RAT MODELS IN OBESITY RESEARCH: FUNCTIONS FOR *PMCH* AND *LPIN1* IN ENERGY HOMEOSTASIS REGULATION

Joram D. Mul

ISBN: 978-94-90371-23-4

Cover image and illustrations: Jessica van der Werff (info@jessicaas.nl)

Layout & printing: Off Page, Amsterdam

RAT MODELS IN OBESITY RESEARCH: FUNCTIONS FOR *PMCH* AND *LPIN1* IN ENERGY HOMEOSTASIS REGULATION

Diermodellen in de rat voor obesitas onderzoek:
Genfuncties voor *Pmch* en *Lpin1*
tijdens de regulatie van energie huishouding

(met een samenvatting in het Nederlands)

PROEFSCHRIFT

ter verkrijging van de graad doctor aan de Universiteit Utrecht
op gezag van de rector magnificus, prof. dr. J.C. Stoof,
ingevolge het besluit van het college voor promoties in het openbaar te verdedigen
op woensdag 30 juni des middags te 2.30 uur

door

Joram David Mul
geboren op 25 juni 1980
te Arnhem

Promotor: Prof. dr. E. P. J. G. Cuppen

The research described in this thesis was performed at the Hubrecht Institute of the Royal Academy of Arts and Sciences (KNAW), within the framework of the Graduate School of Cancer Genomics and Developmental Biology (CGDB) in Utrecht.

Printing of this thesis was financially supported by the J.E. Jurriaanse Stichting.

CONTENTS

1

GENERAL INTRODUCTION

GENERAL INTRODUCTION

The Creation of Knockout Rat Models

The laboratory rat is one of the most extensively studied model organism for various aspects of human health and disease, like physiology, toxicology and neurobiology, as well as for drug development. Moreover, some neurological diseases and disorders affecting higher brain function, including schizophrenia, anxiety, depression, and addiction are best mimicked in the rat. In addition, their relative large size enables surgical manipulations of many organs including the brain (Sutherland, 2004).

At the beginning of the 21st century, the generation of stable knockouts by homologous recombination in embryonic stem (ES) cells, as is widely used for the mouse (Capecchi, 2005), was unavailable in rats due to the unavailability of rat ES cells despite several decades of attempts. Therefore, investigators applied a known technique, called target-selected mutagenesis or TILLING, to the rat and successfully generated the first rat knockout models (Zan et al., 2003; Smits et al., 2004; Smits et al., 2006). In short, male rats are injected with the potent mutagen *N*-ethyl-*N*-nitrosourea (ENU), which introduces random point mutations that become fixed in the germline. Mutagenized males are subsequently mated to untreated females to generate F_1 animals, which carry unique random heterozygous point mutations in their genomes. DNA from each F_1 animal is subsequently screened for induced mutations in genes of interest that affect normal protein function by changing functionally conserved amino acids or introducing premature stop codons (Fig. 1).

A large-scale gene-driven (reverse genetics) screen using this technique in Wistar rats produced several mutant and knockout rat models, including a knockout model for

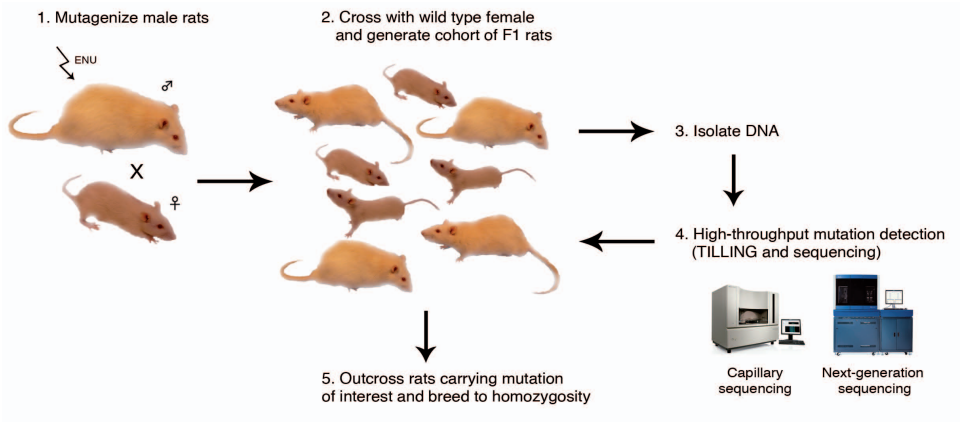

Figure 1. Schematic overview of target-selected mutagenesis procedure. Male founder rats are mutagenized using ENU and mated to wild type females (1), generating a cohort of F_1 animals that carry a large number of random heterozygous mutations (2). After isolation of genetic material (3), DNA of each rat can be screened using a high-throughput screening platform (4) such as a 3730XL capillary sequencer (Applied Biosystems) or a SOLiD™ next-generation sequencer (Applied Biosystems). If a functional mutation is observed in a gene of interest, the rat can be outcrossed and bred to homozygosity (5). Adapted from Smits et al., 2004.

the prehormone precursor *Pmch* (Smits et al., 2006). Another mutant was discovered via a different route: after an accidental brother-sister mating of F_3 generation rats derived from the initial ENU-mutagenesis screen, a nest with phenotypic mutants (paralysis and decreased body weight) was identified. In a phenotype-driven forward genetics approach, a mutation in the *Lpin1* gene was found to be causative to the phenotype.

Both *Pmch* and *Lpin1* are involved in the regulation of lipid metabolism and consequently body weight. Therefore, I will first present a general overview of the current knowledge regarding body weight regulation, which will be followed by a more detailed overview of *Pmch* and *Lpin1* function. Subsequently, 4 chapters describing the initial characterization of both the *Pmch* (chapters 2, 3, and 4) and the *Lpin1* (chapter 5) rat model will be presented. Finally, a general discussion will summarize the findings presented and further directions for research will be discussed.

THE REGULATION OF BODY WEIGHT

The Current Global Obesity Epidemic

Excess energy is stored in the human body predominantly in the form of fat (adipose tissue). This ability to store excess energy as body fat is critical for survival, which may suggest that evolution over time naturally selects biological mechanisms that increase fat storage, thus optimizing the ability to store excess energy as adipose tissue. As food supplies used to be scarce, i.e. food was still hunted or scavenged, times of feeding were unpredictable and irregular and the storage of reserve energy was promoted for survival during meager times. However, food availability, amongst other factors, has improved dramatically during the past few centuries, especially during the last three decades. As the evolutionary favored mechanism of efficient fat storage is still present but no longer needed in most humans in first world countries, this has generated challenges to correctly regulate a healthy body weight.

If the ingestion of energy exceeds ongoing requirements, this will eventually result in overweight, or extreme overweight, also indicated as obesity. Obesity is hallmarked by the accumulation of excess body fat to such an extent that it can have adverse effects on health. Although obesity is seen as a disease on its own, it can also lead to many co-morbidities. These common secondary health problems include diabetes mellitus type 2 (T2D; high blood glucose in the context of insulin resistance and relative insulin deficiency), cardiovascular and heart diseases (high blood pressure), breathing problems, osteoarthritis (degradation of the joints), infertility, and certain types of cancer. The combination of insulin resistance, high blood pressure, high blood levels of triglycerides and high-density lipoproteins are together most often referred to as the 'metabolic syndrome'. This makes obesity one of the leading preventable causes of death worldwide, and applies great medical and financial pressure to the strenuous economy of obesity-prone cultures. In general, obesity is often caused by a combination of high-caloric food intake, decreased physical activity, and genetic susceptibility. A small fraction (~5-10%) is caused by (mono)-genetic mutations, endocrine disorders, or medication (Schwartz et al., 2004).

The current global obesity epidemic occurs predominantly in first world countries that are characterized by wealth and 24-hr high-caloric food availability, thereby promoting caloric intake and a sedentary lifestyle. In 2008, the National Health and Nutrition Examination Survey (NHANES) reported that obesity occurred in approximately 34% of the adult US population, although the strong increase in obesity numbers seen in the last 2 decades has discontinued (Flegal et al., 2010). In US adolescents, obesity occurs in approximately 17% of the population (Ogden et al., 2010). In the Netherlands, a TNO study between 2002 and 2004 found that approximately half of the adult population suffers from overweight, while 11% suffers from obesity (www.TNO.nl). Statistical numbers regarding the Dutch adolescent population are equally alarming, or even more severe. However, in order to successfully treat obesity, we first need to sufficiently understand how body weight is regulated through the process of energy homeostasis.

Energy Homeostasis

The capacity to adjust nutrient intake in response to changes in positive or negative energy requirements is essential for human survival. Unconsciously, we have the ability to decide whether or not to eat specific nutrients with apparent ease. This is an example of the efficiency with which the central nervous system (CNS) processes information of unlimited variety and complexity. Using our eyes, nose, touch, and previous experience, nutrients are identified and distinguished from potentially hazardous environmental components. Although memories based on odor, taste, and vision have no energy content themselves; they are associated with experiences, and thus energy intake, in the past.

During the ingestion of food, taste information will help assess its palatability, and this information will be integrated with signals regarding nutritional state, both short-term (from the stomach or the gastrointestinal [GI] tract) and long-term (from adipose mass) (Fig. 2). As a consequence, the drive to eat will decrease during the ingestion of food. This process is termed 'satiation'.

Changes in behavior or environment cause changes in energy requirements, thus affecting nutrient intake. This process, called energy homeostasis, adjusts energy intake to match energy expenditure over time, thus promoting stability in the amount of stored body energy. Nevertheless, for most humans the composition and amount of food consumed, and thus energy consumed, varies strongly between meals and between days (Edholm, 1977). This discrepancy in short-term energy intake disappears when energy expenditure is compared to energy intake of a longer period that includes multiple meals, and almost always results in a precise match between energy expenditure and energy intake (Edholm, 1977).

Because feeding is such a complex behavior, it is not surprising that over the past three decades many signaling molecules have been discovered that are part of the body weight-regulatory system. Two of these signaling molecules, insulin, produced by the pancreas in proportion to adiposity, and leptin, produced by adipocytes, were among the first hormonal signals to be discovered that affect body weight (Woods et

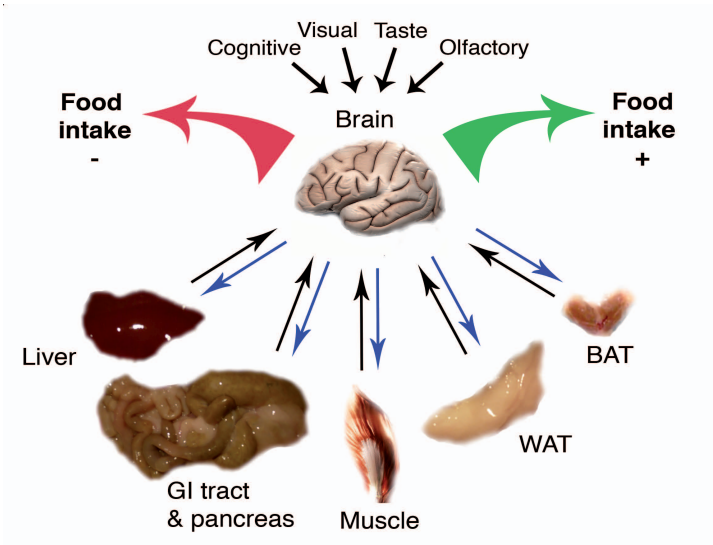

Figure 2. Schematic representation of food intake regulation. Peripheral tissues including liver, gastrointestinal tract, pancreas, muscle, WAT, and BAT have direct or indirect influence on metabolic information processing in the brain. This is achieved by short- or long-term signaling regarding nutritional state (black arrows). The brain stimulates stored energy release or energy uptake in peripheral tissues by releasing hormones or neurotransmitters, or by direct nervous innervation (blue arrows). In addition to the peripheral input, cognitive, visual, taste, and olfactory cues aid in the processing of metabolic information. Continuous metabolic information processing will result in stimulation or inhibition of food intake.

al., 1979; Zhang et al., 1994). Already in mid-fifties the process of energy homeostasis was widely studied and a model was coined in 1953 that suggested that signals generated in proportion to energy (i.e. adipose mass) stored in the body reduce food intake through action on the brain, also known as the 'adiposity-negative feedback' model (Kennedy, 1953). As this model could not directly explain the dynamics of meal initiation and termination, a second model was added twenty years later proposing that inhibitory molecules generated during a meal, this time also including signals from the GI tract, provide information to the brain thus acutely terminating energy intake (Gibbs et al., 1973). 'Adipose-negative feedback' signals should fit three criteria: (1) they must circulate at levels proportionate to body energy (i.e. adipose mass) content and possess the ability to enter the brain; (2) they must be able to promote body weight loss; and (3) blockade of the latter function must result in increased energy intake and body weight gain. Although many signaling molecules have been discovered that possess one or two of the above criteria, to date only insulin and leptin fit all three criteria (Schwartz et al., 2000; Morton et al., 2006).

In summary, by integrating a large variety of hormonal and neural signals regarding body energy levels with visual, cognitive, olfactory, and taste cues, the CNS controls nutrient intake and body weight regulation on an unconscious level (Morton et al., 2006). A subset of these hormonal and neural signals will be discussed below in more detail.

THE NEUROBIOLOGY OF ENERGY HOMEOSTASIS

In this subchapter, a brief and general overview of our current understanding of some of the factors that regulate energy homeostasis will be provided. This will be followed by a more specific overview of two factors involved in this process that have been studied in more detail in this thesis.

Insulin and Leptin

Both insulin and leptin are to date the only discovered 'adiposity negative feedback signals'. This means that both hormones circulate at levels proportionate to body fat content (Bagdade et al., 1967; Considine et al., 1996), enter the CNS in proportion to blood levels (Baura et al., 1993; Schwartz et al., 1996a), and administration of either hormone into the brain or body reduces energy intake (Woods et al., 1979; Campfield et al., 1995; Halaas et al., 1995; Weigle et al., 1995). Moreover, both hormones bind to their own receptors expressed in brain regions regulating energy intake (Elmquist et al., 1998b; Bruning et al., 2000; Elias et al., 2000; Leinninger et al., 2009; Myers et al., 2009), deficiency of leptin in *ob*/*ob* mice results in hyperphagia (overeating) and obesity (Trayhurn, 1984; Zhang et al., 1994), whereas brain deficiency of insulin results in hyperphagia (Sipols et al., 1995). Although both insulin and leptin are important regulators of the energy balance, multiple lines of evidence indicate that leptin has a more significant role than insulin. Loss of leptin results in obesity and hyperphagia, despite high insulin levels, while loss of insulin (diabetes mellitus type 1) does not result in obesity. The latter finding, however, could result from the requirement of insulin for adipocyte growth and differentiation (Saltiel and Kahn, 2001; Louveau and Gondret, 2004). Loss of insulin increases energy intake (Leedom and Meehan, 1989), but as fat deposition is impaired and leptin levels remain relatively low (Havel et al., 1998; Hathout et al., 1999), it results in hyperglycemia (high blood glucose levels) that is largely corrected by loss of glucose through urine. Another complicating factor in the latter findings is that insulin controls leptin secretion through effects on glucose metabolism in adipocytes (Mueller et al., 1998; Wang et al., 1998). Additional evidence for this finding comes from observations that leptin levels drop acutely when food deprivation is induced, while fat depots are still unaffected at that time.

Although both the low leptin and insulin levels can be responsible for 'diabetic hyperphagia', leptin seems to be the more significant of the two hormones, as replenishing leptin levels to non-diabetic levels in diabetic rats prevented the development of 'diabetic hyperphagia' (Sindelar et al., 1999). However, the optimism surrounding leptin as an anti-obesity treatment diminished rapidly with the discovery that many obese individuals are leptin resistant (Heymsfield et al., 1999). Leptin resistance is also well documented in rodents with mutant leptin receptors (Campfield et al., 1995; Chua et al., 1996). As already mentioned, obesity results in peripheral insulin resistance (T2D). To counter this, pancreatic b-cells must increase their basal and post-meal insulin secretion, thereby resulting in relative hyperinsulinemia (Polonsky et al., 1988; Kahn et al., 1993). However, as insulin levels fail to reach a level sufficient to

compensate for the insulin resistance, obesity can develop further, often resulting in T2D and exacerbated hyperglycemia. Not only peripheral tissues, but also the brain of obese rodents develops resistance to insulin as well as leptin (Munzberg et al., 2004; De Souza et al., 2005).

In sum, insulin itself was never a promising therapeutic target due to its complex role in T2D, whereas leptin was found to be promising therapeutic target for obesity treatment. However, leptin has not yet lived up to the expectations despite a large collection of data on its function. To date, a decreased sensitivity to leptin in obese patients seems to be the most significant limitation. Therefore, researchers have subsequently focused on down-stream players of the leptin and insulin pathways.

THE HYPOTHALAMUS

History

A classic lesion and brain stimulation study already performed in 1954 identified the hypothalamus as an important centre controlling energy homeostasis (Stellar, 1954). Within the hypothalamus, the ventromedial hypothalamic nucleus (VMN) was identified as the satiety centre, whereas the lateral hypothalamic centre (LHA) was identified as the hunger centre (Fig. 3; Stellar, 1954). Subsequent research during the past decades has provided immense quantities of information regarding the function of the hypothalamus, and has led to the discovery of other brain regions involved in the regulation of energy homeostasis. Moreover, it has led to the confirmation of the hypothalamus as one of the key regions involved in the energy balance, and has identified many additional anabolic (energy intake stimulating) and catabolic (energy intake limiting) effectors (Flier and Maratos-Flier, 1998; Barsh et al., 2000; Schwartz et al., 2000; Morton et al., 2006). Therefore, the classic view of distinct 'feeding or satiety centers' has been replaced by a more specific view of discrete neuronal pathways that are intertwined and communicate between multiple brain regions.

Arcuate Nucleus and Primary Metabolic Neurons

Blood-borne hormonal signals, such as insulin and leptin, can signal to the brain through passage of the blood-brain barrier. This uptake is facilitated by the appropriate receptors expressed by endothelial cells in the blood-brain barrier (Baura et al., 1993; Bjorbaek et al., 1998). After passage through the blood-brain barrier, insulin and leptin signaling is transformed into a neuronal signal in the arcuate nucleus (ARC), a key brain region of the hypothalamus. The ARC is adjacent to the lower part of the third ventricle (3V; Fig. 3) and contains neurons that express the anabolic neuropeptides neuropeptide-Y (NPY) and Agouti-related peptide (AgRP) neurons (Broberger et al., 1998; Hahn et al., 1998). Loss of either NPY or AgRP has no effect on feeding (Qian et al., 2002; Ste Marie et al., 2005), whereas ablation of NPY/AgRP neurons results in severe hypophagia (Gropp et al., 2005; Luquet et al., 2005). A distinct but adjacent subset of ARC neurons expresses the catabolic neuropeptides pro-opiomelanocortin (POMC) and cocaine- and amphetamine-regulated transcript (CART) (Gee et al., 1983;

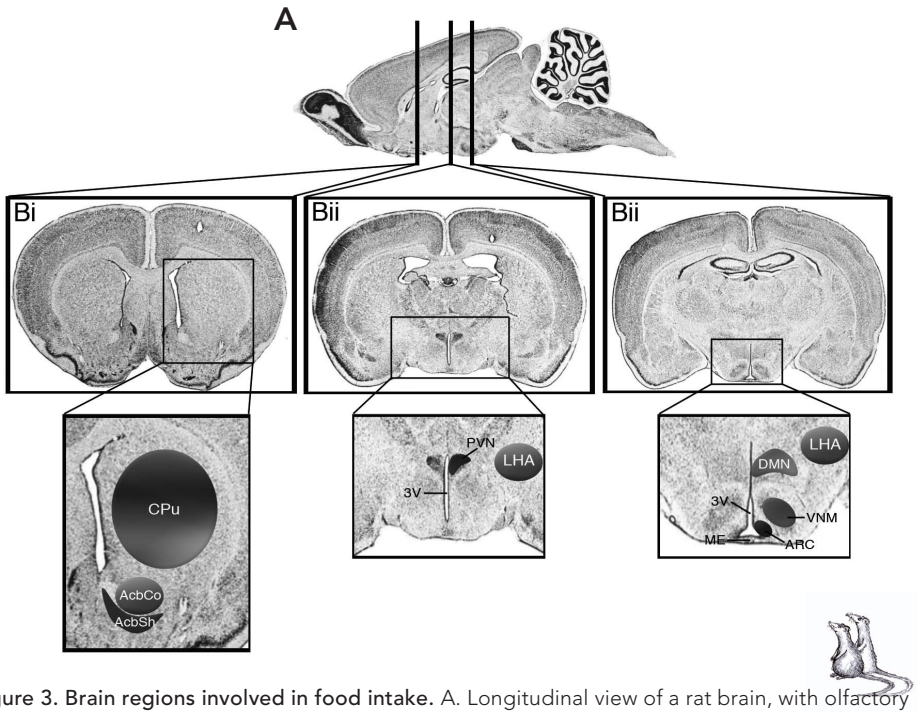

Figure 3. Brain regions involved in food intake. A. Longitudinal view of a rat brain, with olfactory bulb at the anterior end on the left and the caudal hindbrain at the posterior end on the right. B. Cross-sections of the brain (indicated by lines in A). Bi. Cross-section demonstrating location of the caudate putamen (CPu), the nucleus accumbens core (AcbCo), and the nucleus accumbens shell (AcbSh). Bii. Cross-section demonstrating location of the paraventricular nucleus (PVN) and the anterior lateral hypothalamic area (LHA). Biii. Cross-section demonstrating location of the arcuate nucleus (ARC), the ventromedial nucleus (VMN), the dorsomedial nucleus (DMN), and the posterior part of the LHA. Abbreviations: 3V, third ventricle; ME, medial eminence (Brain slide images were obtained from Sherwood and Timiras, 1970).

Douglass and Daoud, 1996; Elias et al., 1998). Processing of the precursor gene *Pomc* generates multiple products, including α-melanocyte stimulating hormone (α-MSH), β-endorphin, and adrenocorticotropic hormone (ACTH), although the variety of products differs between sites (central vs. pituitary) and between models (human vs. rodents) (Coll, 2007). The NPY/AGRP and POMC/CART neuronal populations function in parallel and counterbalance each other to properly regulate energy homeostasis. For example, α-MSH is an agonist of melanocortin-receptors 1, 3, 4 and 5 (MC1R-MC5R), whereas AGRP is an antagonist of MC3R and MC4R function (Ollmann et al., 1997). Both MC3R and MC4R, the two most predominant expressed melanocortin receptors in the brain, are implicated and important for correct body weight regulation (Ollmann et al., 1997). Interestingly, ARC lesions decrease the intracerebroventricular (ICV) injection effects of leptin (Dawson et al., 1997; Tang-Christensen et al., 1999), and leptin administration to the ARC generates an anorexic response (Satoh et al., 1997). Moreover, neurons expressing the above-mentioned neuropeptides express leptin

receptors (Cheung et al., 1997; Baskin et al., 1999), as well as insulin receptors (Baskin et al., 1988; Bohannon et al., 1988b, a). Leptin inhibits NPY/AgRP gene expression, whereas lower leptin levels or insulin deficiency activate these neurons (Williams et al., 1989a; Williams et al., 1989b; Sipols et al., 1995; Stephens et al., 1995; Schwartz et al., 1996b; Broberger et al., 1998; Hahn et al., 1998). On the contrary, lower insulin or leptin levels inhibit POMC/CART gene expression (Schwartz et al., 1997; Thornton et al., 1997; Kristensen et al., 1998). In summary, the ARC is an important mediator of leptin and insulin. The importance of melanocortin signaling in mediating the anorexic function of adiposity signals was further shown by MC3R and MC4R antagonism studies (Seeley et al., 1997; Hagan et al., 1999).

The ARC is a critical brain region that integrates information about energy levels communicated by peripheral adiposity signals such as leptin and insulin. However, recent evidence has shown that additional biological products can contribute to signaling regarding energy homeostasis. For example, acute changes in glucose levels affect feeding behavior, thus suggesting that carbohydrate sensing is physiologically important in the CNS (Levin et al., 2004). For example, central administration of 2-deoxy-D-glucose, a glucose analog that blocks glucose metabolism, strongly increases nutrient intake (Miselis and Epstein, 1975). Subsequent research identified AgRP/NPY neurons as glucose-inhibited cells, whereas POMC neurons are glucose-stimulated (Muroya et al., 1999; Ibrahim et al., 2003).

Basal energy levels are also known to affect peripheral fatty acid metabolism (Jayakumar et al., 1995). Interestingly, neuronal ATP levels are predominantly derived from glucose oxidation and not fat oxidation (Sokoloff et al., 1977). Nevertheless, peripheral but also central inhibition of fatty acid synthase (FAS) function decreases body weight (Clegg et al., 2002; Wortman et al., 2003; Lam et al., 2005). In addition, an increase in hypothalamic FAS-substrate malonyl-CoA, ICV injection of long-chain fatty acid-CoA (LCFA-CoA), and peripheral LCFA-CoAs that cross the blood-brain barrier, all induce weight loss (Loftus et al., 2000; Obici et al., 2002; Hu et al., 2005; He et al., 2006; Pocai et al., 2006). Finally, recent evidence has also shown that amino acids are involved in CNS nutrient sensing. For example, ICV injection of leucine decreases food intake (Cota et al., 2006). This effect is mediated by inhibition of hypothalamic *Agrp* expression, and is effective in obese mice (Morrison et al., 2007; Zhang et al., 2007).

Finally, two protein kinases, AMP-activated protein (AMPK) and mammalian target of rapamycin (mTOR) have recently been shown to play an important role in nutrient sensing in the hypothalamus (Minokoshi et al., 2004; Cota et al., 2006). Hypothalamic AMPK activity can be increased by fasting or AGRP administration, whereas insulin, high glucose, and refeeding decrease AMPK activity (Minokoshi et al., 2004). Leucine or leptin administration increases hypothalamic mTOR activity (Cota et al., 2006). AMPK is thus activated by states of negative energy balance, whereas mTOR is activated by states of positive energy balance (Sandoval et al., 2008). Both AMPK and mTOR seem to colocalize with NPY/AGRP and POMC/CART neurons, and are important downstream signal modifiers of leptin signaling (Minokoshi et al., 2004; Cota et al., 2006).

These initial reports, combined with confirmative studies, established an exclusive and important function for ARC neurons sensing and processing information regarding body energy levels. This led to the hypothesis that secondary neurons receiving input from ARC neurons could play an equal or even more important role in the regulation of energy homeostasis.

Secondary Metabolic Neurons

Initial lesion/stimulation and feeding studies had shown that other hypothalamic nuclei besides the ARC, such as the VMN and LHA, are critical regions involved in energy homeostasis and body weight regulation (Stellar, 1954; Stanley et al., 1993). Moreover, ARC neurons expressing NPY/AGRP or POMC/CART project to many other hypothalamic nuclei, including the paraventricular nucleus (PVN), the zona incerta, perifornical area (PFA), and the LHA (Elmquist et al., 1998a; Elmquist et al., 1999). Neuropeptides expressed predominantly in the PVN, such as corticosterone-releasing hormone (CRH), thyrotropin-releasing hormone (TRH), and oxytocin (OXY) were indeed found to affect food intake, all in an anorectic manner (Kow and Pfaff, 1991; Dallman et al., 1993; Verbalis et al., 1995).

Two neuropeptides expressed predominantly in the LHA, Melanin-concentrating hormone (MCH; extensively discussed below) and orexin (OX) were both also found to affect food intake, this time in an orexigenic manner (Qu et al., 1996; de Lecea et al., 1998; Sakurai et al., 1998; Shimada et al., 1998). More recently, additional hypothalamic neuropeptides have been discovered that affect energy regulation. These include the anorectic peptide Nesfatin-1 (Oh et al., 2006) and the orexigenic peptide FTO (Fischer et al., 2009). In humans, polymorphisms in the *fto* gene were shown to affect body mass and T2D (Dina et al., 2007; Frayling et al., 2007; Scott et al., 2007; Scuteri et al., 2007).

EXTRAHYPOTHALAMIC BRAIN REGIONS INVOLVED IN ENERGY HOMEOSTASIS

The Hindbrain

The decision-making process to start eating (meal initiation) can be influenced by many different factors. These factors include emotional status, time of day, the availability of food, the palatability of the available food, and environmental influences. However, the process that terminates a meal, in the light of *ad-libitum* access, appears to be biologically controlled (Smith, 1996). Information regarding satiety is largely conveyed by afferent fibres of the vagus nerve and by afferent passing into the spinal cord from the upper GI tract (Ritter et al., 1994). Subsequently, a combination of satiety information both from the abdomen (GI tract and liver) and the oral cavity is processed in the nucleus tractus solitarius (NTS) (Travers et al., 1987; Friedman et al., 1999).

Evidence for neuronal talk between hypothalamic signals and hindbrain regions comes from multiple observations. First, reciprocal connections exist between the NTS and the PVN (Ter Horst et al., 1989). Second, genes involved in hypothalamic energy regulation such as *Mc4r*, leptin receptors, and *Pomc* are expressed in the NTS

(Bronstein et al., 1992; Mountjoy et al., 1994; Mercer et al., 1998). Moreover, MC4R-manipulation in the hindbrain affects food intake (Grill et al., 1998), and the hindbrain is critical for the anorexic effect of leptin (Grill et al., 2002).

The Gastrointestinal Tract

The GI tract consists of the upper and the lower GI tracts. The upper GI tract extends from the mouth to the small intestines, while the lower GI tract extends from the small intestines to the anus. When food passes through the GI tract, physical expansion and nutrient sensing initiate the production of multiple hormonal peptides that affect the regulation of energy balance, predominantly by signaling to the hindbrain. These peptides include the incretins glucagon-like peptide-1 (GLP-1) and gastric inhibitory peptide (GIP), which directly increase insulin levels after food ingestion before glucose levels rise. Other examples are gastrin, secretin, vasoactive intestinal peptide (VIP), cholecystokinin (CCK), polypeptide-YY_{3-36}, and oxyntomodulin, of which the latter three together with GLP-1 can decrease food intake by decreasing meal size (Antin et al., 1975; Moran and Schwartz, 1994; Cummings and Overduin, 2007; Chaudhri et al., 2008). To date, one peripheral hormone, ghrelin, is produced by endothelial cells of the stomach and can increase food intake by increasing meal size (Tschop et al., 2000; Cummings and Overduin, 2007; Chaudhri et al., 2008). Administration of ghrelin, either peripheral or central, positively regulates energy homeostasis in both humans and rodents (Tschop et al., 2000; Wren et al., 2001a; Wren et al., 2001b), while plasma ghrelin levels are increased in obese individuals or increase after weight loss in humans (Cummings et al., 2002b; Cummings et al., 2002a).

Interestingly, most GI hormones or their receptors are also expressed in the CNS, thus suggesting a function in the CNS in addition to their peripheral function. For example, GLP-1 is synthesized in the NTS, GLP-1 neurons in the NTS project to the hypothalamus and the amygdala, and GLP-1 receptors are expressed extensively in the amygdala, the PVN, ARC, and the caudal brain stem (Han et al., 1986; Merchenthaler et al., 1999). Although it is clear that GLP-1, and other GI signals, can affect food intake and glucose metabolism, the exact origin of these effects (peripheral, central, or some combination of both) is still elusive.

While the discovery of additional peripheral players in the near future is not excluded, investigators are optimistic that the all-ready known gut hormones will make interesting targets for the treatment of obesity and/or diabetes. For example, liraglutide, a GLP-1 agonist, decreases body weight in overweight individuals (Astrup et al., 2009).

Midbrain and Forebrain Dopaminergic Signaling

If the control of energy regulation were purely homeostatic, feeding behavior would be purely automated and rather dull behavior. However, humans can become very enthusiastic when eating highly palatable food and are willing to pay large sums of money in expensive restaurants to do this. Moreover, most mammals will consume

more than necessary when presented with a large quantity of highly palatable food. This suggests that a hedonic factor adds to the complexity of feeding behavior. Indeed, brain systems that contain the monoamine dopamine (DA) have been implicated in the regulation of the hedonic or rewarding aspect of feeding, and multiple peripheral hormones act on midbrain dopaminergic systems to affect food intake (Narayanan et al., 2009). Drug addiction studies have provided evidence that reward is strongly correlated with substantia negra and ventral tegmental area (VTA) DA-containing neuron function and their projections to the nucleus accumbens (NAc; also indicated as ventral striatum), cortex, and subcortical nuclei (Wise, 1996, 2004). The dopaminergic projections from the VTA to the NAc are also indicated as the 'mesolimbic' projection.

As neurological reward-related processes such as drug abuse, feeding, and sex are intertwined through their shared dopaminergic basis, it has been proposed that DA also mediates the hedonic aspect of feeding (Stricker and Zigmond, 1984; Wang et al., 2001a; Volkow and Wise, 2005; Wise, 2006; Yamamoto, 2006; Narayanan et al., 2009). It is hypothesized that this occurs via the mesolimbic projection (Wise, 2006), and dysfunction of reward processing in either of these regions can promote obesity or leanness (Volkow and Wise, 2005).

Although initial studies did not reveal a striatal function regarding feeding behavior, i.e. NAc ablation did not obviously affect feeding behavior or operant responding for food (Koob et al., 1978; Ikemoto and Panksepp, 1996), other and more recent data have suggested otherwise. For example, depletion of DA through intraventricular 6-hydroxydopamine injections decreased feeding (Zigmond and Stricker, 1972). Nigrostratial or caudate putamen (CPu; also indicated as the dorsal striatum) reinstatement of DA production rescues feeding in normally starved-to-death DA-depleted mice (Szczypka et al., 2001; Hnasko et al., 2006). Additionally, GABA agonist and glutamate antagonist injections in the NAc affected feeding (Maldonado-Irizarry et al., 1995; Stratford and Kelley, 1997; Stratford et al., 1998).

Leptin receptors, which are highly expressed in the ARC, are also expressed in the VTA and leptin administration in the VTA decreases food intake as well as dopaminergic neuron firing, while leptin receptor knockdown in the VTA increases food intake (Hommel et al., 2006). Upstream of this direct VTA effect, leptin can also affect feeding via the VTA through action on LHA neurons that also contain leptin receptors (Leinninger et al., 2009). Ghrelin administered to the VTA or NAc also affects feeding behavior (Naleid et al., 2005; Abizaid et al., 2006).

These findings have provided evidence that peripheral hormones can directly influence mesolimbic DA signaling and thus affect feeding behavior. Recent evidence has emerged that the neuropeptides MCH (discussed below) and OX expressed in secondary neurons in the LHA also affect the DA system and subsequent reward-related behavior (Georgescu et al., 2005; Harris et al., 2005; Smith et al., 2005; Pissios et al., 2008). Although these findings increase the complexity of feeding behavior regulation, they also provide new interesting therapeutic targets for obesity treatment.

MELANIN-CONCENTRATING HORMONE

History

In 1983, MCH (the product of *pMCH1*) was discovered as a 17-amino acid cyclic peptide in the pituitary of the chum salmon where it stimulates the aggregation of melanosomes, thus lightning the skin, in response to stress and other environmental stimuli (Kawauchi et al., 1983). In addition to *pMCH1*, a second fish MCH gene, named *pMCH2*, was described in 1989 (Ono et al., 1988; Takayama et al., 1989). The *pMCH1* gene is an intronless preprohormone and processing results in neuropeptide E-V and MCH (Balm and Groneveld, 1998). Within the salmonid family, peptide sequence homology is high, but homology with other fish is lower (Pissios et al., 2006). The effects of MCH on skin pigmentation, endocrine function, and food intake in fish have been extensively studied (Balm and Groneveld, 1998; Kawauchi, 2006). MCH has a clear effect on skin pigmentation in fish, hence its name. However, in mice no clear effects on skin color have been observed in brown or black coat-colored mice that have disrupted MCH function (Pissios et al., 2006). Therefore, despite its name, a similar function for MCH on mammalian skin pigmentation is possible but unlikely.

Melanin-Concentrating Hormone Genes in Mammals

A peptide discovery study in 1989 identified MCH in the hypothalamus of rats (Vaughan et al., 1989). Other studies further characterized the MCH gene in rats and identified MCH genes in humans and mice (Presse et al., 1990; Thompson and Watson, 1990; Presse et al., 1992; Breton et al., 1993b; Breton et al., 1993a). Mammalian MCH is a 19-amino acid cyclic peptide highly identical to salmon MCH with two additional amino acids and four non-conserved amino acids as compared to salmon MCH (Pissios et al., 2006). The mammalian 165-amino acid precursor gene of MCH (hereafter *Pmch*) contains three exons and two introns. Between multiple mammalian species, including human, rat, and mouse, *Pmch* peptide sequence homology is very high (Pissios et al., 2006). Moreover, MCH primary structure is fully conserved among human, rat, and mouse (Pissios et al., 2006).

Only a single MCH-encoding gene has been found in rodents (Vaughan et al., 1989; Breton et al., 1993b), while two additional '*Pmch*-like' variants (*pMCHL1* and *pMCHL2*) have been described in humans (Breton et al., 1993a; Pedeutour et al., 1994; Viale et al., 1998b; Viale et al., 1998a). *PMCHL1* produces several sense and antisense RNA transcripts, especially in the developing human brain (Miller et al., 1998; Viale et al., 2000), but the exact function of these 'primate-specific' RNA transcripts has remained obscure. Several mature and immature RNAs were also observed in rat brain, thymus, pancreas, and adrenal gland (Hervieu and Nahon, 1995).

Pmch-derived Peptides and *Pmch*-related Peptides in Mammals

Pmch processing generates neuropeptide glycine-glutamic acid (NGE), neuropeptide-glutamatic acid-isoleucine (NEI), as well as MCH (Nahon et al., 1989). Two different post-translational systems can be responsible for the correct cleavage of NEI; first, whereas

almost all prehormone convertase (PC) can cleave MCH from its precursor at the Arg^{145}-Arg^{146} site, only prehormone convertase 2 (PC2) can cleave the Lys^{129}-Arg^{130} site, thus correctly liberating NEI (Viale et al., 1999b). Subsequently, PC2-deficient mice show increased MCH-immunoreactive (IR) and decreased NEI-IR levels, while hypothalamic *Pmch* mRNA levels were unchanged (Viale et al., 1999b). Moreover, processing of prehormones, such as *Pmch*, can differ between organs, and between organs and the brain, due to the presence or absence of particular PCs (Zakarian and Smyth, 1982; Viale et al., 1999b). The second system involves carboxypeptidase E (CpE), as CpE activates NEI by removing three amino acid residues from the carboxyterminal end of NEI (Rovere et al., 1996). Subsequently, *fat*/*fat* rats, which lack CpE, show decreased mature NEI and a compensatory increase in *Pmch* and thus mature MCH (Rovere et al., 1996). Many MCH-neurons, especially the LHA and IHy, are immunoreactive for both MCH and NEI, although some neurons show immunoreactivity to only one of the neuropeptides (Bittencourt and Celis, 2008). This suggests that the above-mentioned post-translational systems can be involved in neurons that show MCH immunoreactivity but not NEI immunoreactivity (Bittencourt and Celis, 2008).

Two additional products of *Pmch* itself have also been described. The first product, named MCH-gene overprinted polypeptide (MGOP)-14 and MGOP-27 was discovered in rats and results from alternative frame translation, thereby excluding exon 2 (Toumaniantz et al., 1996). The second product, named antisense RNA-overlapping MCH (AROM) is transcribed from the opposite strand (Borsu et al., 2000). Multiple transcripts from the AROM gene are derived trough alternative splicing, but all derived coding transcripts do not overlap with *Pmch* cDNA (Borsu et al., 2000). The exact functions of the MGOP and AROM transcripts have remained obscure so far.

MCH Neurons, MCH-Receptors, and MCH-Receptor Signaling

Magnocellular neurons expressing *Pmch* are predominantly present in the LHA and the incerto hypothalamic area and project to many brain regions in the neuroaxis (Bittencourt et al., 1992; Sita et al., 2007). These brain regions include the olfactory bulb, the prefrontal cortex, the striatum, and hindbrain nuclei including the NTS and the parabrachial nucleus. This widespread projection pattern generated the hypothesis that MCH-signaling is involved in a scale of behaviors (Nahon, 1994).

The identification of a MCH-receptor was initially obstructed by high non-specific binding (Hintermann et al., 1999; Kokkotou et al., 2000), but was soon followed by the observation that MCH bound to the orphan GPCR SLC1/GPR24, thus identifying this receptor as MCH1R (Kolakowski et al., 1996; Bachner et al., 1999; Chambers et al., 1999; Lembo et al., 1999; Saito et al., 1999; Shimomura et al., 1999). MCH1R is a highly conserved (human-rat, 96% homology; human-mouse, 95% homology) seven-transmembrane domain GPCR and shares homology (35%) with the somatostatin receptor family (Kolakowski et al., 1996; Pissios and Maratos-Flier, 2003).

To date, only MCH and MCH(Phe13 Tyr19), an iodinatable homologue of MCH, have been found to specifically bind and activate MCH1R in a dose-response manner

(Chambers et al., 1999; Lembo et al., 1999; Saito et al., 1999). Moreover, NEI, NGE, MGOP-14 or -27, somatostatin-14, the somatostatin analogue RC-160, cortistatin-14 or -29, ACTH, α-MSH, and atrial natriuretic peptide were unable to bind or activate MCH1R (Chambers et al., 1999; Lembo et al., 1999; Saito et al., 1999). MCH is unable to bind MC3R or MC4R (Ludwig et al., 1998), suggesting that the antagonistic action of MCH and α-MSH results from the convergence of pathway signaling activation by distinct receptors (Saito et al., 1999).

Mch1r expression in the brain is largely restricted to piriform cortex, olfactory tubercle, the hippocampal formation, the nucleus accumbens shell (AcbSh), the ARC, and the VMN (Kolakowski et al., 1996; Chambers et al., 1999; Lembo et al., 1999; Saito et al., 1999; Hervieu et al., 2000; Saito et al., 2000; Kokkotou et al., 2001). These brain regions are involved in olfactory learning, reinforcement mechanisms, and feeding, and thus important for the complex regulation of feeding behavior (Pissios et al., 2006). *Mch1r* expression was also observed in the locus coeruleus, the orbital cortex, the cingulate gyrus, and the amygdala (Chambers et al., 1999; Lembo et al., 1999; Saito et al., 1999; Mori et al., 2001), generating the hypothesis that MCH-MCH1R signaling could also be involved in arousal and anxiety-related behavior (Saito et al., 2000). The finding that MCH1R-antagonism has antidepressant and anxiolytic effects strengthened this idea (Borowsky et al., 2002).

Peripheral *Pmch* expression has been observed in stomach, intestines, and testis (Hervieu and Nahon, 1995), whereas peripheral *Mch1r* expression was observed in many tissues, including stomach, eye, adipocytes, pituitary, heart, kidney, ovaries, skeletal muscle, and tongue (Kolakowski et al., 1996; Saito et al., 1999; Saito et al., 2000; Bradley et al., 2002). In humans, reports have also demonstrated *Pmch* and *Mch1r* expression in immune-, endothelial-, neuroblastoma-, and melanoma cells (Saito et al., 2001; Hoogduijn et al., 2002; Schlumberger et al., 2002b; Verlaet et al., 2002). Additionally, MCH antagonizes α-MSH action on melanin production in human melanocytes, and vitiligo, a human skin disease involving loss of pigmentation, involves MCH1R (Hoogduijn et al., 2002; Kemp et al., 2002). The latter findings indicate a function for MCH in skin pigmentation, as is widely observed in fish. However, loss of *Pmch* of *Mch1r* in mice does not affect skin color, limiting the possibility that MCH-MCH1R signaling plays an important role in mammalian pigmentation and suggesting a misnomer (Pissios et al., 2006).

MCH binds to MCH1R with strong affinity, and activates G_i, G_o, and G_q proteins and synergizes with G_s pathways (Hawes et al., 2000; Pissios et al., 2003). MCH1R activation has several intracellular effects: (1) increase in phospholipase C (PLC) activity, thus increasing inositol 1,4,5-trisphosphates (IP3) and diacylglycerol (DAG) levels. DAG activates protein kinase C (PKC), whereas IP3 levels increase intracellular free calcium levels (effect of G_q activation; calcium levels might also be influenced by G_i/G_o activation); (2) inhibition of adenylate cyclase (AC), thus lowering cAMP levels and subsequent protein kinase A (PKA) activity (effect of G_i/G_o activation); and (3) the activation of extracellular signal-regulated kinase ERK1 (also known as MAPK3) and

ERK2 (also known as MAPK1) (effect of G_i/G_o activation) (Hawes et al., 2000; Pissios et al., 2003) (Fig. 4).

A second MCH receptor, MCH2R, has been identified in humans, monkeys, dogs and ferrets (An et al., 2001; Hill et al., 2001; Mori et al., 2001; Rodriguez et al., 2001; Sailer et al., 2001; Wang et al., 2001b). In general, *Mch2r* expression overlaps strongly with *Mch1r* expression, both central and peripheral, although *Mch2r* is expressed at lower levels and less abundant (An et al., 2001; Hill et al., 2001; Sailer et al., 2001; Schlumberger et al., 2002a). MCH2R shares low homology (~35%) with both MCH1R or somatostatin receptor 1 (An et al., 2001; Mori et al., 2001; Sailer et al., 2001), and *Mch2r* expression was not found in rodents (Tan et al., 2002). Additionally, MCH2R activation increases intracellular free calcium levels, but apparently does not affect cAMP levels (An et al., 2001; Hill et al., 2001; Sailer et al., 2001).

Two intracellular proteins have been found to bind to MCH1R, although their exact function remains to be elucidated. Periplakin, which binds to actin and intermediate filaments, is coexpressed with MCH1R and potentially interacts with the C-terminus to affect calcium mobilization (Murdoch et al., 2005). MCH1R-interacting zinc-finger protein (MIZIP) also interacts with the C-terminus and is hypothesized to be a modulator of MCH-MCH1R signaling (Bachner et al., 2002). MIZIP expression, central and peripheral, shows strong overlap with *Pmch* and MCH1R expression (Bachner et al., 2002).

So far, several amino acid residues have been found to be crucial for MCH1R function: three consensus N-glycosylation sites, an process important for correct folding of proteins, and several potential phosphorylation sites have been found in intracellular loops (Lakaye et al., 1998); a 3rd transmembrane domain aspartatic acid residue (Asp^{123}) is crucial for ligand binding (Macdonald et al., 2000); an extracellular N-terminal aspargine residue (Asn^{23}) is important for N-linked glycosylation and

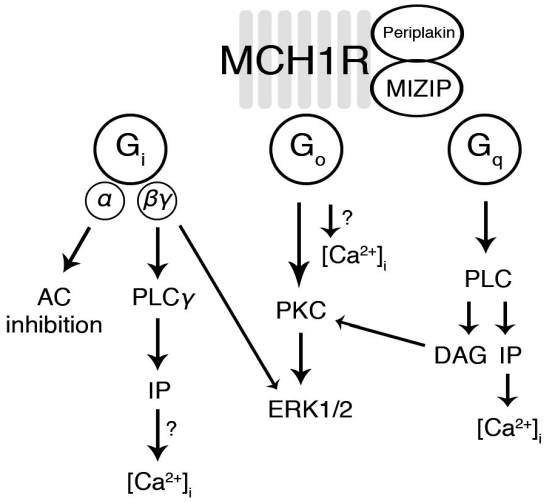

Figure 4. MCH1R activates multiple signaling pathways. The 7-transmemberane receptor MCH1R interacts with the intracellular proteins Periplakin and MIZIP. Through coupling to different G-proteins, MCH1R decreases adenylate cyclase (AC) activity, increases intracellular calcium (Ca^{2+}_i) levels, and activates extracellular-signal-regulated kinases (ERKs) 1 and 2 (sometimes also referred to as mitogen-activated protein kinase [MAPKs]) (based on Hawes et al., 2000; Pissios et al., 2003; Pissios et al., 2006).

cell surface expression (Saito et al., 2003); an arginine residue in the 2nd intracellular loop (Arg^{155}) is important for signal transduction initiation (Saito et al., 2005); and the C-terminus tail is important for receptor function (Tetsuka et al., 2004).

MCH Function and Animal Models

The role of MCH in energy regulation emerged when increased *Pmch* mRNA levels were observed in the hypothalami of leptin-deficient *ob*/*ob* mice (Qu et al., 1996). Moreover, fasting increased *Pmch* mRNA levels in both wild type and *ob*/*ob* mice, suggesting an orexigenic function for MCH which was confirmed by the acute increase of feeding resulting from third ventricle MCH injections (Qu et al., 1996; Rossi et al., 1997). Ablation of *Pmch* in mice generated mice with a decreased body weight and hypophagia (Shimada et al., 1998). *Pmch* knockout (KO) mice showed increased energy expenditure (if data were normalized for body weight), decreased adipose tissue, decreased plasma leptin levels, and decreased hypothalamic POMC expression (Shimada et al., 1998). Additionally, *Pmch* KO mice demonstrated normal activity, normal length, normal expression of hypothalamic expression of OX, NPY and AgRP, and normal plasma glucose insulin, thyroxine, and corticosterone levels (Shimada et al., 1998). Lean *Pmch*-deficient mice also showed resistance to age-related increases in body weight and insulin resistance (Jeon et al., 2006).

Overexpression of *Pmch* results in obesity and insulin resistance (Ludwig et al., 2001), whereas injection of MCH for 14 days strongly increased body weight (Della-Zuana et al., 2002; Gomori et al., 2003; Ito et al., 2003).

Another murine model was developed in which MCH neurons were ablated using genetic expression of the toxin ataxin-3 under the MCH promoter (Alon and Friedman, 2006). Mice expressing this transgenic gene have lost about ~65% of the MCH neurons at 15 weeks of age, resulting in leanness, hypophagia, and increased energy expenditure (the latter was observed after correction for body weight) (Alon and Friedman, 2006). Strong similarity between *Pmch*-KO mice and *Pmch*-neuron ablated mice suggests that MCH, but also the two other *Pmch*-derived neuropeptides NEI and NGE, are critical mediators of the energy regulation effects of MCH neurons (Pissios et al., 2006).

Low levels of plasma leptin would normally increase food intake, but in *Pmch* KO mice the leptin-signaling pathway seems dysregulated, suggesting a function of MCH downstream of leptin. This hypothesis was studied in mice carrying both a deletion of *Pmch* and leptin. These double KO mice were still obese, but markedly leaner than *ob*/*ob* mice (Segal-Lieberman et al., 2003). Interestingly, the decreased body weight compared to *ob*/*ob* mice rather resulted from increased energy expenditure than from a decrease in feeding, as double KO mice consumed equal amounts of food compared to *ob*/*ob* mice (Segal-Lieberman et al., 2003). Additional studies in mouse lines (129/SvEV and C57BL6) have also suggested that the leanness of *Pmch*-deficient mice results from an increased energy expenditure rather than a decrease in feeding (Kokkotou et al., 2005).

Mch1r-deficiency in mice results in leanness, characterized by decreased adipose tissue, but, quite surprisingly, also results in hyperphagia and hyperactivity (Chen et al., 2002; Marsh et al., 2002). Additionally, *Mch1r*-KO mice showed osteoporosis, anxiolytic-like behavior, and an aberrant DA system (Bohlooly et al., 2004; Smith et al., 2005; Smith et al., 2006).

Acute blockade of *Mch1r* using *Mch1r*-specific antagonistic peptidic compounds blocks the orexigenic action of MCH (Shearman et al., 2003; Mashiko et al., 2005; Morens et al., 2005). Moreover, long-term (2-4 wk) blockade of *Mch1r* decreased food intake and body weight gain in rats or obese mice (Shearman et al., 2003; Mashiko et al., 2005), whereas *Mch1r*-antagonism was ineffective in *Mch1r* KO mice (Mashiko et al., 2005). Multiple studies have described the anorectic effects of small molecule *Mch1r*-antagonists such as SNAP-7491, GW803430, or T-226296 (Borowsky et al., 2002; Takekawa et al., 2002; Kowalski et al., 2004; Lynch et al., 2006; Tavares et al., 2006; Gehlert et al., 2009). However, is has been noted that most of theses studies have not reported the effects of *Mch1r*-antagonism on energy expenditure (Pissios, 2009). Finally, administration of SNAP-7491 or GW803430 resulted in antidepressant and anxiolytic effects (Borowsky et al., 2002; Gehlert et al., 2009). The latter observations are of particular interest as depression is regularly observed in obese individuals. As functional deletion of *Pmch* or acute *Mch1r* blockade can decrease food intake, it has been interpreted that the hyperactivity and hyperphagia in chronic *Mch1r*-KO mice results from a compensatory mechanism (Pissios, 2009).

Sites of MCH action and additional observations in MCH models

Central MCH injections identified hypothalamic regions involved in the orexigenic effect of MCH, as MCH injections in the PVN, the dorsomedial hypothalamic nucleus (DMH), and ARC resulted in an acute increase of feeding (Abbott et al., 2003). In addition, MCH injection into the AcbSh also increased food intake (Georgescu et al., 2005). Additional research will be needed to investigate if the PVN, DMH, ARC, and AcbSh are the only physiological important brain sites for MCH action.

In addition to the orexigenic affect of MCH, several studies have reported increased water intake independent of food intake, increased alcohol intake, and increased sucrose intake after central MCH administration (Clegg et al., 2003; Duncan et al., 2005; Sakamaki et al., 2005). It is however not known if this is mediated via independent mechanisms or via a common reward-mediated behavioral mechanism.

Recent evidence has emerged that MCH affects limbic dopaminergic function, and that the AcbSh is important for this effect. *Pmch* or *Mch1r* KO mice showed increased limbic dopaminergic sensitivity or a dysregulated mesolimbic dopamine system (Smith et al., 2005; Zhou et al., 2005; Smith et al., 2006; Tyhon et al., 2006; Pissios et al., 2008; Smith et al., 2008). Although many studies have been recently published on this matter, no clear explanations on how MCH increases feeding are available to date.

The hypothalamus is in close proximity to the 3V, whereas *Mch1r* is also expressed in the hindbrain, in close proximity to the fourth ventricle (4V). However, MCH injections in

the 4V had no effect on feeding behavior or locomotor activity, but did decrease body temperature (Zheng et al., 2005). Infusions of MCH into the medial NTS decreased rat blood pressure and heart rate (Brown et al., 2007; Messina and Overton, 2007), whereas *Mch1r* KO mice demonstrated increased sympathetic activity and increased heart rate (Astrand et al., 2004).

Several studies have shown that MCH can affect thermogenesis through effects on *Ucp1* expression. For example, *Pmch-ob/ob* double KO mice showed increased *Ucp1* expression in brown adipose tissue (BAT) and increased cold tolerance (Segal-Lieberman et al., 2003). In addition, central administration in rats of a MCH antisense oligonucleotide increased UCP1 protein levels in BAT compared to rats after saline administration during a cold exposure experiment (Pereira-da-Silva et al., 2005).

Finally, a recent study demonstrated that MCH is capable of stimulating neurite outgrowth (Cotta-Grand et al., 2009). This suggests that loss of chronic loss of *Pmch* might have potential developmental effects in neuron development.

MCH and effects on hormone levels

Initially it was shown that MCH failed to release CRH *in vitro* in hypothalamic explants (Navarra et al., 1990). Paradoxically, a second study showed that central injection of MCH increased plasma corticosterone levels (Jezova et al., 1992). However, *Pmch* KO mice showed normal plasma corticosterone levels compared to wild type mice (Shimada et al., 1998). Subsequently it was shown that MCH or NEI did not affect basal *in vivo* secretion of growth hormone (GH) or prolactin (PRL), whereas MCH did lower adrenocorticotropic hormone (ACTH; a product of POMC) secretion during the end of the light phase (Bluet-Pajot et al., 1995). Interestingly, NEI antagonized the effect of MCH on ACTH release when co-administered (Bluet-Pajot et al., 1995). Finally, MCH suppresses thyroid-stimulating hormone release *in vivo* and *in vitro* (Kennedy et al., 2001). A suppressed hypothalamic-pituitary-thyroid (HPT) axis, translated by TRH and TSH suppression and lower thyroxine levels, could potentially decrease energy consumption. However, *Pmch* KO mice showed normal thyroxine levels compared to wild type mice (Shimada et al., 1998).

Putative Functions for Neuropeptide-GE

Although MCH and NEI (discussed below) seem to have specific biological functions, NGE to date has remained much less studied; thereby fueling the discussion that NGE has no biological function. However, NGE was shown to increase neurofilaments *in vitro*, albeit only at a very high concentration (2500nM vs. no effect with 25-750nM) (Kistler-Heer et al., 1998). This effect was also found for NEI, although NEI shows already an effect at 250nM and a maximal effect at a concentration of 750nM (Kistler-Heer et al., 1998). NGE increased melanin synthesis in murine B16 melanoma cells *in vitro* at 100nM, 1μM, and 10μM concentrations (Hintermann et al., 2001). However, the latter effect was also found for NEI (1μM, and 10μM), MCH (100nM, 1μM, and 10μM), and α-MSH (1pM, 0.1nM, 10nM, and 1μM) (Hintermann et al., 2001).

Cyclic-AMP (cAMP) synthesis increased ~8-fold compared to controls after administration of 1pM α-MSH, while administration of 1μM MCH, NEI, or NGE had hardly any effect (Hintermann et al., 2001). Moreover, only α-MSH and agouti-related protein were able to replace radioactive-labeled α-MSH from MC1R, MC3R, MC4R, or MC5R, expressed in transfected cells while MCH, NEI, nor NGE lacked this ability (Hintermann et al., 2001).

In summary, NGE seems to exert minimal effects, if any, at relatively high concentrations, generating the discussion if these concentrations and thus these effects are physiologically important and relevant. However, NGE might have biological functions that have remained elusive to date.

Putative Functions for Neuropeptide-EI

As co-expression and co-secretion of NEI and MCH was observed in early studies (Parkes and Vale, 1992; Viale et al., 1999b), NEI was hypothesized to have a distinct biological function and was subsequently studied in more detail.

For example, NEI or α-MSH administration to the VTA (1μM) or intraventricular (1μM) increased grooming, rearing and locomotor activity (Sanchez et al., 1997; Sanchez et al., 2001a), while MCH antagonized the induced behavior of either peptide (Sanchez et al., 1997). Interestingly, α-MSH also antagonized rearing and locomotor activity induced by NEI (Sanchez et al., 1997). Moreover, NEI and MCH increased cAMP levels, although only after administration of a high dose (3.6μM vs. no effect with 0.6μM), and interacted, negatively at low dose and positively at a high dose, with α-MSH in *ex vivo* striatal brain slices, (Sanchez et al., 1999). MCH also increased inositol trisphosphate (IP_3) levels at a concentration of 3.6μM, an effect that was blocked by co-administration of NEI or α-MSH (Sanchez et al., 2002).

NEI administration, at 15μM or 45μM but not at 5μM, stimulated binding affinity of a DA receptor 1 (D_1R) agonist to D_1R, suggesting that NEI can affect D_1R-binding potentially by modulating receptors or their environment (Sanchez et al., 2001b). Only α-MSH administration, but not NEI administration, to the VTA affected DA levels in the NAc, whereas both α-MSH or NEI lowered DA levels and increased 3,4-dihydroxyphenylacetic acid (DOPAC; a metabolite of DA) levels in the CPu (Sanchez et al., 2001a). In female rats, NEI injections in VMN stimulated motor activity, increased anxiety, and reduced both DA and DOPAC release in the VMN (Gonzalez et al., 1998). NEI injections in the medial preoptic area (MPOA), where many gonadotropin-releasing hormone (GnRH) neurons are located, had no such effect (Gonzalez et al., 1998). Moreover, NEI in the MPOA, but not in the VMN, stimulated sexual behavior (Gonzalez et al., 1998). The effect of NEI on grooming behavior might be influenced by the cholinergic system, as the ICV-administered muscarinic acetylcholine receptor antagonist atropine suppresses NEI-induced-grooming and activity, while a general nicotinic acetylcholine receptor antagonist does not (Berberian et al., 2002). This suggests that the cholinergic system might be involved, which in turn can project to the DA system (Berberian et al., 2002; Bittencourt and Celis, 2008). Interestingly, manipulation of the cholinergic system can

increase grooming, motor activity, and striatal DA release (Bittencourt and Celis, 2008). An additional study has also demonstrated involvement of the β1-adrenoreceptor, suggesting a neuromodulating effect of NEI on the CNS (Sanchez-Borzone et al., 2007).

Multiple studies have investigated the effect of NEI on the hypothalamo-pituitary-adrenal (HPA) and hypothalamo-pituitary-thyroid (HPT) axes regarding hormone regulation (Bittencourt and Celis, 2008). For example, MCH or NEI did not affect basal *in vivo* secretion of growth hormone (GH) or prolactin (PRL), whereas MCH did lower plasma ACTH (a product of POMC) secretion during the end of the light phase (Bluet-Pajot et al., 1995). Interestingly, when co-administered NEI antagonized the effect of MCH on ACTH release (Bluet-Pajot et al., 1995). A subsequent study however showed increased circulating ACTH and corticosterone after MCH injection in the PVN or ICV injection (Kennedy et al., 2003). Moreover, both NEI and MCH increased corticotropin-releasing hormone (CRH) release in hypothalamic explants (Kennedy et al., 2003).

Additionally, intracerebroventricular (ICV) injection of MCH reduced plasma thyroid-stimulating hormone (TSH; affects thyroid function), whereas both MCH and NEI inhibited thyrotropin-releasing hormone (TRH; stimulates the release of TSH and PRL from pituitary) release from hypothalamic explants (Kennedy et al., 2001). It is interesting that in this study NEI and MCH show a converging function in contrast to the often-observed antagonistic function, whereas the effect of α-MSH is opposite to MCH (Kim et al., 2000). Additional studies showed a possible interaction between NEI and luteinizing hormone (LH) in macaque monkeys (Viale et al., 1999a), whereas NEI released LH in rats *in vivo* and *in vitro* (Attademo et al., 2004; De Paul et al., 2009). NEI treatment in posterior pituitary explants decreased arginine vasopressin (AVP) release whereas it increased OXY release (Parkes and Vale, 1993).

In testis, NEI potentiated human chorionic gonadotrophin (hCG)-stimulated testosterone synthesis, whereas MCH lacked this action (Hervieu et al., 1996).

NEI had no effect on feeding behavior, whereas $PMCH_{131-164}$ (i.e. NEI-MCH) functions as a super-agonist, inducing increased hyperphagia compared to MCH administration alone (Rossi et al., 1997; Maulon-Feraille et al., 2002). The latter effect is likely due to a decreased susceptibility of NEI-MCH to proteases (Maulon-Feraille et al., 2002).

Finally, both NEI and α-MSH have quite similar epitopes recognized by α-MSH antibodies: Pro-Ile-NH_2 for NEI compared to Pro-Val-NH_2 for α-MSH, resulting in regularly observed cross-immunoreactivity of α-MSH and NEI (Bittencourt and Celis, 2008).

In summary, NEI and α-MSH show much similarity in structure as well in biological function. NEI often antagonizes MCH function, like α-MSH, in the HPA axis, HPT axis or in the hypothalamo-pituitary-gonadal (HPG) axis. This is also observed in the behavioral studies regarding motor activity and grooming. Only regarding TRH-release, both MCH and NEI seem to act in the same direction (Kennedy et al., 2001). The similarity between NEI and α-MSH function suggests that NEI mimics α-MSH, either by modulating MCH1R binding or melanocortin receptor binding. MCH1R can synergize with G_s pathways and affect PKA activity via G_i signaling, whereas melanocortin receptors affect PKA activity

via G_s signaling (Gantz et al., 1993b; Gantz et al., 1993a; Hawes et al., 2000; Czyzyk et al., 2008). Therefore, manipulation of either receptor can affect PKA activity. However, due to the inconsistent nature of some results, more data is needed to elute the exact mechanism(s) how NEI, possibly through α-MSH-like action, antagonizes some MCH functions.

Summary

MCH function is involved in many processes, including memory, depression, and anxiety (Monzon et al., 1999; Borowsky et al., 2002). However, most attention has been focused on the effects of MCH on feeding behavior and energy regulation (Shimada et al., 1998; Pissios and Maratos-Flier, 2003; Pissios et al., 2006; Pissios, 2009). Although much insight regarding MCH function has been generated in the last decade, many questions still remain. Two important questions that have remained incompletely answered are what are the functions of NEI and NGE? In addition, despite the increased knowledge to date, no suitable pharmaceutical treatment based on MCH-signaling has been produced. Future research will have reveal new findings to determine if this will ever be feasible.

LIPIN 1

History

In 1988, a natural occurring autosomal recessive mutation in BALB/cByJ mice, called *fatty liver dystrophy* (*fld*), was reported (Sweet et al., 1988). These BALB/cByJ-*fld* mice (hereafter *Lpin1*^{fld}) are characterized by a neonatal fatty liver that resolves at weaning, a progressive demyelinating neuropathy affecting peripheral nerves visible from postnatal day (PND) 10 onwards, a reduced body size, a floppy gait, tremors, hepatic genetic adaptations, and lipodystrophy (Langner et al., 1989; Langner et al., 1991; Rehnmark et al., 1998; Klingenspor et al., 1999; Peterfy et al., 2001). A second murine line, C3H/HeJ-*fld*^{2J} (hereafter *Lpin1*^{fld2J}), demonstrated the same phenotype and carried a mutation allelic to *fld* (Peterfy et al., 2001). In 2001, using a positional cloning approach in *fld* mice, Peterfy and colleagues identified the gene *Lpin1* to be responsible for the phenotype (Peterfy et al., 2001). In *fld* mice, the *Lpin1* gene was rearranged in a complex manner (combination of deletion, inversion, and duplication), whereas *fld*^{2J} mice carried a Gly84Arg substitution in a highly conserved region (Peterfy et al., 2001).

Biochemical characterization of Lipin 1 indicates that it is an Mg^{2+}-dependent phosphatidate phosphatase (PAP1) enzyme catalyzing the dephosporylation of phosphatidic acid (PA), yielding inorganic phosphate and diacylglycerol needed for the synthesis of triacylglycerol, phosphatidylcholine, and phosphatidylethanolamine in mammals (Han et al., 2006; Donkor et al., 2007; Harris et al., 2007; Carman and Han, 2009). The mammalian lipin protein family consists of three members, Lipin 1, Lipin 2, and Lipin 3 (Peterfy et al., 2001), which differ in tissue expression (Donkor et al., 2007). Human *Lpin1* is expressed in multiple tissues with highest levels in adipose

and muscle (Donkor et al., 2007). Alternate splicing of *Lpin1* generates two Lipin 1 isoforms that play distinct, but complementary, roles in adipogenesis: Lipin 1α, which is predominantly nuclear and affects adipocyte differentiation, and Lipin 1β, which is mostly cytoplasmic and induces lipogenic gene expression (Peterfy et al., 2005). The amino-terminal and carboxy-terminal regions of Lipin 1 (NLIP and CLIP, respectively), and a predicted nuclear localization signal (NLS) are highly conserved among the three mammalian lipin family members and among species (Peterfy et al., 2001). The CLIP domain contains multiple key protein functional domains: four haloacid dehalogenase motifs and a transcription factor-binding motif (LXXIL) (Finck et al., 2006; Han et al., 2006; Donkor et al., 2009). Moreover, Lipin 1 and Lipin 2 have been predicted to possess the same structural organization as previously characterized HAD protein family members (Donkor et al., 2009). The transcriptional coactivation role of Lipin 1 has been shown in murine hepatocytes where it regulates expression of genes involved in fatty acid oxidation (Finck et al., 2006).

Models to study Lipin 1 function

Lpin1$^{fld/fld}$ mice carry a spontaneous null mutation for *Lpin1*, whereas *Lpin1*$^{fld2J/fld2J}$ mice carry a Gly84Arg substitution in the highly conserved NLIP domain (Peterfy et al., 2001). Both alleles result in a severe phenotype, including neuropathy and lipodystrophy (Peterfy et al., 2001). *Lpin1* mRNA levels were undetectable in sciatic nerve and adipose tissue of *Lpin1*$^{fld/fld}$ mice. Moreover, *Lpin1* mRNA levels were increased in adipose tissue of *Lpin1*$^{fld2J/fld2J}$ mice, suggesting transcriptional feedback regulation due to impaired lipin 1 function (Peterfy et al., 2001). In addition, the observed neuropathy manifests itself during the second postnatal week, is progressive, and persists through adulthood (Langner et al., 1991). Overexpression of *Lpin1* in either adipose tissue or skeletal muscle promotes obesity (Phan and Reue, 2005).

As *Lpin1*$^{fld/fld}$ mice demonstrated affected WAT, liver, and peripheral nerves, mice with a Schwann cell (SC)-specific deletion of *Lpin1* were created resulting in SC abnormalities and a neuropathy similar to the complete *Lpin1* knockout (*Lpin1*$^{fld/fld}$) mice (Peterfy et al., 2001; Nadra et al., 2008). SC-specific deletion of *Lpin1* also revealed an interaction between PA and the MEK-Erk pathway mediating SC dedifferentiation and proliferation (Nadra et al., 2008). This indicated that the observed neuropathy is a direct consequence of the absence op Lipin-1 – and the subsequent dysregulation of lipid metabolism – within the nerve itself. In addition, the observed neuropathy manifests itself during the second postnatal week, is progressive, and persists through adulthood (Nadra et al., 2008).

The recently characterized mouse line 20884 show adult-onset transitory hindlimb paralysis, characterized by a floppy gait and a tendency to clench the hind limbs in toward the body when suspended by the tail (Douglas et al., 2009). The phenotype is caused by two concurrent mutations, a missense mutation in *Lpin1* (Tyr873Asn) and a nonsense mutation in *Nrcam* (Gln1033X) (Douglas et al., 2009). These 20844 mutant mice develop a hindlimb paralysis between postnatal week 5 and 7, which becomes

less clear after postnatal week 14. Moreover, between 8 months and 1 year of age the 20844 mutant mice regain the ability to both grip structures and walk, although still with a floppy gait (Douglas et al., 2009). To study the mutations in an independent manner, 20884 mutant mice were outcrossed to generate *Lpin1*^{20884} and *Nrcam*^{20884} lines. The *Lpin1*^{20884} phenotype was less severe compared to *Lpin1*$^{fld/fld}$ mice, due to partial loss of PAP activity, and additionally, *Lpin1*^{20884} mice lack the fatty liver, the delayed hair growth, and the small size seen in preweaning *Lpin1*$^{fld/fld}$ mice (Douglas et al., 2009). In addition, *Lpin1*^{20884} mice show no difference in body weight or forelimb grip strength compared to wild type mice (Douglas et al., 2009). *Lpin1*^{20884} mice did show a slight transitory weakness in hindlimb grip strength (Douglas et al., 2009).

In humans, mutations in *Lpin1* resulted in recurrent myoglobinuria (rapid breakdown of muscle tissue) or statin-induced myopathy (muscular weakness) (Zeharia et al., 2008). Unfortunately, these patients were not tested for peripheral neuropathy. In addition, although patients, aged 8-10 years, showed low height and weight, no aberrant fat distribution was observed (Zeharia et al., 2008).

Summary
Lipin 1 function is involved in lipid metabolism. Aberrant Lipin 1 function disrupts lipid metabolism in WAT but also affects nerve function. Future research will have to reveal if Lipin 1 is also involved in additional processes, and additional research will determine if Lipin 1 function might be suitable as a pharmaceutical target to treat disorders associated with altered cholesterol metabolism (such as Tangier disease and Smith-Lemli-Opitz-syndrome) or fatty acid metabolism (such as Refsum's disease and diabetes mellitus).

OUTLINE OF THIS THESIS

Recent decennia have shown the fast rise of a global obesity epidemic, predominantly in first world countries. Accordingly, knowledge regarding the correct regulation of body weight has grown exponentially. Despite this increased understanding, long-term successful and safe pharmacological anti-obesity treatments have not been generated yet. In this thesis we have studied two rat models carrying a genetic mutation in either *Pmch* or *Lpin1*, both showing reduced adipose mass. Although the reduction in adipose mass is generated through different mechanisms, enhanced knowledge on how these genes affect body weight regulation can potentially help the generation of adequate anti-obesity treatments.

Chapter 1 has given a general introduction into the regulation of energy homeostasis. Brain regions and neuropeptides involved in energy homeostasis regulation were explored, as well as a more detailed introduction regarding *Pmch* and *Lpin1* function.

In **Chapter 2** we describe the initial characterization of the *Pmch* knockout rat model. Rats lacking functional *Pmch* are lean and hypophagic. In addition, we describe the observation that, although functional in adult rats during times of starvation, *Pmch* expression appears especially important during early development and puberty.

In **Chapter 3** we study the motivational adaptations of the *Pmch* rat model. Rats lacking functional *Pmch* show decreased willingness to exert work for food rewards, while showing increased willingness to exert work for cocaine rewards. We describe molecular changes that might partially underlie this uncoupling behavior and propose a potential mechanism.

In **Chapter 4** we focus on adipose tissue function in the *Pmch* rat model. Although hypophagia is the predominant cause of the decreased adipose mass in this model, we investigate whether other factors add to the lean phenotype. Catecholaminergic signaling, a mechanism that can increase lipolysis appears affected in rats lacking functional *Pmch*.

In **Chapter 5** we describe the initial characterization of the *Lpin1* mutant rat model. Lipin 1 is a bifunctional protein with PAP1 activity and transcriptional activity. Rats homozygous for a mutated form of *Lpin1* are lean and show severe peripheral neuropathy. However, the neuropathy, caused by malformation of neuronal myelin sheets, regresses during rat maturation. In addition, the severe lipodystrophy improves too. We show that loss of PAP1 activity induces the neuropathy, and propose that correct function of its transcriptional motif positively affects lipid metabolism over time. These changes in lipid metabolism ameliorate myelin sheet morphology and lipodystrophy, resulting in near-complete rescue of the phenotype.

In **Chapter 6** I summarize the results presented, and discuss the current status and potential of anti-obesity treatments using drugs targeting the functional pathways of *Pmch* or *Lpin1*. Furthermore, I speculate on the possibility of using drug-based obesity treatments and other treatments to counter the current worldwide obesity epidemic.

Taken together, we describe two new lean rat models. Our findings provide new knowledge on how these genes regulate energy homeostasis and nerve functionality. With this increased knowledge, the creation of a pharmaceutical anti-obesity treatment or a treatment improving paralysis might be a step closer.

REFERENCES

Abbott CR, Kennedy AR, Wren AM et al. (2003) Identification of hypothalamic nuclei involved in the orexigenic effect of melanin-concentrating hormone. Endocrinology 144:3943-3949.

Abizaid A, Liu ZW, Andrews ZB et al. (2006) Ghrelin modulates the activity and synaptic input organization of midbrain dopamine neurons while promoting appetite. J Clin Invest 116:3229-3239.

Alon T, Friedman JM (2006) Late-onset leanness in mice with targeted ablation of melanin concentrating hormone neurons. J Neurosci 26:389-397.

An S, Cutler G, Zhao JJ et al. (2001) Identification and characterization of a melanin-concentrating hormone receptor. Proc Natl Acad Sci U S A 98:7576-7581.

Antin J, Gibbs J, Holt J et al. (1975) Cholecystokinin elicits the complete behavioral sequence of satiety in rats. Journal of comparative and physiological psychology 89:784-790.

Astrand A, Bohlooly YM, Larsdotter S et al. (2004) Mice lacking melanin-concentrating hormone receptor 1 demonstrate increased heart rate associated with altered autonomic activity. Am J Physiol Regul Integr Comp Physiol 287:R749-758.

Astrup A, Rossner S, Van Gaal L et al. (2009) Effects of liraglutide in the treatment of obesity: a randomised, double-blind, placebo-controlled study. Lancet 374:1606-1616.

Attademo AM, Sanchez-Borzone M, Lasaga M et al. (2004) Intracerebroventricular injection of neuropeptide EI increases serum LH in male and female rats. Peptides 25:1995-1999.

Bachner D, Kreienkamp HJ, Richter D (2002) MIZIP, a highly conserved, vertebrate specific melanin-concentrating hormone receptor 1 interacting zinc-finger protein. FEBS Lett 526:124-128.

Bachner D, Kreienkamp H, Weise C et al. (1999) Identification of melanin concentrating hormone (MCH) as the natural ligand for the orphan somatostatin-like receptor 1 (SLC-1). FEBS Lett 457:522-524.

Bagdade JD, Bierman EL, Porte D, Jr. (1967) The significance of basal insulin levels in the evaluation of the insulin response to glucose in diabetic and nondiabetic subjects. J Clin Invest 46:1549-1557.

Balm PH, Groneveld D (1998) The melanin-concentrating hormone system in fish. Ann N Y Acad Sci 839:205-209.

Barsh GS, Farooqi IS, O'Rahilly S (2000) Genetics of body-weight regulation. Nature 404:644-651.

Baskin DG, Breininger JF, Schwartz MW (1999) Leptin receptor mRNA identifies a subpopulation of neuropeptide Y neurons activated by fasting in rat hypothalamus. Diabetes 48:828-833.

Baskin DG, Wilcox BJ, Figlewicz DP et al. (1988) Insulin and insulin-like growth factors in the CNS. Trends Neurosci 11:107-111.

Baura GD, Foster DM, Porte D, Jr. et al. (1993) Saturable transport of insulin from plasma into the central nervous system of dogs *in vivo*. A mechanism for regulated insulin delivery to the brain. J Clin Invest 92:1824-1830.

Berberian V, Sanchez MS, Celis ME (2002) Participation of the cholinergic system in the excessive grooming behavior induced by neuropeptide (N) glutamic acid (E) isoleucine (I) amide (NEI). Neurochem Res 27:1713-1717.

Bittencourt J, Celis ME (2008) Anatomy, function and regulation of neuropeptide EI (NEI). Peptides 29:1441-1450.

Bittencourt JC, Presse F, Arias C et al. (1992) The melanin-concentrating hormone system of the rat brain: an immuno- and hybridization histochemical characterization. The Journal of comparative neurology 319:218-245.

Bjorbaek C, Elmquist JK, Michl P et al. (1998) Expression of leptin receptor isoforms in rat brain microvessels. Endocrinology 139:3485-3491.

Bluet-Pajot MT, Presse F, Voko Z et al. (1995) Neuropeptide-E-I antagonizes the action of melanin-concentrating hormone on stress-induced release of adrenocorticotropin in the rat. J Neuroendocrinol 7:297-303.

Bohannon NJ, Corp ES, Wilcox BJ et al. (1988a) Localization of binding sites for insulin-like growth factor-I (IGF-I) in the rat brain by quantitative autoradiography. Brain Res 444:205-213.

Bohannon NJ, Corp ES, Wilcox BJ et al. (1988b) Characterization of insulin-like growth factor I receptors in the median eminence of the brain and their modulation by food restriction. Endocrinology 122:1940-1947.

Bohlooly YM, Mahlapuu M, Andersen H et al. (2004) Osteoporosis in MCHR1-deficient mice. Biochem Biophys Res Commun 318:964-969.

Borowsky B, Durkin MM, Ogozalek K et al. (2002) Antidepressant, anxiolytic and anorectic effects of a melanin-concentrating hormone-1 receptor antagonist. Nat Med 8:825-830.

Borsu L, Presse F, Nahon JL (2000) The AROM gene, spliced mRNAs encoding new DNA/RNA-binding proteins are transcribed from the opposite strand of the melanin-concentrating hormone gene in mammals. J Biol Chem 275:40576-40587.

Bradley RL, Mansfield JP, Maratos-Flier E et al. (2002) Melanin-concentrating hormone activates signaling pathways in 3T3-L1 adipocytes. Am J Physiol Endocrinol Metab 283:E584-592.

Breton C, Schorpp M, Nahon JL (1993a) Isolation and characterization of the human melanin-concentrating hormone gene and a variant gene. Brain Res Mol Brain Res 18:297-310.

Breton C, Presse F, Hervieu G et al. (1993b) Structure and regulation of the mouse melanin-concentrating hormone mRNA and gene. Mol Cell Neurosci 4:271-284.

Broberger C, Johansen J, Johansson C et al. (1998) The neuropeptide Y/agouti gene-related protein (AGRP) brain circuitry in normal, anorectic, and monosodium glutamate-treated mice. Proc Natl Acad Sci U S A 95:15043-15048.

Bronstein DM, Schafer MK, Watson SJ et al. (1992) Evidence that beta-endorphin is synthesized in cells in the nucleus tractus solitarius: detection of POMC mRNA. Brain Res 587:269-275.

Brown SN, Chitravanshi VC, Kawabe K et al. (2007) Microinjections of melanin concentrating hormone into the nucleus tractus solitarius of the rat elicit depressor and bradycardic responses. Neuroscience 150:796-806.

Bruning JC, Gautam D, Burks DJ et al. (2000) Role of brain insulin receptor in control of body weight and reproduction. Science (New York, NY 289:2122-2125.

Campfield LA, Smith FJ, Guisez Y et al. (1995) Recombinant mouse OB protein: evidence for a peripheral signal linking adiposity and central neural networks. Science (New York, NY 269:546-549.

Capecchi MR (2005) Gene targeting in mice: functional analysis of the mammalian genome for the twenty-first century. Nat Rev Genet 6:507-512.

Carman GM, Han GS (2009) Phosphatidic acid phosphatase, a key enzyme in the regulation of lipid synthesis. J Biol Chem 284:2593-2597.

Chambers J, Ames RS, Bergsma D et al. (1999) Melanin-concentrating hormone is the cognate ligand for the orphan G-protein-coupled receptor SLC-1. Nature 400:261-265.

Chaudhri OB, Field BC, Bloom SR (2008) Gastrointestinal satiety signals. Int J Obes (Lond) 32 Suppl 7:S28-31.

Chen Y, Hu C, Hsu CK et al. (2002) Targeted disruption of the melanin-concentrating hormone receptor-1 results in hyperphagia and resistance to diet-induced obesity. Endocrinology 143:2469-2477.

Cheung CC, Clifton DK, Steiner RA (1997) Proopiomelanocortin neurons are direct targets for leptin in the hypothalamus. Endocrinology 138:4489-4492.

Chua SC, Jr., Chung WK, Wu-Peng XS et al. (1996) Phenotypes of mouse diabetes and rat fatty due to mutations in the OB (leptin) receptor. Science (New York, NY 271:994-996.

Clegg DJ, Wortman MD, Benoit SC et al. (2002) Comparison of central and peripheral administration of C75 on food intake, body weight, and conditioned taste aversion. Diabetes 51:3196-3201.

Clegg DJ, Air EL, Benoit SC et al. (2003) Intraventricular melanin-concentrating hormone stimulates water intake independent of food intake. Am J Physiol Regul Integr Comp Physiol 284:R494-499.

Coll AP (2007) Effects of pro-opiomelanocortin (POMC) on food intake and body weight: mechanisms and therapeutic potential? Clin Sci (Lond) 113:171-182.

Considine RV, Sinha MK, Heiman ML et al. (1996) Serum immunoreactive-leptin concentrations in normal-weight and obese humans. N Engl J Med 334:292-295.

Cota D, Proulx K, Smith KA et al. (2006) Hypothalamic mTOR signaling regulates food intake. Science (New York, NY 312:927-930.

Cotta-Grand N, Rovere C, Guyon A et al. (2009) Melanin-concentrating hormone induces neurite outgrowth in human neuroblastoma SH-SY5Y cells through p53 and MAPKinase signaling pathways. Peptides 30:2014-2024.

Cummings DE, Overduin J (2007) Gastrointestinal regulation of food intake. J Clin Invest 117:13-23.

Cummings DE, Weigle DS, Frayo RS et al. (2002a) Plasma ghrelin levels after diet-induced weight loss or gastric bypass surgery. N Engl J Med 346:1623-1630.

Cummings DE, Clement K, Purnell JQ et al. (2002b) Elevated plasma ghrelin levels in Prader Willi syndrome. Nat Med 8:643-644.

Czyzyk TA, Sikorski MA, Yang L et al. (2008) Disruption of the RIIbeta subunit of PKA reverses the obesity syndrome of Agouti lethal yellow mice. Proc Natl Acad Sci U S A 105:276-281.

Dallman MF, Strack AM, Akana SF et al. (1993) Feast and famine: critical role of glucocorticoids with insulin in daily energy flow. Front Neuroendocrinol 14:303-347.

Dawson R, Pelleymounter MA, Millard WJ et al. (1997) Attenuation of leptin-mediated effects by monosodium glutamate-induced arcuate nucleus damage. Am J Physiol 273:E202-206.

de Lecea L, Kilduff TS, Peyron C et al. (1998) The hypocretins: hypothalamus-specific peptides with neuroexcitatory activity. Proc Natl Acad Sci U S A 95:322-327.

De Paul AL, Attademo AM, Caron RW et al. (2009) Neuropeptide glutamic-isoleucine (NEI) specifically stimulates the secretory activity of gonadotrophs in primary cultures of female rat pituitary cells. Peptides 30:2081-2087.

De Souza CT, Araujo EP, Bordin S et al. (2005) Consumption of a fat-rich diet activates a proinflammatory response and induces insulin resistance in the hypothalamus. Endocrinology 146:4192-4199.

Della-Zuana O, Presse F, Ortola C et al. (2002) Acute and chronic administration of melanin-concentrating hormone enhances food intake and body weight in Wistar and Sprague-Dawley rats. Int J Obes Relat Metab Disord 26:1289-1295.

Dina C, Meyre D, Gallina S et al. (2007) Variation in FTO contributes to childhood obesity and severe adult obesity. Nat Genet 39:724-726.

Donkor J, Sariahmetoglu M, Dewald J et al. (2007) Three mammalian lipins act as phosphatidate phosphatases with distinct tissue expression patterns. J Biol Chem 282:3450-3457.

Donkor J, Zhang P, Wong S et al. (2009) A conserved serine residue is required for the phosphatidate phosphatase activity but not the transcriptional coactivator functions of lipin-1 and lipin-2. J Biol Chem 284:29968-29978.

Douglas DS, Moran JL, Bermingham JR, Jr. et al. (2009) Concurrent Lpin1 and Nrcam mouse mutations result in severe peripheral neuropathy with transitory hindlimb paralysis. J Neurosci 29:12089-12100.

Douglass J, Daoud S (1996) Characterization of the human cDNA and genomic DNA encoding CART: a cocaine- and amphetamine-regulated transcript. Gene 169:241-245.

Duncan EA, Proulx K, Woods SC (2005) Central administration of melanin-concentrating hormone increases alcohol and sucrose/quinine intake in rats. Alcohol Clin Exp Res 29:958-964.

Edholm OG (1977) Energy balance in man studies carried out by the Division of Human Physiology, National Institute for Medical Research. J Hum Nutr 31:413-431.

Elias CF, Kelly JF, Lee CE et al. (2000) Chemical characterization of leptin-activated neurons in the rat brain. The Journal of comparative neurology 423:261-281.

Elias CF, Lee C, Kelly J et al. (1998) Leptin activates hypothalamic CART neurons projecting to the spinal cord. Neuron 21:1375-1385.

Elmquist JK, Elias CF, Saper CB (1999) From lesions to leptin: hypothalamic control of food intake and body weight. Neuron 22:221-232.

Elmquist JK, Maratos-Flier E, Saper CB et al. (1998a) Unraveling the central nervous system pathways underlying responses to leptin. Nat Neurosci 1:445-450.

Elmquist JK, Bjorbaek C, Ahima RS et al. (1998b) Distributions of leptin receptor mRNA isoforms in the rat brain. The Journal of comparative neurology 395:535-547.

Finck BN, Gropler MC, Chen Z et al. (2006) Lipin 1 is an inducible amplifier of the hepatic PGC-1alpha/PPARalpha regulatory pathway. Cell Metab 4:199-210.

Fischer J, Koch L, Emmerling C et al. (2009) Inactivation of the Fto gene protects from obesity. Nature 458:894-898.

Flegal KM, Carroll MD, Ogden CL et al. (2010) Prevalence and trends in obesity among US adults, 1999-2008. JAMA 303:235-241.

Flier JS, Maratos-Flier E (1998) Obesity and the hypothalamus: novel peptides for new pathways. Cell 92:437-440.

Frayling TM, Timpson NJ, Weedon MN et al. (2007) A common variant in the FTO gene is associated with body mass index and predisposes to childhood and adult obesity. Science (New York, NY 316:889-894.

Friedman MI, Harris RB, Ji H et al. (1999) Fatty acid oxidation affects food intake by altering hepatic energy status. Am J Physiol 276:R1046-1053.

Gantz I, Miwa H, Konda Y et al. (1993a) Molecular cloning, expression, and gene localization of a fourth melanocortin receptor. J Biol Chem 268:15174-15179.

Gantz I, Konda Y, Tashiro T et al. (1993b) Molecular cloning of a novel melanocortin receptor. J Biol Chem 268:8246-8250.

Gee CE, Chen CL, Roberts JL et al. (1983) Identification of proopiomelanocortin neurones in rat hypothalamus by in situ cDNA-mRNA hybridization. Nature 306:374-376.

Gehlert DR, Rasmussen K, Shaw J et al. (2009) Preclinical evaluation of melanin-concentrating hormone receptor 1 antagonism for the treatment of obesity and depression. J Pharmacol Exp Ther 329:429-438.

Georgescu D, Sears RM, Hommel JD et al. (2005) The hypothalamic neuropeptide melanin-concentrating hormone acts in the nucleus accumbens to modulate feeding behavior and forced-swim performance. J Neurosci 25:2933-2940.

Gibbs J, Young RC, Smith GP (1973) Cholecystokinin decreases food intake in rats. Journal of comparative and physiological psychology 84:488-495.

Gomori A, Ishihara A, Ito M et al. (2003) Chronic intracerebroventricular infusion of MCH causes obesity in mice. Melanin-concentrating hormone. Am J Physiol Endocrinol Metab 284:E583-588.

Gonzalez MI, Baker BI, Hole DR et al. (1998) Behavioral effects of neuropeptide E-I (NEI) in the female rat: interactions with alpha-MSH, MCH and dopamine. Peptides 19:1007-1016.

Grill HJ, Ginsberg AB, Seeley RJ et al. (1998) Brainstem application of melanocortin receptor ligands produces long-lasting effects on feeding and body weight. J Neurosci 18:10128-10135.

Grill HJ, Schwartz MW, Kaplan JM et al. (2002) Evidence that the caudal brainstem is a target for the inhibitory effect of leptin on food intake. Endocrinology 143:239-246.

Gropp E, Shanabrough M, Borok E et al. (2005) Agouti-related peptide-expressing neurons are mandatory for feeding. Nat Neurosci 8:1289-1291.

Hagan MM, Rushing PA, Schwartz MW et al. (1999) Role of the CNS melanocortin system in the response to overfeeding. J Neurosci 19:2362-2367.

Hahn TM, Breininger JF, Baskin DG et al. (1998) Coexpression of Agrp and NPY in fasting-activated hypothalamic neurons. Nat Neurosci 1:271-272.

Halaas JL, Gajiwala KS, Maffei M et al. (1995) Weight-reducing effects of the plasma protein encoded by the obese gene. Science (New York, NY 269:543-546.

Han GS, Wu WI, Carman GM (2006) The Saccharomyces cerevisiae Lipin homolog is a Mg2+-dependent phosphatidate phosphatase enzyme. J Biol Chem 281:9210-9218.

Han VK, Hynes MA, Jin C et al. (1986) Cellular localization of proglucagon/glucagon-like peptide I messenger RNAs in rat brain. J Neurosci Res 16:97-107.

Harris GC, Wimmer M, Aston-Jones G (2005) A role for lateral hypothalamic orexin neurons in reward seeking. Nature 437:556-559.

Harris TE, Huffman TA, Chi A et al. (2007) Insulin controls subcellular localization and multisite phosphorylation of the phosphatidic acid phosphatase, lipin 1. J Biol Chem 282:277-286.

Hathout EH, Sharkey J, Racine M et al. (1999) Changes in plasma leptin during the treatment of diabetic ketoacidosis. J Clin Endocrinol Metab 84:4545-4548.

Havel PJ, Uriu-Hare JY, Liu T et al. (1998) Marked and rapid decreases of circulating leptin in streptozotocin diabetic rats: reversal by insulin. Am J Physiol 274:R1482-1491.

Hawes BE, Kil E, Green B et al. (2000) The melanin-concentrating hormone receptor couples to multiple G proteins to activate diverse intracellular signaling pathways. Endocrinology 141:4524-4532.

He W, Lam TK, Obici S et al. (2006) Molecular disruption of hypothalamic nutrient sensing induces obesity. Nat Neurosci 9:227-233.

Hervieu G, Nahon JL (1995) Pro-melanin concentrating hormone messenger ribonucleic acid and peptides expression in peripheral tissues of the rat. Neuroendocrinology 61:348-364.

Hervieu G, Segretain D, Nahon JL (1996) Developmental and stage-dependent expression of melanin-concentrating hormone in mammalian germ cells. Biol Reprod 54:1161-1172.

Hervieu GJ, Cluderay JE, Harrison D et al. (2000) The distribution of the mRNA and protein products of the melanin-concentrating hormone (MCH) receptor gene, slc-1, in the central nervous system of the rat. Eur J Neurosci 12:1194-1216.

Heymsfield SB, Greenberg AS, Fujioka K et al. (1999) Recombinant leptin for weight loss in obese and lean adults: a randomized, controlled, dose-escalation trial. Jama 282:1568-1575.

Hill J, Duckworth M, Murdock P et al. (2001) Molecular cloning and functional characterization of MCH2, a novel human MCH receptor. J Biol Chem 276:20125-20129.

Hintermann E, Drozdz R, Tanner H et al. (1999) Synthesis and characterization of new radioligands for the mammalian melanin-concentrating hormone (MCH) receptor. J Recept Signal Transduct Res 19:411-422.

Hintermann E, Tanner H, Talke-Messerer C et al. (2001) Interaction of melanin-concentrating hormone (MCH), neuropeptide E-I (NEI), neuropeptide G-E (NGE), and alpha-MSH with melanocortin and MCH receptors on mouse B16 melanoma cells. J Recept Signal Transduct Res 21:93-116.

Hnasko TS, Perez FA, Scouras AD et al. (2006) Cre recombinase-mediated restoration of nigrostriatal dopamine in dopamine-deficient mice reverses hypophagia and bradykinesia. Proc Natl Acad Sci U S A 103:8858-8863.

Hommel JD, Trinko R, Sears RM et al. (2006) Leptin receptor signaling in midbrain dopamine neurons regulates feeding. Neuron 51:801-810.

Hoogduijn MJ, Ancans J, Suzuki I et al. (2002) Melanin-concentrating hormone and its receptor are expressed and functional in human skin. Biochem Biophys Res Commun 296:698-701.

Hu Z, Dai Y, Prentki M et al. (2005) A role for hypothalamic malonyl-CoA in the control of food intake. J Biol Chem 280:39681-39683.

Ibrahim N, Bosch MA, Smart JL et al. (2003) Hypothalamic proopiomelanocortin neurons are glucose responsive and express K(ATP) channels. Endocrinology 144:1331-1340.

Ikemoto S, Panksepp J (1996) Dissociations between appetitive and consummatory responses by pharmacological manipulations of reward-relevant brain regions. Behav Neurosci 110:331-345.

Ito M, Gomori A, Ishihara A et al. (2003) Characterization of MCH-mediated obesity in mice. Am J Physiol Endocrinol Metab 284:E940-945.

Jayakumar A, Tai MH, Huang WY et al. (1995) Human fatty acid synthase: properties and molecular cloning. Proc Natl Acad Sci U S A 92:8695-8699.

Jeon JY, Bradley RL, Kokkotou EG et al. (2006) MCH-/- mice are resistant to aging-associated increases in body weight and insulin resistance. Diabetes 55:428-434.

Jezova D, Bartanusz V, Westergren I et al. (1992) Rat melanin-concentrating hormone stimulates adrenocorticotropin secretion: evidence for a site of action in brain regions protected by the blood-brain barrier. Endocrinology 130:1024-1029.

Kahn SE, Prigeon RL, McCulloch DK et al. (1993) Quantification of the relationship between insulin sensitivity and beta-cell function in human subjects. Evidence for a hyperbolic function. Diabetes 42:1663-1672.

Kawauchi H (2006) Functions of melanin-concentrating hormone in fish. J Exp Zool A Comp Exp Biol 305:751-760.

Kawauchi H, Kawazoe I, Tsubokawa M et al. (1983) Characterization of melanin-concentrating hormone in chum salmon pituitaries. Nature 305:321-323.

Kemp EH, Waterman EA, Hawes BE et al. (2002) The melanin-concentrating hormone receptor 1, a novel target of autoantibody responses in vitiligo. J Clin Invest 109:923-930.

Kennedy AR, Todd JF, Stanley SA et al. (2001) Melanin-concentrating hormone (MCH) suppresses thyroid stimulating hormone (TSH) release, *in vivo* and *in vitro*, via the hypothalamus and the pituitary. Endocrinology 142:3265-3268.

Kennedy AR, Todd JF, Dhillo WS et al. (2003) Effect of direct injection of melanin-concentrating hormone into the paraventricular nucleus: further evidence for a stimulatory role in the adrenal axis via SLC-1. J Neuroendocrinol 15:268-272.

Kennedy GC (1953) The role of depot fat in the hypothalamic control of food intake in the rat. Proc R Soc Lond B Biol Sci 140:578-596.

Kim MS, Small CJ, Stanley SA et al. (2000) The central melanocortin system affects the hypothalamo-pituitary thyroid axis and may mediate the effect of leptin. J Clin Invest 105:1005-1011.

Kistler-Heer V, Schlumpf M, Lichtensteiger W (1998) Melanocortin and MCH precursor-derived NEI effects on striatum-midbrain co-cultures. Peptides 19:1317-1327.

Klingenspor M, Xu P, Cohen RD et al. (1999) Altered gene expression pattern in the fatty liver dystrophy mouse reveals impaired insulin-mediated cytoskeleton dynamics. J Biol Chem 274:23078-23084.

Kokkotou E, Jeon JY, Wang X et al. (2005) Mice with MCH ablation resist diet-induced obesity through strain-specific mechanisms. Am J Physiol Regul Integr Comp Physiol 289:R117-124.

Kokkotou E, Mastaitis JW, Qu D et al. (2000) Characterization of [Phe(13), Tyr(19)]-MCH analog binding activity to the MCH receptor. Neuropeptides 34:240-247.

Kokkotou EG, Tritos NA, Mastaitis JW et al. (2001) Melanin-concentrating hormone receptor is a target of leptin action in the mouse brain. Endocrinology 142:680-686.

Kolakowski LF, Jr., Jung BP, Nguyen T et al. (1996) Characterization of a human gene related to genes encoding somatostatin receptors. FEBS Lett 398:253-258.

Koob GF, Riley SJ, Smith SC et al. (1978) Effects of 6-hydroxydopamine lesions of the nucleus accumbens septi and olfactory tubercle on feeding, locomotor activity, and amphetamine anorexia in the rat. Journal of comparative and physiological psychology 92:917-927.

Kow LM, Pfaff DW (1991) The effects of the TRH metabolite cyclo(His-Pro) and its analogs on feeding. Pharmacol Biochem Behav 38:359-364.

Kowalski TJ, Farley C, Cohen-Williams ME et al. (2004) Melanin-concentrating hormone-1 receptor antagonism decreases feeding by reducing meal size. European journal of pharmacology 497:41-47.

Kristensen P, Judge ME, Thim L et al. (1998) Hypothalamic CART is a new anorectic peptide regulated by leptin. Nature 393:72-76.

Lakaye B, Minet A, Zorzi W et al. (1998) Cloning of the rat brain cDNA encoding for the SLC-1 G protein-coupled receptor reveals the presence of an intron in the gene. Biochim Biophys Acta 1401:216-220.

Lam TK, Pocai A, Gutierrez-Juarez R et al. (2005) Hypothalamic sensing of circulating fatty acids is required for glucose homeostasis. Nat Med 11:320-327.

Langner CA, Birkenmeier EH, Roth KA et al. (1991) Characterization of the peripheral neuropathy in neonatal and adult mice that are homozygous for the fatty liver dystrophy (fld) mutation. J Biol Chem 266:11955-11964.

Langner CA, Birkenmeier EH, Ben-Zeev O et al. (1989) The fatty liver dystrophy (fld) mutation. A new mutant mouse with a developmental abnormality in triglyceride metabolism and associated tissue-specific defects in lipoprotein lipase and hepatic lipase activities. J Biol Chem 264:7994-8003.

Leedom LJ, Meehan WP (1989) The psychoneuroendocrinology of diabetes mellitus in rodents. Psychoneuroendocrinology 14:275-294.

Leinninger GM, Jo YH, Leshan RL et al. (2009) Leptin acts via leptin receptor-expressing lateral hypothalamic neurons to modulate the mesolimbic dopamine system and suppress feeding. Cell Metab 10:89-98.

Lembo PM, Grazzini E, Cao J et al. (1999) The receptor for the orexigenic peptide melanin-concentrating hormone is a G-protein-coupled receptor. Nat Cell Biol 1:267-271.

Levin BE, Routh VH, Kang L et al. (2004) Neuronal glucosensing: what do we know after 50 years? Diabetes 53:2521-2528.

Loftus TM, Jaworsky DE, Frehywot GL et al. (2000) Reduced food intake and body weight in mice treated with fatty acid synthase inhibitors. Science (New York, NY 288:2379-2381.

Louveau I, Gondret F (2004) Regulation of development and metabolism of adipose tissue by growth hormone and the insulin-like growth factor system. Domest Anim Endocrinol 27:241-255.

Ludwig DS, Mountjoy KG, Tatro JB et al. (1998) Melanin-concentrating hormone: a functional melanocortin antagonist in the hypothalamus. Am J Physiol 274:E627-633.

Ludwig DS, Tritos NA, Mastaitis JW et al. (2001) Melanin-concentrating hormone overexpression in transgenic mice leads to obesity and insulin resistance. J Clin Invest 107:379-386.

Luquet S, Perez FA, Hnasko TS et al. (2005) NPY/AgRP neurons are essential for feeding in adult mice but can be ablated in neonates. Science (New York, NY 310:683-685.

Lynch JK, Freeman JC, Judd AS et al. (2006) Optimization of chromone-2-carboxamide melanin concentrating hormone receptor 1 antagonists: assessment of potency, efficacy, and cardiovascular safety. J Med Chem 49:6569-6584.

Macdonald D, Murgolo N, Zhang R et al. (2000) Molecular characterization of the melanin-concentrating hormone/receptor complex: identification of critical residues involved in binding and activation. Mol Pharmacol 58:217-225.

Maldonado-Irizarry CS, Swanson CJ, Kelley AE (1995) Glutamate receptors in the nucleus accumbens shell control feeding behavior via the lateral hypothalamus. J Neurosci 15:6779-6788.

Marsh DJ, Weingarth DT, Novi DE et al. (2002) Melanin-concentrating hormone 1 receptor-deficient mice are lean, hyperactive, and hyperphagic and have altered metabolism. Proc Natl Acad Sci U S A 99:3240-3245.

Mashiko S, Ishihara A, Gomori A et al. (2005) Antiobesity effect of a melanin-concentrating hormone 1 receptor antagonist in diet-induced obese mice. Endocrinology 146:3080-3086.

Maulon-Feraille L, Della Zuana O, Suply T et al. (2002) Appetite-boosting property of pro-melanin-concentrating hormone(131-165) (neuropeptide-glutamic acid-isoleucine) is associated with proteolytic resistance. J Pharmacol Exp Ther 302:766-773.

Mercer JG, Moar KM, Hoggard N (1998) Localization of leptin receptor (Ob-R) messenger ribonucleic acid in the rodent hindbrain. Endocrinology 139:29-34.

Merchenthaler I, Lane M, Shughrue P (1999) Distribution of pre-pro-glucagon and glucagon-like peptide-1 receptor messenger RNAs in the rat central nervous system. The Journal of comparative neurology 403:261-280.

Messina MM, Overton JM (2007) Cardiovascular effects of melanin-concentrating hormone. Regul Pept 139:23-30.

Miller CL, Burmeister M, Thompson RC (1998) Antisense expression of the human pro-melanin-concentrating hormone genes. Brain Res 803:86-94.

Minokoshi Y, Alquier T, Furukawa N et al. (2004) AMP-kinase regulates food intake by responding to hormonal and nutrient signals in the hypothalamus. Nature 428:569-574.

Miselis RR, Epstein AN (1975) Feeding induced by intracerebroventricular 2-deoxy-D-glucose in the rat. Am J Physiol 229:1438-1447.

Monzon ME, de Souza MM, Izquierdo LA et al. (1999) Melanin-concentrating hormone (MCH) modifies memory retention in rats. Peptides 20:1517-1519.

Moran TH, Schwartz GJ (1994) Neurobiology of cholecystokinin. Crit Rev Neurobiol 9:1-28.

Morens C, Norregaard P, Receveur JM et al. (2005) Effects of MCH and a MCH1-receptor antagonist on (palatable) food and water intake. Brain Res 1062:32-38.

Mori M, Harada M, Terao Y et al. (2001) Cloning of a novel G protein-coupled receptor, SLT, a subtype of

the melanin-concentrating hormone receptor. Biochem Biophys Res Commun 283:1013-1018.

Morrison CD, Xi X, White CL et al. (2007) Amino acids inhibit Agrp gene expression via an mTOR-dependent mechanism. Am J Physiol Endocrinol Metab 293:E165-171.

Morton GJ, Cummings DE, Baskin DG et al. (2006) Central nervous system control of food intake and body weight. Nature 443:289-295.

Mountjoy KG, Mortrud MT, Low MJ et al. (1994) Localization of the melanocortin-4 receptor (MC4-R) in neuroendocrine and autonomic control circuits in the brain. Mol Endocrinol 8:1298-1308.

Mueller WM, Gregoire FM, Stanhope KL et al. (1998) Evidence that glucose metabolism regulates leptin secretion from cultured rat adipocytes. Endocrinology 139:551-558.

Munzberg H, Flier JS, Bjorbaek C (2004) Region-specific leptin resistance within the hypothalamus of diet-induced obese mice. Endocrinology 145:4880-4889.

Murdoch H, Feng GJ, Bachner D et al. (2005) Periplakin interferes with G protein activation by the melanin-concentrating hormone receptor-1 by binding to the proximal segment of the receptor C-terminal tail. J Biol Chem 280:8208-8220.

Muroya S, Yada T, Shioda S et al. (1999) Glucose-sensitive neurons in the rat arcuate nucleus contain neuropeptide Y. Neuroscience letters 264:113-116.

Myers MG, Jr., Munzberg H, Leinninger GM et al. (2009) The geometry of leptin action in the brain: more complicated than a simple ARC. Cell Metab 9:117-123.

Nadra K, de Preux Charles AS, Medard JJ et al. (2008) Phosphatidic acid mediates demyelination in Lpin1 mutant mice. Genes Dev 22:1647-1661.

Nahon JL (1994) The melanin-concentrating hormone: from the peptide to the gene. Crit Rev Neurobiol 8:221-262.

Nahon JL, Presse F, Bittencourt JC et al. (1989) The rat melanin-concentrating hormone messenger ribonucleic acid encodes multiple putative neuropeptides coexpressed in the dorsolateral hypothalamus. Endocrinology 125:2056-2065.

Naleid AM, Grace MK, Cummings DE et al. (2005) Ghrelin induces feeding in the mesolimbic reward pathway between the ventral tegmental area and the nucleus accumbens. Peptides 26:2274-2279.

Narayanan NS, Guarnieri DJ, Dileone RJ (2009) Metabolic hormones, dopamine circuits, and feeding. Front Neuroendocrinol.

Navarra P, Tsagarakis S, Coy DH et al. (1990) Rat melanin concentrating hormone does not modify the release of CRH-41 from rat hypothalamus or ACTH from the anterior pituitary *in vitro*. J Endocrinol 127:R1-4.

Obici S, Feng Z, Morgan K et al. (2002) Central administration of oleic acid inhibits glucose production and food intake. Diabetes 51:271-275.

Ogden CL, Carroll MD, Curtin LR et al. (2010) Prevalence of high body mass index in US children and adolescents, 2007-2008. JAMA 303:242-249.

Oh IS, Shimizu H, Satoh T et al. (2006) Identification of nesfatin-1 as a satiety molecule in the hypothalamus. Nature 443:709-712.

Ollmann MM, Wilson BD, Yang YK et al. (1997) Antagonism of central melanocortin receptors *in vitro* and *in vivo* by agouti-related protein. Science (New York, NY 278:135-138.

Ono M, Wada C, Oikawa I et al. (1988) Structures of two kinds of mRNA encoding the chum salmon melanin-concentrating hormone. Gene 71:433-438.

Parkes D, Vale W (1992) Secretion of melanin-concentrating hormone and neuropeptide-EI from cultured rat hypothalamic cells. Endocrinology 131:1826-1831.

Parkes DG, Vale WW (1993) Contrasting actions of melanin-concentrating hormone and neuropeptide-E-I on posterior pituitary function. Ann N Y Acad Sci 680:588-590.

Pedeutour F, Szpirer C, Nahon JL (1994) Assignment of the human pro-melanin-concentrating hormone gene (PMCH) to chromosome 12q23-q24 and two variant genes (PMCH1 and PMCHL2) to chromosome 5p14 and 5q12-q13. Genomics 19:31-37.

Pereira-da-Silva M, De Souza CT, Gasparetti AL et al. (2005) Melanin-concentrating hormone induces insulin resistance through a mechanism independent of body weight gain. J Endocrinol 186:193-201.

Peterfy M, Phan J, Reue K (2005) Alternatively spliced lipin isoforms exhibit distinct expression pattern, subcellular localization, and role in adipogenesis. J Biol Chem 280:32883-32889.

Peterfy M, Phan J, Xu P et al. (2001) Lipodystrophy in the fld mouse results from mutation of a new gene encoding a nuclear protein, lipin. Nat Genet 27:121-124.

Phan J, Reue K (2005) Lipin, a lipodystrophy and obesity gene. Cell Metab 1:73-83.

Pissios P (2009) Animals models of MCH function and what they can tell us about its role in energy balance. Peptides 30:2040-2044.

Pissios P, Maratos-Flier E (2003) Melanin-concentrating hormone: from fish skin to skinny mammals. Trends Endocrinol Metab 14:243-248.

Pissios P, Bradley RL, Maratos-Flier E (2006) Expanding the scales: The multiple roles of MCH in regulating energy balance and other biological functions. Endocr Rev 27:606-620.

Pissios P, Trombly DJ, Tzameli I et al. (2003) Melanin-concentrating hormone receptor 1 activates extracellular signal-regulated kinase and synergizes with G(s)-coupled pathways. Endocrinology 144:3514-3523.

Pissios P, Frank L, Kennedy AR et al. (2008) Dysregulation of the mesolimbic dopamine system and reward in MCH-/- mice. Biol Psychiatry 64:184-191.

Pocai A, Lam TK, Obici S et al. (2006) Restoration of hypothalamic lipid sensing normalizes energy and

glucose homeostasis in overfed rats. J Clin Invest 116:1081-1091.

Polonsky KS, Given BD, Van Cauter E (1988) Twenty-four-hour profiles and pulsatile patterns of insulin secretion in normal and obese subjects. J Clin Invest 81:442-448.

Presse F, Nahon JL, Fischer WH et al. (1990) Structure of the human melanin concentrating hormone mRNA. Mol Endocrinol 4:632-637.

Presse F, Hervieu G, Imaki T et al. (1992) Rat melanin-concentrating hormone messenger ribonucleic acid expression: marked changes during development and after stress and glucocorticoid stimuli. Endocrinology 131:1241-1250.

Qian S, Chen H, Weingarth D et al. (2002) Neither agouti-related protein nor neuropeptide Y is critically required for the regulation of energy homeostasis in mice. Mol Cell Biol 22:5027-5035.

Qu D, Ludwig DS, Gammeltoft S et al. (1996) A role for melanin-concentrating hormone in the central regulation of feeding behaviour. Nature 380:243-247.

Rehnmark S, Giometti CS, Slavin BG et al. (1998) The fatty liver dystrophy mutant mouse: microvesicular steatosis associated with altered expression levels of peroxisome proliferator-regulated proteins. J Lipid Res 39:2209-2217.

Ritter S, Dinh TT, Friedman MI (1994) Induction of Fos-like immunoreactivity (Fos-li) and stimulation of feeding by 2,5-anhydro-D-mannitol (2,5-AM) require the vagus nerve. Brain Res 646:53-64.

Rodriguez M, Beauverger P, Naime I et al. (2001) Cloning and molecular characterization of the novel human melanin-concentrating hormone receptor MCH2. Mol Pharmacol 60:632-639.

Rossi M, Choi SJ, O'Shea D et al. (1997) Melanin-concentrating hormone acutely stimulates feeding, but chronic administration has no effect on body weight. Endocrinology 138:351-355.

Rovere C, Viale A, Nahon J et al. (1996) Impaired processing of brain proneurotensin and promelanin-concentrating hormone in obese fat/fat mice. Endocrinology 137:2954-2958.

Sailer AW, Sano H, Zeng Z et al. (2001) Identification and characterization of a second melanin-concentrating hormone receptor, MCH-2R. Proc Natl Acad Sci U S A 98:7564-7569.

Saito Y, Nothacker HP, Civelli O (2000) Melanin-concentrating hormone receptor: an orphan receptor fits the key. Trends Endocrinol Metab 11:299-303.

Saito Y, Tetsuka M, Yue L et al. (2003) Functional role of N-linked glycosylation on the rat melanin-concentrating hormone receptor 1. FEBS Lett 533:29-34.

Saito Y, Nothacker HP, Wang Z et al. (1999) Molecular characterization of the melanin-concentrating-hormone receptor. Nature 400:265-269.

Saito Y, Wang Z, Hagino-Yamagishi K et al. (2001) Endogenous melanin-concentrating hormone receptor SLC-1 in human melanoma SK-MEL-37 cells. Biochem Biophys Res Commun 289:44-50.

Saito Y, Tetsuka M, Saito S et al. (2005) Arginine residue 155 in the second intracellular loop plays a critical role in rat melanin-concentrating hormone receptor 1 activation. Endocrinology 146:3452-3462.

Sakamaki R, Uemoto M, Inui A et al. (2005) Melanin-concentrating hormone enhances sucrose intake. Int J Mol Med 15:1033-1039.

Sakurai T, Amemiya A, Ishii M et al. (1998) Orexins and orexin receptors: a family of hypothalamic neuropeptides and G protein-coupled receptors that regulate feeding behavior. Cell 92:573-585.

Saltiel AR, Kahn CR (2001) Insulin signalling and the regulation of glucose and lipid metabolism. Nature 414:799-806.

Sanchez M, Baker BI, Celis M (1997) Melanin-concentrating hormone (MCH) antagonizes the effects of alpha-MSH and neuropeptide E-I on grooming and locomotor activities in the rat. Peptides 18:393-396.

Sanchez MS, Cremer MC, Celis ME (1999) Effects and interactions between alpha-MSH and MCH/NEI upon striatal cAMP levels. Peptides 20:611-614.

Sanchez MS, Berberian V, Celis ME (2002) Effects of MCH/NEI in the striatum and interactions between them and with alpha-MSH on IP3 levels. Peptides 23:877-880.

Sanchez MS, Barontini M, Armando I et al. (2001a) Correlation of increased grooming behavior and motor activity with alterations in nigrostriatal and mesolimbic catecholamines after alpha-melanotropin and neuropeptide glutamine-isoleucine injection in the rat ventral tegmental area. Cell Mol Neurobiol 21:523-533.

Sanchez MS, Salvatierra NA, Vettori G et al. (2001b) Effect of neuropeptide-EI on the binding of [3H]SCH 23390 to the dopamine D1 receptor in rat striatal membranes. Neurochem Res 26:533-537.

Sanchez-Borzone ME, Attademo A, Baiardi G et al. (2007) Effect of beta-adrenoceptors on the behaviour induced by the neuropeptide glutamic acid isoleucine amide. European journal of pharmacology 568:186-191.

Sandoval D, Cota D, Seeley RJ (2008) The integrative role of CNS fuel-sensing mechanisms in energy balance and glucose regulation. Annu Rev Physiol 70:513-535.

Satoh N, Ogawa Y, Katsuura G et al. (1997) The arcuate nucleus as a primary site of satiety effect of leptin in rats. Neuroscience letters 224:149-152.

Schlumberger SE, Talke-Messerer C, Zumsteg U et al. (2002a) Expression of receptors for melanin-concentrating hormone (MCH) in different tissues and cell lines. J Recept Signal Transduct Res 22:509-531.

Schlumberger SE, Jaggin V, Tanner H et al. (2002b) Endogenous receptor for melanin-concentrating hormone in human neuroblastoma Kelly cells. Biochem Biophys Res Commun 298:54-59.

Schwartz MW, Peskind E, Raskind M et al. (1996a) Cerebrospinal fluid leptin levels: relationship to plasma levels and to adiposity in humans. Nat Med 2:589-593.

Schwartz MW, Woods SC, Porte D, Jr. et al. (2000) Central nervous system control of food intake. Nature 404:661-671.

Schwartz MW, Seeley RJ, Woods SC et al. (1997) Leptin increases hypothalamic pro-opiomelanocortin mRNA expression in the rostral arcuate nucleus. Diabetes 46:2119-2123.

Schwartz MW, Baskin DG, Bukowski TR et al. (1996b) Specificity of leptin action on elevated blood glucose levels and hypothalamic neuropeptide Y gene expression in ob/ob mice. Diabetes 45:531-535.

Schwartz TL, Nihalani N, Jindal S et al. (2004) Psychiatric medication-induced obesity: a review. Obes Rev 5:115-121.

Scott LJ, Mohlke KL, Bonnycastle LL et al. (2007) A genome-wide association study of type 2 diabetes in Finns detects multiple susceptibility variants. Science (New York, NY 316:1341-1345.

Scuteri A, Sanna S, Chen WM et al. (2007) Genome-wide association scan shows genetic variants in the FTO gene are associated with obesity-related traits. PLoS Genet 3:e115.

Seeley RJ, Yagaloff KA, Fisher SL et al. (1997) Melanocortin receptors in leptin effects. Nature 390:349.

Segal-Lieberman G, Bradley RL, Kokkotou E et al. (2003) Melanin-concentrating hormone is a critical mediator of the leptin-deficient phenotype. Proc Natl Acad Sci U S A 100:10085-10090.

Shearman LP, Camacho RE, Sloan Stribling D et al. (2003) Chronic MCH-1 receptor modulation alters appetite, body weight and adiposity in rats. European journal of pharmacology 475:37-47.

Sherwood NM, Timiras PS (1970) A stereotaxic atlas of the developing rat brain. Berkeley, Los Angeles, London: University of California Press.

Shimada M, Tritos NA, Lowell BB et al. (1998) Mice lacking melanin-concentrating hormone are hypophagic and lean. Nature 396:670-674.

Shimomura Y, Mori M, Sugo T et al. (1999) Isolation and identification of melanin-concentrating hormone as the endogenous ligand of the SLC-1 receptor. Biochem Biophys Res Commun 261:622-626.

Sindelar DK, Havel PJ, Seeley RJ et al. (1999) Low plasma leptin levels contribute to diabetic hyperphagia in rats. Diabetes 48:1275-1280.

Sipols AJ, Baskin DG, Schwartz MW (1995) Effect of intracerebroventricular insulin infusion on diabetic hyperphagia and hypothalamic neuropeptide gene expression. Diabetes 44:147-151.

Sita LV, Elias CF, Bittencourt JC (2007) Connectivity pattern suggests that incerto-hypothalamic area belongs to the medial hypothalamic system. Neuroscience 148:949-969.

Smith DG, Qi H, Svenningsson P et al. (2008) Behavioral and biochemical responses to d-amphetamine in MCH1 receptor knockout mice. Synapse 62:128-136.

Smith DG, Davis RJ, Rorick-Kehn L et al. (2006) Melanin-concentrating hormone-1 receptor modulates neuroendocrine, behavioral, and corticolimbic neurochemical stress responses in mice. Neuropsychopharmacology 31:1135-1145.

Smith DG, Tzavara ET, Shaw J et al. (2005) Mesolimbic dopamine super-sensitivity in melanin-concentrating hormone-1 receptor-deficient mice. J Neurosci 25:914-922.

Smith GP (1996) The direct and indirect controls of meal size. Neurosci Biobehav Rev 20:41-46.

Smits BM, Mudde J, Plasterk RH et al. (2004) Target-selected mutagenesis of the rat. Genomics 83:332-334.

Smits BM, Mudde JB, van de Belt J et al. (2006) Generation of gene knockouts and mutant models in the laboratory rat by ENU-driven target-selected mutagenesis. Pharmacogenet Genomics 16:159-169.

Sokoloff L, Reivich M, Kennedy C et al. (1977) The [14C]deoxyglucose method for the measurement of local cerebral glucose utilization: theory, procedure, and normal values in the conscious and anesthetized albino rat. J Neurochem 28:897-916.

Stanley BG, Willett VL, 3rd, Donias HW et al. (1993) The lateral hypothalamus: a primary site mediating excitatory amino acid-elicited eating. Brain Res 630:41-49.

Ste Marie L, Luquet S, Cole TB et al. (2005) Modulation of neuropeptide Y expression in adult mice does not affect feeding. Proc Natl Acad Sci U S A 102:18632-18637.

Stellar E (1954) The physiology of motivation. Psychol Rev 61:5-22.

Stephens TW, Basinski M, Bristow PK et al. (1995) The role of neuropeptide Y in the antiobesity action of the obese gene product. Nature 377:530-532.

Stratford TR, Kelley AE (1997) GABA in the nucleus accumbens shell participates in the central regulation of feeding behavior. J Neurosci 17:4434-4440.

Stratford TR, Swanson CJ, Kelley A (1998) Specific changes in food intake elicited by blockade or activation of glutamate receptors in the nucleus accumbens shell. Behav Brain Res 93:43-50.

Stricker EM, Zigmond MJ (1984) Brain catecholamines and the central control of food intake. Int J Obes 8 Suppl 1:39-50.

Sutherland S (2004) Embracing the rat. Drug Discov Today 9:468.

Sweet HO, Birkenmeier EH, Davisson MT (1988) Mouse News Letter 81.

Szczypka MS, Kwok K, Brot MD et al. (2001) Dopamine production in the caudate putamen restores feeding in dopamine-deficient mice. Neuron 30:819-828.

Takayama Y, Wada C, Kawauchi H et al. (1989) Structures of two genes coding for melanin-concentrating hormone of chum salmon. Gene 80:65-73.

Takekawa S, Asami A, Ishihara Y et al. (2002) T-226296: a novel, orally active and selective melanin-concentrating hormone receptor antagonist. European journal of pharmacology 438:129-135.

Tan CP, Sano H, Iwaasa H et al. (2002) Melanin-concentrating hormone receptor subtypes 1 and 2: species-specific gene expression. Genomics 79:785-792.

Tang-Christensen M, Holst JJ, Hartmann B et al. (1999) The arcuate nucleus is pivotal in mediating the anorectic effects of centrally administered leptin. Neuroreport 10:1183-1187.

Tavares FX, Al-Barazanji KA, Bigham EC et al. (2006) Potent, selective, and orally efficacious antagonists of melanin-concentrating hormone receptor 1. J Med Chem 49:7095-7107.

Ter Horst GJ, de Boer P, Luiten PG et al. (1989) Ascending projections from the solitary tract nucleus to the hypothalamus. A Phaseolus vulgaris lectin tracing study in the rat. Neuroscience 31:785-797.

Tetsuka M, Saito Y, Imai K et al. (2004) The basic residues in the membrane-proximal C-terminal tail of the rat melanin-concentrating hormone receptor 1 are required for receptor function. Endocrinology 145:3712-3723.

Thompson RC, Watson SJ (1990) Nucleotide sequence and tissue-specific expression of the rat melanin concentrating hormone gene. DNA Cell Biol 9:637-645.

Thornton JE, Cheung CC, Clifton DK et al. (1997) Regulation of hypothalamic proopiomelanocortin mRNA by leptin in ob/ob mice. Endocrinology 138:5063-5066.

Toumaniantz G, Bittencourt JC, Nahon JL (1996) The rat melanin-concentrating hormone gene encodes an additional putative protein in a different reading frame. Endocrinology 137:4518-4521.

Travers JB, Travers SP, Norgren R (1987) Gustatory neural processing in the hindbrain. Annu Rev Neurosci 10:595-632.

Trayhurn P (1984) The development of obesity in animals: the role of genetic susceptibility. Clin Endocrinol Metab 13:451-474.

Tschop M, Smiley DL, Heiman ML (2000) Ghrelin induces adiposity in rodents. Nature 407:908-913.

Tyhon A, Adamantidis A, Foidart A et al. (2006) Mice lacking the melanin-concentrating hormone receptor-1 exhibit an atypical psychomotor susceptibility to cocaine and no conditioned cocaine response. Behav Brain Res 173:94-103.

Vaughan JM, Fischer WH, Hoeger C et al. (1989) Characterization of melanin-concentrating hormone from rat hypothalamus. Endocrinology 125:1660-1665.

Verbalis JG, Blackburn RE, Hoffman GE et al. (1995) Establishing behavioral and physiological functions of central oxytocin: insights from studies of oxytocin and ingestive behaviors. Adv Exp Med Biol 395:209-225.

Verlaet M, Adamantidis A, Coumans B et al. (2002) Human immune cells express ppMCH mRNA and functional MCHR1 receptor. FEBS Lett 527:205-210.

Viale A, Kerdelhue B, Nahon JL (1999a) 17beta-estradiol regulation of melanin-concentrating hormone and neuropeptide-E-I contents in cynomolgus monkeys: a preliminary study. Peptides 20:553-559.

Viale A, Ortola C, Vernier P et al. (1998a) Structure, expression, and evolution of the variant MCH gene in primates. Ann N Y Acad Sci 839:214-218.

Viale A, Courseaux A, Presse F et al. (2000) Structure and expression of the variant melanin-concentrating hormone genes: only PMCHL1 is transcribed in the developing human brain and encodes a putative protein. Mol Biol Evol 17:1626-1640.

Viale A, Ortola C, Richard F et al. (1998b) Emergence of a brain-expressed variant melanin-concentrating hormone gene during higher primate evolution: a gene "in search of a function". Mol Biol Evol 15:196-214.

Viale A, Ortola C, Hervieu G et al. (1999b) Cellular localization and role of prohormone convertases in the processing of pro-melanin concentrating hormone in mammals. J Biol Chem 274:6536-6545.

Volkow ND, Wise RA (2005) How can drug addiction help us understand obesity? Nat Neurosci 8:555-560.

Wang GJ, Volkow ND, Logan J et al. (2001a) Brain dopamine and obesity. Lancet 357:354-357.

Wang J, Liu R, Hawkins M et al. (1998) A nutrient-sensing pathway regulates leptin gene expression in muscle and fat. Nature 393:684-688.

Wang S, Behan J, O'Neill K et al. (2001b) Identification and pharmacological characterization of a novel human melanin-concentrating hormone receptor, mchr2. J Biol Chem 276:34664-34670.

Weigle DS, Bukowski TR, Foster DC et al. (1995) Recombinant ob protein reduces feeding and body weight in the ob/ob mouse. J Clin Invest 96:2065-2070.

Williams G, Gill JS, Lee YC et al. (1989a) Increased neuropeptide Y concentrations in specific hypothalamic regions of streptozocin-induced diabetic rats. Diabetes 38:321-327.

Williams G, Lee YC, Ghatei MA et al. (1989b) Elevated neuropeptide Y concentrations in the central hypothalamus of the spontaneously diabetic BB/E Wistar rat. Diabet Med 6:601-607.

Wise RA (1996) Neurobiology of addiction. Curr Opin Neurobiol 6:243-251.

Wise RA (2004) Dopamine, learning and motivation. Nat Rev Neurosci 5:483-494.

Wise RA (2006) Role of brain dopamine in food reward and reinforcement. Philos Trans R Soc Lond B Biol Sci 361:1149-1158.

Woods SC, Lotter EC, McKay LD et al. (1979) Chronic intracerebroventricular infusion of insulin reduces food intake and body weight of baboons. Nature 282:503-505.

Wortman MD, Clegg DJ, D'Alessio D et al. (2003) C75 inhibits food intake by increasing CNS glucose metabolism. Nat Med 9:483-485.

Wren AM, Seal LJ, Cohen MA et al. (2001a) Ghrelin enhances appetite and increases food intake in humans. J Clin Endocrinol Metab 86:5992.

Wren AM, Small CJ, Abbott CR et al. (2001b) Ghrelin causes hyperphagia and obesity in rats. Diabetes 50:2540-2547.

Yamamoto T (2006) Neural substrates for the processing of cognitive and affective aspects of taste in the brain. Arch Histol Cytol 69:243-255.

Zakarian S, Smyth DG (1982) beta-Endorphin is processed differently in specific regions of rat pituitary and brain. Nature 296:250-252.

Zan Y, Haag JD, Chen KS et al. (2003) Production of knockout rats using ENU mutagenesis and a yeast-based screening assay. Nat Biotechnol 21:645-651.

Zeharia A, Shaag A, Houtkooper RH et al. (2008) Mutations in LPIN1 cause recurrent acute myoglobinuria in childhood. Am J Hum Genet 83:489-494.

Zhang Y, Proenca R, Maffei M et al. (1994) Positional cloning of the mouse obese gene and its human homologue. Nature 372:425-432.

Zhang Y, Guo K, LeBlanc RE et al. (2007) Increasing dietary leucine intake reduces diet-induced obesity and improves glucose and cholesterol metabolism in mice via multimechanisms. Diabetes 56:1647-1654.

Zheng H, Patterson LM, Morrison C et al. (2005) Melanin concentrating hormone innervation of caudal brainstem areas involved in gastrointestinal functions and energy balance. Neuroscience 135:611-625.

Zhou D, Shen Z, Strack AM et al. (2005) Enhanced running wheel activity of both Mch1r- and Pmch-deficient mice. Regul Pept 124:53-63.

Zigmond MJ, Stricker EM (1972) Deficits in feeding behavior after intraventricular injection of 6-hydroxydopamine in rats. Science (New York, NY 177:1211-1214.

2

PMCH EXPRESSION DURING EARLY DEVELOPMENT IS CRITICAL FOR NORMAL ENERGY HOMEOSTASIS

Joram D. Mul, Chun-Xia Yi, Sjoerd A.A. van den Berg, Marieke Ruiter,
Pim W. Toonen, Martine C.J. van der Elst, Peter J. Voshol,
Bart A. Ellenbroek, Andries Kalsbeek, Susanne E. la Fleur and Edwin Cuppen

Adapted from American Journal of Physiology –
Endocrinology and Metabolism. 2010 Mar; 298(3): E477-88

ABSTRACT

Postnatal development and puberty are times of strong physical maturation and require large quantities of energy. The hypothalamic neuropeptide Melanin-Concentrating Hormone (MCH) regulates nutrient intake and energy homeostasis, but the underlying mechanisms are not completely understood. Here we use a novel rat knockout model in which the MCH-precursor *Pmch* has been inactivated to study the effects of loss of MCH on energy regulation in more detail. *Pmch*$^{-/-}$ rats are lean, hypophagic, osteoporotic, and although endocrine parameters were changed in *pmch*$^{-/-}$ rats, endocrine dynamics were normal, indicating an adaptation to new homeostatic levels rather than disturbed metabolic mechanisms. Detailed body weight growth and feeding behavior analysis revealed that *Pmch* expression is particularly important during early rat development and puberty, i.e. the first 8 postnatal weeks. Loss of *Pmch* resulted in a 20% lower set point for body weight that was determined solely during this period and remained unchanged during adulthood. Although the final body weight is diet-dependent, the *Pmch*-deficiency effect was similar for all diets tested in this study. Loss of *Pmch* affected energy expenditure in both young and adult rats, although these effects seem secondary to the observed hypophagia. Our findings show an important role for *Pmch* in energy homeostasis determination during early development, and indicate that the MCH-Melanin-Concentrating Hormone Receptor 1-system is a plausible target for childhood obesity treatment, currently a major health issue in first world countries.

INTRODUCTION

Childhood obesity is now widely recognized as a severe public health issue (Ogden et al., 2006). Treatment with drugs aimed at neural systems involved in the determination of the energy balance could potentially result in a lower energy balance during puberty as well as later in adulthood. Therefore, neuropeptides involved in body weight regulation during early development and puberty are attractive targets for anti-childhood obesity drugs.

The neuronal metabolic systems in humans and primates develop prenatally while in rodents these systems develop during the first three postnatal weeks (Grove et al., 2005; Bouret and Simerly, 2006). This results in the activation and optimization of neuronal systems during early rodent development. A second important metabolic period is puberty, a period of major growth, hormonal changes, and sexual maturation. In the rat, puberty is characterized by different responses of young-adolescent (postnatal day [PND] 40) and young-adult (PND 60) male rats to environmental cues like stress and cold (Gomez and Dallman, 2001; Gomez et al., 2002). In addition to these age-dependent behavioral differences, the amount of food consumed during early rodent life plays an important role in determining subsequent food intake in later life (Oscai and McGarr, 1978). Following this initial observation, many studies have shown that postnatal nutrition is important for the regulation of appetite in adult rodents, suggesting that the energy balance is predominantly determined during early development (McMillen et al., 2005).

MCH has been shown to be a critical mammalian hypothalamic effecter of energy homeostasis by various genetic and pharmacological studies (Pissios et al., 2006). The MCH-precursor gene (*Pmch*) is expressed predominantly in neurons of the lateral hypothalamic area (LHA) and the incerto hypothalamic area (IHy), which project throughout the brain (Bittencourt et al., 1992; Sita et al., 2007). *Pmch* is also expressed in some peripheral tissues, such as the testes, although at lower levels than in brain (Hervieu and Nahon, 1995). Processing of *Pmch* results in the production of three neuropeptides: neuropeptide glycine-glutamic acid (N-GE), neuropeptide glutamic acid-isoleucine (N-EI) and MCH (Nahon et al., 1989). *Pmch* mRNA is up regulated after fasting or leptin deficiency (Qu et al., 1996; Kokkotou et al., 2001), 3rd ventricle ICV injections of MCH increase food intake and body weight (Rossi et al., 1997; Della-Zuana et al., 2002; Gomori et al., 2003; Ito et al., 2003; Guesdon et al., 2009), *Pmch* knockout mice are lean due to a decreased food intake and an increased metabolic rate (Shimada et al., 1998; Kokkotou et al., 2005), and overexpression of MCH causes obesity (Ludwig et al., 2001). In rodents MCH binds to Melanin-Concentrating Hormone Receptor 1 (MCH1R), a G-protein coupled receptor expressed throughout the brain (Chambers et al., 1999; Lembo et al., 1999; Saito et al., 1999; Saito et al., 2001). MCH1R is particularly enriched in the nucleus accumbens shell (AcbSh) (Lembo et al., 1999; Saito et al., 1999; Pissios et al., 2008), thus forming a potential hypothalamic-limbic circuit modulating the hedonic, or rewarding, aspects of feeding (Georgescu et al., 2005; Pissios et al., 2008). Recently it was indeed shown that the MCH system affects motivation for feeding or

drugs of abuse (Chung et al., 2009; Nair et al., 2009). Rodents only express MCH1R, whereas humans also express a second MCH receptor, MCH2R (Sailer et al., 2001). Recent studies have focused on MCH1R, demonstrating that MCH1R-antagonism decreases food intake and weight gain in adult rodents (Shearman et al., 2003; Mashiko et al., 2005; Palani et al., 2005; Handlon and Zhou, 2006; Luthin, 2007).

Most MCH-related studies using genetic models or MCH antagonists have primarily focused on the function of MCH during adulthood. Therefore the effect of loss of *Pmch* expression on energy regulation during early development is largely unexplored. To study nutrient intake during this period, we utilized a novel rat knockout model that was generated recently using an ENU-driven target-selected mutagenesis approach (Smits et al., 2006). Preliminary studies in young-adult animals showed that the caloric intake of *pmch*$^{-/-}$ rats was unchanged compared to control littermates when nutrient intake data were normalized for body weight. Following this initial observation we have analyzed the metabolic characteristics of the *Pmch* knockout rat model on three different diets (maintenance [M], semi-high-protein [SHP], and high-fat [HF]) by following body weight and food intake during development and adulthood, and by measuring endocrine values. Furthermore, the metabolic profile of *pmch*$^{-/-}$ rats was analyzed using indirect calorimetry. Our results show that *Pmch* plays an important role in the energy balance determination during the first 8 postnatal weeks, and that loss of *Pmch* results in a 20% decreased body weight during adulthood regardless of diet.

MATERIAL AND METHODS

Animals. The Animal Care Committee of the Royal Dutch Academy of Science and the Leiden University Medical Center approved all experiments according to the Dutch legal ethical guidelines. The *Pmch* knockout rat (*Pmch*^{1Hubr}) was generated by target-selected ENU-driven mutagenesis (see Smits et al., 2006). Briefly, high-throughput resequencing of genomic target sequences in progeny from mutagenized rats revealed an ENU-induced premature stopcodon in exon 1 (K50X) of *Pmch* in a rat (Wistar/Crl background). The heterozygous mutant animal was backcrossed to wild type Wistar background for six generations to eliminate confounding effects from background mutations induced by ENU. Assuming that the total amount of coding DNA in a male rat is approximately 28.6 x10^6 bp (Cuppen et al., 2007) and the used ENU treatment resulted in a mutation frequency of 1 per 1.5x10^6 bp (Smits et al., 2006), approximately 19 mutations can be expected in protein-coding sequences of the founder animal. Backcrossing six times would therefore decrease the total number of random background mutations to 1. Furthermore, the maximal number of nonsense inducing mutations (NIMs) is much lower than 19, i.e. 3 (Cuppen et al., 2007). However, as part of the donor chromosome harboring the *Pmch* mutation is still present after six backcrosses (Keays et al., 2006), we cannot fully exclude the presence of tightly linked confounding mutations in our rat model. To further control for possible contributions of confounding mutations, we repeated several measurements in different outcross generations and could replicate previous findings in each generation. Additionally, we always generated experimental *pmch*$^{+/+}$ and *pmch*$^{-/-}$ rats by crossing *pmch*$^{+/-}$ rats. Experimental rats were obtained at the expected Mendelian frequency. Furthermore, littermates (with similar genetic backgrounds) were used as much as possible for experiments. *Pmch*$^{-/-}$ rats were viable into adulthood and fertile, and appeared phenotypically normal despite their lower body weight. Two rats were housed together, unless noted otherwise, under controlled experimental conditions (12 h light/dark cycle,

light period 0600-1800, 21±1°C, ~60% relative humidity). The standard fed diet in our animal facility (semi high-protein chow: RM3, 26.9% crude protein, 11.5% fat, and 61.6% carbohydrates; 3.33 kcal/g AFE; SDS, Witham, United Kingdom) was provided *ad libitum* together with water, unless noted otherwise (maintenance chow: RM1, 17.5% crude protein, 7.4% fat, and 75.1% carbohydrates; 3.29 kcal/g AFE, SDS, Witham, United Kingdom; high-fat chow: 45%-AFE, 20% crude protein, 45% fat, and 35% carbohydrates; 4.54 kcal/g AFE SDS, Witham, United Kingdom). Only male rats were used in the present study.

Genotyping. Genotyping was done using the KASPar SNP Genotyping System (KBiosciences, Hoddesdon, United Kingdom; as described in van Boxtel et al., 2008) using gene-specific primers (forward common, TTAAT ACATT CAGGA TGGGG AAAGC CTTT; reverse wild type, GAAGG TGACC AAGTT CATGCT CGATC TTTCT GCGGT ATCTT CCTT; reverse homozygous, GAAGG TCGGA GTCAA CGGAT TCGAT CTTTC TGCGG TATCT TCCTA). All pups were genotyped at 3 weeks of age. Genotypes were reconfirmed when experimental procedures were completed.

Northern Blot analysis. Northern Blot analysis (as described in Homberg et al., 2007) was done using a *Pmch* specific radiolabeled PCR-derived probe covering the first exon of the gene. The following primers were used for probe generation: forward primer: ATTCT CCTTC GGCTT TACG; reverse primer: TCCAG AGAAG GAGCA ACAAC.

Body weight and nutrient intake. Animals were housed individually at PND 21. Until weaning, animals had access to SHP diet in their maternal home cage. Body weight, water intake, and food intake was monitored biweekly for 18 weeks. Food (M, SHP, or HF diet) and water were provided *ad libitum*. At 8 and 17 weeks of age, nutrient intake was measured for 6 consecutive days at 06:00 (dark phase intake) and at 18:00 (light phase intake).

WAT and organ weight. A WAT fat pad sample (containing the right side of the subcutaneous WAT pad, the whole epididymal WAT pad, the right side of the perirenal WAT pad, the whole mesenteric WAT pad), liver, adrenals, and the thymus were isolated from 26-week-old rats.

Jugular vein catheter. 22-week-old rats were anaesthetized with isoflurane and equipped with a jugular vein catheter (headpiece: Connector Pedestal 20GA, Plastics One, Roanoke, VA, USA). Before surgery, rats received one dose of Temgesic® (0.05 mg/kg, subcutaneous; Schering-Plough, Utrecht, the Netherlands). Rats were allowed to recover for 7 days during which they were handled to minimize stress.

Indirect calorimetry. Indirect calorimetry was measured in an 8-cage combined, open circuit indirect calorimetry system (LabMaster system, TSE systems, Bad Homburg, Germany). After a 20hr acclimatization period, parameters of indirect calorimetry (O_2 uptake [VO_2] and CO_2 [VCO_2] production) and caloric intake (SHP diet) were measured for 3 consecutive days. Respiratory exchange rate (RER) as a measure for metabolic substrate choice was calculated using the following formula, with VO_2 and VCO_2 given in ml/h: $RER=VCO_2/VO_2$. Carbohydrate and fat oxidation rates were calculated from VO_2 and VCO_2 using the following formulas: carbohydrate oxidation (cal/h) = $(4.585*VCO_2 - 3.226*VO_2)*4$ and fat oxidation (cal/h) = $(1.695*VO_2 - 1.701*VCO_2)*9$. Total energy expenditure (EE) was calculated from the sum of carbohydrate and fat oxidation. Physical activity was measured using infrared sensor frames. Interruptions of infrared sensor pairs were detected by a control unit and registered by a computer with the relevant software (ActiMot2, TSE systems). Body composition and bone mass density were measured by dual-energy X-ray absorptiometry (DEXA) using a Norland pDEXA Sabre scanner (Norland Stratec, Fort Atkinson, WI, USA). Fecal samples were collected, freeze-dried, and analyzed for gross energy content using adiabatic bomb calorimetry (Ika-calorimeter system C4000 Heitersheim, Germany). The energetic ratio was calculated as the EE (kcal/day) divided by the metabolisable energy (kcal/day; kcal ingested minus kcal lost in feces). All measurements were done at PND 40 and 120. At PND 130, an indirect

calorimetric analysis was performed during 48hr caloric starvation (no SHP diet; water freely available), followed by 72hr of refeeding.

Statistical analysis. Data are expressed as mean ± S.E.M. Longitudinal body weight, longitudinal endocrine (leptin, insulin, glucose), IVITT, IVGTT, and longitudinal body core temperature data were analyzed using a repeated-measures ANOVA followed by a Tukey-HSD *post hoc* analysis. The statistical analysis included the within-subjects factors of *time* (days or hours) and *genotype* (*pmch*$^{+/+}$, *pmch*$^{-/-}$). All other data were analyzed using a Students' *t*-test. All data were analyzed using a commercially available statistical program (SPSS for Macintosh, version 16.0). The null hypothesis was rejected at the 0.05 level.

RESULTS

Generation of the Pmch knockout rat. In a large ENU-driven target-selected mutagenesis screen we identified a rat carrying a heterozygous mutation in *Pmch* (Smits et al., 2006). The mutation (K50X) resulted in a premature stop codon in exon 1 (Fig. 1*A*). Northern blot analysis showed that *Pmch* mRNA is almost completely absent in *pmch*$^{-/-}$ animals, most likely as a result of nonsense-mediated decay (Fig. 1*B*). Furthermore, *Pmch* expression is gene dose-dependent reduced in *pmch*$^{+/-}$ rats. The knockout phenotype was confirmed by immunohistochemistry, which showed that all three neuropeptides derived from *Pmch*, N-GE, N-EI, and MCH, are absent in sections of the lateral hypothalamus of *pmch*$^{-/-}$ animals (Fig. 1*C*).

Pmch knockout rats are lean and hypophagic. The body weight of *pmch*$^{+/+}$ and *pmch*$^{-/-}$ rats was monitored on three different diets (M, SHP, and HF) for 18 weeks starting at PND 21. At the end of the study, *pmch*$^{-/-}$ animals showed a lower body weight compared to *pmch*$^{+/+}$ rats on all three diets (Fig. 2, *A-C*). Body weight did not differ between genotypes at birth, or between birth and the 3rd postnatal week (data not shown), but started to diverge approximately 3 weeks after birth. Furthermore, *pmch*$^{-/-}$ rats showed a reduction in naso-anal body length at 6 and 13 weeks (M, SHP diet) and 12 weeks (HF diet) of age (Supplementary Figure S1), suggesting an impaired growth that could be a secondary effect of the decreased caloric intake. When the study was completed, relative body weight of *pmch*$^{-/-}$ rats was 78% (M), 79% (SHP), and 82% (HF) compared to *pmch*$^{+/+}$ rats (Fig. 2, *A-C*). *Pmch*$^{+/+}$ as well as *pmch*$^{-/-}$ rats on HF diet showed a higher body weight at the end of the study compared to M or SHP diet (109% and 112% increase in *pmch*$^{+/+}$ rats and 114% and 117% in *pmch*$^{-/-}$ rats, respectively; Fig. 2, *A-C*). This indicates that *pmch*$^{-/-}$ animals are capable of increasing their body weight when presented with a HF diet. Longitudinal analysis of caloric intake showed that *pmch*$^{-/-}$ animals were hypophagic on M diet (Fig. 2*D*), SHP diet (Fig. 2*E*), and HF diet (Fig. 2*F*). Caloric intake measured during 6 consecutive days in 8-week and 17-week-old rats confirmed these observations (Supplemental Fig. S2*A*), and showed the hypophagia occurred both during the light and dark phase (Supplemental Fig. S2*C*). Water intake was decreased in 8-week-old *pmch*$^{-/-}$ rats on all diets, and unchanged (M diet), decreased (SHP diet), or increased (HF diet) in 17-week-old *pmch*$^{-/-}$ rats compared to *pmch*$^{+/+}$ rats (data not shown).

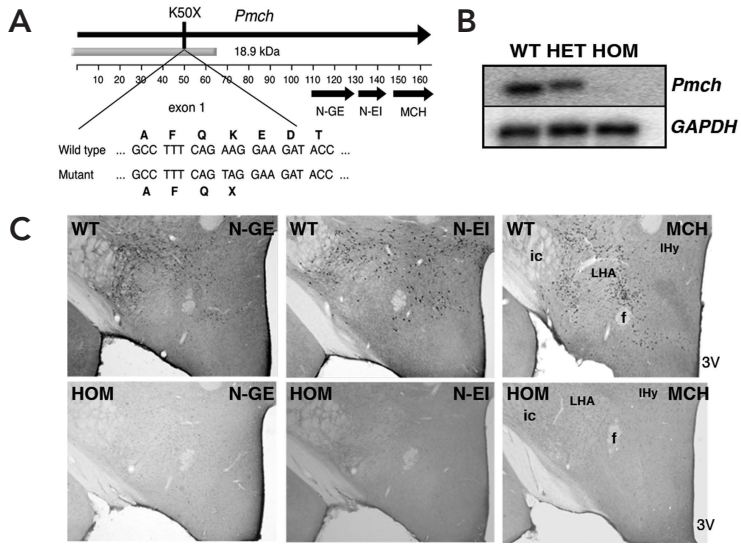

Fig. 1. Confirmation of the *Pmch* knockout rat. *A*: Sequencing revealed an induced premature stop codon in the first exon (K50X) in the MCH precursor gene (indicated in schematic overview). The light grey bar indicates the probe used for the Northern Blot analysis. *B*: Northern Blot analysis of whole brain tissue demonstrated that the premature stopcodon results in almost complete loss of *Pmch* mRNA in animals homozygous for the mutation, and showed a gene dose-dependent reduction in *Pmch* expression in heterozygous rats (53% expression compared to WT). *C*: Immunohistochemistry (250x enlargement) revealed that all three neuropeptides derived from the *Pmch* precursor, N-GE, N-EI, and MCH, are absent in hypothalamic sections derived from *pmch*$^{-/-}$ animals. Abbreviations: 3V, third ventricle; ic, internal capsule; f, fornix; IHy, incerto hypothalamic area; LHA, lateral hypothalamic area.

Body analysis and endocrine profile of Pmch knockout rats. Body analysis of 26-week-old *pmch*$^{-/-}$ rats (M, SHP, and HF diet) revealed a decrease in adipose tissue, even if adipose tissue was normalized for total body weight (Fig. 3*A*). Liver weights were lower, but showed no difference when normalized for total body weight, indicating that liver weights were proportional to the body weights (Fig. 3*A*). Blood analysis in 24-week-old *pmch*$^{-/-}$ rats revealed lower plasma leptin concentrations on all three diets compared to *pmch*$^{+/+}$ rats (Fig. 3*B*). Plasma glucose concentrations did not differ on M diet and tended to be higher in *pmch*$^{-/-}$ rats on SHP diet, while on HF diet *pmch*$^{-/-}$ rats showed higher plasma glucose concentrations compared to *pmch*$^{+/+}$ rats (Fig. 3*C*). Plasma insulin concentrations were lower in *pmch*$^{-/-}$ rats on M or SHP diet, but did not differ between genotypes on HF diet (Fig. 3*D*). Plasma insulin concentrations in *pmch*$^{-/-}$ rats seemed lower during the end of the dark phase (04:00) on all three diets (Fig. 3*D*). A hyperinsulinemic-euglycemic clamp study in body weight-matched *pmch*$^{+/+}$ and *pmch*$^{-/-}$ rats revealed no difference in basal glucose levels (*pmch*$^{+/+}$: 5.73 ± 0.09 mmol/L; *pmch*$^{-/-}$: 5.50 ± 0.12 mmol/L; $P = 0.14$ by Students' *t*-test) or insulin levels (*pmch*$^{+/+}$: 1.23 ± 0.15 ng/ml; *pmch*$^{-/-}$: 1.00 ± 0.18 ng/ml; $P = 0.36$ by Students' *t*-test) during an equilibrium

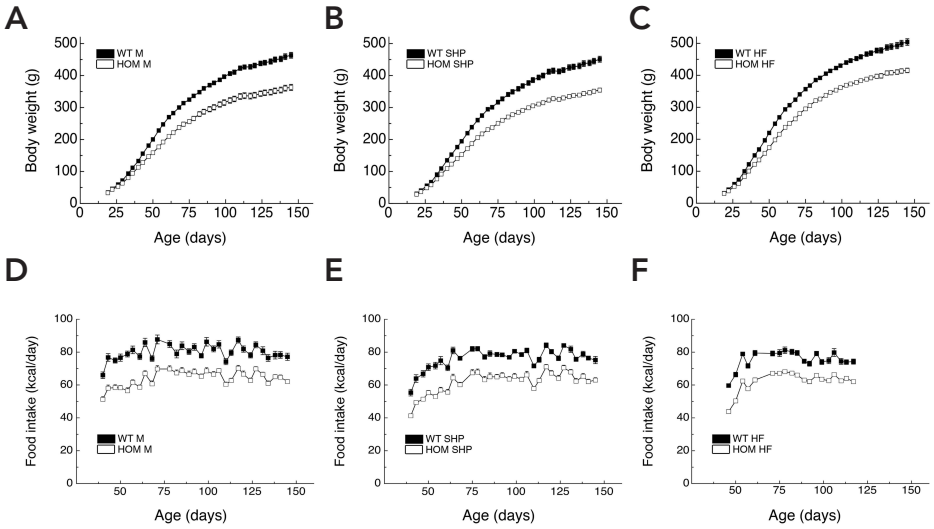

Fig. 2. *Pmch* knockout rats show a lower body weight and decreased caloric intake on three different diets. *A*: Body weight of *pmch*$^{-/-}$ rats was lower compared to *pmch*$^{+/+}$ rats on M diet (squares; $F_{(1, 20)} = 72.2$, $P < 0.001$). *B*: Body weight of *pmch*$^{-/-}$ rats was lower compared to *pmch*$^{+/+}$ rats on SHP diet (triangles; $F_{(1, 19)} = 82.6$, $P < 0.001$). *C*: Body weight of *pmch*$^{-/-}$ rats was lower compared to *pmch*$^{+/+}$ rats on HF diet (circles; $F_{(1, 29)} = 101.6$, $P < 0.001$). Rats on HF diet increased their body weight compared to rats on M or SHP diet with both genotypes (*Pmch*$^{+/+}$ HF vs. *Pmch*$^{+/+}$ M: $F_{(1, 25)} = 18.6$, $P < 0.001$; *Pmch*$^{-/-}$ HF vs. *Pmch*$^{-/-}$ M: $F_{(1, 24)} = 22.9$, $P < 0.001$; *Pmch*$^{+/+}$ HF vs. *Pmch*$^{+/+}$ SHP: $F_{(1, 24)} = 26.9$, $P < 0.001$; *Pmch*$^{-/-}$ HF vs. *Pmch*$^{-/-}$ SHP: $F_{(1, 24)} = 51.7$, $P < 0.001$). Animals on M or SHP diet showed no difference in body weight within genotype (*Pmch*$^{+/+}$ M vs. *Pmch*$^{+/+}$ SHP: $F_{(1, 21)} = 1.6$, $P = 0.23$; *Pmch*$^{-/-}$ M vs. *Pmch*$^{-/-}$ SHP: $F_{(1, 18)} = 1.2$, $P = 0.29$). Statistical analysis also revealed an effect for *time* and a *time* x *genotype* interaction for all groups. *Pmch*$^{-/-}$ rats started showing a reduced body weight per individual measurement after 22 days of age (SHP and HF diet) or 26 days of age (M diet). *D*: *Pmch*$^{-/-}$ rats on M diet ingested fewer calories compared to *pmch*$^{+/+}$ rats ($P < 0.001$ for all individual measurements, Students' *t*-test). *E*: *Pmch*$^{-/-}$ rats on SHP diet ingested fewer calories compared to *pmch*$^{+/+}$ rats ($P < 0.001$ for all individual measurements, Students' *t*-test). *F*: *Pmch*$^{-/-}$ rats on HF diet ingested fewer calories compared to *pmch*$^{+/+}$ rats ($P < 0.001$ for all individual measurements, Students' *t*-test). Data are expressed as means ± S.E.M. (n = 10-16 per group).

state in the early afternoon. However, *pmch*$^{-/-}$ rats showed a lower basal endogenous glucose production (EGP) compared to *pmch*$^{+/+}$ rats, reflecting a decreased metabolic clearance rate (MCR) (Fig. 3*E*). Under hyperinsulinemia (*pmch*$^{+/+}$: 2.16 ± 0.08 ng/ml; *pmch*$^{-/-}$: 2.24 ± 0.09 ng/ml; $P = 0.25$ by Students' *t*-test), both *pmch*$^{+/+}$ and *pmch*$^{-/-}$ rats showed a reduction in EGP, but no differences were found between groups (Fig. 3*E*). When comparing hyperinsulinemic to basal values, insulin-mediated suppression on the EGP did not differ between genotypes (*pmch*$^{+/+}$: -63.07 ± 3.67%; *pmch*$^{-/-}$: -62.13 ± 2.86%; $P = 0.84$ by Students' *t*-test). In addition, glucose disappearance rate (Rd) did also not differ between genotypes (*pmch*$^{+/+}$: 94.21 ± 5.43 μmol/kg.min; *pmch*$^{-/-}$: 99.01 ± 5.74 μmol/kg.min; $P = 0.56$ by Students' *t*-test). These data indicate that *pmch*$^{-/-}$ rats have a functional and dynamic insulin system for maintaining the basal

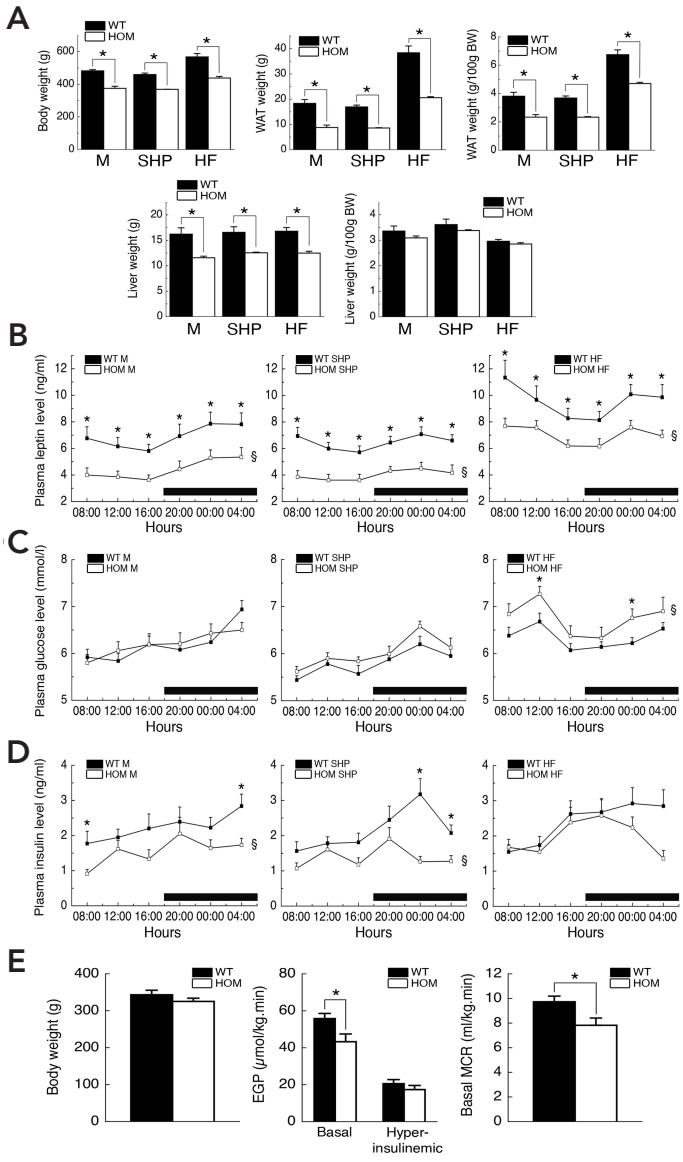

Fig. 3. *Pmch* knockout rats show a changed endocrine profile on three different diets although dynamics are intact. *A*: *Pmch*$^{-/-}$ rats showed decreased body-, total WAT fat pad-, and liver weights compared to *pmch*$^{+/+}$ rats on three different diets (M, SHP, and HF) (n = 3-6 per group). Relative body weight is 78% (M), 80% (SHP), and 77% (HF). Relative total WAT weight is 48% (M), 51% (SHP), 54% (HF), and 61% (M), 63% (SHP), and 70% (HF) when normalized for body weight. Relative liver weight is 71% (M), 75% (SHP), and 74% (HF). However, if liver weights were normalized for body weight, no difference was found between genotypes. *B*: *Pmch*$^{-/-}$ rats showed decreased plasma leptin levels during 24 hrs on M, SHP, and HF diet compared to *pmch*$^{+/+}$ rats ($^{\S}P < 0.05$; $F_{(1, 17)}$ = 7.4, $F_{(1, 20)}$ = 12.6, $F_{(1, 15)}$ = 7.0, respectively; n = 8-12 per group). *C*: *Pmch*$^{-/-}$ rats showed unchanged plasma glucose levels on M diet ($F_{(1, 21)}$ = 0.0001, *P* = 0.98), an elevated trend on SHP diet ($F_{(1, 23)}$ = 3.9, *P* = 0.06), and elevated glucose levels on HF diet ($F_{(1, 16)}$ = 7.0, $^{\S}P < 0.05$) compared to *pmch*$^{+/+}$ rats (n = 9-13 per group). *D*: *Pmch*$^{-/-}$ rats showed decreased plasma insulin levels on M and SHP diet ($F_{(1, 18)}$ = 10.0 and $F_{(1, 20)}$ = 13.1 respectively; $^{\S}P < 0.05$), but unchanged insulin levels on HF diet ($F_{(1, 15)}$ = 1.5, *P* = 0.24) compared to *pmch*$^{+/+}$ rats (n = 8-12 per group). *E*: *Pmch*$^{-/-}$ rats body weight-matched to *pmch*$^{+/+}$ rats showed a decreased basal endogenous glucose production (EGP) and a decreased basal metabolic clearing rate (MCR) compared to *pmch*$^{+/+}$ rats during a hyperinsulinemic-euglycemic clamp analysis (n = 6 per group). EGP levels under hyperinsulinemic conditions did not differ significantly between genotypes (*P* = 0.33 by Students' *t*-test; n = 6 per group). $^{*}P < 0.05$ by Students' *t*-test. Data are expressed as means ± S.E.M. The black bars on the x-axes in panels' *B*, *C*, and *D* indicate the dark phase.

glucose production and utilization. In line with this, intravenous insulin-tolerance tests (IVITT) revealed no difference between genotypes in whole-body insulin sensitivity (Supplemental Fig. S3*A*). Interestingly, intravenous glucose-tolerance tests (IVGTT) showed a trend towards a slightly delayed glucose removal in response to a glucose bolus in *pmch*$^{-/-}$ rats on SHP or HF diet (Supplemental Fig. S3*A*). The Hypothalamic-Pituitary-Adrenal (HPA) axis activity was also investigated in the 26-week-old *pmch*$^{-/-}$ rats, finding a decreased thymus weight in *pmch*$^{-/-}$ rats on SHP diet (*pmch*$^{+/+}$: 0.351 ± 0.018 g, *pmch*$^{-/-}$: 0.263 ± 0.014 g; $P < 0.05$ by Student's *t*-test; n = 3-4 per group), but no difference on the other two diets (data not shown). Weight of the adrenals did not differ on any diet (data not shown). Plasma corticosterone levels at 08:00 and 20:00 also showed no differences between *pmch*$^{+/+}$ and *pmch*$^{-/-}$ rats on M diet (data not shown).

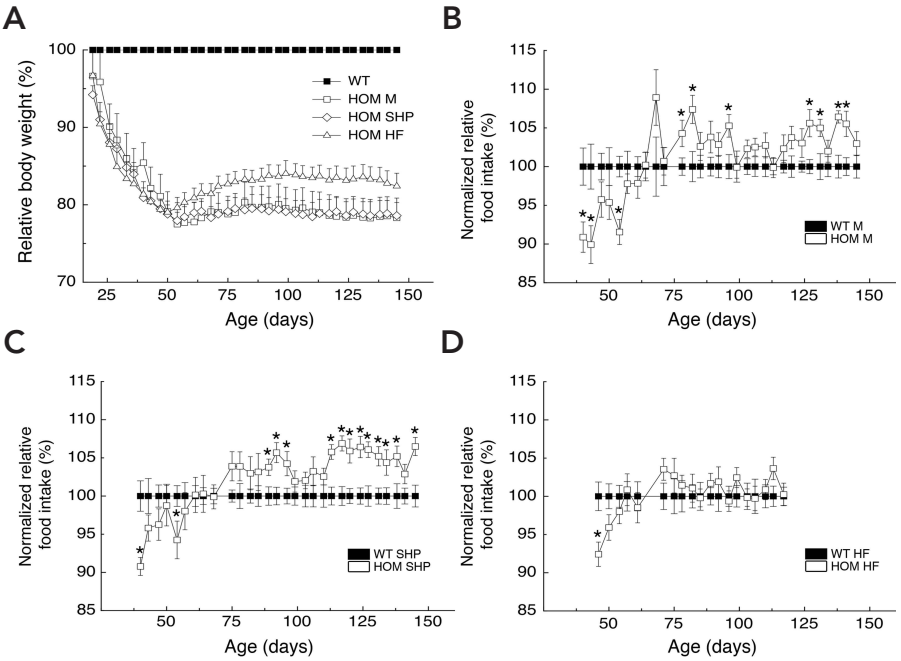

Fig. 4. *Pmch* knockout rats show a switch in caloric intake and relative body weight stabilization during development. *A*: *Pmch*$^{-/-}$ rats showed a stabilization of relative body weight difference during week 8 (PND 50-56) on all three diets (M, SHP, and HF) compared to *pmch*$^{+/+}$ rats. *B*: *Pmch*$^{-/-}$ rats showed a switch in relative caloric intake normalized for body weight compared to *pmch*$^{+/+}$ rats on M diet. Average relative caloric intake from day 40 till day 57 is 94%. However, average relative intake from day 61 till day 145 is 103%. *C*: *Pmch*$^{-/-}$ rats showed a switch in relative caloric intake normalized for body weight compared to *pmch*$^{+/+}$ rats on SHP diet. Average relative caloric intake from day 40 till day 57 was 96%. However, average relative intake from day 61 till day 145 was 104%. *D*: *Pmch*$^{-/-}$ rats showed a switch in relative caloric intake normalized for body weight compared to *pmch*$^{+/+}$ rats on HF diet. Average relative caloric intake from day 46 till day 57 was 97%. However, average relative intake from day 61 till day 117 was 102%. *$P < 0.05$ by Students' *t*-test. Data are expressed as means ± S.E.M. (n = 10-16 per group).

Basal physical activity and body core temperature. Basal physical activity measured in 10-week-old (M, SHP, and HF) or 19-week-old (HF) rats using a home-cage monitoring system did not differ between *pmch*$^{+/+}$ and *pmch*$^{-/-}$ rats (Supplemental Fig. S4*A*). Body core temperature measured using telemetry revealed no significant difference between 25-week-old *pmch*$^{+/+}$ and *pmch*$^{-/-}$ rats on SHP diet (Supplemental Fig. S4*B*). However, *pmch*$^{-/-}$ rats showed two small peaks in body core temperature during the night phase compared to *pmch*$^{+/+}$ rats (Supplemental Fig. S4*B*).

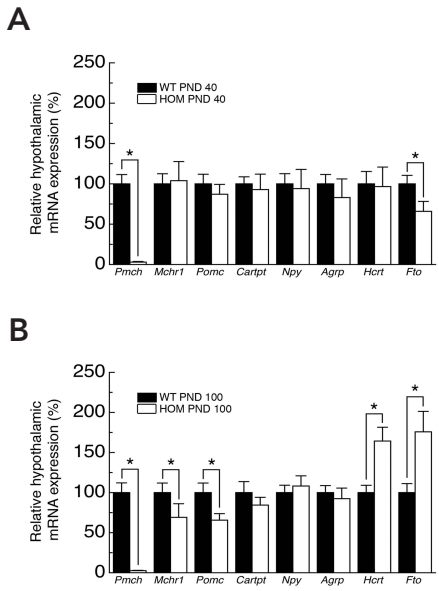

Fig. 5. Hypothalamic gene expression in *Pmch* knockout rats. *A*: Gene expression of a selection of hypothalamic neuropeptides at PND 40. Relative expression of *Pmch* and *Fto* is decreased in *pmch*$^{-/-}$ rats compared to *pmch*$^{+/+}$ rats (*$P < 0.05$ by Students' *t*-test). *B*: Gene expression of a selection of hypothalamic neuropeptides at PND 100. Relative expression of *Pmch*, *Mchr1*, and *Pomc* is decreased while expression of *Hcrt* and *Fto* is increased in *pmch*$^{-/-}$ rats compared to *pmch*$^{+/+}$ rats (*$P < 0.05$ by Students' *t*-test). Data are expressed as means ± S.E.M. (n = 9 per group).

***Pmch* knockout rats have an altered energy balance set point.** The relative body weight of *pmch*$^{-/-}$ rats on all diets decreased approximately 20% during the first 7 weeks compared to *pmch*$^{+/+}$ rats, but this difference stabilized quite abruptly during week 8 (Fig. 4*A*). After this stabilization, the relative body weight difference stayed stable during the remainder of the study and the average remained approximately 79%, 79%, and 83% (M, SHP, and HF respectively) compared to *pmch*$^{+/+}$ rats (Fig. 4*A*). The observed stabilization occurred exactly during the same week of age, postnatal week 8 (PNDs 50-56), with all three diets. These results indicate that the energy balance is set differently in *pmch*$^{-/-}$ rats when entering adulthood and is maintained at a lower level during adulthood. The observed deviation in body weight between *pmch*$^{+/+}$ and *pmch*$^{-/-}$ rats during the first 8 weeks is mirrored by the weekly body weight growth rate, which is decreased in *pmch*$^{-/-}$ rats during the first 8 weeks compared to *pmch*$^{+/+}$ rats on all three diets, but approaches the level of *pmch*$^{+/+}$ rats during adulthood (Supplemental Fig. S5*A*-*C*). This indicates that the body weight growth rate is only decreased in *pmch*$^{-/-}$ rats during the first 8 weeks. Body weight growth per calories was increased in 7-week-old *pmch*$^{-/-}$ rats compared to *pmch*$^{+/+}$ rats, although not significantly on M diet (Supplemental Fig. S5*D*). The same pattern was observed in 14-week-old rats (Supplemental Fig.

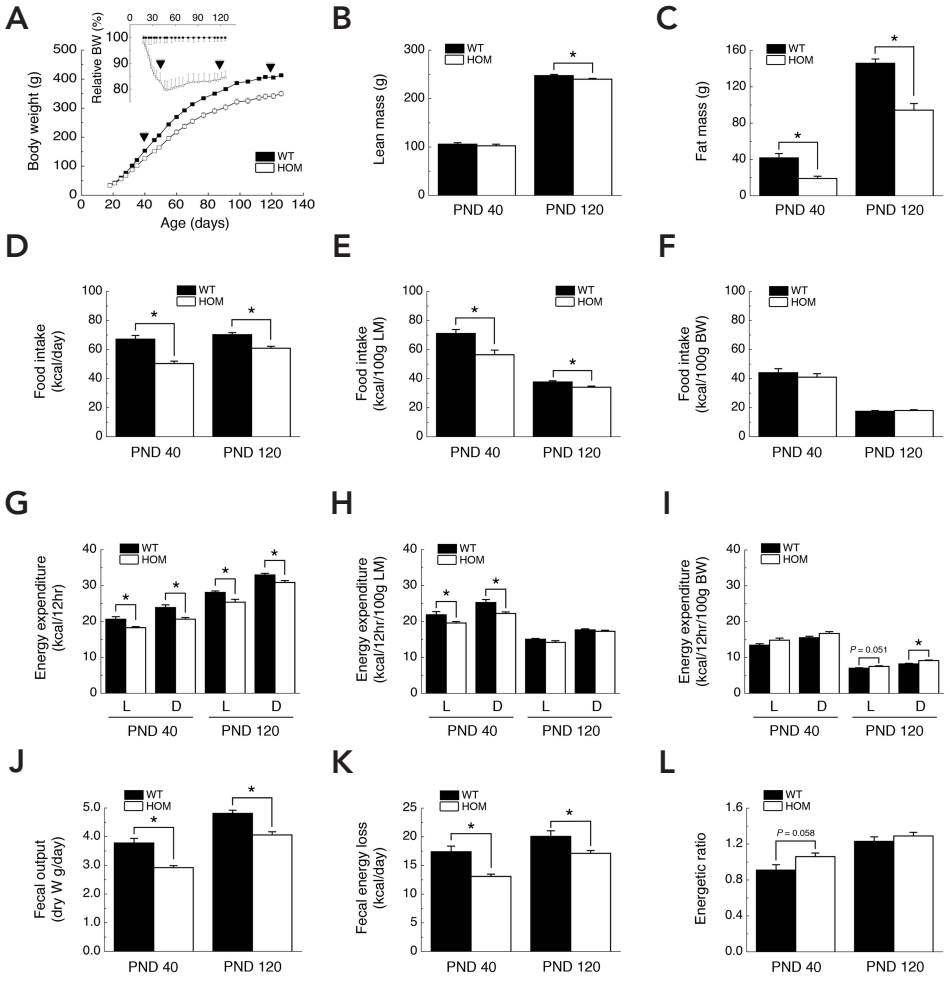

Fig. 6. Energy expenditure in *Pmch* knockout rats. *A*: Body weight is decreased in *pmch*$^{-/-}$ rats compared to *pmch*$^{+/+}$ rats ($F_{(1, 18)} = 36.3$, $P < 0.001$). Relative body weight stabilizes during week 7 (insert). Metabolic measurements are indicated by a triangle. *B*: Lean mass was decreased in *pmch*$^{-/-}$ rats at PND 120, but not at PND 40 compared to *pmch*$^{+/+}$ rats (*$P < 0.05$ by Students' *t*-test). *C*: Fat mass was decreased in *pmch*$^{-/-}$ rats at PND 40 and 120 compared to *pmch*$^{+/+}$ rats (*$P < 0.05$ by Students' *t*-test). *D*: Food intake was decreased in *pmch*$^{-/-}$ rats at PND 40 and 120 compared to *pmch*$^{+/+}$ rats (*$P < 0.05$ by Students' *t*-test). *E*: Food intake normalized for lean mass (LM) was decreased in *pmch*$^{-/-}$ rats at PND 40 and 120 compared to *pmch*$^{+/+}$ rats (*$P < 0.05$ by Students' *t*-test). *F*: Food intake normalized for body weight (BW) was equal between genotypes at PND 40 and 120 (93 and 103%, respectively). *G*: Energy expenditure was decreased in *pmch*$^{-/-}$ rats at PND 40 and 120, both during the light (L) and dark (D) phase compared to *pmch*$^{+/+}$ rats (*$P < 0.05$ by Students' *t*-test). *H*: Energy expenditure normalized for lean mass was decreased in *pmch*$^{-/-}$ rats during the PND 40 light and dark phase (*$P < 0.05$ by Students' *t*-test), but showed no difference during the PND 120 dark phase compared to *pmch*$^{+/+}$ rats. *I*: Energy expenditure normalized for body weight showed increased trends in *pmch*$^{-/-}$ rats during the PND 40 light and dark phase and the PND 120 light phase ($P = 0.07$, $P = 0.09$, and $P = 0.051$, respectively, by Students' *t*-test), and was increased during the PND 120 dark phase compared to *pmch*$^{+/+}$ rats (*$P < 0.05$ by Students' *t*-test). *J*: Fecal output (dry weight per day) was decreased in *pmch*$^{-/-}$ rats ▷

▷ at PND 40 and 120 compared to *pmch*$^{+/+}$ rats (*P < 0.05 by Students' *t*-test). *K*: Fecal energy loss (kcal per day) was decreased in *pmch*$^{-/-}$ rats at PND 40 and 120 compared to *pmch*$^{+/+}$ rats (*P < 0.05 by Students' *t*-test). *L*: The energetic ratio (EE per day divided by metabolisable energy per day) showed an increased trend in *pmch*$^{-/-}$ rats at PND 40 (116%; P = 0.058 by Students' *t*-test), but was equal between genotypes at PND 120 compared to *pmch*$^{+/+}$ rats (105%; P = 0.32 by Students' *t*-test). Data are expressed as means ± S.E.M. (n = 8 per group)

S5*E*), indicating that although lean, the growth efficiency of *pmch*$^{-/-}$ rats is improved compared to *pmch*$^{+/+}$ rats after ingesting the same amount of calories.

Pmch knockout rats show relative hypophagia during early development and relative hyperphagia during adulthood. To investigate the sudden stabilization of relative body weight, we normalized caloric intake for body weight. After normalization for body weight and shown as relative caloric intake, young *pmch*$^{-/-}$ rats (<PND 55) showed slight hypophagia, while adult *pmch*$^{-/-}$ rats (>PND 60) showed slight hyperphagia on M diet (Fig. 4*B*), SHP diet (Fig. 4*C*), and HF diet (Fig. 4*D*) compared to *pmch*$^{+/+}$ rats. Caloric intake measured during 6 consecutive days in 8-week and 17-week-old rats confirmed these observations (Supplemental Fig. S2, *B* and *D*). A same 'biphasic' pattern was observed for relative water intake on all diets (data not shown).

Hypothalamic gene expression. Because the hypothalamus is an important brain region regulating energy balance, the relative expression of a subset of hypothalamic genes in young (PND 40) and adult (PND 100) rats was investigated. At both PND 40 and 100, expression of *Pmch* was almost undetectable in *pmch*$^{-/-}$ rats compared to *pmch*$^{+/+}$ rats (Fig. 5, *A* and *B*). At PND 40, expression of Fatso (*Fto*) was decreased, while expression of Melanin-Concentrating Hormone Receptor 1 (*Mchr1*), Pro-opiomelanocortin (*Pomc*), Cocaine- and amphetamine-regulated Transcript (*Cartpt*), Neuropeptide-Y (*Npy*), Agouti-related peptide (*Agrp*), and Hypocretin (*Hcrt*; also known as Orexin) was unchanged in *pmch*$^{-/-}$ rats compared to *pmch*$^{+/+}$ rats (Fig. 5*A*). At PND 100, expression of *Hcrt* and *Fto* was increased, expression of *Mchr1* and *Pomc* was decreased, and expression of *Cartpt*, *Npy*, and *Agrp* was unchanged in *pmch*$^{-/-}$ animals compared to *pmch*$^{+/+}$ rats (Fig. 5*B*).

Energy expenditure in _Pmch_ knockout rats. To investigate how loss of *Pmch* affects energy expenditure, indirect calorimetric analysis was performed using metabolic cages at PND 40 and 120. *Pmch*$^{-/-}$ rats showed a lower body weight gain over time, again characterized by a sudden stabilization of relative body weight difference (Fig. 6*A*). Lean mass did not differ between genotypes at PND 40, but was decreased at PND 120 (Fig. 6*B*). Fat mass was decreased in *pmch*$^{-/-}$ rats at both PNDs compared to *pmch*$^{+/+}$ rats (Fig. 6*C*). Food intake was lower in *pmch*$^{-/-}$ rats at both PNDs compared to *pmch*$^{+/+}$ rats (Fig. 6*D*). After normalization for lean mass, food intake remained lower compared to *pmch*$^{+/+}$ rats (Fig. 6*E*). In contrast, if data were normalized for total body mass food intake did not differ between genotypes (Fig. 6*F*). Absolute energy expenditure (EE) in *pmch*$^{-/-}$ rats was decreased at PND 40 and 120 compared to *pmch*$^{+/+}$

rats, both during the light and dark phase (Fig. 6*G*). The decreased EE in *pmch*$^{-/-}$ rats was characterized by a decreased carbohydrate oxidation, while fat oxidation was equal between genotypes (data not shown). EE normalized for lean mass in *pmch*$^{-/-}$ rats was decreased at PND 40 during the light and dark phase, and showed a decreased trend during the PND 120 light and dark phase compared to *pmch*$^{+/+}$ rats (Fig. 6*H*). EE normalized for total body mass was increased at PND 120 in *pmch*$^{-/-}$ rats during the dark phase and showed an increased trend during the PND 40 light and dark phase and the PND 120 light phase compared to *pmch*$^{+/+}$ rats (Fig. 6*I*). Fecal output per day and fecal energy content were decreased in *pmch*$^{-/-}$ rats at both PNDs compared to *pmch*$^{+/+}$ rats (Fig. 6, *J* and *K*). The energetic ratio, i.e. the fraction of EE per kcal metabolisable energy, showed an increased trend in *pmch*$^{-/-}$ rats at PND 40 compared to *pmch*$^{+/+}$ rats, but did not differ between genotypes at PND 120 (Fig. 6*L*).

Caloric restriction. At PND 130, body weights of *pmch*$^{+/+}$ and *pmch*$^{-/-}$ rats decreased equally during 48hr starvation (Supplemental Fig. S6*A*). If body weight loss was expressed as a percentage of the body weight at the start of the starvation, *pmch*$^{-/-}$ rats showed an increased trend compared to *pmch*$^{+/+}$ rats ($P = 0.06$; Supplemental Fig. S6*B*). During 72hr refeeding, the body weight regain showed an increased trend in *pmch*$^{+/+}$ rats compared to *pmch*$^{-/-}$ rats ($P = 0.11$; Supplemental Fig. S6*C*). However, this trend was not observed if the body weight regain was expressed as a percentage of the body weight at the end of the starvation (Supplemental Fig. S6*D*). During the starvation, no difference in EE was observed between genotypes (Supplemental Fig. S6*E*). However, approaching the end of the starvation, *pmch*$^{-/-}$ rats showed lower EE compared to *pmch*$^{+/+}$ rats (data not shown). The decreased body weight regain trend in *pmch*$^{-/-}$ rats was reflected by an impaired refeeding response compared to *pmch*$^{+/+}$ rats (Supplemental Fig. S6*F*). Additionally, both *pmch*$^{+/+}$ and *pmch*$^{-/-}$ rats showed hyperphagia compared to basal caloric intake levels at PND 120 (87.5 vs. 70.2 and 73.2 vs. 60.9 kcal/day, respectively; Fig. 6*D*, Supplemental Fig. S6*F*).

Testosterone does not induce the observed stabilization of relative body weight. As the observed stabilization of relative body weight and 'switch' in nutrient intake behavior appeared around the end of rat puberty (approximately between PNDs 55 and 65), we tested the hypothesis that changes in blood testosterone levels induced our observed phenotype. Orchiectomy during postnatal week 5 reduced the body weight of *pmch*$^{+/+}$ and *pmch*$^{-/-}$ rats compared to sham-operated *pmch*$^{+/+}$ and *pmch*$^{-/-}$ rats (Supplemental Fig. S7*A*). Both orchiectomized *pmch*$^{+/+}$ and *pmch*$^{-/-}$ rats showed a decrease in relative body weight compared to sham-operated rats, although no clear stabilization pattern is observed around week 8 (Supplemental Fig. S7, *B* and *C*). Sham-operated *pmch*$^{-/-}$ rats showed a clear stabilization of relative body weight compared to sham-operated *pmch*$^{+/+}$ rats around week 8, confirming observations from untreated animals (Fig. 4*C*, Supplemental Fig. S7*D*). However, orchiectomized *pmch*$^{-/-}$ rats also showed a stabilization of relative body weight compared to orchiectomized *pmch*$^{+/+}$ rats around week 8 (Supplemental Fig. S7*E*). Serum free testosterone levels in *pmch*$^{-/-}$ rats

showed no difference on SHP diet around PND 40, a decreased trend on PND 60, and levels were decreased on PND 120 compared to *pmch*$^{+/+}$ rats (Supplemental Fig. S7*F*). Orchiectomy resulted in almost undetectable levels in both genotypes (Supplemental Fig. S7*F*).

***Pmch* knockout rats develop osteoporosis.** Bone mass density was reduced in *pmch*$^{-/-}$ rats at both PND 40 and 120 compared to *pmch*$^{+/+}$ rats (Supplemental Fig. S8).

DISCUSSION

The key findings of this work is the demonstration that *Pmch* expression during early development and puberty is of critical importance for a normal energy balance, and that loss of *Pmch* results in a 20% decreased energy balance that is maintained during adulthood.

While the role of MCH in energy regulation is well established, it should be noted that the entire *Pmch* gene is inactivated in our rat model and that the less well-characterized neuropeptides N-GE and N-EI are not expressed. Although N-GE so far does not seem to have a biological function, N-EI is implicated in modulatory action on anxiety- and sexual-related behavior in female rats (Gonzalez et al., 1998), increases luteinizing hormone release (Attademo et al., 2004), and stimulates grooming, locomotion, and rearing in male rats (Sanchez et al., 1997). These additional neuropeptides could perform as of yet unknown functions, thereby contributing to phenotypes observed in this study.

Pmch$^{-/-}$ rats have a lower body weight and are hypophagic. Plasma leptin levels were lower in *pmch*$^{-/-}$ rats, correlating with the lower adipose amounts. Two independent studies showed that MCH is a positive regulator of insulin release (Tadayyon et al., 2000; Pissios et al., 2007), thus loss of *Pmch* expression could explain the decreased basal plasma insulin levels and the delayed glucose clearance in the IVGTT studies. Basal insulin levels were lower especially at the end of the dark phase, suggesting a combinatorial effect of decreased caloric intake and loss of MCH-stimulated insulin release. Basal EGP levels in the *pmch*$^{-/-}$ rats were 22% lower compared to *pmch*$^{+/+}$ rats). However, under hyperinsulinemic conditions, this significant difference disappeared, although on average levels were still 16% lower in *pmch*$^{-/-}$ rats. The inhibition of EGP levels by the hyperinsulinemic conditions was equal between genotypes. Moreover, IVITT studies also showed no difference between genotypes. These findings indicate that *pmch*$^{-/-}$ rats react normal to insulin. Plasma leptin, insulin, and glucose levels showed normal circadian patterns in general, and insulin sensitivity was unchanged between genotypes, indicating that the system dynamics in *pmch*$^{-/-}$ rats are intact and functional, although adapted to new homeostatic levels. Additionally, thymus weight, adrenal weight, and plasma corticosterone levels showed no clear differences between *pmch*$^{+/+}$ and *pmch*$^{-/-}$ rats, suggesting that the HPA axis is not severely affected in male *Pmch*-deficient rats.

Chronic loss of *Pmch* in mice resulted in hypophagia (Shimada et al., 1998); however this was characterized in adult mice only. Detailed longitudinal analysis of feeding behavior in *pmch*$^{-/-}$ rats confirmed the hypophagia but also revealed a more complex phenotype. First, food intake corrected for lean mass was lower in young and adult *pmch*$^{-/-}$ rats compared to *pmch*$^{+/+}$ rats. Secondly, when caloric intake was normalized for total body mass, young *pmch*$^{-/-}$ rats (<PND 55) showed a slight hypophagia, while adult young *pmch*$^{-/-}$ rats (>PND 60) showed a slight hyperphagia compared to *pmch*$^{+/+}$ rats. This indicated that adult *pmch*$^{-/-}$ rats consumed approximately equal or higher amounts of calories per body weight compared to *pmch*$^{+/+}$ rats. The switch in caloric intake occurred in the same week for all three diets, suggesting that the effect is genetic and not dietary, and overlapped precisely with the stabilization in relative body weight. Moreover, not only male but also female *pmch*$^{-/-}$ rats showed a stabilization of relative body weight around week 8 compared to *pmch*$^{+/+}$ rats (data not shown). The body weight growth per week mirrored the above-mentioned longitudinal feeding pattern, being lower in *pmch*$^{-/-}$ rats compared to *pmch*$^{+/+}$ rats until ~PND 60, but approaching the level of *pmch*$^{+/+}$ rats afterwards. The increased body weight growth per calories in *pmch*$^{-/-}$ rats is in line with a previous report showing that a caloric restriction induces adipocyte adaptations thus promoting fat storage (Sugden et al., 1999). It is however important to note that loss of *Pmch* does not mimic temporary caloric restriction with accompanying body weight regain after refeeding, but results in a model of chronic voluntary caloric restriction as rats were allowed to feed *ad-libitum* throughout their life. Our findings suggest that *Pmch* expression drives energy intake and storage to levels exceeding the minimal need to grow during early development and puberty, but that this 'overstimulation' disappears around postnatal week 8. During adulthood, *Pmch* expression remains functional during times of starvation (Qu et al., 1996). However, our findings indicate that *Pmch* expression is especially relevant during early development and puberty. This is supported by the observation that the energy balance in *pmch*$^{-/-}$ rats remained ~80% compared to *pmch*$^{+/+}$ rats during the remainder of our study. Moreover, nest-size induced food restriction of pups until PND 25 decreases relative body weight, and this difference in relative body weight diminishes again when animals are given *ad-libitum* access to chow after PND 25 (Remmers et al., 2008). However, the catch-up growth is incomplete as relative body weight stabilizes around week 9, reflected by an increased growth velocity in restricted rats until week 8 and no difference in growth velocity after week 8 (Remmers et al., 2008).

The relative body weight of *pmch*$^{+/+}$ and *pmch*$^{-/-}$ rats started to divert during postnatal week 3, when the pups start to feed at their own, and stabilized around postnatal week 8 for the remainder of the study. Increased oxygen consumption has been shown for 20-week-old mice with a loss of *Pmch* and 17-week-old transgenic mice with a severe loss of MCH neurons (Shimada et al., 1998; Alon and Friedman, 2006). It is however important to note that in both situations data were normalized for body weight. As it is unknown if the metabolic activity of white adipose tissue (WAT) is altered in *pmch*$^{-/-}$ rats, and has been demonstrated that WAT has a minimal

contribution to EE (Even et al., 2001), we chose to show EE not normalized, normalized for lean mass, and normalized for body weight. EE data normalized for body weight showed increased or a trend towards increased EE levels in *pmch*$^{-/-}$ rats compared to *pmch*$^{+/+}$ rats, which is in line with findings that oxygen consumption levels are increased in MCH$^{-/-}$ mice if normalized for body weight (Shimada et al., 1998; Alon and Friedman, 2006). However, EE not normalized or EE normalized for lean mass showed decreased or a trend towards decreased levels in *pmch*$^{-/-}$ rats compared to *pmch*$^{+/+}$ rats. Therefore, the higher amount of non-metabolically active WAT in *pmch*$^{+/+}$ rats might be a confounding factor underlying the calculation of EE, and normalization for body weight can result in incorrect conclusions.

The energetic ratio, calculated by correcting EE values for the amount of metabolisable energy, i.e. the energy absorbed by the rat, showed an increased trend at PND 40, but did not differ at PND 120. These data explain why young *pmch*$^{-/-}$ rats (< PND 55) increase their body weight at a slower pace compared to *pmch*$^{+/+}$ rats, whereas older *pmch*$^{-/-}$ rats increase their body weight at a similar pace compared to *pmch*$^{+/+}$ rats. We therefore conclude that loss of *Pmch* decreases rather than increases EE in the rat, and that the change in EE is secondary to the change in caloric intake. This hypothesis is strengthened by our observations that body weight loss is equal between genotypes during 48hr starvation and that *pmch*$^{-/-}$ rats show a refeeding deficit compared to *pmch*$^{+/+}$ rats during 72hr refeeding. The lower absolute EE values might be related to the lower caloric intake due to a lower thermic effect of food (Even et al., 1994).

Basal locomotor activity did not differ between genotypes at various ages (PND 40 or 120, week 10/11 or 19), with various diets (M, SHP, or HF), and with different techniques (metabolic cage or Phenotyper®). This indicates that physical activity does not contribute to the lean phenotype of *Pmch*-deficient rats, and supports the idea that loss of *Pmch* primarily results in a decrease of caloric intake. Interestingly, the *Mchr1* knockout mice show hyperphagia and an increased physical activity (Chen et al., 2002; Marsh et al., 2002). Although loss of *Pmch* or *Mchr1* both produces a lean phenotype, the aberrant behavior resulting in leanness is different (i.e. normal activity versus hyperactivity, and hypophagia versus hyperphagia), and no explaining mechanisms have been proposed to date.

Hypothalamic *Pmch* mRNA expression increases slowly during early development, increasing more rapidly after weaning, and stabilizes in 8-week-old rats (Presse et al., 1992). *Pmch* is also expressed in Sertoli cells in rat testis where expression increased strongly between PND 15 and adulthood (Hervieu and Nahon, 1995). Relative hypothalamic *Pmch* expression was almost undetectable in *pmch*$^{-/-}$ rats at PND 40 and PND 100 compared to *pmch*$^{+/+}$ rats, confirming our Northern Blot analysis. Relative *Mchr1* expression did not differ between genotypes at PND 40, while being decreased at PND 100 compared to *pmch*$^{+/+}$ rats, suggesting a feedback system affecting *Mchr1* expression during adulthood. Relative *Fto* expression in *pmch*$^{-/-}$ rats was decreased at PND 40 and increased at PND 100 compared to *pmch*$^{+/+}$ rats, while relative expression

of *Pomc* and *Hcrt* was normal at PND 40, but was decreased and increased, respectively, in *pmch*$^{-/-}$ rats compared to *pmch*$^{+/+}$ rats at PND 100. The expression profiles of *Npy* and *Agrp* in adult rats confirm findings in adult mice, however the expression profiles of *Pomc* and *Hcrt* either partially agree or disagree with findings in adult mice (Shimada et al., 1998; Alon and Friedman, 2006). In sum, the time-related differences in expression profiles and a likely interaction between *Pmch* and the orexigenic and anorectic systems studied here could offer an explanation to the sudden stabilization of relative body weight but remain to be studied in more detail.

The stabilization of relative body weight during the end of puberty suggested a functional interaction between *Pmch* and gonadal steroids, such as testosterone. However, free testosterone levels on PND 40 did not differ between genotypes and orchiectomy during postnatal week 5 lowered the body weight of orchiectomized rats compared to sham-operated rats within genotypes, but did not affect the observed stabilization in relative body weight between *pmch*$^{+/+}$ and *pmch*$^{-/-}$ rats around week 8. This indicates that testosterone affects the energy balance but is not essential to induce the observed stabilization of relative body weight. Moreover, free testosterone levels were decreased in *pmch*$^{-/-}$ rats on PND 120, suggesting that the decreased energy balance level influenced free testosterone levels.

The osteoporotic phenotype in *pmch*$^{-/-}$ rats was already observed at PND 40 and confirms the finding that MCHR1 knockout mice develop high bone turnover osteoporosis (Bohlooly et al., 2004). Energy-restriction is known to decrease bone mass density in adult rats (Mardon et al., 2008), indicating that the decreased energy balance in *pmch*$^{-/-}$ rats could result in osteoporosis. Hypogonadism is another known inducer of osteoporosis (Francis et al., 1986; Stepan et al., 1989). However, *pmch*$^{-/-}$ rats were already osteoporotic while serum free testosterone levels were indifferent compared to *pmch*$^{+/+}$ rats at PND 40, suggesting that loss of MCH signaling leads to osteoporosis independently of androgen deficiency.

The body weight of adult humans is normally relatively stable, with only a very small variance over a long period of time (Khosla and Billewicz, 1964; Robinson and Watson, 1965). Classic studies in rodents have shown that stable body weights are actively maintained when animals receive caloric restriction or when the rat's body weight is experimentally elevated; animals quickly restored their body weight to the level appropriate for their age and gender when returned to standard conditions (Steffens, 1975). In humans, dieting strategies combining energy restriction and physical activity have shown moderate success for the reduction of body weight (Hill et al., 1987; Hammer et al., 1989). However, many individuals who have lost weight using a dieting strategy will regain a large proportion or all of the weight lost within 5 years from the end of the treatment (van Dale et al., 1990; Brownell and Wadden, 1992; Foreyt and Goodrick, 1993), although low-fat intake in combination with high activity can successfully slow the regain of weight (Wing and Hill, 2001; Leser et al., 2002). Even though 'short-term' (≤ 4 weeks) MCH1R-antagonism studies are successful in decreasing body weight in adult rats and mice (Mashiko et al., 2005; Palani et al.,

2005; Handlon and Zhou, 2006; Luthin, 2007), it would be very interesting to see if 'long-term' (> 4 weeks) MCH1R antagonism can chronically alter the energy balance of adult animals successfully. Because our data indicate that loss of *Pmch* can lower the energy balance, and that *Pmch* expression is important during early development and puberty, it would be even more interesting to study the effect of MCH1R-antagonism on the determination of the energy balance in young animals.

ACKNOWLEDGEMENTS

We gratefully acknowledge Mark Verheul for help with genotyping, Ruud Bueters for preliminary studies, Ies Nijman and Victor Guryev for computational help, Linda Verhagen for help with statistical analysis, and Judith Homberg for scientific discussion.

GRANTS

Part of this work was supported by grants from the Dutch Diabetes Foundation (grant 2004.00.027), the Nutrigenomics Consortium/Top Institute Food and Nutrition (NGC/TIFN), and the Center of Medical Systems Biology (CMSB) established by The Netherlands Genomics Initiative/Netherlands Organization for Scientific Research (NGI/NWO).

REFERENCES

Ackermans MT, Pereira Arias AM, Bisschop PH et al. (2001) The quantification of gluconeogenesis in healthy men by (2)H2O and [2-(13)C]glycerol yields different results: rates of gluconeogenesis in healthy men measured with (2)H2O are higher than those measured with [2-(13)C]glycerol. The Journal of clinical endocrinology and metabolism 86:2220-2226.

Alon T, Friedman JM (2006) Late-onset leanness in mice with targeted ablation of melanin concentrating hormone neurons. J Neurosci 26:389-397.

Attademo AM, Sanchez-Borzone M, Lasaga M et al. (2004) Intracerebroventricular injection of neuropeptide EI increases serum LH in male and female rats. Peptides 25:1995-1999.

Bittencourt JC, Presse F, Arias C et al. (1992) The melanin-concentrating hormone system of the rat brain: an immuno- and hybridization histochemical characterization. J Comp Neurol 319:218-245.

Bohlooly YM, Mahlapuu M, Andersen H et al. (2004) Osteoporosis in MCHR1-deficient mice. Biochem Biophys Res Commun 318:964-969.

Bouret SG, Simerly RB (2006) Developmental programming of hypothalamic feeding circuits. Clin Genet 70:295-301.

Brownell KD, Wadden TA (1992) Etiology and treatment of obesity: understanding a serious, prevalent, and refractory disorder. J Consult Clin Psychol 60:505-517.

Chambers J, Ames RS, Bergsma D et al. (1999) Melanin-concentrating hormone is the cognate ligand for the orphan G-protein-coupled receptor SLC-1. Nature 400:261-265.

Chen Y, Hu C, Hsu CK et al. (2002) Targeted disruption of the melanin-concentrating hormone receptor-1 results in hyperphagia and resistance to diet-induced obesity. Endocrinology 143:2469-2477.

Chung S, Hopf FW, Nagasaki H et al. (2009) The melanin-concentrating hormone system modulates cocaine reward. Proc Natl Acad Sci U S A.

Cuppen E, Gort E, Hazendonk E et al. (2007) Efficient target-selected mutagenesis in Caenorhabditis elegans: toward a knockout for every gene. Genome research 17:649-658.

Della-Zuana O, Presse F, Ortola C et al. (2002) Acute and chronic administration of melanin-concentrating hormone enhances food intake and body weight in Wistar and Sprague-Dawley rats. Int J Obes Relat Metab Disord 26:1289-1295.

Even PC, Mokhtarian A, Pele A (1994) Practical aspects of indirect calorimetry in laboratory animals. Neurosci Biobehav Rev 18:435-447.

Even PC, Rolland V, Roseau S et al. (2001) Prediction of basal metabolism from organ size in the rat: relationship to strain, feeding, age, and obesity. Am J Physiol Regul Integr Comp Physiol 280:R1887-1896.

Foreyt JP, Goodrick GK (1993) Evidence for success of behavior modification in weight loss and control. Ann Intern Med 119:698-701.

Francis RM, Peacock M, Aaron JE et al. (1986) Osteoporosis in hypogonadal men: role of decreased plasma 1,25-dihydroxyvitamin D, calcium malabsorption, and low bone formation. Bone 7:261-268.

Georgescu D, Sears RM, Hommel JD et al. (2005) The hypothalamic neuropeptide melanin-concentrating hormone acts in the nucleus accumbens to modulate feeding behavior and forced-swim performance. J Neurosci 25:2933-2940.

Gomez F, Dallman MF (2001) Manipulation of androgens causes different energetic responses to cold in 60- and 40-day-old male rats. Am J Physiol Regul Integr Comp Physiol 280:R262-273.

Gomez F, Houshyar H, Dallman MF (2002) Marked regulatory shifts in gonadal, adrenal, and metabolic system responses to repeated restraint stress occur within a 3-week period in pubertal male rats. Endocrinology 143:2852-2862.

Gomori A, Ishihara A, Ito M et al. (2003) Chronic intracerebroventricular infusion of MCH causes obesity in mice. Melanin-concentrating hormone. Am J Physiol Endocrinol Metab 284:E583-588.

Gonzalez MI, Baker BI, Hole DR et al. (1998) Behavioral effects of neuropeptide E-I (NEI) in the female rat: interactions with alpha-MSH, MCH and dopamine. Peptides 19:1007-1016.

Grove KL, Grayson BE, Glavas MM et al. (2005) Development of metabolic systems. Physiol Behav 86:646-660.

Guesdon B, Paradis E, Samson P et al. (2009) Effects of intracerebroventricular and intra-accumbens melanin-concentrating hormone agonism on food intake and energy expenditure. Am J Physiol Regul Integr Comp Physiol 296:R469-475.

Hammer RL, Barrier CA, Roundy ES et al. (1989) Calorie-restricted low-fat diet and exercise in obese women. Am J Clin Nutr 49:77-85.

Handlon AL, Zhou H (2006) Melanin-concentrating hormone-1 receptor antagonists for the treatment of obesity. J Med Chem 49:4017-4022.

Hervieu G, Nahon JL (1995) Pro-melanin concentrating hormone messenger ribonucleic acid and peptides expression in peripheral tissues of the rat. Neuroendocrinology 61:348-364.

Hill JO, Sparling PB, Shields TW et al. (1987) Effects of exercise and food restriction on body composition and metabolic rate in obese women. Am J Clin Nutr 46:622-630.

Homberg JR, Olivier JD, Smits BM et al. (2007) Characterization of the serotonin transporter knockout rat: a selective change in the functioning of the serotonergic system. Neuroscience 146:1662-1676.

Ito M, Gomori A, Ishihara A et al. (2003) Characterization of MCH-mediated obesity in mice. Am J Physiol Endocrinol Metab 284:E940-945.

Keays DA, Clark TG, Flint J (2006) Estimating the number of coding mutations in genotypic- and phenotypic-driven N-ethyl-N-nitrosourea (ENU) screens. Mamm Genome 17:230-238.

Khosla T, Billewicz WZ (1964) Measurement of Change in Body-Weight. Br J Nutr 18:227-239.

Kokkotou E, Jeon JY, Wang X et al. (2005) Mice with MCH ablation resist diet-induced obesity through strain-specific mechanisms. Am J Physiol Regul Integr Comp Physiol 289:R117-124.

Kokkotou EG, Tritos NA, Mastaitis JW et al. (2001) Melanin-concentrating hormone receptor is a target of leptin action in the mouse brain. Endocrinology 142:680-686.

Lembo PM, Grazzini E, Cao J et al. (1999) The receptor for the orexigenic peptide melanin-concentrating hormone is a G-protein-coupled receptor. Nat Cell Biol 1:267-271.

Leser MS, Yanovski SZ, Yanovski JA (2002) A low-fat intake and greater activity level are associated with lower weight regain 3 years after completing a very-low-calorie diet. J Am Diet Assoc 102:1252-1256.

Ludwig DS, Tritos NA, Mastaitis JW et al. (2001) Melanin-concentrating hormone overexpression in transgenic mice leads to obesity and insulin resistance. J Clin Invest 107:379-386.

Luthin DR (2007) Anti-obesity effects of small molecule melanin-concentrating hormone receptor 1 (MCHR1) antagonists. Life sciences 81:423-440.

Mardon J, Zangarelli A, Walrand S et al. (2008) Impact of energy and casein or whey protein intake on bone status in a rat model of age-related bone loss. Br J Nutr 99:764-772.

Marsh DJ, Weingarth DT, Novi DE et al. (2002) Melanin-concentrating hormone 1 receptor-deficient mice are lean, hyperactive, and hyperphagic and have altered metabolism. Proc Natl Acad Sci U S A 99:3240-3245.

Mashiko S, Ishihara A, Gomori A et al. (2005) Antiobesity effect of a melanin-concentrating hormone 1 receptor antagonist in diet-induced obese mice. Endocrinology 146:3080-3086.

McMillen IC, Adam CL, Muhlhausler BS (2005) Early origins of obesity: programming the appetite regulatory system. J Physiol 565:9-17.

Nahon JL, Presse F, Bittencourt JC et al. (1989) The rat melanin-concentrating hormone messenger ribonucleic acid encodes multiple putative neuropeptides coexpressed in the dorsolateral hypothalamus. Endocrinology 125:2056-2065.

Nair SG, Adams-Deutsch T, Pickens CL et al. (2009) Effects of the MCH1 receptor antagonist SNAP 94847 on high-fat food-reinforced operant responding and reinstatement of food seeking in rats. Psychopharmacology (Berl).

Ogden CL, Carroll MD, Curtin LR et al. (2006) Prevalence of overweight and obesity in the United States, 1999-2004. Jama 295:1549-1555.

Oscai LB, McGarr JA (1978) Evidence that the amount of food consumed in early life fixes appetite in the rat. The American journal of physiology 235:R141-144.

Palani A, Shapiro S, McBriar MD et al. (2005) Biaryl ureas as potent and orally efficacious melanin concentrating hormone receptor 1 antagonists for the treatment of obesity. J Med Chem 48:4746-4749.

Pissios P, Bradley RL, Maratos-Flier E (2006) Expanding the scales: The multiple roles of MCH in regulating energy balance and other biological functions. Endocrine reviews 27:606-620.

Pissios P, Frank L, Kennedy AR et al. (2008) Dysregulation of the mesolimbic dopamine system and reward in MCH-/- mice. Biological psychiatry 64:184-191.

Pissios P, Ozcan U, Kokkotou E et al. (2007) Melanin concentrating hormone is a novel regulator of islet function and growth. Diabetes 56:311-319.

Presse F, Hervieu G, Imaki T et al. (1992) Rat melanin-concentrating hormone messenger ribonucleic acid expression: marked changes during development and after stress and glucocorticoid stimuli. Endocrinology 131:1241-1250.

Qu D, Ludwig DS, Gammeltoft S et al. (1996) A role for melanin-concentrating hormone in the central regulation of feeding behaviour. Nature 380:243-247.

Remmers F, Fodor M, Delemarre-van de Waal HA (2008) Neonatal food restriction permanently alters rat body dimensions and energy intake. Physiology & behavior 95:208-215.

Risold PY, Fellmann D, Rivier J et al. (1992) Immunoreactivities for antisera to three putative neuropeptides of the rat melanin-concentrating hormone precursor are coexpressed in neurons of the rat lateral dorsal hypothalamus. Neuroscience letters 136:145-149.

Robinson MF, Watson PE (1965) Day-to-Day Variations in Body-Weight of Young Women. Br J Nutr 19:225-235.

Rossi M, Choi SJ, O'Shea D et al. (1997) Melanin-concentrating hormone acutely stimulates feeding, but chronic administration has no effect on body weight. Endocrinology 138:351-355.

Sailer AW, Sano H, Zeng Z et al. (2001) Identification and characterization of a second melanin-concentrating hormone receptor, MCH-2R. Proc Natl Acad Sci U S A 98:7564-7569.

Saito Y, Cheng M, Leslie FM et al. (2001) Expression of the melanin-concentrating hormone (MCH) receptor mRNA in the rat brain. J Comp Neurol 435:26-40.

Saito Y, Nothacker HP, Wang Z et al. (1999) Molecular characterization of the melanin-concentrating-hormone receptor. Nature 400:265-269.

Sanchez M, Baker BI, Celis M (1997) Melanin-concentrating hormone (MCH) antagonizes the effects of alpha-MSH and neuropeptide E-I on grooming and locomotor activities in the rat. Peptides 18:393-396.

Shearman LP, Camacho RE, Sloan Stribling D et al. (2003) Chronic MCH-1 receptor modulation alters appetite, body weight and adiposity in rats. European journal of pharmacology 475:37-47.

Shimada M, Tritos NA, Lowell BB et al. (1998) Mice lacking melanin-concentrating hormone are hypophagic and lean. Nature 396:670-674.

Sita LV, Elias CF, Bittencourt JC (2007) Connectivity pattern suggests that incerto-hypothalamic area belongs to the medial hypothalamic system. Neuroscience 148:949-969.

Smits BM, Mudde JB, van de Belt J et al. (2006) Generation of gene knockouts and mutant models in the laboratory rat by ENU-driven target-selected mutagenesis. Pharmacogenetics and genomics 16:159-169.

Steffens AB (1975) Influence of reversible obesity on eating behavior, blood glucose, and insulin in the rat. Am J Physiol 228:1738-1744.

Stepan JJ, Lachman M, Zverina J et al. (1989) Castrated men exhibit bone loss: effect of calcitonin treatment on biochemical indices of bone remodeling. J Clin Endocrinol Metab 69:523-527.

Sugden MC, Grimshaw RM, Holness MJ (1999) Caloric restriction leads to regional specialisation of adipocyte function in the rat. Biochim Biophys Acta 1437:202-213.

Tadayyon M, Welters HJ, Haynes AC et al. (2000) Expression of melanin-concentrating hormone receptors in insulin-producing cells: MCH stimulates insulin release in RINm5F and CRI-G1 cell-lines. Biochem Biophys Res Commun 275:709-712.

van Boxtel R, Toonen PW, van Roekel HS et al. (2008) Lack of DNA mismatch repair protein MSH6 in the rat results in hereditary non-polyposis colorectal cancer-like tumorigenesis. Carcinogenesis 29:1290-1297.

van Dale D, Saris WH, ten Hoor F (1990) Weight maintenance and resting metabolic rate 18-40 months after a diet/exercise treatment. Int J Obes 14:347-359.

Wing RR, Hill JO (2001) Successful weight loss maintenance. Annu Rev Nutr 21:323-341.

SUPPLEMENTAL MATERIAL AND METHODS

Immunohistochemistry. Rats were anaesthetized by intraperitoneal administration of sodium pentobarbital (120 mg/kg), and transcardially perfused with 50 ml 0.9% sodium chloride (NaCl) in distilled water, followed by 300 ml 4% paraformaldehyde in 0.1 M sodium phosphate-buffered saline (PBS; pH 7.3). Brains were removed and postfixed in the same fixative, for 16 hrs at 4˚C. Coronal vibratome (Leica, Nussloch, Germany) sections (50 µm) were rinsed in PBS and in 0.3% H_2O_2 in PBS. Subsequently, sections were pretreated with PBS containing 0.1% bovine serum albumin (BSA) and 0.3% Triton-X-100 for 30 min, and then incubated with rat anti-MCH, anti-NGE and anti-NEI serum for 16 hrs (all 1:20000; kindly provided by P.Y Risold, Faculté de Médicine et de Pharmacie, Besançon, France; information on antibody specificity is provided in (Risold et al., 1992). After rinsing, sections were incubated in donkey-anti-rabbit (1:1500, Vector Laboratories, Burlingame, Canada) for 90 min, rinsed, and incubated with an Avidin-Biotin Complex (ABC; Vector ABC Elite, Vector Laboratories, Burlingame, CA, USA) for 90 min. After ABC incubation and rinsing, sections were treated with 0.025% 3'3'-diaminobenzidine (DAB) containing 0.15% nickel ammonium sulphate for 10 min. Subsequently the immunostaining was developed by treating the sections with the former solution containing 0.00015% H_2O_2, for 10 min, and rinsed. Serial sections were mounted on gelatine-coated slides, dehydrated and coverslipped with Entellan®.

Hyperinsulinemic-euglycemic clamp. Rats received a jugular vein catheter and a carotid catheter (as described in the jugular vein catheter placement section) and were allowed to recover for 7 days during which they were handled to minimize stress. Rats received standard fed diet (SHP) and water *ad libitum*. Body-weight matched rats (11-15 weeks of age; n = 6 per group) were fasted starting at the beginning of the light period (0600) until the start of the experiment (1100; 5 hr fast). A tracer dilution technique that measures the enrichment (tracer:tracee ratio) of [6,6-D2] glucose (Cambridge Isotope Laboratories, Cambridge, USA) was applied to calculate the basal glucose turnover as well as hepatic insulin and whole body insulin sensitivity during hyperinsulinemic-euglycemic clamp. The clamp study consisted of a basal equilibration period (t = 0 – t = 100), and a hyperinsulinemic-euglycemic clamp period (t = 110 – t = 250). After a primed (8.0 µmol in 5 min)-continuous (16.6 µmol/h) [6,6-D2] glucose intravenous infusion, carotid artery blood samples were taken at t = 90, t = 95 and t = 100 for determining enrichment during the equilibration state. After the last equilibration blood sample, insulin was administered in a primed (7.2 mU/kg/min, 4 min)-continuous intravenous infusion. A variable infusion of a 25% glucose solution (containing 2.35% [6,6-D2] glucose) through the jugular vein catheter was used to maintain euglycemia (5.5 ± 0.2 mmol/L), as determined by 10 min carotid catheter blood sampling and a glucometer (Freestyle, TheraSense, Disetronic Medical Systems BV, Vianen, the Netherlands). At the end of the clamp, five blood samples were taken with a 10 min interval from t = 210 to t = 250. Blood samples were immediately chilled on ice in tubes containing a 5µl heparin solution and centrifuged at 4°C. Plasma was then stored at -20°C until analysis. Plasma glucose concentrations were determined using a glucose/glucose oxidase-perid method (Boehringer Mannheim, Mannheim, Germany). Plasma insulin concentrations were measured using radioimmunoassay kits (LINCO Research, St. Charles, MO, USA and ICN Biomedicals, Costa Mesa, CA, USA, respectively). Plasma [6,6-D2] glucose enrichment was measured by gas chromatography-mass spectrometry (GCMS) (Ackermans et al., 2001).

Naso-anal length. Naso-anal length was measured at 6 and 13 weeks of age by gentle fixation.

Blood analysis. Blood samples (0.3 ml) were obtained at 24:00, 04:00, 08:00, 12:00, 16:00, and 20:00. Blood was collected in EDTA tubes (BD Vacutainer tubes, Plymouth, United Kingdom) containing 20µl aprotinin (Sigma-Aldrich, Zwijndrecht, the Netherlands). Samples were collected on ice and instantly centrifuged at 2150 rcf for 15' at 4°C. Samples were then aliquoted and stored at -80°C until analysis. Plasma leptin levels were determined *in duplo* using a leptin ELISA (EZRL-

83K, Linco Research, St. Charles, Missouri, USA) according to the manufacturer's instructions. The assay sensitivity limit was 0.04 ng/ml. The intra- and interassay coefficients of variation were 2.17 and 3.40%, respectively. Plasma insulin levels were determined *in duplo* using an insulin ELISA (EZRMI-13K, Linco Research, St. Charles, Missouri, USA) according to the manufacturer's instructions. The assay sensitivity limit was 0.2 ng/ml. The intra- and interassay coefficients of variation were 1.91 and 7.63%, respectively. Plasma glucose levels were determined *in duplo* using an OneTouch® Ultrameter® (LifeScan Benelux, Beerse, Belgium) according to the manufacturer's instructions. Plasma corticosterone levels were determined *in duplo* using a Corticosterone EIA (DSL Deutschland GMBH – Benelux, Assendelft, NL) according to the manufacturer's instructions. The assay sensitivity limit was 1.6 ng/ml. The intra- and interassay coefficients of variation were 3.23 and 4.77%, respectively.

IVITT and IVGTT measurements. Intravenous insulin tolerance tests (IVITT) were performed 7 days after longitudinal blood samples were obtained. Rats were fasted for 3 hrs and subsequently injected in the early afternoon with bovine insulin (0.5 IU/kg body weight, Sigma, Zwijndrecht, NL) as a bolus via the jugular vein catheter. First, a blood sample (0.2 ml) was collected (t = 0), immediately followed by the insulin injection, and subsequent blood samples (0.2 ml) were collected at t = 5, 10, 20, 30, 60, and 90 min. Plasma glucose levels were determined *in duplo* using an OneTouch® Ultrameter® (LifeScan Benelux, Beerse, BE) according to the manufacturer's instructions. Intravenous glucose tolerance tests (IVGTT) were performed 4 days after the IVITT studies. Rats were fasted for 3 hrs and subsequently injected in the early afternoon with D(+)-glucose monohydrate (0.5 ml, 500 mg/kg body weight, J.T. Baker, Deventer, NL) as a bolus via the jugular vein catheter. The same procedure as for the IVITT studies was used. Plasma glucose levels were determined *in duplo* using an OneTouch® Ultrameter® (LifeScan Benelux, Beerse, BE) according to the manufacturer's instructions. Unfortunately, not enough rats on M diet with a functional catheter remained to perform an IVGTT.

Basal physical activity. Basal physical activity of *pmch*$^{+/+}$ and *pmch*$^{-/-}$ rats was measured at 11 weeks of age (M, SHP diet) and 10 or 19 weeks of age (HF diet) using the Phenotyper® home-cage monitoring system (Noldus Information Technology BV, Wageningen, NL). Rats were allowed to adjust to the room for 4 hours before measurements were started. All experiments started in the early afternoon and basal physical activity was measured during 72 hr. Standard fed diet (SHP) and water was available *ad libitum*. Data was analyzed using Ethovision® software (Noldus Information Technology BV, Wageningen, NL) in combination with in-house developed software.

Body core temperature. Adult *pmch*$^{+/+}$ and *pmch*$^{-/-}$ rats were anaesthetized with isoflurane and equipped with a temperature-sensitive radio-transmitter (PhysioLinQ®, Telemetronics Biometry BV, Lelystad, NL) in the peritoneal cavity. After surgery, the rats were individually housed in test cages and allowed to recover for 5 days before measurements were started. The cages were placed on base plates connected to a receiver, which was connected to a PC-based data acquisition and analysis system (LinQcontrol®, Telemetronics Biometry BV, Lelystad, NL). The system demodulated the signals and converted the raw telemetry data into degrees Celsius, and was configured to measure temperature every minute on a 24-hr basis. A total of seven days were measured per animal. Standard fed diet (SHP) and water was available *ad libitum*.

Body weight growth. The weekly body weight growth was expressed as the percentage body weight growth normalized to the body weight at the start of the experiment (PND 19). The body weight on PND 19 was 34.32 g (*Pmch*$^{+/+}$; M diet), 33.16 g (*Pmch*$^{-/-}$; M diet), 30.36 g (*Pmch*$^{+/+}$; SHP diet), 28.61 g (*Pmch*$^{-/-}$; SHP diet), 31.44 g (*Pmch*$^{+/+}$; HF diet), and 30.40 g (*Pmch*$^{-/-}$; HF diet). This means that a hypothetical growth of 100% by *pmch*$^{+/+}$ rats on an M diet during a week indicates that the rats grew 34.32 g in body weight during that week.

Growth per calories. The growth per calories was expressed as the percentage body weight growth during 1 week per 100 calories intake, normalized to the body weight at the start of the week when the measurement was done. Analysis was performed on week 7 and week 14. This means that a hypothetical growth of 4.7% by *pmch*$^{+/+}$ rats on an M diet (average weight 181g at the start of week 7) during week 7 indicates that the rats grew 8.51g in body weight during that week per 100 calories intake.

Hypothalamic mRNA expression. Rats were sacrificed at PND 40 and 100 during the early afternoon. The hypothalamus was rapidly dissected and snap-frozen in liquid nitrogen. Total RNA was isolated using a Trizol method and RNA quantity and quality was assessed using a Nanodrop® ND-1000 spectrophotometer (Thermo-Scientific, Wilmington, DE, USA). cDNA was synthesized from 2.5μg of total RNA using a RetroScript® kit (Applied Biosystems, Nieuwerkerk a/d Ijssel, NL) as described by the manufacturer, and diluted in MQ (1:8). Gene expression was quantified with a 7900 HT Real-Time PCR machine (ABI Prism®). Primers for *Cyclophilin*, *Pmch*, *Mchr1*, *Pomc*, *Cartpt*, *Npy*, *Agrp*, *Hcrt*, and *Fto* were designed using SciTools PrimerQuest (IDT; primers shown in Supplementary Table 1). Primers were optimized to amplify cDNA but not genomic DNA and to generate a single PCR product. PCR efficiency was between 80% and 120%. In general, 2μl template, 10μM primers, and 5μl SYBRGreen Mix (Applied Biosystems) was used in a 10μl PCR reaction. Thermocycler conditions comprised an initial holding stage at 50°C for 2 min followed by 95°C for 3 min followed by a PCR program consisting of 95°C for 30 sec and 60°C for 30 sec for 40 cycles. Samples were run in triplicates. To control for input, *Cyclophilin* was run on the same plate and used as a control gene. Calculations were performed by a comparative method ($2^{-\Delta\Delta Ct}$), taking the efficiency of the PCR into account (1.8-2.2). All experiments were repeated after a new cDNA synthesis reaction. Average *pmch*$^{-/-}$ rat gene expression from the two experiments is expressed as a percentage of average *pmch*$^{+/+}$ gene expression.

Orchiectomy and free testosterone levels. Testis and epididymides were removed during postnatal week 5 under anesthesia with isoflurane. Sham-operated rats were anaesthetized with isoflurane, after which a small incision was made and closed again. Body weight of operated and sham-operated rats was monitored until 16 weeks of age. At 16 weeks of age, rats were sacrificed by decapitation and blood was isolated. Blood samples were allowed to clot at room temperature and centrifuged at 2150 rcf for 15' at 4°C. Serum samples were then aliquoted and stored at -20°C until analysis. Untreated *pmch*$^{+/+}$ and *pmch*$^{-/-}$ rats were sacrificed around PND 40, and serum samples were isolated as mentioned above. Serum free testosterone levels were determined *in quattro* using a Free Testosterone RIA (DSL Deutschland GMBH – Benelux, Assendelft, NL) according to the manufacturers instructions. The assay sensitivity limit was 0.18 pg/ml. The intra- and interassay coefficients of variation were 5.03 and 8.30%, respectively. If serum free testosterone levels were below detection levels, 0.18 pg/ml was taken as data value.

SUPPLEMENTAL FIGURES AND TABLES

Table S1. Forward and reverse primer sequences for qPCR analysis of hypothalamic gene expression

Gene	Forward primer	Reverse Primer
Cyclophilin	ACTTCATGATCCAGGGTGGAGACT	AAGTTCTCATCTGGGAAGCGCTCA
Pmch	TCGGTTGTTGCTCCTTCTCTGGAA	TGGAGCCTGTGTTCTTTGTGGTCT
Mchr1	TCCGATGGCCAGGATAATCTCACA	AGATGGTACCAAACACGGAAGGCA
Pomc	TCCATAGACGTGTGGAGCTGGT	TTCATCTCCGTTGCCTGGAAACAC
Cart	TGGACATCTACTCTGCCGTGGAT	TTCCTGCAGCGCTTCAATCTGCAA
Npy	AGAGGACATGGCCAGATACTACTC	AATCAGTGTCTCAGGGCTGGATCT
AgRP	TCCCAGAGTTCTCAGGTGAGTATGGT	TCTGCCAAAGCTTCTGCCTTCT
Hcrt	TTTGGACCACTGCACCGAAGATAC	CCCAGGGAACCTTTGTAGAAGGAA
Fto	ACCATGACGAGAACTTGGTGGACA	AGCTGGACTCGTCATCGCTTTCAT

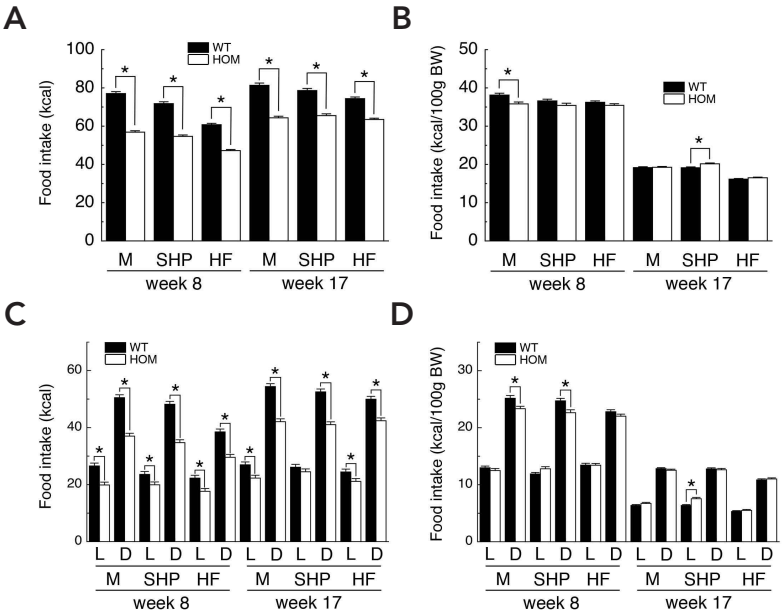

Fig. S1. *Pmch* knockout rats show a decreased nutrient intake during light and dark phase on three different diets. *A*: *Pmch*$^{-/-}$ rats ingested fewer calories compared to *pmch*$^{+/+}$ rats (M: -26% and -21%, 8 and 17 weeks of age, respectively; SHP: -24% and -17%, 8 and 17 weeks of age, respectively; HF: -22% and -15%, 8 and 17 weeks of age, respectively). *B*: The hypophagic character of *pmch*$^{-/-}$ rats fades at a younger age, and disappears during adulthood when data are normalized for body weight (M: -6% and +0%, 8 and 17 weeks of age, respectively; SHP: -3% and +5%, 8 and 17 weeks of age, respectively; HF: -2% and +2%, 8 and 17 weeks of age, respectively). *C*: Caloric intake is decreased in 8-week and 17-week-old *pmch*$^{-/-}$ rats on three diets (M, SHP, and HF) during both light (L) and dark phase (D). *D*: The hypophagic character of *pmch*$^{-/-}$ rats fades when data are normalized for body weight, except for caloric intake in 8-week-old *pmch*$^{-/-}$ rats on M or SHP diet during the dark phase. **P* < 0.05 by Students' *t*-test. Data are expressed as means ± S.E.M. (n = 10-16 per group).

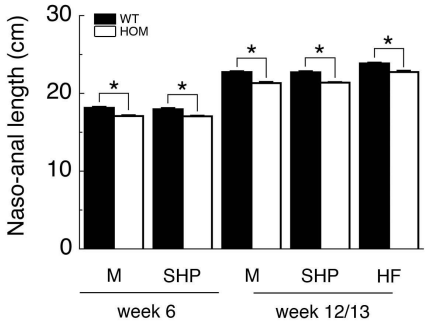

Fig. S2. *Pmch* knockout rats have a decreased body length. *Pmch*$^{-/-}$ rats showed a decreased body length compared to *pmch*$^{+/+}$ rats on three different diets (M, SHP, and HF) at a different age (M, SHP: 6 and 13 weeks; HF: 12 weeks). Relative body length was 94.2% (M) and 94.9% (SHP) at 6 weeks of age, and 93.8% (M), 94.2% (SHP), and 95.4% (HF) at 12/13 weeks of age. **P* < 0.05 by Students' *t*-test. Data are expressed as means ± S.E.M. (n = 10-16 per group).

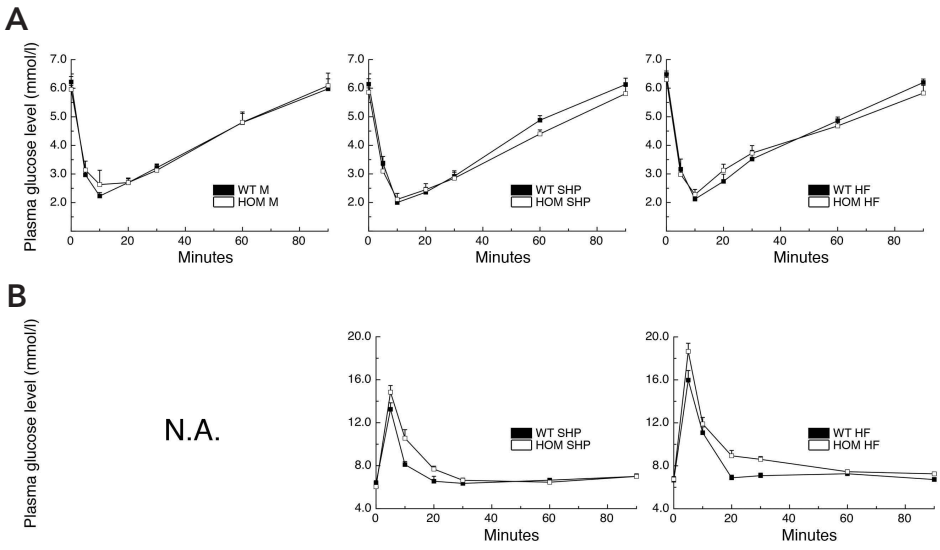

Fig. S3. *Pmch* knockout rats show no change in whole-body insulin sensitivity. *A*: No difference in whole-body insulin sensitivity is observed between 23-week-old *pmch*$^{+/+}$ and *pmch*$^{-/-}$ rats on M, SHP, or HF diet ($F_{(1, 14)}$ = 0.03, P = 0.86; $F_{(1, 15)}$ = 0.9, P = 0.37; $F_{(1, 7)}$ = 0.02, P = 0.90; respectively) during an IVITT (n = 4-9 per group). *B*: *Pmch*$^{-/-}$ rats on SHP diet showed a trend towards slower glucose removal during an IVGTT compared to *pmch*$^{+/+}$ rats ($F_{(1, 5)}$ = 3.7, P = 0.11), while glucose removal in *pmch*$^{-/-}$ rats on HF diet was delayed ($F_{(1, 7)}$ = 20.9, $P < 0.05$). N.A. = data not available. Data are expressed as means ± S.E.M. (n = 3-5 per group).

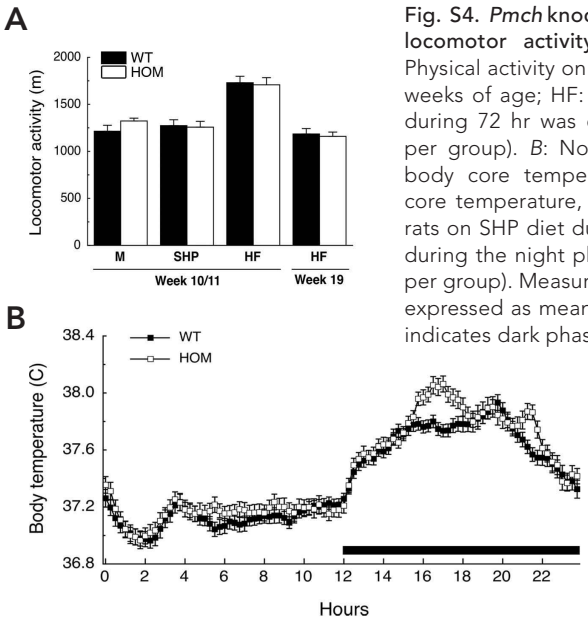

Fig. S4. *Pmch* knockout rats show no change in basal locomotor activity or body core temperature. A: Physical activity on three different diets (M and SHP: 11 weeks of age; HF: 10 and 19 weeks of age) measured during 72 hr was equal between genotypes (n = 7-8 per group). *B*: No statistical difference was found in body core temperature, depicted as average body core temperature, between adult *pmch*$^{+/+}$ and *pmch*$^{-/-}$ rats on SHP diet during 24 hr ($F_{(1, 15)}$ = 0.3, P = 0.60), or during the night phase ($F_{(1, 15)}$ = 0.8, P = 0.40; n = 7-10 per group). Measurement is average of 6 days. Data are expressed as means ± S.E.M. The black bar in panel *B* indicates dark phase.

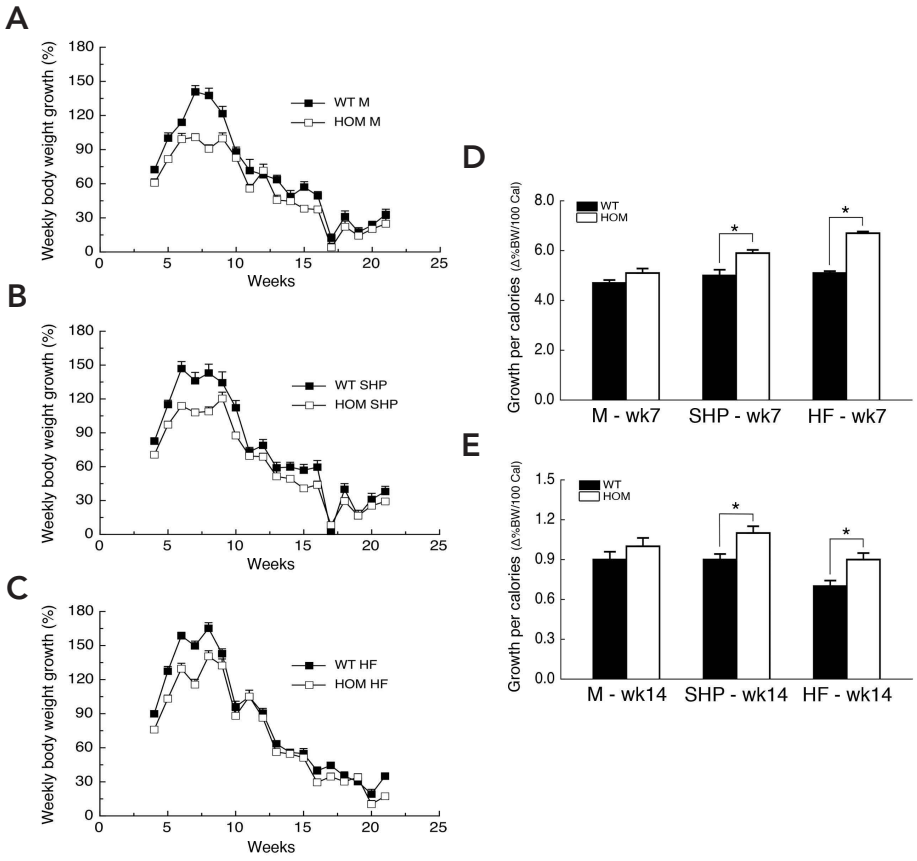

Fig. S5. Weekly growth rate and growth per calories during early development and puberty. *A*: The weekly body weight growth is decreased in *pmch*$^{-/-}$ rats on M diet during the first 8 postnatal weeks. After week 8, the difference in weekly body weight growth between genotypes fades. The same effect is observed for *pmch*$^{-/-}$ rats on SHP diet (*B*) or HF diet (*C*). *D*: Growth per calories (% body weight gained during 1 week/100 calories) in 7-week-old rats on M-, SHP-, or HF diet. *E*: Growth per calories (% body weight gained during 1 week/100 calories) in 14-week-old rats on M, SHP, or HF diet. *$P < 0.05$ by Students' *t*-test. Data are expressed as means ± S.E.M. (n = 10-16 per group).

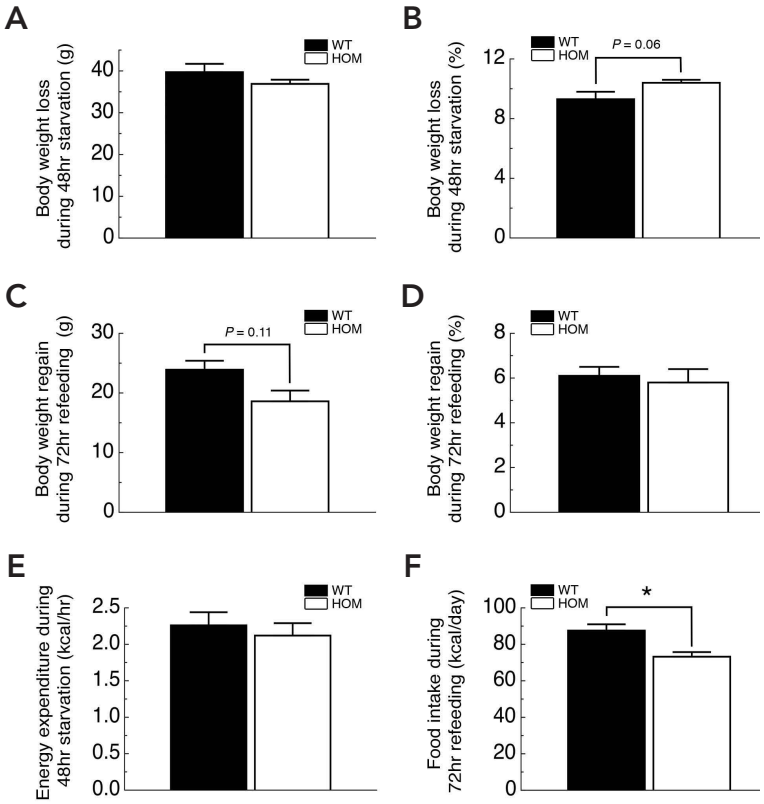

Fig. S6. Caloric restriction analysis. *A*: Body weight reduction was equal between 19-week-old *pmch*$^{+/+}$ and *pmch*$^{-/-}$ rats during 48hr starvation. *B*: *Pmch*$^{-/-}$ rats showed an increased trend in body weight reduction compared to *pmch*$^{+/+}$ rats when data is expressed as a percentage of the body weight at the start of the starvation ($P = 0.06$ by Students' *t*-test). *C*: Body weight regain during 72hr refeeding on SHP diet showed a decreased trend in *pmch*$^{-/-}$ rats compared to *pmch*$^{+/+}$ rats ($P = 0.11$ by Students' *t*-test). *D*: Body weight regain was equal between genotypes when data is expressed as a percentage of the body weight at the start of the refeeding. *E*: No difference in energy expenditure is observed between genotypes during the 48hr starvation. *F*: Average caloric intake per day was lower in *pmch*$^{-/-}$ rats compared to *pmch*$^{+/+}$ rats during 72hr refeeding (*$P < 0.05$ by Students' *t*-test). Data are expressed as means ± S.E.M. (n = 8-6 per group).

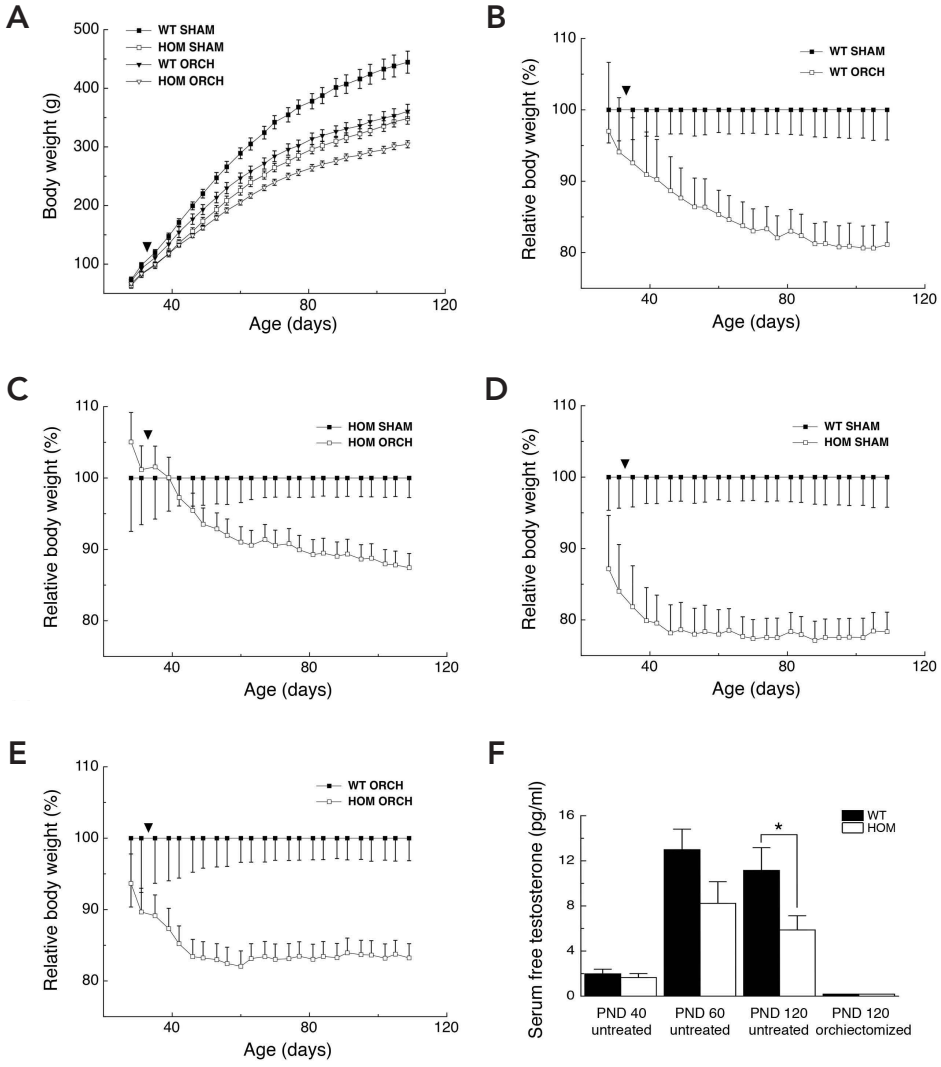

Fig. S7. Testosterone is not critical to induce relative body weight stabilization. *A*: Orchiectomy during postnatal week 5 (indicated by the arrowhead) decreased the body weight of *pmch*$^{+/+}$ rats compared to sham-operated *pmch*$^{+/+}$ rats ($F_{(1, 16)} = 12.3$, $P < 0.005$; n = 8-10 per group). Orchiectomy also lowered the body weight of *pmch*$^{-/-}$ rats ($F_{(1, 21)} = 7.8$, $P < 0.05$; n = 9-14 per group) compared to sham-operated *pmch*$^{-/-}$ rats. Orchiectomized rats started showing a reduced body weight per individual measurement after 49 days of age (*Pmch*$^{+/+}$; $P < 0.05$ by Students' *t*-test) or 60 days of age (*Pmch*$^{-/-}$; $P < 0.05$ by Students' *t*-test). At 16 weeks of age, the body weight of orchiectomized *pmch*$^{+/+}$ rats is 81% compared to the body weight of sham-operated *pmch*$^{+/+}$ rats. During the same week, the body weight of orchiectomized *pmch*$^{-/-}$ rats is 87% compared to the body weight of sham-operated *pmch*$^{-/-}$ rats. *B*: The relative body weight of orchiectomized *pmch*$^{+/+}$ rats showed no clear stabilization around week 8 compared to sham-operated *pmch*$^{+/+}$ rats (n = 8-10 per group). *C*: The relative body weight of orchiectomized *pmch*$^{-/-}$ rats showed no clear stabilization around week 8 compared to sham-operated *pmch*$^{-/-}$ rats (n = 9-14 per group). *D*: The relative body weight of sham-operated *pmch*$^{-/-}$ rats showed a stabilization of relative ▷

▷ body weight around week 8 compared to sham-operated *pmch*$^{+/+}$ rats (n = 8-9 per group). *E*: The relative body weight of orchiectomized *pmch*$^{-/-}$ rats showed a stabilization of relative body weight around week 8 compared orchiectomized *pmch*$^{+/+}$ rats (n = 10-14 per group). *F*: Serum free testosterone levels did not differ between *pmch*$^{+/+}$ and *pmch*$^{-/-}$ rats on PND 40 (n = 14 per group) or PND 60 (n = 8-10 per group), but were decreased on PND 120 in *pmch*$^{-/-}$ rats compared to *pmch*$^{+/+}$ rats ($P < 0.05$ by Students' *t*-test n = 8 per group). Serum free testosterone levels were undetectable in orchiectomized *pmch*$^{+/+}$ and *pmch*$^{-/-}$ rats on PND 120 (n = 10-14 per group). Data are expressed as means ± S.E.M.

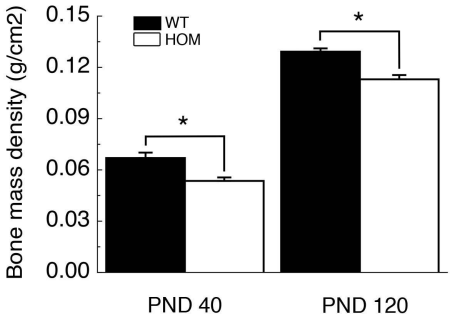

Fig. S8. *Pmch* knockout rats develop osteoporosis. *Pmch*$^{-/-}$ rats showed a decreased bone-mass density compared to *pmch*$^{+/+}$ rats at PND 40 and 120 ($P < 0.05$ by Students' *t*-test; n = 7-8 per group). Data are expressed as means ± S.E.M.

3

LOSS OF MELANIN-CONCENTRATING HORMONE IN THE RAT UNCOUPLES OPERANT RESPONDING FOR FOOD AND COCAINE AND AFFECTS STRIATAL DOPAMINE FUNCTION

Joram D. Mul[1], Robert M. Sears[2,§], Susanne E. la Fleur[3,§§], Anthonieke Afrasiab-Middelman[4], Michel M.M. Verheij[5], Dustin Schetters[6], Judith R. Homberg[4], Anton N.M. Schoffelmeer[6], Roger A.H. Adan[3], Ralph J. DiLeone[2,7], Taco J. De Vries[6] and Edwin Cuppen[1,8,†]

[1]Hubrecht Institute-KNAW & University Medical Center Utrecht, Utrecht, The Netherlands
[2]Department of Psychiatry, Ribicoff Research Facilities, Yale University School of Medicine, New Haven, Connecticut, USA
[3]Rudolf Magnus Institute of Neuroscience, Department of Neuroscience and Pharmacology, University Medical Center Utrecht, Utrecht, The Netherlands
[4]Department of Cognitive Neuroscience, [5]Department of Molecular Animal Physiology, Donders Institute for Brain, Cognition, and Behavior, Radboud University, Nijmegen, The Netherlands.
[6]Department of Anatomy and Neurosciences, Center for Neurogenomics and Cognitive Research, Free University Medical Center, Amsterdam, The Netherlands
[7]Department of Neurobiology, Yale University School of Medicine, New Haven, CT, USA
[8]Department of Medical Genetics, University Medical Center Utrecht, Utrecht, The Netherlands
[§]Current address: Center for Neural Science, New York University, New York, NY, USA
[§§]Current address: Department of Endocrinology and Metabolism, Academic Medical Center, University of Amsterdam, Amsterdam, The Netherlands

ABSTRACT

The nucleus accumbens and the lateral hypothalamic area form a hypothalamic-limbic neuropeptide feeding circuit mediated by Melanin-Concentrating Hormone (MCH). MCH promotes feeding behavior via MCH receptor-1 (MCH1R) in the accumbens shell subregion (AcbSh), although this relationship has not been fully characterized. Given the AcbSh mediates the reinforcing properties of food and drugs of abuse, we hypothesized that MCH may modulate motivational aspects of these behaviors. Functional loss of the rat MCH-precursor *Pmch* reduced meal size and highly palatable food-reinforced operant responding, while it increased cocaine-reinforced operant responding. To our best knowledge, this is the first rat model that shows this clear motivational uncoupling. *Pmch*$^{-/-}$ rats showed increased *ex vivo* electrically evoked dopamine (DA) release, although basal and cocaine-evoked DA levels measured using *in vivo* microdialysis did not differ between genotypes. *Pmch*$^{-/-}$ rats also showed adaptations in genes related to presynaptic dopaminergic release capacity. Finally, *pmch*$^{-/-}$ rats showed increased postsynaptic DA-pathway signaling sensitivity in the AcbSh after a cocaine stimulus. In sum, loss of *Pmch* had presynaptic and postsynaptic effects on the striatal DA system. Our findings support the MCH-MCH1R system as a mediator of both natural and drug rewards, reinforcing this system as a target for treatment of obesity and drug abuse. Also, we propose that MCH signaling positively mediates motivation for food, thus providing a crucial signal with which hypothalamic neural circuits controlling energy balance guide frontal brain areas to shift motivation towards food. Without MCH signaling, motivation away from food prevails.

INTRODUCTION 

The Melanin-Concentrating Hormone (MCH) precursor (*Pmch*) is predominantly expressed in neurons of the lateral hypothalamic area (LHA) and the incerto hypothalamic area (sometimes referred to as zona incerta), which project throughout the brain (Bittencourt et al., 1992; Sita et al., 2007). *Pmch* processing generates glycine-glutamic acid (N-GE), glutamic acid-isoleucine (N-EI), and MCH (Nahon et al., 1989). MCH affects energy homeostasis positively; *Pmch* mRNA is upregulated after fasting (Qu et al., 1996; Silva et al., 2009), *Pmch*-deficient rats or mice show leanness and a reduced appetite (Shimada et al., 1998; Alon and Friedman, 2006; Mul et al., 2010), while *Pmch* overexpression results in obesity and an increased appetite (Ludwig et al., 2001). In addition, central injection of MCH increases caloric intake (Qu et al., 1996; Rossi et al., 1997; Della-Zuana et al., 2002; Abbott et al., 2003; Gomori et al., 2003; Ito et al., 2003; Georgescu et al., 2005; Guesdon et al., 2009).

In rodents MCH binds to MCH receptor-1 (MCH1R), which is present at high levels in limbic regions (Chambers et al., 1999; Lembo et al., 1999; Saito et al., 1999; Hervieu et al., 2000). Moreover, the accumbens shell subregion (AcbSh) modulates the orexigenic action of MCH (Georgescu et al., 2005). MCH1R knockout mice are lean (Chen et al., 2002; Marsh et al., 2002), and blockade of MCH1R lowers body weight and caloric intake through several mechanisms (Ito et al., 2009). Moreover, impaired MCH-MCH1R signaling results in a dysregulated mesolimbic dopamine (DA) system (Smith et al., 2005; Pissios et al., 2008). MCH1r is expressed in medium spiny neurons (MSNs) of the AcbSh, coexpressed with D_1R and D_2R DA receptors, and activation of MCH1R reduces MSN excitability (Robert Sears unpublished data; Georgescu et al., 2005; Chung et al., 2009). MCH1R signals via multiple G-proteins, including $G_{i/o}$ (Bachner et al., 1999; Hawes et al., 2000; Gao and van den Pol, 2001; Pissios et al., 2003), thus potentially affecting phosphorylation sensitivity of several phosphoproteins via striatal neuron protein kinase cascades (Greengard, 2001). AMPA-type glutamate receptor (AMPAR) modulation in the AcbSh affects feeding and brain reward (Maldonado-Irizarry et al., 1995; Stratford et al., 1998; Todtenkopf et al., 2006), and MCH administration affects AMPAR-subunit GluR1 phosphorylation induced by a D_1R agonist (Georgescu et al., 2005).

These findings link the hypothalamic MCH feeding-stimulatory circuit with the mesolimbic DA system that influences behavioral responses to addictive stimuli including food and drugs of abuse. In rats, acute MCH1R-antagonism effects on food-reward and cocaine-reward behavior have been studied (Chung et al., 2009; Nair et al., 2009). Taking advantage of the strong cognitive performance of rats (Snyder et al., 2009) and relatively large size, we investigated meal patterns during development and reward-related behavior in the recently characterized *Pmch*-deficient (*pmch*$^{-/-}$) rats (Mul et al., 2010), using an array of behavioral and biochemical assays. As described below, loss of MCH-MCH1R signaling in the rat affected DA-signaling in the AcbSh, and uncoupled operant responding for highly palatable food and cocaine.

MATERIAL & METHODS

Animals. The Animal Care Committee of the Royal Dutch Academy of Science and the Free University of Amsterdam approved all experiments according to the Dutch legal ethical guidelines. *Pmch*$^{+/+}$ and *pmch*$^{-/-}$ rats, on a Wistar background (Mul et al., 2010), were socially housed (2 per cage) unless noted otherwise in a temperature- and humidity-controlled room (21 ± 2°C and 60% relative humidity) under a 12-h light-dark cycle (lights on at 06.00 h) with standard fed diet (semi-high-protein: RM3, 27% crude protein and 12% fat, 3.33kcal/g AFE, SDS, Witham, United Kingdom) and water available *ad libitum* unless noted otherwise. Rats used for the self-administration experiments were under a reversed 12-h light-dark cycle with diet (Teklan Global 2016, 16.3% crude protein and 4.2% fat, 3.2kcal/g AFE, Harlan, Horst, The Netherlands) and water available *ad libitum*. Only male rats were used in the present study.

Genotyping. Rats were genotyped using the KASPar SNP Genotyping System (KBiosciences, Hoddesdon, UK) as described before (Mul et al., 2010). Rats were genotyped at three weeks of age and genotypes were reconfirmed after experimental procedures were completed.

Meal Pattern Analysis. Rats were placed individually into monitoring cages, and allowed to acclimatize for 2 days. Body weight, food and water intake were measured daily. Water and diet (RM3, 27% crude protein and 12% fat, 3.33kcal/g AFE, SDS, Witham, United Kingdom) were available *ad-libitum*. Meal patterns were determined from 2 consecutive days in each experimental time point using data collected by Scales (Department Biomedical Engineering, UMC Utrecht, the Netherlands). This program records the weight of food hoppers in the home cage automatically every 12 seconds, as well as the amount of licks from water bottles. A meal was defined as an episode of food intake with a minimal consumption of 1 kilocalorie (0.3 g of chow) and a minimal intermeal interval of 5 minutes. Parameters (total food intake, total meal duration, average meal duration, meal frequency, average meal size, rate of eating, average intermeal interval and satiety ratio) were measured at postnatal day (PNDs) 40, 58, 70, 84, and 98. If not in the monitoring cages, rats were housed together (2 per cage) in their home cage. The intermeal interval was defined as the interval between two meals. Rates of eating were calculated by dividing the average meal size by the average duration of a meal. Finally, the satiety ratio, an index of the noneating (i.e., satiety) time produced by each gram of food consumed, was calculated as the average intermeal interval divided by the average meal size (Zorrilla et al., 2005).

Acute Hyperphagia Assay. Adult rats (≥12 weeks old) were housed individually and after 3 days of acclimatizing, food intake was measured for 5 consecutive days. On day 6, rats received HF diet (45%-AFE, 20% crude protein and 45% fat, 4.54kcal/g AFE, SDS, Witham, United Kingdom) for 4 consecutive days. To measure acute hypophagia, rats were grown up on an HF diet after weaning, and were presented with standard SHP diet at adult age (≥12 weeks old) with the same set-up as described above.

Drugs. Cocaine HCl (O.P.G., Utrecht, The Netherlands) and Yohimbine HCl (Sigma-Aldrich, Zwijndrecht, The Netherlands) were dissolved in sterile saline solution (NaCl, 0.9%).

Food Self-Administration. The food self-administration experiments were conducted in standard, ventilated, and sound-attenuating operant conditioning test chambers (Med Associates Inc.). The chambers were fitted with a dim red house light and two small levers separated 15 cm from each other. Water was available *ad-libitum*. A pellet receptacle was placed in between the levers. One lever was designated as 'active'; lever pressing on this lever resulted in the delivery of one pellet (Dustless Precision pellets®, 45 mg, 10.9% crude protein, 45% fat, and 33.9% carbohydrates; 4.84% kcal/g AFE; Bio-Serv, USA). At the same time a cue light above the active lever was turned on for 5 sec and 6 sound clicks were produced during 3 sec (compound cue). Lever presses on the inactive lever were monitored, but were without consequences. A 15-s time-out period immediately

followed each pellet delivery during which lever pressing was without consequences. A computer interfaced to the chambers was used for equipment operation and data collection. Med PC IV software (Med Associates Inc.) was used to analyze data.

Acquisition (FR1) and progressive ratio (PR) schedules. Adult (≥12 weeks old) *pmch*$^{+/+}$ rats weighing between 330-350 g and *pmch*$^{-/-}$ rats weighing between 280-300g at the beginning of the experiment were used. Body weight and food intake was measured daily during the course of the study. Acquisition phase sessions (3 hr duration, with cues: cue light on for 5 s, 6 sound clicks during 3 s) commenced after 7 days of acclimation to the animal facility and were performed between 1000-1300 h. Rats were allowed to self-administer pellets during 12 daily sessions on an intermittent (1 day) fixed ratio 1 (FR1) schedule of reinforcement. After the FR1 schedule, rats were allowed to self-administer pellets on a progressive ratio (PR) schedule during 4 intermittent (1 day) sessions (3 hr duration, with cues: cue light on for 5 s, 6 sound clicks during 3 s). The successive increase in number of lever presses required to obtain a pellet delivery was calculated by the following equation: Response ratio = (5^(0.2*reward number))-5, rounded to the nearest integer (Richardson and Roberts, 1996). This equation produced the following sequence of required lever presses: 1, 2, 4, 6, 9, 12, 15, 20, 35, 40, 50, 62, 77 etcetera. The final ratio attained was defined as the animal's breakpoint. PR data are also shown as the mean of last 3 PR sessions.

Extinction phases and reinstatement. After the PR sessions, rats were allowed to self-administer pellets at an FR1 schedule for 4 intermittent (1 day) sessions (3 hr duration, with cues: cue light on for 5 s, 6 sound clicks during 3 s). Rats then entered an extinction phase of 22 consecutive daily sessions (1 hr duration, no reward, no cues). After all rats showed stable extinction values (<10 active responses, 5 consecutive sessions), rats were tested for cue-induced relapse (1 hr duration, no reward, 1 cue series at start of session and the ability to respond for the compound cue on an FR1 schedule). Rats then entered an extinction phase of 9 consecutive daily sessions during which responding for the cues was extinguished (1 hr duration, no reward, with cues). After all rats showed stable extinction values (<10 active responses, 5 consecutive sessions), rats were tested for pellet-induced relapse (1 hr duration, no reward, 1 pellet at start of session, with cues). Following 14 additional extinction sessions rats were tested for yohimbine-induced (α_2-andrenergic receptor antagonist; pharmacological stressor) relapse (1 hr duration, no reward, yohimbine (2 mg/kg, 1 ml/kg, intraperitoneal; 30 min prior to start of session, with cues).

Cocaine Self-Administration. Cocaine self-administration experiments were conducted in standard, ventilated, and sound-attenuating operant conditioning test chambers (Med Associates Inc.) as described previously (De Vries et al., 2001). The chambers were fitted with a dim red house light and two small nose-poke holes (2.5 cm i.d.) separated 15 cm from each other. One hole was designated as 'active'; nose poking in this hole resulted in the delivery of 42.52 µl of the drug solution over a period of 2 s. At the same time a yellow cue light inside the nose poke hole was turned on for 2 sec and 6 sound clicks were produced during 3 sec (compound cue). Pokes in the inactive hole were monitored, but were without consequences. A 15-s time-out period immediately followed each infusion during which further nose poking was without consequences. A computer interfaced to the chambers was used for equipment operation and data collection. Med PC IV (Med Associates Inc.) software was used to analyze data.

Surgery. Intravenous silicon catheters (0.6 mm outside diameter, 0.3 mm inside diameter) were surgically implanted in the right jugular vein under isoflurane gas anesthesia. The catheter was secured to the vein with two sutures and passed subcutaneously to the top of the skull. The distal end of the catheter was attached to a connector pedestal (Plastics One, Düsseldorf, DE) anchored to the skull with four surgical screws and dental cement. Catheter potency was maintained by daily infusion of 0.15 ml of a sterile saline solution containing heparin (20 units/ml) and gentamycin (0.08 mg/ml). During the following 7-day recovery period, the rats were housed individually and

handled daily to minimize non-specific stress. Experimental procedures were only performed when the bodyweight recovered to pre-surgery level.

Acquisition (FR1) and progressive ratio (PR) schedules. Adult (≥12 weeks old) *pmch*$^{+/+}$ rats weighing between 340-360 g and *pmch*$^{-/-}$ rats weighing between 280-300 g at the beginning of the experiment were used. Body weight and food intake was measured daily during the course of the study. Acquisition phase sessions (1 hr duration, with cues: cue light on for 2 s, 6 sound click during 3 s) commenced 7 days after surgery while acclimating to the new environment and were performed between 1000-1300 h. Rats were allowed to self-administer cocaine (100 µg/inf. during 6 daily sessions, 200 µg/inf. during 5 daily sessions, and 300 µg/inf. during 5 daily sessions) on a continuous schedule of reinforcement (FR1). The number of cocaine infusions was limited to 40 per session. Under these conditions all rats with intact catheters acquired stable self-administration, i.e. > 90% accuracy (active versus inactive presses). After the rats had reached stable responding for cocaine, they were switched to a PR schedule of reinforcement. Rats were allowed to self-administer during 13 daily PR sessions (300 µg/inf. during 5 sessions, 200 µg/inf. during 4 sessions, and 100 µg/inf. during 4 sessions; 3 hr duration). The number of cocaine infusions was not limited. The successive increase in number of nose pokes required to obtain a drug infusion was calculated by the following equation: Response ratio = (5^(0.2* reward number))-5, rounded to the nearest integer (Richardson and Roberts, 1996). This equation produced the following sequence of required lever presses: 1, 2, 4, 6, 9, 12, 15, 20, 35, 40, 50, 62, 77 etcetera. The final ratio attained was defined as the animal's breakpoint. Daily PR sessions lasted 3 hr or were terminated when 30 min elapsed without a drug infusion. PR data are also shown as the mean of the last 3 PR sessions.

Extinction phases and reinstatement. After the PR sessions, rats were allowed to self-administer cocaine at an FR1 schedule for another 2 sessions Rats then entered an extinction phase of 16 consecutive daily sessions (1 hr duration, no reward, no cues). After all rats showed stable extinction values (<10 active responses, 5 consecutive sessions), rats were tested for cue-induced relapse (1 hr duration, no reward, ability to respond for the compound cue on an FR1 schedule). As rats did not receive rewards, no limit was installed. Rats then entered an extinction phase of 9 consecutive daily sessions during which responding for the cue was extinguished. After all rats showed stable extinction values (<25 active responses, 5 consecutive sessions), rats were tested for drug-primed relapse (1 hr duration, no reward, one cocaine infusion at start of session [10 mg/kg, 1 ml/kg, intraperitoneal], with cues).

Western Blot Procedure and Antibodies. Adult rats (≥10 weeks old) received a saline, a 10mg/kg, or a 20mg/kg intraperitoneal cocaine solution injection (0.5 ml/kg; O.P.G., Utrecht, The Netherlands). Rats were sacrificed during the early afternoon after 10 min and brains were snap-frozen in isopentane. For the dark phase experiment, rats were sacrificed during the 3rd hour of the dark phase after receiving a saline injection. Frozen brains were cut on a cryostat at 250µm and the AcbSh and AcbCo were microdissected in the cryostat (while frozen) for tissue processing and western blotting. Immediately prior to sonication of slices, 70µL of boiling 1% SDS including protease and phosphatase inhibitor cocktails 1 and 2 was added to each tube (Sigma, St. Louis, MO, USA). Following sonication, lysate was boiled for 10 minutes. Tissue was quantitated using a Bio-Rad Laboratories DC assay (Hercules, CA, USA), and 15µg protein was loaded on an Invitrogen Bis-Tris Midi or Mini gel (4-12%) (Carslbad, CA, USA) following the manufacturers instructions. For GluR1 protein detection, membranes were first blotted with the phospho-antibody at 1:500 (rabbit polyclonal, Ser845 and Ser831 antibodies from PhosphoSolutions, Aurora, CO, USA). After secondary detection, membranes were stripped and blotted with a total GluR1 antibody (rabbit polyclonal, 1:1000, Abcam, Cambridge, MA, USA). DARPP-32 antibodies were a generous gift from Dr. Angus Nairn. Rabbit α-Thr^{34} (1:1000) and mouse α-DARPP-32 (1:10,000) were co-

incubated. Following overnight incubation in 1° antibodies at 4°C, blots were incubated in Alexa-conjugated secondary antibodies for 1 hour at 4°C (1:5000, Invitrogen Carlsbad, CA, USA and/or Rockland Immunochemicals, Gilbertsville, PA, USA). Blots were scanned and quantified using a LiCor Odyssey scanner (Lincoln, NE, USA). Fluorescent images were converted to grayscale for figures.

Neurochemical analysis. Adult rats (≥12 weeks old) were decapitated and the caudate putamen (CPu) and nucleus accumbens (NAc) were rapidly dissected from the coronal brain slices. Samples (0.3 x 0.3 x 2 mm) were prepared using a McIlwain tissue chopper, incubated and superfused essentially as described before (Schoffelmeer et al., 1988). Samples were washed twice with Krebs-Ringer bicarbonate medium (in mM; NaCl, 121; KCL, 1.87; KH_2PO_4, 1.17; $MgSO_4$, 1.17; $NaHCO_3$, 25; $CaCl_2$, 1.22 and D-(+)-glucose, 10), followed by preincubation for 15 min in this medium in a constant atmosphere of 95% O_2-5% CO_2 at 37 °C. After preincubation, the samples were washed rapidly with the Krebs-Ringer and incubated for 15 min in 2.5 mL of this medium containing 5 µCi [^{3}H]dopamine in an atmosphere of 95% O_2-5% CO_2 at 37 °C with or without 6 µM GBR-12909 (dopamine reuptake inhibitor; Sigma-Aldrich, Zwijndrecht, the Netherlands). As the CPu and the NAc have a dense noradrenergic innervation, 3.6 µM desipramine (3-isobutyl-1-methyl-xantine [DMI]; Sigma, St. Louis, MO, USA) was added to the medium of these brain structures to prevent accumulation of [^{3}H]dopamine in noradrenergic nerve terminals. After labeling, the samples were washed rapidly and transferred to a chamber of the superfusion apparatus (approximately 4 mg tissue in 0.2 mL volume) and superfused (0.2 mL/min) with medium gassed with 95% O_2-5% CO_2 at 37 °C. In each observation, neurotransmitter release from samples of *pmch*$^{+/+}$ and *pmch*$^{-/-}$ rats was studied simultaneously. After 40 min of superfusion (t = 40 min), the superfusate was collected as 10-min samples. Neurotransmitter release was induced by exposing the samples to electrical biphasic block-pulses (1 Hz, 4 ms at 30 mA) for 10 min at t = 50. The radioactivity remaining at the end of the experiment was extracted from the tissue with 0.1 N HCl. The radioactivity in superfusion fractions and tissue extracts was determined by liquid scintillation counting. The efflux of radioactivity during each collection was expressed as a percentage of the amount of radioactivity in the slices at the beginning of the respective collection period. The electrically evoked release of neurotransmitter was calculated by subtracting the spontaneous efflux of radioactivity from the total overflow of radioactivity during stimulation and the next 10 min. A linear decline from the 10-min interval before to that 20-30 min after the start of stimulation was assumed for calculation of the spontaneous efflux of radioactivity. The evoked release was expressed as percentage of the content of radioactivity of the samples at the start of the stimulation period.

Autoradiographic DAT Assay. Cryostatic coronal sections (10 µm) through mid-striatum from adult rats (≥12 weeks old) were preincubated (20 min, 20°C) in 50mM Tris-HCl 120mM NaCl (pH 7.4), then 60 min in fresh buffer containing 10 pM RTI-55 (2200 Ci/mmol; Perkin Elmer) and 1µM Citalopram and Nisoxetine (Sigma-Aldrich, Zwijndrecht, the Netherlands), with nonspecific binding defined with 100 µM GBR-12909 (Sigma-Aldrich, Zwijndrecht, the Netherlands). Slides were washed twice for 10 min in fresh buffer (4°C), dipped in ice-cold deionised water, airflow dried, exposed to tritium-sensitive film for 5 days with tritium standards, photodeveloped, and analyzed using NIH freeware ImageJ®.

Microdialysis surgery. Rats were anesthetized using isoflurane (2.5%, 400ml/min N_2O, 600ml/min O_2). Lidocaine (10% m/v) was used for local anesthesia. The animals were fixed in a stereotaxic frame and unilaterally implanted with a stainless steel guide cannula (8mm) aimed at the right AcbSh according to previously described procedures (Verheij and Cools, 2007; Verheij et al., 2008). The following coordinates were used: anteroposterior +10.2mm; lateral -0.8mm; dorsoventral -6.0mm (Paxinos and Watson, 2005). The anteroposterior coordinate is relative to the interaural line; the lateral coordinate is relative to the midline suture and the dorsoventral coordinate is

relative to the skull surface. The cannula was fixed onto the skull and anchored with dental cement and stainless steel screws. The guide cannula contained an inner cannula to prevent infections and occlusions. The rats were allowed to recover from surgery for at least 7 days in Plexiglas microdialysis cages (25x25x35cm) for the rest of the experiment. On 3 consecutive days, prior to the start of the microdialysis experiment, each rat was gently picked up and lifted above the top of the home cage in order to habituate them to handling.

Microdialysis procedure. A detailed description of the microdialysis procedure has been published elsewhere (Verheij et al., 2008). In short, a dialysis probe (type A-I-8-02, outer diameter: 0.22mm, 50,000 molecular-weight cut-off) was carefully inserted into the guide cannula. The probe was secured to the guide cannula using a screw. The tip of the dialysis probe protruded 2mm below the distal end of the guide cannula. The probes had an *in vitro* recovery of 10–12% for DA. The inlet and outlet of the probe were connected to a swivel that allowed the rat to move freely inside the microdialysis cage. The dialysis probe was perfused at a rate of 2.0µl/min with Modified Ringer solution (147mM NaCl, 4mM KCl, 1.1mM $CaCl_2.2H_2O$ and 1.1 mM $MgCl_2.6H_2O$, dissolved in ultra pure water, pH7.4). The outflow was collected every 15 minutes in a tube containing 8µl of 0.02M formic acid and kept at -80°C until analyzed. The samples were manually injected into a high performance liquid chromatography (HPLC) system. DA was separated from the remaining neurotransmitters by means of reversed phase, ion-paring liquid chromatography using an Eicompak PP-ODS column (particle size: 2µm, 4.6mm x 30mm) in combination with a mobile phase (0.1M phosphate buffer ($NaH_2PO_4.2H_2O$: $Na_2HPO_4.12H_2O$, ratio 25:4), 2.0mM sodium 1-decanesulphonate and 0.1mM di-sodium EDTA, dissolved in ultra pure water (>18MΩ), pH6.0) containing 1% of methanol. The flow rate was 500µl/min and the system temperature was 25°C. The concentration of DA was measured using electrochemical detection. The working electrode was set at +400 mV against a silver / silver-chloride reference electrode. The accuracy of measurement was within 1.3% and the detection limit was about 30 fg per sample. The system was calibrated using a standard DA solution before each measurement. On the experimental day, a stable baseline level of DA (± 10%) was reached at 4 hr after insertion of the probe (Verheij and Cools, 2007; Verheij et al., 2008), followed by the start of the experiment. After collection of 3 basal samples, a palatable food reward (Kinderchocolade®) was given to the rat and 4 subsequent samples were collected. Subsequently, a saline injection (intraperitoneal) was given followed by the collection of 4 samples. Finally, rats were injected with cocaine (15 mg/kg cocaine, intraperitoneal), followed by the collection of 6 samples. Basal DA levels are expressed as pg DA in a 15 min dialysate sample, and food, saline and cocaine effects are expressed as % of the baseline sample before each manipulation. Only data for the cocaine challenge are shown, because neither food, nor saline elicited a significant DA response.

Microdialysis histology. At the end of the experiment, rats were given an overdose of sodium-pentobarbital (250mg/kg, i.p.) and were intracardially perfused with 60ml 4% paraformaldehyde solution. Vibratome sections (150µm) were cut to determine the correct location of the microdialysis probe.

NAc mRNA expression. Adult rats (≥12 weeks old) were sacrificed during the early afternoon. The NAc was rapidly dissected and snap-frozen in liquid nitrogen**.** Total RNA was isolated using a Trizol method and RNA quantity and quality was assessed using a Nanodrop® ND-1000 spectrophotometer (Thermo-Scientific, Wilmington, DE, USA). cDNA was synthesized from 1µg of total RNA using a RetroScript® kit (Applied Biosystems, Nieuwerkerk a/d Ijssel, NL) as described by the manufacturer, and diluted in MQ (1:2 for *Th* and *Vmat2*; 1:8 for all other genes). Gene expression was quantified with a 7900 HT Real-Time PCR machine (ABI Prism®). Primers for *Cyclophilin*, *Drd1a*, *Drd2*, *GluR1*, *DARPP32*, *Th*, *Vmat2*, *Syn1*, and *Htr2c* were designed using SciTools PrimerQuest (IDT; primers shown in Supplementary Table S1). Primers were optimized

to amplify cDNA but not genomic DNA and to generate a single PCR product. PCR efficiency was between 80% and 120%. In general, 2μl template, 10μM primers, and 5μl SYBRGreen Mix (Applied Biosystems) was used in a 10μl PCR reaction. Thermocycler conditions comprised an initial holding stage at 50°C for 2 min followed by 95°C for 3 min followed by a PCR program consisting of 95°C for 30 sec and 60°C for 30 sec for 40 cycles. Samples were run in triplicates. To control for input, *Cyclophilin* was run on the same plate and used as a control gene. Calculations were performed by a comparative method ($2.0^{-\Delta\Delta Ct}$), taking the efficiency of the PCR into account (1.8-2.2). All experiments were repeated twice after a new cDNA synthesis reaction. Average *pmch*$^{-/-}$ rat gene expression from the three experiments is expressed as a percentage of average *pmch*$^{+/+}$ gene expression.

Data Analysis. Data are expressed as mean ± S.E.M. In figures 3*A* and 3*B*, overall results were analyzed using a two-way Analysis of Variance (ANOVA) with a Bonferroni *post-hoc* correction for multiple comparisons. Meal pattern characteristics (Fig. 1*A-I*), acute hyperphagia (Fig. 1*J*), acute hypophagia (Fig. 1*K*), ongoing food-reinforced responding (Fig. 2*C*, 2*D*), ongoing cocaine-reinforced responding (Fig. 2*F*, 2*G*), the amount of rewards (Fig. S1*A*, S2*A*), and TO lever presses (Fig. S1*B*, S2*B*) data were analyzed by multifactorial analysis of variance, with repeated-measures. If an effect was observed for the meal pattern characteristics (Fig. 1*A-I*), the repeated-measures ANOVA was followed by a Students' *t*-test analysis. For the acute hyperphagia and hypophagia assays, we used a special contrast to investigate if the intake on the test day (HF day1 or SHP day1) was different from the average intake of 5 preceding days (SHP days1-5 or HF days1-5). All other data were analyzed using a Students' *t*-test. All data were analyzed using a commercially available statistical program (SPSS for Macintosh, version 16.0). The null hypothesis was rejected at the 0.05 level.

RESULTS

Feeding behavior in *pmch*$^{-/-}$ rats. *Pmch*$^{-/-}$ rats show diurnal and nocturnal hypophagia (Mul et al., 2010). To investigate which elements of feeding behavior are changed, we analyzed the meal pattern of *pmch*$^{+/+}$ and *pmch*$^{-/-}$ rats at postnatal days [PNDs] 40, 58, 70, 84, and 98. The statistical analysis for body weight revealed significant effects of *time* ($F_{(2,24)} = 1372$; $P < 0.001$), *genotype* ($F_{(1,14)} = 10$; $P < 0.01$), and a *time* x *genotype* interaction ($F_{(2,24)} = 5$; $P < 0.05$; Fig. 1*A*). Body weight of *pmch*$^{-/-}$ rats was reduced at all PNDs ($P < 0.05$, Student's *t*-test; Fig. 1*A*). The statistical analysis for caloric intake revealed significant effects of *time* ($F_{(4,56)} = 10$; $P < 0.001$) and *genotype* ($F_{(1,14)} = 8$; $P < 0.05$), but no *time* x *genotype* interaction ($F_{(4,56)} = 1$; $P = 0.44$; Fig. 1*B*). Caloric intake was reduced in *pmch*$^{-/-}$ rats at PND 40, 84, and 98, and showed a decreased trend at PND 58 and 70 ($P = 0.07$ and $P = 0.12$, respectively, Student's *t*-test; Fig. 1*B*). The statistical analysis for total meal duration revealed significant effects of *time* ($F_{(4,56)} = 15$; $P < 0.001$), but not of *genotype* ($F_{(1,14)} = 0.2$; $P = 0.63$), and no *time* x *genotype* interaction ($F_{(4,56)} = 1$; $P = 0.28$; Fig. 1*C*). Total meal duration did not differ at any PND (Fig. 1*C*). The statistical analysis for average meal duration revealed significant effects of *time* ($F_{(4,56)} = 19$; $P < 0.001$), but not of *genotype* ($F_{(1,14)} = 0.5$; $P = 0.47$), and no *time* x *genotype* interaction ($F_{(4,56)} = 3$; $P = 0.14$; Fig. 1*D*). Average meal duration was only reduced at PND 40 in *pmch*$^{-/-}$ rats compared to *pmch*$^{+/+}$ rats (Fig. 1*D*). The statistical analysis for meal frequency revealed significant effects of *time* ($F_{(4,56)} = 3$; $P < 0.05$), but

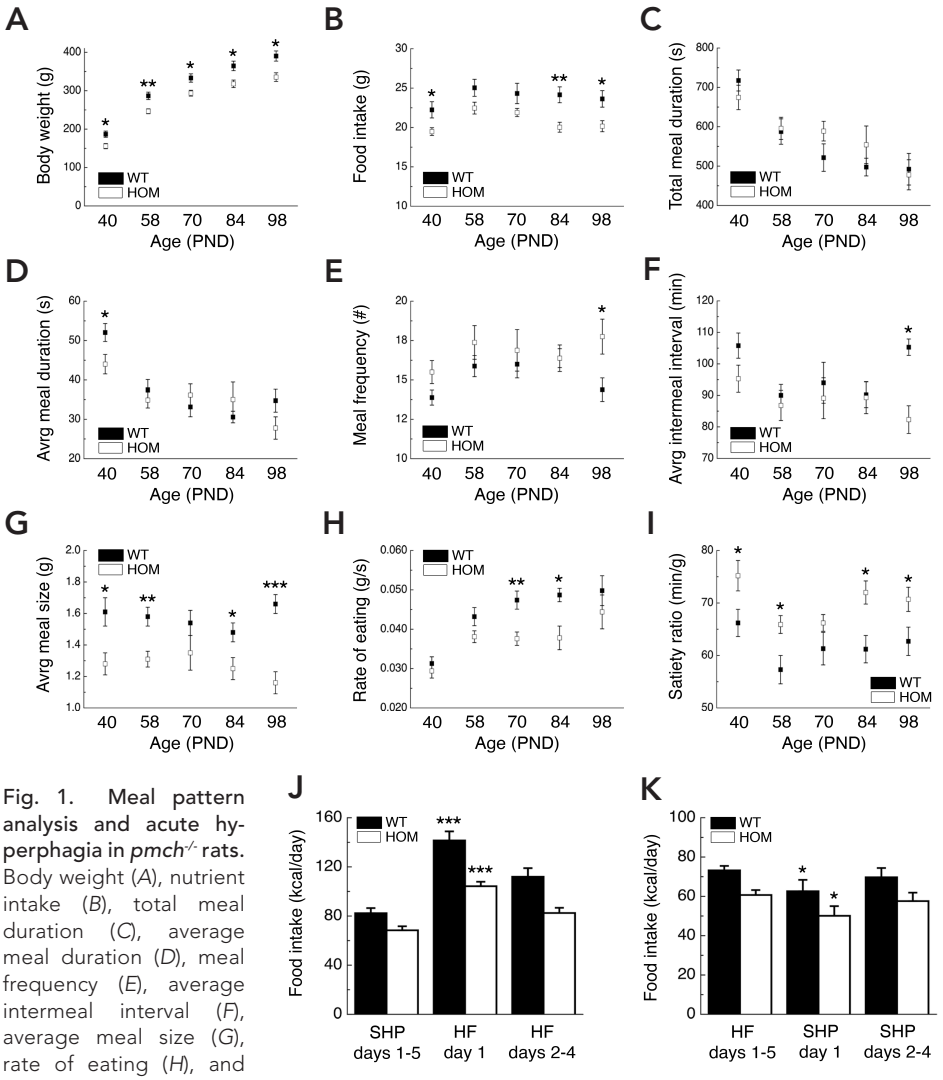

Fig. 1. Meal pattern analysis and acute hyperphagia in *pmch*$^{-/-}$ rats. Body weight (*A*), nutrient intake (*B*), total meal duration (*C*), average meal duration (*D*), meal frequency (*E*), average intermeal interval (*F*), average meal size (*G*), rate of eating (*H*), and satiety ratio (*I*) in *pmch*$^{+/+}$ and *pmch*$^{-/-}$ rats at postnatal day [PND] 40, 58, 70, 84, and 98. Body weight (*A*), nutrient intake (*B*), and average meal size (*G*) are predominantly decreased in *pmch*$^{-/-}$ rats, while satiety ratios (*I*) are predominantly increased in *pmch*$^{-/-}$ rats. Total meal duration (*C*) seems unaffected, while average meal duration (*D*), meal frequency (*E*), and average intermeal interval (*F*) seem unaffected except for PND 40 and 98. Eating rates (*H*) are affected in *pmch*$^{-/-}$ rats at PND 70 and 84 (*$P < 0.05$, **$P < 0.005$, ***$P < 0.001$ by Students' *t*-test; n = 8 per group). (*J*) Adult *pmch*$^{+/+}$ and *pmch*$^{-/-}$ rats showed acute hyperphagia when high-fat palatable food (HF) was presented after being presented with standard chow for 5 consecutive days. However, acute hyperphagia was attenuated in *pmch*$^{-/-}$ rats (172% increase in wild type rats compared to 152% increase in *pmch*$^{-/-}$ rats; ***$P < 0.001$ versus SHP days1-5, by repeated-measures ANOVA with special contrast analysis; n = 7-8 per group). (*K*) Adult *pmch*$^{+/+}$ and *pmch*$^{-/-}$ rats showed acute hypophagia when standard chow was presented after being grown on high-fat palatable food (HF), however in equal quantities (14% decrease in wild type rats compared to 17% decrease in *pmch*$^{-/-}$ rats; *$P < 0.05$ versus HF days1-5, by repeated-measures ANOVA with special contrast analysis; n = 6-8 per group). Data are shown as mean ± S.E.M.

not of *genotype* ($F_{(1,14)}$ = 3; P = 0.13), and no *time* x *genotype* interaction ($F_{(4,56)}$ = 2; P = 0.15; Fig. 1*E*). The statistical analysis for average intermeal interval revealed significant effects of *time* ($F_{(4,56)}$ = 3; $P < 0.05$), but not of *genotype* ($F_{(1,14)}$ = 3; P = 0.13), and no *time* x *genotype* interaction ($F_{(4,56)}$ = 2; P = 0.12; Fig. 1*F*). Both average meal frequency and average intermeal interval were increased at PND 90 in *pmch*$^{-/-}$ rats compared to *pmch*$^{+/+}$ rats, but did not differ at the other PNDs (Fig. 1*E* and *F*). The statistical analysis for average meal size revealed no significant effect of *time* ($F_{(4,56)}$ = 1; P = 0.35), but significant effect of *genotype* ($F_{(1,14)}$ = 14; $P < 0.005$), and a *time* x *genotype* interaction ($F_{(4,56)}$ = 3; $P < 0.05$; Fig. 1*G*). Average meal size in *pmch*$^{-/-}$ rats was reduced at all PNDs compared to *pmch*$^{+/+}$ rats, except for PND 70 (P = 0.20, Student's *t*-test; Fig. 1*G*). The statistical analysis for rate of eating revealed significant effects of *time* ($F_{(4,56)}$ = 19; $P <$ 0.001) and *genotype* ($F_{(1,14)}$ = 7; $P < 0.05$), but no *time* x *genotype* interaction ($F_{(4,56)}$ = 2; P = 0.18; Fig. 1*H*). The rate of eating was reduced at PND 70 and 84 in *pmch*$^{-/-}$ rats compared to *pmch*$^{+/+}$ rats, but did not differ at the other PNDs (Fig. 1*H*). The statistical analysis for satiety ratio revealed significant effects of *time* ($F_{(4,56)}$ = 11; $P < 0.001$) and *genotype* ($F_{(1,14)}$ = 8; $P < 0.05$), but no *time* x *genotype* interaction ($F_{(4,56)}$ = 1; P = 0.35; Fig. 1*H*). Satiety ratios were decreased in *pmch*$^{-/-}$ rats compared to *pmch*$^{+/+}$ rats at all PNDs except PND 70 (Fig. 1*I*). Thus, while the meal pattern dynamics (frequency, duration) seemed relatively unaltered in *pmch*$^{-/-}$ rats, the caloric intake per meal is reduced. To investigate whether the reduced caloric intake per meal was the result of perturbed reward signaling, we measured acute hyperphagia of adult *pmch*$^{+/+}$ and *pmch*$^{-/-}$ rats when offered a palatable high-fat (HF) diet. In addition, acute hypophagia in response to standard chow offered to adult rats grown-up on an HF diet was also investigated. The statistical analysis for acute hyperphagia revealed significant effects of *time* ($F_{(6,77)}$ = 41; $P < 0.001$), *genotype* ($F_{(1,13)}$ = 16; $P < 0.005$), and a *time* x *genotype* interaction ($F_{(6,77)}$ = 41; $P < 0.005$; Fig. 1*J*). Although both *pmch*$^{+/+}$ and *pmch*$^{-/-}$ rats increased their caloric intake significantly during the first day on HF diet ($F_{(1,13)}$ = 191.9; $P < 0.001$), the increase in caloric intake was higher in *pmch*$^{+/+}$ rats compared to *pmch*$^{-/-}$ rats (172% versus 152%, respectively). This indicated a perturbation in reward signaling in *pmch*$^{-/-}$ rats. The statistical analysis for acute hypophagia revealed significant effects of *time* ($F_{(4,46)}$ = 5; $P < 0.005$) and *genotype* ($F_{(1,12)}$ = 14; $P < 0.005$), but no *time* x *genotype* interaction ($F_{(4,77)}$ = 0.5; P = 0.73; Fig. 1*K*). Both *pmch*$^{+/+}$ and *pmch*$^{-/-}$ rats reduced their caloric intake during the first day on SHP diet ($F_{(1,12)}$ = 8; $P < 0.05$), although the decrease was equal between *pmch*$^{+/+}$ and *pmch*$^{-/-}$ rats (86% versus 83%, respectively).

Loss of *Pmch* reduces operant responding for food. As *pmch*$^{-/-}$ rats showed a perturbation in feeding behavior, we set out to investigate if *pmch*$^{-/-}$ rats have a decreased incentive, or motivation, to work for high palatable food pellets. Adult male *pmch*$^{+/+}$ and *pmch*$^{-/-}$ rats were tested in a self-administration paradigm where rats could lever press for high palatable food pellets (Fig. 2*A*). The statistical analysis for total active lever presses during acquisition phase progression (FR1 schedule) revealed significant effects of *time* ($F_{(4,71)}$ = 4; $P < 0.05$), but not of *genotype* ($F_{(1,18)}$ = 1; P = 0.25) and no *time* x *genotype* interaction ($F_{(4,71)}$ = 2; P = 0.19; Fig. 2*C*). *Pmch*$^{+/+}$ rats thus showed an

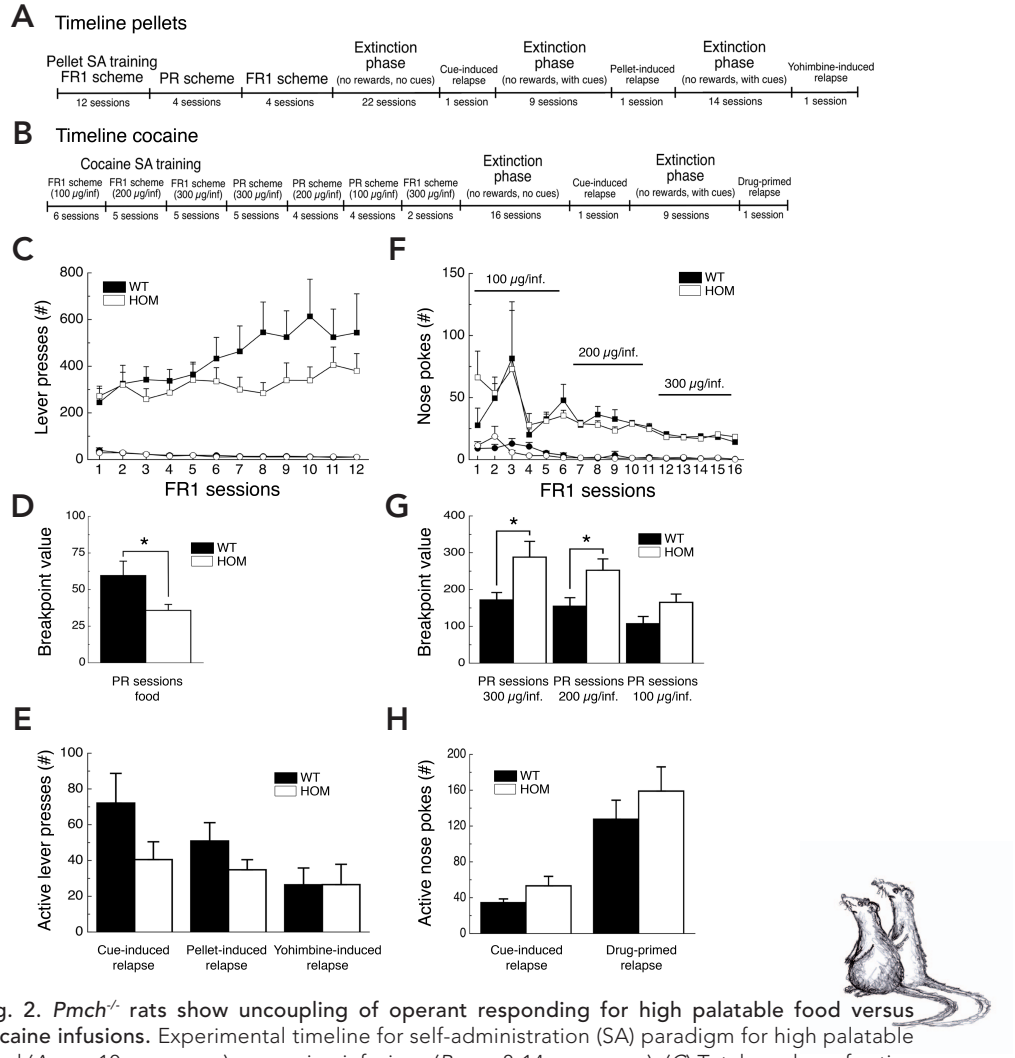

Fig. 2. *Pmch*$^{-/-}$ rats show uncoupling of operant responding for high palatable food versus cocaine infusions. Experimental timeline for self-administration (SA) paradigm for high palatable food (*A*; n = 10 per group) or cocaine infusions (*B*; n = 8-14 per group). (*C*) Total number of active lever presses (squares) and inactive lever presses (circles) for high palatable food pellets. Total number of active lever presses showed an escalation-like effect over time in *pmch*$^{+/+}$ rats on the FR1 schedule of reinforcement compared to *pmch*$^{-/-}$ rats, although this was not significant ($F_{(1,18)}$ = 1.5, P = 0.25). (*D*) Mean breakpoint value of the last 3 PR sessions was decreased in *pmch*$^{-/-}$ rats compared to *pmch*$^{+/+}$ rats. *P < 0.05 by Students' *t*-test. (*E*) *Pmch*$^{-/-}$ rats showed a trend towards decreased responding during cue- or pellet-induced reinstatement of food seeking, but not during a yohimbine-induced reinstatement session (P = 0.12, P = 0.19, P = 0.99, respectively). (*F*) Total number of active nose pokes (squares) and inactive nose pokes (circles) for intravenous cocaine infusions at different infusion concentrations. Total number of active nose pokes was equal between *pmch*$^{+/+}$ and *pmch*$^{-/-}$ rats on an FR1 schedule. (*G*) Mean breakpoint value of the last 3 PR sessions was increased in *pmch*$^{-/-}$ rats compared to *pmch*$^{+/+}$ rats with 300 and 200µg/inf. (*P < 0.05 by Students' *t*-test), and showed an increased trend with 100µg/inf (P = 0.08 by Students' *t*-test). (*H*) *Pmch*$^{-/-}$ rats showed a trend towards increased responding during cue-, or drug-induced (cocaine, 10mg/kg, 1ml/kg intraperitoneal) reinstatement of cocaine seeking (P = 0.15, and P = 0.37, respectively). Data are shown as mean ± S.E.M.

escalation-like effect over time, although not significant compared to *pmch*$^{-/-}$ rats, for total active lever presses. This behavior can be interpreted as a measure of compulsive food-taking behavior (Ghitza et al., 2006). This behavior was however blunted in *pmch*$^{-/-}$ rats. Total inactive lever presses did not differ between genotypes during training (Fig. 2*C*). As the amount of rewards remained stable during the acquisition phase (Fig. S1*A*), the slight increase over time in total active lever presses, predominantly in *pmch*$^{+/+}$ rats, resulted from an escalation-like effect in time out (TO) presses (Fig. S1*B*). Subsequently, the motivation to work for high palatable pellets was determined using a progressive ratio (PR) schedule (Richardson and Roberts, 1996). The mean breakpoint value of the last 3 PR sessions was decreased in *pmch*$^{-/-}$ rats ($P < 0.05$, Student's *t*-test; Fig. 2*D*), indicating that *pmch*$^{-/-}$ rats are less motivated to work for the high palatable food pellets tested here. After extinction (Fig. S1*C*), active lever presses during cue-induced or pellet-induced reinstatement showed a decreased trend in *pmch*$^{-/-}$ rats ($P = 0.12$ and $P = 0.19$, respectively; Student's *t*-test; Fig. 2*E*). Brief exposure to stress can trigger relapse-like behavior, as was shown recently for cocaine seeking in monkeys (Lee et al., 2004). However, reinstatement induced by the pharmacological stressor yohimbine revealed no differences between genotypes ($P = 0.99$, Student's *t*-test; Fig. 2*E*, S1*C*).

Loss of *Pmch* increases operant responding for cocaine. We also set out to investigate whether chronic loss of *Pmch* affects the motivation to obtain drugs of abuse. *Pmch*$^{+/+}$ and *pmch*$^{-/-}$ rats were tested in a self-administration paradigm where rats could nose poke for intravenous cocaine infusions (Fig. 2*B*). During the acquisition phase an FR1 schedule was used with increasing doses of cocaine (100, 200, and 300µg/inf.). The statistical analysis for total active nose pokes during acquisition revealed a significant effect of *time* ($F_{(2,46)} = 3.9$, $P < 0.05$), but no effect of *genotype* ($F_{(1,20)} = 0.02$, $P = 0.88$) and no *time* x *genotype* interaction ($F_{(2,46)} = 3.9$, $P = 0.64$; Fig. 2*F*). Total inactive nose pokes did not differ between genotypes during training (Fig. 2*F*), nor did the amount of infusions (Fig. S2*A*) or active TO nose pokes (Fig. S2*B*). Next, the motivation of the rats to work for intravenous cocaine infusions was tested using a PR schedule (Richardson and Roberts, 1996). The mean breakpoint value of the last 3 PR sessions of each dose was increased in *pmch*$^{-/-}$ rats for the 200 and 300µg/inf. dose ($P < 0.05$, Student's *t*-test), and showed an increased trend for the 100µg/inf. dose ($P = 0.08$, Student's *t*-test; Fig. 2*G*). This indicates that *pmch*$^{-/-}$ rats are more willing to work for the cocaine infusions, an effect that becomes more obvious with a higher cocaine dosage. After extinction (Fig. S2*C*), active nose pokes in *pmch*$^{-/-}$ rats during cue-induced and drug-primed (cocaine, 10mg/kg, 1ml/kg) reinstatement were slightly but not significantly elevated ($P = 0.15$, and $P = 0.37$, respectively; Student's *t*-test; Fig. 2*H*, S2*C*).

Loss of *Pmch* affects the postsynaptic DA system. The above-mentioned behavioral observations indicated changes in reward-related neurochemical signaling in *pmch*$^{-/-}$ rats. For example, it is known that loss of MCH-MCH1R signaling results in a dysregulated mesolimbic DA system (Smith et al., 2005; Pissios et al., 2008). MCH1R is expressed in medium spiny neurons (MSNs) of the AcbSh, coexpressed with D_1R and

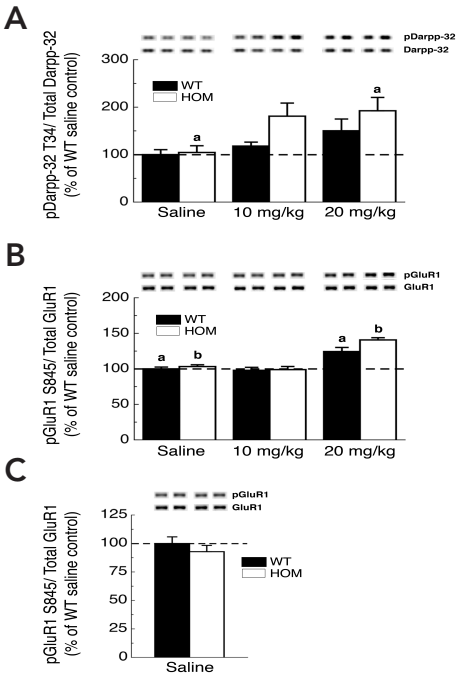

Fig. 3. *Pmch*$^{-/-}$ rats show increased postsynaptic AcbSh DA-related phosphoprotein phosphorylation sensitivity after *in vivo* cocaine treatment. Graphs represent the ratio of phosphorylated signal to total protein signal for all treatments. Representative western blot bands are shown above graphs. Data is shown in comparison to saline-treated *pmch*$^{+/+}$ controls as 100% (dotted line). (*A*) Phosphorylated DARPP32^{Thr34} levels are increased in the AcbSh of *pmch*$^{-/-}$ rats after a 20mg/kg cocaine stimulus compared to saline-treated *pmch*$^{-/-}$ rats, whereas *pmch*$^{+/+}$ rats do not show this effect. Groups labeled with the same letter are statistically different ($P < 0.05$, by 2-way ANOVA, Bonferroni *post-hoc* analysis; n = 4-6 per group). (*B*) Phosphorylated GluR1^{Ser845} levels are increased in the AcbSh of both *pmch*$^{+/+}$ and *pmch*$^{-/-}$ rats after a 20mg/kg cocaine stimulus compared to saline-treated rats. However, pGluR1^{ser845} levels in *pmch*$^{-/-}$ rats after a 20mg/kg cocaine stimulus showed an increased trend compared to 20mg/kg cocaine-treated *pmch*$^{+/+}$ rats ($P = 0.08$, by 2-way ANOVA, Bonferroni *post-hoc* analysis). Groups labeled with the same letter are statistically different ($P < 0.01$, by 2-way ANOVA, Bonferroni *post-hoc* analysis; n = 5-6 per group). (*C*) Basal phosphorylated GluR1^{Ser845} levels in the AcbSh during the 3rd hour of the dark phase were equal between *pmch*$^{+/+}$ and *pmch*$^{-/-}$ rats (n = 10 per group). Data are shown as mean ± S.E.M.

D_2R DA receptors, and signals via multiple G-proteins, including $G_{i/o}$ (Bachner et al., 1999; Hawes et al., 2000; Gao and van den Pol, 2001; Pissios et al., 2003; Georgescu et al., 2005; Chung et al., 2009). MCH1R-$G_{i\alpha}$ activation depresses adenylate cyclase (AC) activation, whereas D_1R activation increases AC activity (Hawes et al., 2000; Greengard, 2001). Cocaine competitively inhibits the DA transporter (DAT), thereby elevating extracellular DA levels preferentially in limbic regions (Carboni et al., 1989; Jones et al., 1995). Cocaine also affects mobilization of a synapsin- and vesicular monoamine transporter (VMAT)-dependent DA reserve pool independent of transporter blockade (Venton et al., 2006; Verheij et al., 2008). Therefore we hypothesized that loss of MCH-MCH1R signaling, through its negative modulation of AC activity, increases phosphorylation of several postsynaptic phosphoproteins, including dopamine and cAMP-regulated phosphoprotein-32 (DARPP-32), via protein kinase and phosphatase cascades that have been described for DA signaling in striatal neurons (Greengard, 2001). To investigate this, *pmch*$^{+/+}$ and *pmch*$^{-/-}$ rats were injected with saline, 10- or 20mg/kg cocaine, and phosphorylation levels of GluR1^{Ser845} and DARPP32^{Thr34} were analyzed.

Immunoblotting for pDARPP32^{Thr34} levels revealed an effect of *treatment* ($F_{(2,24)}$ = 6.6, $P < 0.01$) and *genotype* ($F_{(1,24)}$ = 5.2, $P < 0.05$), but no interaction between them ($F_{(2,24)}$ = 1.1, $P = 0.34$; Fig. 3*A*). Furthermore, pDARPP32^{Thr34} levels of 20mg/kg cocaine-treated *pmch*$^{-/-}$ rats were increased compared to saline-treated *pmch*$^{-/-}$ rats ($P < 0.05$, by 2-way ANOVA, Bonferroni *post-hoc* analysis; Fig. 3*A*), and pDARPP32^{Thr34} levels of 10mg/kg cocaine-treated *pmch*$^{-/-}$ rats showed an increased trend compared to saline-treated *pmch*$^{-/-}$ rats ($P = 0.14$, by 2-way ANOVA, Bonferroni *post-hoc* analysis; Fig. 3*A*). Thus, (1) phosphorylated DARPP32^{Thr34} levels were slightly elevated, although not significant, after a 10mg/kg cocaine stimulus in *pmch*$^{-/-}$ rats, but not in *pmch*$^{+/+}$ rats, and (2) pDARPP32^{Thr34} levels were similarly elevated in *pmch*$^{-/-}$ rats after either a 10- or a 20mg/kg cocaine stimulus (Fig. 3*A*).

Immunoblotting for pGluR1^{ser845} levels revealed an effect of *treatment* ($F_{(2,25)}$ = 18.2, $P < 0.001$), but no effect of *genotype* ($F_{(1,25)}$ = 1.1, $P = 0.31$) and no interaction between them ($F_{(2,25)}$ = 0.2, $P = 0.82$; Fig. 3*B*). Phosphorylated GluR1^{ser845} levels after a 10mg/kg cocaine stimulus did not differ from saline-treated levels in both genotypes, nor were there differences between genotypes (Fig. 3*B*). However, pGluR1^{ser845} levels of a 20mg/kg cocaine stimulus were elevated in both genotypes compared to saline-treated rats ($P < 0.01$, by 2-way ANOVA, Bonferroni *post-hoc* analysis), while pGluR1^{ser845} levels in *pmch*$^{-/-}$ rats showed an increased trend ($P = 0.08$, by 2-way ANOVA, Bonferroni *post-hoc* analysis) compared to *pmch*$^{+/+}$ rats (Fig. 3*B*). All the observed changes were found to be specific for phosphorylation states, as no difference was seen in basal DARPP32 or GluR1 protein levels (Fig. 3*A* and *B*). Taken together, these findings suggest that loss of MCH-MCH1r signaling, including loss of negative modulation of AC activity, increases phosphorylation sensitivity of several phosphoproteins involved in the postsynaptic DA pathway in the AcbSh.

Rats are nocturnal and therefore predominantly feed during the dark phase, although *pmch*$^{-/-}$ rats are hypophagic both during the day and night (Mul et al., 2010). PKA-mediated phosphorylation of GluR1^{ser845} increases channel conductance (Roche et al., 1996), thereby enhancing glutamatergic transmission through the AMPAR, and blockade of AMPARs in the AcbSh increases feeding (Maldonado-Irizarry et al., 1995; Stratford et al., 1998). Therefore we hypothesized that increased phosphorylation sensitivity of D_1R-signaling target pathways leads to increased GluR1-containing AMPAR conductance in *pmch*$^{-/-}$ rats, thus depressing in caloric intake. However, immunoblotting revealed that *ad libitum*-fed saline-treated *pmch*$^{-/-}$ rats have equal pGluR1^{Ser845} levels compared to *pmch*$^{+/+}$ rats during the light phase (Fig. 3*A* and *B*). Moreover, pGluR1^{Ser845} levels were also equal between genotypes during the 3rd hour of the dark phase (Fig. 3*C*). Finally, basal GluR1 protein levels during the 3rd hour of the dark phase were equal between genotypes (Fig. 3*C*). Thus, phosphorylation of GluR1 does not seem responsible for the observed hypophagia after functional loss of *Pmch* in rats.

Loss of *Pmch* affects the presynaptic DA system. The cocaine-induced phosphorylation experiments revealed increased phosphorylation sensitivity for proteins involved in

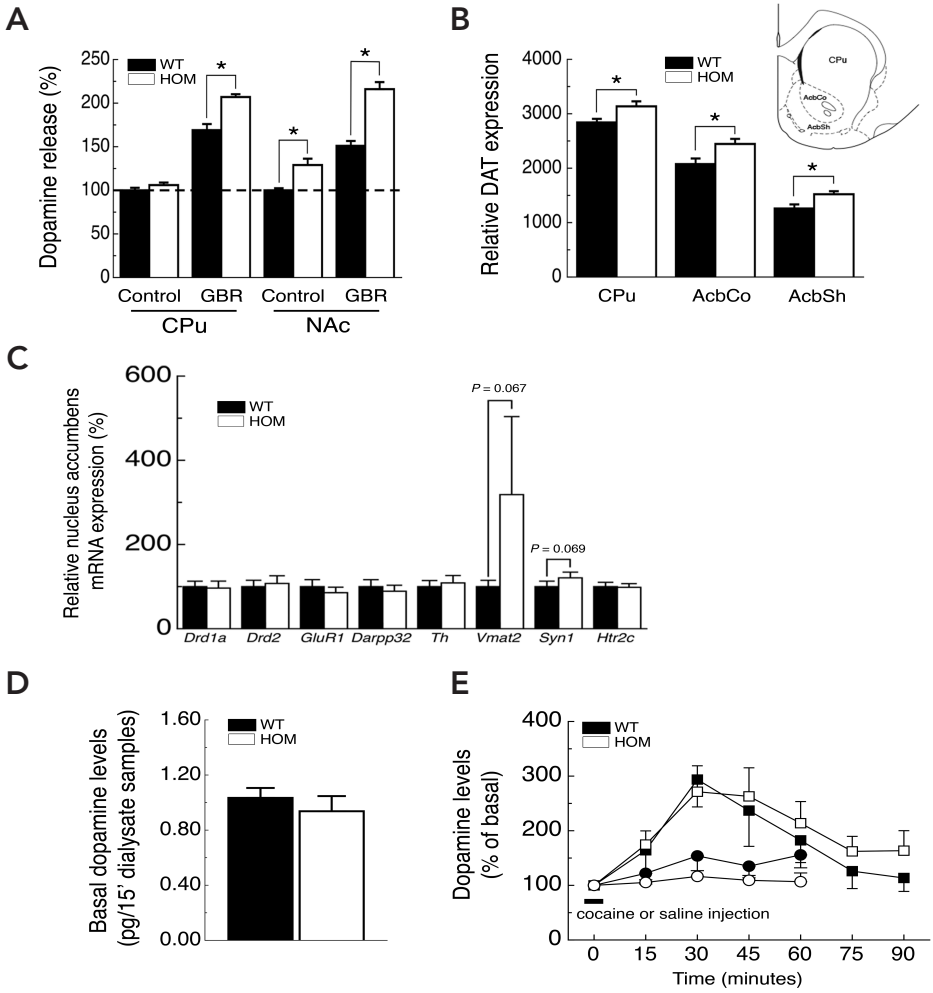

Fig. 4. DA system function in *pmch*$^{-/-}$ rats. (*A*) Electrically evoked control DA release is similar between genotypes in the CPu, but is increased in the NAc of *pmch*$^{-/-}$ rats compared to *pmch*$^{+/+}$ rats. Electrically evoked DA release in both the CPu and NAc of *pmch*$^{-/-}$ rats is increased compared to *pmch*$^{+/+}$ rats after treatment with GBR12909, a highly specific dopamine transporter (DAT) inhibitor. Data is shown in comparison to WT control release as 100% (dotted line). (*$P < 0.05$ by Students' *t*-test; n = 4 per group). (*B*) DAT expression is increased in the CPu, AcbCo, and the AcbSh of *pmch*$^{-/-}$ rats compared to *pmch*$^{+/+}$ rats. Brain areas are indicated on an atlas section from Paxinos and Watson (Paxinos and Watson, 2005) (*$P < 0.05$, by Students' *t*-test; n = 8-11 per group). (*C*) Relative gene expression of a subset of genes involved in dopaminergic storage capacity and DA signaling in the NAc of adult *pmch*$^{+/+}$ and *pmch*$^{-/-}$ rats revealed an increased trend of *Vmat2* and *Syn1* in *pmch*$^{-/-}$ rats compared to *pmch*$^{+/+}$ rats ($P = 0.067$ and $P = 0.069$ by Students' *t*-test, respectively; n = 8-9 per group). (*D*) Basal extracellular DA levels in the AcbSh did not differ between genotypes. (*E*) Extracellular DA levels in the AcbSh after a 15mg/kg cocaine administration (squares) were elevated compared to basal levels ($F_{(5,60)} = 10.2$, $P < 0.005$), but did not differ between genotypes ($F_{(1,12)} = 0.35$, $P = 0.57$). Extracellular DA levels in the AcbSh after a saline administration (circles) did not differ between genotypes ($F_{(1,12)} = 1.7$, $P = 0.22$), or compared to basal levels ($F_{(3,42)} = 2.3$, $P = 0.08$) (n = 7 per group). Data are shown as mean ± S.E.M.

postsynaptic DA signaling. As the increased sensitivity can result from a postsynaptic effect, a presynaptic effect, or a combination of both, we investigated how the DA system is affected in *pmch*$^{-/-}$ rats.

First we investigated if NAc DA release differs between genotypes using challenged conditions in neurochemical experiments (i.e. using electric stimulation). This revealed that electrically evoked DA release *ex vivo* was elevated in acute coronal NAc brain slice preparations from untreated *ad libitum*-fed *pmch*$^{-/-}$ rats compared to untreated *pmch*$^{+/+}$ rats (Fig. 4*A*). Moreover, sample treatment with GBR12909, a highly specific DA transporter (DAT) inhibitor, increased the difference in evoked NAc DA release even further (129% at basal levels vs. 161% with GBR12909 treatment compared to *pmch*$^{+/+}$ rats; Fig. 4*A*), suggesting that NAc DAT protein levels were increased in *pmch*$^{-/-}$ rats, as was recently shown for MCH$^{-/-}$ mice (Pissios et al., 2008). Radioactive ligand binding analysis revealed that NAc DAT protein expression was indeed increased in *pmch*$^{-/-}$ rats, both in the nucleus accumbens core (AcbCo; 118%) and in the AcbSh (121%; Fig. 4*B*). Similar results were observed for the caudate putamen (CPu) in *pmch*$^{-/-}$ rats (Fig. 4*A* and *B*), whereas MCH$^{-/-}$ mice did not show a difference for CPu DAT levels (Pissios et al., 2008).

As *ex vivo* DA release seems to be affected in *pmch*$^{-/-}$ rats, we studied relative gene expression of a subset of genes, involved in dopaminergic storage capacity or signaling, in the NAc of adult *pmch*$^{+/+}$ and *pmch*$^{-/-}$ rats. Relative expression of D_1R (*Drd1a*), D_2R (*Drd2*), GluR1 (*Gria1*), DARPP32 (*Darpp32*), tyrosine hydroxylase (*Th*), and 5-hydroxytryptamine (serotonin) receptor 2c (*Htr2c*) was unchanged between genotypes (Fig. 4*C*). However, relative expression of VMAT2 (*Vmat2*) and Synapsin 1 (*Syn1*) showed an increased trend in *pmch*$^{-/-}$ rats compared to *pmch*$^{+/+}$ rats (P = 0.067 and P = 0.069 by Students' t-test, respectively; Fig. 5). *Vmat2* is responsible for transmitter loading of synaptic vesicles (Edwards, 1992), is preferentially expressed in the CNS (Peter et al., 1995; Erickson et al., 1996), and increased expression of *Vmat2* increases NAc dopaminergic storage capacity (Verheij et al., 2008). The G protein subunits, G_{o2} and $G_{\alpha o2}$, are involved in the negative regulation of VMAT2 activity (Holtje et al., 2000), whereas the MCH-MCH1r system signals via $G_{i/o}$ (Hawes et al., 2000). Synapsin 1 controls the fraction of synaptic vesicles available for release (Greengard et al., 1993), and elevated *Syn1* expression can thereby increase the efficiency of DA release observed in *pmch*$^{-/-}$ rats in this study. Therefore, our data indicate that loss of the negative modulation of MCH-MCH1R signaling via $G_{i/o}$ also results in an additional effect on vesicle dynamics in the presynaptic terminal. In addition, the elevated DAT levels in *pmch*$^{-/-}$ rats can amplify the increased dopaminergic release capacity.

Subsequently we investigated if the postsynaptic phosphorylation sensitivity in *pmch*$^{-/-}$ rats results from intracellular postsynaptic adaptations, or predominantly from presynaptic adaptations (i.e. elevated extracellular DA levels). To study this, we measured *in vivo* extracellular DA levels using classical microdialysis under non-challenged conditions (i.e. in habituated rats) after intraperitoneal administration of a saline stimulus or after a 15mg/kg cocaine stimulus. Basal *in vivo* extracellular

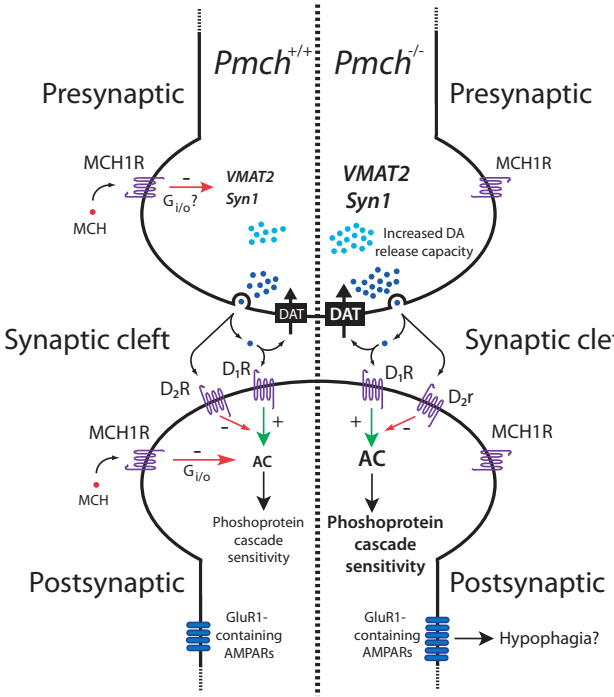

Fig. 5. Simplified schematic overview of the dopaminergic system in the NAc of *pmch*$^{+/+}$ and *pmch*$^{-/-}$ rats. Loss of presynaptic MCH-MCH1R signaling, likely mediated via $G_{i/o}$, increases dopaminergic release capacity in *pmch*$^{-/-}$ rats by affecting gene expression of *Vmat2* and *Syn1*. Indeed, increased DA amounts in the reserve pool (light blue circles) and the release-ready pool (dark blue circles) can be observed under challenged conditions *ex vivo*. DAT protein levels are increased in the NAc of *pmch*$^{-/-}$ rats to compensate for this effect. Binding of DA to the D1 subclass of dopamine receptors increases AC activity, whereas binding of DA to the D2 subclass of dopamine receptors inhibits the D_1R-mediated increase of AC activity. Loss of postsynaptic MCH1R-$G_{i/o}$-mediated negative modulation of AC activity increases AC activity in *pmch*$^{-/-}$ rats. As a result, increased phosphoprotein cascade sensitivity is observed in these rats. A recent report has shown that MCH can decrease the amount of cell surface GluR1-containing AMPARs, subsequently depressing MSN excitability (Robert Sears, unpublished data). Loss of functional *Pmch* can thus potentially result in an increased amount of cell surface GluR1-containing AMPARs, thus increasing MSN excitability and potentially inducing hypophagia of *pmch*$^{-/-}$ rats. Multiple additional neurotransmitters affect dopaminergic signaling in MSNs (Greengard, 2001). Therefore, a role for additional putative effectors in our proposed scheme should not be excluded. Green line (+) = stimulatory; red line (-) = inhibitory.

AcbSh DA levels did not differ between genotypes (Fig. 4*D*), and *in vivo* saline-evoked extracellular AcbSh DA levels revealed no effect of *time* ($F_{(3,42)}$ = 2.3, P = 0.08), no effect of *genotype* ($F_{(1,12)}$ = 1.7, P = 0.22) and no *time* x *genotype* interaction ($F_{(3,42)}$ = 1.2, P = 0.31; Fig. 4*E*). In contrast, *in vivo* cocaine-evoked extracellular AcbSh DA levels did reveal an effect of *time* ($F_{(5,60)}$ = 10.2, P < 0.005), but no effect of *genotype* ($F_{(1,12)}$ = 0.35, P = 0.57) and no *time* x *genotype* interaction ($F_{(5,60)}$ = 0.4, P = 0.87; Fig. 4*E*).

Taken together, our findings indicate that loss of MCH-MCH1R signaling has a presynaptic effect on striatal DA storage and release capacity, in addition to a postsynaptic effect on DA signaling. Moreover, they also indicate that the postsynaptic phosphorylation sensitivity in *pmch*$^{-/-}$ rats observed in this study resulted solely from loss of the negative AC modulation via $G_{i/o}$-mediated MCH-MCH1R signaling during non-challenged conditions. However, during challenged conditions (i.e. a single high dose or repeated cocaine stimuli), the presynaptic adaptations can amplify postsynaptic phosphorylation sensitivity in *pmch*$^{-/-}$ rats through elevation of extracellular DA levels. In summary, the increased DAT levels after functional loss of *Pmch* appear to be a crucial compensatory mechanism to minimize relative increased extracellular DA levels under challenged-conditions, thereby depressing postsynaptic phosphorylation sensitivity.

DISCUSSION

Here we showed that loss of *Pmch* in the rat reduced meal size and operant responding for high palatable food pellets, but increased operant responding for cocaine infusions. To the best of our knowledge, this is the first rat model that shows this clear behavioral uncoupling. Moreover, using an array of behavioral and biochemical assays, we show that loss of *Pmch* affected the striatal DA system on a presynaptic and postsynaptic level. Although parts of our rat data strengthen findings in mice models, the majority of our observations is novel and provides strong heuristic value to reward-related research regarding MCH.

A selective reduction in meal size in *pmch*$^{-/-}$ rats is consistent with the finding that acute MCH1R-antagonism decreased meal size, and not meal frequency (Kowalski et al., 2004). MCH immunoreactive fibers innervate nucleus of the solitary tract regions (NTS) (Bittencourt and Elias, 1998). Therefore, MCH-deficiency potentially removes the inhibitory effect of MCH on glutamate transmission between primary vagal afferents and NTS neurons (Zheng et al., 2005), decreasing meal size and caloric intake. However, 4th ventricle MCH injections had no effect on caloric intake (Zheng et al., 2005). Thus, it is unlikely that a reduced meal size results from lack of MCH signaling at the level of the brainstem. However, we cannot exclude that satiety factors integrated outside the brain stem are affected in our rat model. This leaves the Arc, PVN, DMN, and the AcbSh as primary effecter sites of MCH (Abbott et al., 2003; Georgescu et al., 2005; Zheng et al., 2005). Changes in reward-related neurochemistry and behavior observed here and other studies (Georgescu et al., 2005; Smith et al., 2005; Pissios et al., 2008) indicate that the AcbSh is a likely converging site to exert the orexigenic action of MCH.

During acute hyperphagia, induced by exposure to palatable food, *pmch*$^{-/-}$ rats showed a blunted caloric intake increase compared to *pmch*$^{+/+}$ rats, while during induced acute hypophagia, the reduction in caloric intake was equal. This indicates that the perturbed reward-related behavior in *pmch*$^{-/-}$ rats is only observed under acute reward stimulatory conditions. MCH$^{-/-}$ mice, bred on a C57BL6 background, demonstrated no acute overfeeding, and surprisingly, displayed no hypophagia (Pissios et al., 2008).

Pmch$^{-/-}$ rats were less motivated to work for high palatable food. Our observations align with recent findings that acute MCH1R blockade reduces food-reinforced operant responding (Nair et al., 2009). Loss of *Pmch* also tended to decrease pellet- or cue-induced reinstatement of food seeking, but these effects did not reach statistical significance. Relapse induced by the pharmacological stressor yohimbine, a measure of stress-induced relapse behavior (Ghitza et al., 2006), was similar between genotypes. In contrast, *pmch*$^{-/-}$ rats were more motivated to work for cocaine. *Pmch*$^{-/-}$ rats also tended to be more sensitive to cocaine- or cue-induced reinstatement of cocaine seeking following extinction, a validated animal model of relapse (Epstein et al., 2006).

The latter observations are in clear contrast to the recently published data of Chung *et al.*, showing that acute MCH1R blockade in the rat AcbSh decreased motivation to work for cocaine (Chung et al., 2009). As the used self-administration paradigms were practically identical, an explanation for the different observations must lie in the different animal models (acute blockade of MCH1R-signaling versus chronic loss of *Pmch*). It suggests that the adult drug phenotype in *pmch*$^{-/-}$ rats results from developmental abnormalities, or compensations by other neural systems. For example, it was recently shown that MCH affects neurite outgrowth (Cotta-Grand et al., 2009). Therefore, loss of MCH signaling during early development could affect neuronal differentiation. Additionally, to date, only MCH has been shown to bind and activate MCH1R (Chambers et al., 1999; Lembo et al., 1999; Saito et al., 1999), whereas *Pmch* also encodes N-EI and N-GE (Nahon et al., 1989). Although N-GE so far does not seem to have a biological function, N-EI has been implicated in DA system modulation in several brain regions (Bittencourt and Celis, 2008). Therefore, loss of these two neuropeptides could contribute to the phenotype observed in this study. Finally, a difference in rat strains used (Wistar versus Sprague-Dawley) might also play a role.

Loss of *Pmch* had a postsynaptic effect on the striatal DA system. Our observations indicated increased postsynaptic phosphorylation sensitivity of DARPP32 and GluR1 in *pmch*$^{-/-}$ rats compared to *pmch*$^{+/+}$ rats after a systemic cocaine stimulus. MCH administration decreases phosphorylation of DA-signaling targets through $G_{i/o}$-mediated signaling (Robert Sears, unpublished data). Thus, as observed in this study, loss of MCH-MCH1R signaling can relatively increase *in vivo* phosphorylation of DARPP32 and GluR1 compared to a wild type situation (Fig. 5). In addition, basal extracellular *in vivo* DA levels and cocaine-evoked extracellular *in vivo* DA levels in the AcbSh did not differ between genotypes with a 15mg/kg dose. This indicates that the increased phosphorylation of DARPP32 and GluR1 in *pmch*$^{-/-}$ rats compared to *pmch*$^{+/+}$ rats, observed after a cocaine dose in the same range (10- or 20mg/kg), resulted solely from direct postsynaptic adaptations. Activation of MCH1R-$G_{i\alpha}$ depresses adenylate cyclase (AC) activity (Hawes et al., 2000), whereas D_1R activation increases AC activity (Greengard, 2001). Therefore, lack of MCH1R-signaling enhances D_1R-mediated activation of AC, thus increasing postsynaptic phosphorylation sensitivity (Fig. 5).

Loss of *Pmch* also affects the presynaptic DA system, in addition to a postsynaptic effect. We observed increased DAT levels and increased presynaptic dopaminergic

release capacity in the NAc of *pmch*$^{-/-}$ rats. The latter observation seems to result from elevated relative expression of *Vmat2* and *Syn1*. We propose that this effect results from loss of presynaptic MCH1R-$G_{i/o}$ signaling (Fig. 5). Interestingly, mice overexpressing DAT showed reduced operant responding for milk, and increased sensitivity to the rewarding effects of amphetamine (Salahpour et al., 2008). Although the behavioral uncoupling in these mice is not as clear or well documented as in this study, both studies demonstrate the importance of DAT levels regarding the correct regulation of DA-induced reward mechanisms.

Pmch$^{-/-}$ rats are hypophagic (Mul et al., 2010), but the exact mechanism behind the hypophagia is still unknown. MCH blocks DA-induced phosphorylation of GluR1^{ser845} in the AcbSh (Georgescu et al., 2005). As we did not observe differences in pGluR1^{ser845} levels between genotypes during the light or the dark phase, we exclude that changes in pGluR1^{ser845} levels are causal to the hypophagia observed in *pmch*$^{-/-}$ rats. Also, it has been demonstrated that MCH reduced MSN excitability by decreasing the amount of cell-surface GluR1-containing AMPARs (Robert Sears, unpublished data). This indicates that not the relative phosphorylation state, but rather the amount of GluR1-containing AMPARs could be causal to the hypophagia in *pmch*$^{-/-}$ rats (Fig. 5). Finally, involvement of MCH1R-signaling in other areas, such as the PVN and DMN can also contribute to the phenotypes observed in this study, and therefore remain to be studied in more detail.

Pmch$^{-/-}$ rats showed increased cocaine-reinforced operant responding. Elevation of PKA activity within the NAc increases responding for cocaine in a PR schedule, and results in persistent motivational changes (Lynch and Taylor, 2005). Increased PKA activation, resulting from a loss of postsynaptic inhibitory MCH-MCH1R signaling in combination with increased extracellular DA levels through DAT blockade by repeated cocaine administration, could therefore be at the basis of the drug phenotype observed *in pmch*$^{-/-}$ rats in this study.

MCH signaling between the LHA and the NAc has been implicated in communicating the hedonic, or rewarding aspects of feeding (Saper et al., 2002). Since repeated exposure to sugar sensitizes the response to drugs of abuse, it has been proposed that common neural substrates mediate these effects (Le Merrer and Stephens, 2006). Thus one would expect that loss of MCH signaling would effect motivation to obtain palatable food or drugs of abuse in a similar manner. We here showed that this is not the case and propose that MCH signaling selectively mediates motivation for food and thus provides a crucial signal with which hypothalamic neural circuits controlling energy balance guide frontal brain areas to shift motivation towards food. Without MCH signaling, motivation away from food prevails.

In summary, we confirm that MCH is an important regulator of motivational behavior by affecting limbic DA function (Pissios et al., 2008; Chung et al., 2009), an ability that is shared by other LHA factors (Harris et al., 2005; Leinninger et al., 2009). Incorrect control of caloric intake is one of the hallmarks for developing or maintaining obesity, and the development of MCH1R-antagonists could be a possible way to reverse obesity. We

have recently shown that *Pmch* expression is important during early development and puberty, and that loss of MCH-MCH1R signaling lowers the body weight set point (Mul et al., 2010), indicating that an MCH1R-antagonist-based treatment could be especially effective in obese children. However, potential use of long-term MCH1R-antagonism as an anti-obesity treatment in young children might result in developmental effects that increase vulnerability to drugs of abuse during adulthood.

ACKNOWLEDGEMENTS

We gratefully acknowledge Pim Toonen animal genotyping, Sabine Grol, Delphi Coppens, and Wendy de Vries for initial animal studies and data analysis, Mieneke Luijendijk for initial meal pattern analysis, Rea van Rozen for help with the autoradiographic DAT assay, and François Hogenboom, Rob Binnekade and Yvar van Mourik for excellent animal care and tissue isolation.

REFERENCES

Abbott CR, Kennedy AR, Wren AM et al. (2003) Identification of hypothalamic nuclei involved in the orexigenic effect of melanin-concentrating hormone. Endocrinology 144:3943-3949.

Alon T, Friedman JM (2006) Late-onset leanness in mice with targeted ablation of melanin concentrating hormone neurons. J Neurosci 26:389-397.

Bachner D, Kreienkamp H, Weise C et al. (1999) Identification of melanin concentrating hormone (MCH) as the natural ligand for the orphan somatostatin-like receptor 1 (SLC-1). FEBS Lett 457:522-524.

Bittencourt J, Celis ME (2008) Anatomy, function and regulation of neuropeptide EI (NEI). Peptides 29:1441-1450.

Bittencourt JC, Elias CF (1998) Melanin-concentrating hormone and neuropeptide EI projections from the lateral hypothalamic area and zona incerta to the medial septal nucleus and spinal cord: a study using multiple neuronal tracers. Brain Res 805:1-19.

Bittencourt JC, Presse F, Arias C et al. (1992) The melanin-concentrating hormone system of the rat brain: an immuno- and hybridization histochemical characterization. The Journal of comparative neurology 319:218-245.

Carboni E, Imperato A, Perezzani L et al. (1989) Amphetamine, cocaine, phencyclidine and nomifensine increase extracellular dopamine concentrations preferentially in the nucleus accumbens of freely moving rats. Neuroscience 28:653-661.

Chambers J, Ames RS, Bergsma D et al. (1999) Melanin-concentrating hormone is the cognate ligand for the orphan G-protein-coupled receptor SLC-1. Nature 400:261-265.

Chen Y, Hu C, Hsu CK et al. (2002) Targeted disruption of the melanin-concentrating hormone receptor-1 results in hyperphagia and resistance to diet-induced obesity. Endocrinology 143:2469-2477.

Chung S, Hopf FW, Nagasaki H et al. (2009) The melanin-concentrating hormone system modulates cocaine reward. Proc Natl Acad Sci U S A.

Cotta-Grand N, Rovere C, Guyon A et al. (2009) Melanin-concentrating hormone induces neurite outgrowth in human neuroblastoma SH-SY5Y cells through p53 and MAPKinase signaling pathways. Peptides 30:2014-2024.

De Vries TJ, Shaham Y, Homberg JR et al. (2001) A cannabinoid mechanism in relapse to cocaine seeking. Nat Med 7:1151-1154.

Della-Zuana O, Presse F, Ortola C et al. (2002) Acute and chronic administration of melanin-concentrating hormone enhances food intake and body weight in Wistar and Sprague-Dawley rats. Int J Obes Relat Metab Disord 26:1289-1295.

Edwards RH (1992) The transport of neurotransmitters into synaptic vesicles. Curr Opin Neurobiol 2:586-594.

Epstein DH, Preston KL, Stewart J et al. (2006) Toward a model of drug relapse: an assessment of the validity of the reinstatement procedure. Psychopharmacology (Berl) 189:1-16.

Erickson JD, Schafer MK, Bonner TI et al. (1996) Distinct pharmacological properties and distribution in neurons and endocrine cells of two isoforms of the human vesicular monoamine transporter. Proc Natl Acad Sci U S A 93:5166-5171.

Gao XB, van den Pol AN (2001) Melanin concentrating hormone depresses synaptic activity of glutamate and GABA neurons from rat lateral hypothalamus. J Physiol 533:237-252.

Georgescu D, Sears RM, Hommel JD et al. (2005) The hypothalamic neuropeptide melanin-concentrating hormone acts in the nucleus accumbens to modulate feeding behavior and forced-swim performance. J Neurosci 25:2933-2940.

Ghitza UE, Gray SM, Epstein DH et al. (2006) The anxiogenic drug yohimbine reinstates palatable food seeking in a rat relapse model: a role of CRF1 receptors. Neuropsychopharmacology 31:2188-2196.

Gomori A, Ishihara A, Ito M et al. (2003) Chronic intracerebroventricular infusion of MCH causes obesity in mice. Melanin-concentrating hormone. Am J Physiol Endocrinol Metab 284:E583-588.

Greengard P (2001) The neurobiology of slow synaptic transmission. Science (New York, NY 294:1024-1030.

Greengard P, Valtorta F, Czernik AJ et al. (1993) Synaptic vesicle phosphoproteins and regulation of synaptic function. Science (New York, NY 259:780-785.

Guesdon B, Paradis E, Samson P et al. (2009) Effects of intracerebroventricular and intra-accumbens melanin-concentrating hormone agonism on food intake and energy expenditure. Am J Physiol Regul Integr Comp Physiol 296:R469-475.

Harris GC, Wimmer M, Aston-Jones G (2005) A role for lateral hypothalamic orexin neurons in reward seeking. Nature 437:556-559.

Hawes BE, Kil E, Green B et al. (2000) The melanin-concentrating hormone receptor couples to multiple G proteins to activate diverse intracellular signaling pathways. Endocrinology 141:4524-4532.

Hervieu GJ, Cluderay JE, Harrison D et al. (2000) The distribution of the mRNA and protein products of the melanin-concentrating hormone (MCH) receptor gene, slc-1, in the central nervous system of the rat. Eur J Neurosci 12:1194-1216.

Holtje M, von Jagow B, Pahner I et al. (2000) The neuronal monoamine transporter VMAT2 is regulated by the trimeric GTPase Go(2). J Neurosci 20:2131-2141.

Ito M, Gomori A, Ishihara A et al. (2003) Characterization of MCH-mediated obesity in mice. Am J Physiol Endocrinol Metab 284:E940-945.

Ito M, Ishihara A, Gomori A et al. (2009) Mechanism of the anti-obesity effects induced by a novel Melanin-concentrating hormone 1-receptor antagonist in mice. Br J Pharmacol.

Jones SR, Garris PA, Wightman RM (1995) Different effects of cocaine and nomifensine on dopamine uptake in the caudate-putamen and nucleus accumbens. J Pharmacol Exp Ther 274:396-403.

Kowalski TJ, Farley C, Cohen-Williams ME et al. (2004) Melanin-concentrating hormone-1 receptor antagonism decreases feeding by reducing meal size. Eur J Pharmacol 497:41-47.

Le Merrer J, Stephens DN (2006) Food-induced behavioral sensitization, its cross-sensitization to cocaine and morphine, pharmacological blockade, and effect on food intake. J Neurosci 26:7163-7171.

Lee B, Tiefenbacher S, Platt DM et al. (2004) Pharmacological blockade of alpha2-adrenoceptors induces reinstatement of cocaine-seeking behavior in squirrel monkeys. Neuropsychopharmacology 29:686-693.

Leinninger GM, Jo YH, Leshan RL et al. (2009) Leptin acts via leptin receptor-expressing lateral hypothalamic neurons to modulate the mesolimbic dopamine system and suppress feeding. Cell Metab 10:89-98.

Lembo PM, Grazzini E, Cao J et al. (1999) The receptor for the orexigenic peptide melanin-concentrating hormone is a G-protein-coupled receptor. Nat Cell Biol 1:267-271.

Ludwig DS, Tritos NA, Mastaitis JW et al. (2001) Melanin-concentrating hormone overexpression in transgenic mice leads to obesity and insulin resistance. J Clin Invest 107:379-386.

Lynch WJ, Taylor JR (2005) Persistent changes in motivation to self-administer cocaine following modulation of cyclic AMP-dependent protein kinase A (PKA) activity in the nucleus accumbens. Eur J Neurosci 22:1214-1220.

Maldonado-Irizarry CS, Swanson CJ, Kelley AE (1995) Glutamate receptors in the nucleus accumbens shell control feeding behavior via the lateral hypothalamus. J Neurosci 15:6779-6788.

Marsh DJ, Weingarth DT, Novi DE et al. (2002) Melanin-concentrating hormone 1 receptor-deficient mice are lean, hyperactive, and hyperphagic and have altered metabolism. Proc Natl Acad Sci U S A 99:3240-3245.

Mul JD, Yi CX, van den Berg SA et al. (2010) Pmch expression during early development is critical for normal energy homeostasis. Am J Physiol Endocrinol Metab 298:E477-488.

Nahon JL, Presse F, Bittencourt JC et al. (1989) The rat melanin-concentrating hormone messenger ribonucleic acid encodes multiple putative neuropeptides coexpressed in the dorsolateral hypothalamus. Endocrinology 125:2056-2065.

Nair SG, Adams-Deutsch T, Pickens CL et al. (2009) Effects of the MCH1 receptor antagonist SNAP 94847 on high-fat food-reinforced operant responding and reinstatement of food seeking in rats. Psychopharmacology (Berl).

Paxinos G, Watson C (2005) The Rat Brain in Stereotaxic Coordinates. New York: Academic Press.

Peter D, Liu Y, Sternini C et al. (1995) Differential expression of two vesicular monoamine transporters. J Neurosci 15:6179-6188.

Pissios P, Trombly DJ, Tzameli I et al. (2003) Melanin-concentrating hormone receptor 1 activates extracellular signal-regulated kinase and synergizes with G(s)-coupled pathways. Endocrinology 144:3514-3523.

Pissios P, Frank L, Kennedy AR et al. (2008) Dysregulation of the mesolimbic dopamine system and reward in MCH-/- mice. Biol Psychiatry 64:184-191.

Qu D, Ludwig DS, Gammeltoft S et al. (1996) A role for melanin-concentrating hormone in the central regulation of feeding behaviour. Nature 380:243-247.

Richardson NR, Roberts DC (1996) Progressive ratio schedules in drug self-administration studies in rats: a method to evaluate reinforcing efficacy. J Neurosci Methods 66:1-11.

Roche KW, O'Brien RJ, Mammen AL et al. (1996) Characterization of multiple phosphorylation sites on the AMPA receptor GluR1 subunit. Neuron 16:1179-1188.

Rossi M, Choi SJ, O'Shea D et al. (1997) Melanin-concentrating hormone acutely stimulates feeding, but chronic administration has no effect on body weight. Endocrinology 138:351-355.

Saito Y, Nothacker HP, Wang Z et al. (1999) Molecular characterization of the melanin-concentrating-hormone receptor. Nature 400:265-269.

Salahpour A, Ramsey AJ, Medvedev IO et al. (2008) Increased amphetamine-induced hyperactivity and reward in mice overexpressing the dopamine transporter. Proc Natl Acad Sci U S A 105:4405-4410.

Saper CB, Chou TC, Elmquist JK (2002) The need to feed: homeostatic and hedonic control of eating. Neuron 36:199-211.

Schoffelmeer AN, Rice KC, Jacobson AE et al. (1988) Mu-, delta- and kappa-opioid receptor-mediated inhibition of neurotransmitter release and adenylate cyclase activity in rat brain slices: studies with fentanyl isothiocyanate. European journal of pharmacology 154:169-178.

Shimada M, Tritos NA, Lowell BB et al. (1998) Mice lacking melanin-concentrating hormone are hypophagic and lean. Nature 396:670-674.

Silva JP, von Meyenn F, Howell J et al. (2009) Regulation of adaptive behaviour during fasting by hypothalamic Foxa2. Nature 462:646-650.

Sita LV, Elias CF, Bittencourt JC (2007) Connectivity pattern suggests that incerto-hypothalamic area belongs to the medial hypothalamic system. Neuroscience 148:949-969.

Smith DG, Tzavara ET, Shaw J et al. (2005) Mesolimbic dopamine super-sensitivity in melanin-concentrating hormone-1 receptor-deficient mice. J Neurosci 25:914-922.

Snyder JS, Choe JS, Clifford MA et al. (2009) Adult-born hippocampal neurons are more numerous, faster maturing, and more involved in behavior in rats than in mice. J Neurosci 29:14484-14495.

Stratford TR, Swanson CJ, Kelley A (1998) Specific changes in food intake elicited by blockade or activation of glutamate receptors in the nucleus accumbens shell. Behav Brain Res 93:43-50.

Todtenkopf MS, Parsegian A, Naydenov A et al. (2006) Brain reward regulated by AMPA receptor subunits in nucleus accumbens shell. J Neurosci 26:11665-11669.

Venton BJ, Seipel AT, Phillips PE et al. (2006) Cocaine increases dopamine release by mobilization of a synapsin-dependent reserve pool. J Neurosci 26:3206-3209.

Verheij MM, Cools AR (2007) Differential contribution of storage pools to the extracellular amount of accumbal dopamine in high and low responders to novelty: effects of reserpine. J Neurochem 100:810-821.

Verheij MM, de Mulder EL, De Leonibus E et al. (2008) Rats that differentially respond to cocaine differ in their dopaminergic storage capacity of the nucleus accumbens. J Neurochem 105:2122-2133.

Zheng H, Patterson LM, Morrison C et al. (2005) Melanin concentrating hormone innervation of caudal brainstem areas involved in gastrointestinal functions and energy balance. Neuroscience 135:611-625.

Zorrilla EP, Inoue K, Fekete EM et al. (2005) Measuring meals: structure of prandial food and water intake of rats. Am J Physiol Regul Integr Comp Physiol 288:R1450-1467.

SUPPLEMENTAL MATERIALS

Table S1. Gene name, gene ID, and forward and reverse primer sequences for qPCR analysis of NAc gene expression.

Gene	Gene ID	Forward primer	Reverse Primer
Cyclophilin	ENSRNOG00000016781	ACTTCATGATCCAGGGTGGAGACT	AAGTTCTCATCTGGGAAGCGCTCA
Drd1a	ENSRNOG00000023688	AACAGTTGCTATGCTGACTGGGCT	CCAAATGCCCTCTTGCTTTAGGGT
Drd2	ENSRNOG00000008428	TTGATAGTCAGCCTTGCTGTGGCT	TCCTGCTGAATTTCCACTCACCCA
GluR1	ENSRNOG00000002422	TGCGGTTGTGGGTGCCAATTT	AGCCGCATGTTCCTGTGATTGTTG
Darpp32	ENSRNOG00000028404	ACCCAAAGTCGAAGAGACCCAA	TCTCACTCAGGTTGCTGATGGTCT
Th	ENSRNOG00000020410	TTCCTACGGAGAGCTCCTGCACT	GTTTGATCTTGGTAGGGCTGCACA
Vmat2	ENSRNOG00000008890	TCACCGTCGTGGTTCCCATCAT	TGGTGGTCTGGATTTCCGTAGAGT
Syn1	ENSRNOG00000010365	GGTTCGACTACACAAGAAGCTTGG	ACTACAGGGTATGTTGTGCTGCTG
Htr2c	ENSRNOG00000030877	ATAGCCGGTTCAATTCGCGGACTA	TGCTTTCGTCCCTCAGTCCAATCA

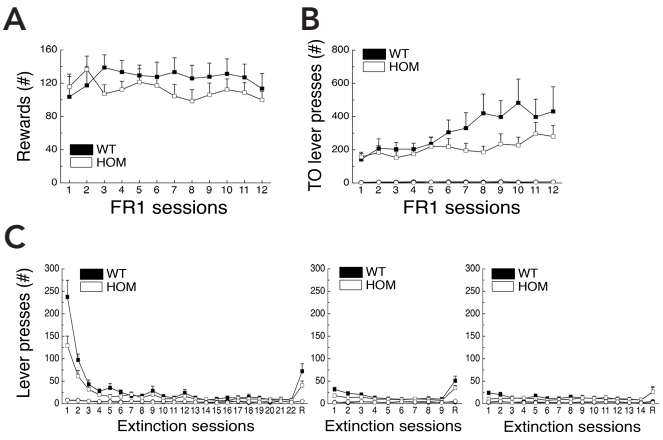

Fig. S1. Supplementary analysis of high palatable food self-administration. (*A*) Number of high palatable food pellets earned during the FR1 sessions. The statistical analysis for total amount of pellets earned during the FR1 sessions revealed no significant effects for *time* ($F_{(7,128)}$ = 0.7, P = 0.70), *genotype* ($F_{(1,18)}$ = 0.7, P = 0.40) and no *time* x *genotype* interaction ($F_{(7,128)}$ = 1.0, P = 0.43). (*B*) Total number of active lever presses (squares) and inactive lever presses (circles) during 15-s time out (TO) periods of the FR1 sessions. The statistical analysis for active TO lever presses revealed an significant effect for *time* ($F_{(3,56)}$ = 5.0, P < 0.005), but not for *genotype* ($F_{(1,18)}$ = 1.6, P = 0.23) and no *time* x *genotype* interaction ($F_{(3,56)}$ = 1.7, P = 0.17). (*C*) Total number of active lever presses (squares) and inactive lever presses (circles) during the extinction phase before cue-induced reinstatement (left panel), pellet-induced reinstatement (middle panel), and yohimbine-induced reinstatement (right panel). R = reinstatement session (n = 10 per group). Data are shown as mean ± S.E.M.

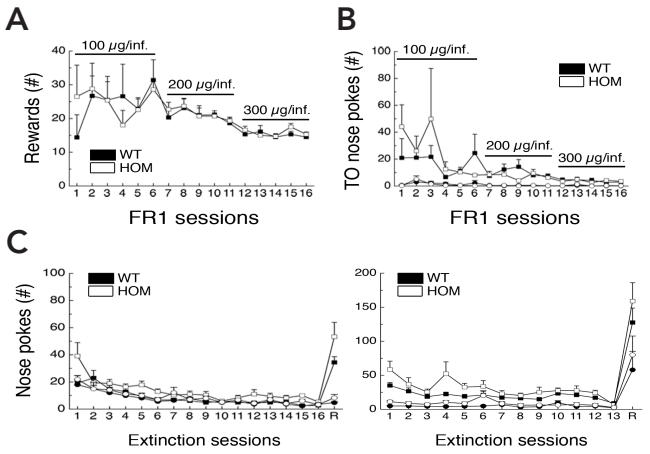

Fig. S2. Supplementary analysis of cocaine self-administration. (*A*) Number of cocaine infusions earned during the FR1 sessions. The statistical analysis for total number of cocaine infusions revealed a significant effect for *time* ($F_{(5,109)}$ = 2.8, P < 0.05), but not for *genotype* ($F_{(1,20)}$ = 0.5, P = 0.83) and no *time* x *genotype* interaction ($F_{(5,109)}$ = 0.6, P = 0.72). (*B*) Total number of active nose pokes (squares) and inactive nose pokes (circles) during 15-s time out (TO) periods of the FR1 sessions. The statistical analysis for active TO responses revealed no significant effects for *time* ($F_{(2,35)}$ = 3.3, P = 0.06), *genotype* ($F_{(1,20)}$ = 0.3, P = 0.87) or a *time* x *genotype* interaction ($F_{(2,35)}$ = 0.3, P = 0.74). (*C*) Total number of active responses (squares) and inactive responses (circles) during the extinction phase before cue-induced reinstatement (left panel) or drug-primed reinstatement (right panel). R = reinstatement session (n = 8-14 per group). Data are shown as mean ± S.E.M.

4

ADIPOSE FUNCTION IN *PMCH*-DEFICIENT RATS

Joram D. Mul[1], Eoghan O'Duibhir[1], Peter Vargoviç[2], Pim W. Toonen[1], Jeroen Korving[1], Arjen Koppen[3], Eric Kalkhoven[3], Richard Kvetnansky[2] and Edwin Cuppen[1,4]

[1]Hubrecht Institute-KNAW & University Medical Center Utrecht, Utrecht, The Netherlands
[2]Laboratory for Stress Research, Institute of Experimental Endocrinology, Bratislava, Slovakia
[3]Department of Metabolic and Endocrine Diseases, UMC Utrecht, Utrecht, The Netherlands
[4]Department of Medical Genetics, University Medical Center Utrecht, Utrecht, The Netherlands

ABSTRACT

The lateral hypothalamic neuropeptide Melanin-Concentrating Hormone (MCH) regulates energy homeostasis. Loss of the MCH-precursor *Pmch* in the rat (hereafter *Pmch*$^{-/-}$) results in decreased body weight (BW) and white adipose tissue (WAT), primarily mediated by hypophagia. As WAT levels are stronger reduced than BW levels (~50% and ~20%, respectively), we investigated whether this discrepancy is induced in *pmch*$^{-/-}$ rats by chronic hypophagia, by WAT-specific adaptations, or by a combination of both. Weight of WAT and brown adipose tissue (BAT), WAT morphology, expression of genes involved in thermogenesis in WAT and BAT, and catecholamine content of WAT and plasma were investigated in *pmch*$^{+/+}$ and *pmch*$^{-/-}$ rats. In addition, the effects of feeding on WAT function was investigated in *pmch*$^{+/+}$ rats pair-fed to *pmch*$^{-/-}$ rats. We observed that *pmch*$^{-/-}$ rats have decreased visceral and subcutaneous WAT at different time points during rat maturation, predominantly resulting from a decrease in adipocyte size. Pair-feeding *pmch*$^{+/+}$ rats to *ad-libitum* fed *pmch*$^{-/-}$ rats resulted in increased WAT levels in pair-fed *pmch*$^{+/+}$ rats as compared to *ad-libitum* fed *pmch*$^{-/-}$ rats. This indicated that in addition to the hypophagia, other mechanisms negatively affect lipid storage in *pmch*$^{-/-}$ rats. Expression of genes involved in thermogenesis, such as *Ucp1*, were elevated in subcutaneous WAT but not in BAT or visceral WAT of *pmch*$^{-/-}$ rats. In addition, plasma catecholamine content, but not WAT catecholamine content, was elevated in *pmch*$^{-/-}$ rats as compared to *pmch*$^{+/+}$ rats. We propose that, in addition to the direct effects of chronic hypophagia on adipose storage in *pmch*$^{-/-}$ rats, *Pmch*-deficiency also resulted in secondary effects on WAT, likely mediated by an increased sympathetic input and consequently increased lipolysis.

INTRODUCTION

Excess energy in the form of lipids can be stored in white adipose tissue (WAT), and the stored amount reflects the cumulative sum over time of the excess energy intake over energy expenditure (Rosenbaum et al., 1997). WAT deposition beyond physical needs results in obesity, generating several adverse health consequences (Spiegelman and Flier, 2001). Brown adipose tissue (BAT) converts energy into heat via cold- or diet-induced nonshivering thermogenesis, essentially through the mitochondrial BAT-specific protein UCP1 (Cannon and Nedergaard, 2004). Although BAT is important for young organisms, recently it has been shown that adult humans have physiological functional BAT levels as well (Cypess et al., 2009; van Marken Lichtenbelt et al., 2009; Virtanen et al., 2009).

The sympathetic nervous system (SNS) innervates both WAT and BAT (Wirsen and Hamberger, 1967; Slavin and Ballard, 1978; Bartness and Bamshad, 1998), and net caloric deprivation triggers the SNS to release catecholamines (epinephrine [Epi] and norepinephrine [NE]; (Migliorini et al., 1997). However, as BAT receives more SNS innervation compared to WAT, neural-derived catecholamines are believed to play a more important role in BAT, whereas catecholamines derived from the circulation are supposed to play a relatively greater role in WAT (Robidoux et al., 2004). Circulatory catecholamines are produced in the adrenal glands in response to stress, activity, and hypoglycemia (Garber et al., 1976; Cryer, 1980). NE and Epi are physiological agonists of adrenergic receptor β_3 (β_3AR), which is the dominant receptor in differentiated adipocytes (Feve et al., 1991; Dixon et al., 2001). Activation of β_3AR results in lipolysis (WAT and BAT) and thermogenesis (BAT, muscle), and affects adipocyte proliferation and differentiation (Cannon and Nedergaard, 2004).

Increased BAT activity promoted energy expenditure and reduced adiposity in the mouse, thus being beneficial for overall health (Kopecky et al., 1995). Interestingly, BAT-like cells are also interspersed within WAT in rodents (Cousin et al., 1992; Xue et al., 2007), and stimulation of β_3AR increases the presence of UCP1-positive BAT-like cells in rodent WAT (Nagase et al., 1996; Ghorbani et al., 1997; Ghorbani and Himms-Hagen, 1997; Umekawa et al., 1997; Guerra et al., 1998; Yoshida et al., 1998; Himms-Hagen et al., 2000).

The orexigenic hypothalamic neuropeptide Melanin-Concentrating Hormone (MCH) positively affects energy balance regulation (Pissios et al., 2006; Richard, 2007; Pissios, 2009). Deletion of the MCH-precursor *Pmch* in rats resulted in a lean anti-obesity model, characterized by decreased food intake, fat mass, leptin levels, and energy expenditure (Mul et al., 2010). However, WAT levels were stronger reduced than BW levels (~50% and ~20%, respectively) (Mul et al., 2010). This suggested that other pathways in addition to the hypophagia might add to the decreased WAT levels in *pmch*$^{-/-}$ rats. For example, MCH affects leptin expression *in vitro* in primary rat adipocytes through MCH1R, the receptor for MCH in rodents (Bradley et al., 2000). MCH also activates signaling pathways *in vitro* in 3T3-L1 cell lines (Bradley et al., 2002).

However, MCH does not affect lipolysis directly *in vitro* in murine adipocytes (Bradley et al., 2005).

Here we investigated whether the discrepancy between decreased BW and WAT levels in *pmch*$^{-/-}$ rats is induced by chronic hypophagia, by WAT-specific adaptations, or by a combination of both. To study this, we used an array of histological and gene expression techniques in *pmch*$^{+/+}$ and *pmch*$^{-/-}$ rats. In addition, we analyzed catecholamine content in WAT and blood plasma, and used a pair-feeding paradigm to differentiate between the hypophagic effects on adipose function and additional effects on adipose function in *pmch*$^{-/-}$ rats.

MATERIAL & METHODS

Animals. The Animal Care Committee of the Royal Dutch Academy of Science approved all experiments according to the Dutch legal ethical guidelines. Previously described *pmch*$^{-/-}$ rats (Mul et al., 2010) were used in the present study. Two rats were housed together, unless noted otherwise, under controlled experimental conditions (12 h light/dark cycle, light period 0600-1800, 21±1°C, ~60% relative humidity). Standard fed diet (semi high-protein chow: RM3, 27% CP and 12% F, 3.33 kcal/g AFE, SDS, Witham, United Kingdom) and water was provided *ad libitum* unless noted otherwise. Genotyping was done as previously described (Mul et al., 2010). Genotypes were reconfirmed when experimental procedures were completed. Only male rats were used in this study.

WAT weight and morphology. Rats were sacrificed at postnatal day (PND) 40, 60, or 120 by decapitation after measuring BW. The left and right subcutaneous (SWAT) and perirenal (PWAT) fat pads, the left lateral liver lobe, and the adrenal glands were isolated and weighed together, and adipose tissue volume was measured. Afterwards, WAT samples were collected in 4% formaldehyde, rotated overnight at room temperature (RT), rinsed with 70% ethanol for 2 hrs, 96% ethanol for 2 hrs, twice with 100% ethanol for 1.5 hrs, 2 hrs in xylene, and embedded in paraffin overnight. Samples were then cut in 14μm sections and stained with eosin. Per animal, 10 sections were cut at positions distributed equally throughout the tissue to minimize for local effects. Average adipocyte cell diameter was then measured using NIH ImageJ software. Using the average adipocyte cell diameter, adipose tissue volume, and correcting for the percentage non-adipocyte tissue, an estimated number of total adipocyte cells was calculated.

Hormone measurements. *Pmch*$^{+/+}$ and *pmch*$^{-/-}$ rats were sacrificed at PND 40, 60, or 120 by decapitation, and whole blood was collected. Blood samples were allowed to clot at RT for 30' and centrifuged at 2150 rcf for 15' at 4°C. Serum samples were then aliquoted and stored at -80°C until analysis. Serum leptin and insulin levels were measured as previously described (Mul et al., 2010).

IBAT weight. After BW measurement, rats were sacrificed at PND 140 by decapitation and the interscapular BAT (IBAT) fat pad was isolated and weighed.

Pair-feeding (PF) experiment. All *pmch*$^{+/+}$ and *pmch*$^{-/-}$ pups had access to SHP diet in their maternal home cage and were weaned and housed individually at PND 25. After weaning, SHP diet and water was provided *ad libitum*. A second group of *pmch*$^{+/+}$ rats was pair-fed (PF) to *pmch*$^{-/-}$ rats from PND 25 until PND 59. BW, food intake, and water intake of all three groups were monitored every other day between PND 25 and 59. The average food intake of the *pmch*$^{-/-}$ rats of the previous two days was calculated and provided to the PF group. PF rats thus received chow every other day. At PND 60, the left whole SWAT fat pad, the left whole PWAT fat pad, the

interscapular BAT fat pad were, and the hypothalamus were isolated during the early afternoon, snap-frozen in liquid nitrogen, and stored at -80°C until analysis. The right whole SWAT fat pad, the right whole PWAT fat pad, and the whole liver were isolated and weighed.

Qualitative RT-PCR. For the determination of relative gene expression levels in IBAT and WAT we used left SWAT, left PWAT, and IBAT samples derived from *pmch*$^{+/+}$ and *pmch*$^{-/-}$ rats at PND 40 during the early afternoon. All samples were processed and analyzed as described before (Mul et al., 2010). Primers for *Cyclophilin* forward: ACTTC ATGAT CCAGG GTGGA GACT; reverse: AAGTT CTCAT CTGGG AAGCG CTCA), *Ucp1* (forward: TCAGC TTTGC TTCCC TCAGG ATTG; reverse: AGCCG AGATC TTGCT TCCCA AAGA), *Cox8b* forward: AGCCA AATCT CCCAC TTCTG CCAT; reverse: TAAGA CCCAT CCTGC TGGAA CCAT), and *Adr3B* forward: AGTCC ACCGC TCAAC AGGTT TGAT; reverse: AGCTT CCTTG CTGGA TCTTC ACG) were designed using SciTools PrimerQuest (IDT).

Immunohistochemistry. Paraffin sections from SWAT and PWAT samples of young (PND 40) and adult (PND 120) *pmch*$^{+/+}$ and *pmch*$^{-/-}$ rats were incubated with anti-UCP1 antibody for 18 hrs (1/1000, Abcam, Cambridge, UK). After rinsing, sections were incubated with Envision® (Dako, Heverlee, Belgium) for 30', rinsed, and incubated with 3'3'-diaminobenzidine (DAB) containing 0.15% nickel ammonium sulphate for 10'. Subsequently, the slides were background stained for 2', rinsed, dehydrated and coverslipped with Pertex® (Histolab, Gothenburg, Sweden).

Catecholamine measurements. We measured plasma norepinephrine and epinephrine by radioenzymatic assay as described before (Peuler and Johnson, 1977). Assay sensitivity was 5 pg/tube. Frozen mesenteric adipose tissue (MWAT) and SWAT samples were weighed and placed into 10 ml tubes containing 2 ml of 0.01 M $HClO_4$. Samples were completely homogenized using a tissue homogenizer (Heidolph Diax 900) at maximum speed, and placed on ice for 1 hr. All samples were diluted to 145 mg/ml (MWAT) and 395 mg/ml (SWAT) using ddH_2O. After vortexing, 0.5 ml of every sample was transferred to a new tube containing 0.1 ml of chloroform, and samples were spinned down at 16100xg, at 4°C for 10'. Supernatant was transferred to a new tube and used for CA measurement. For CA measurement, aliquots containing 5 mg of mesenteric adipose tissue (34µl of supernatant) or 12 mg of subcutaneous adipose tissue (30µl of supernatant) were used. CA adipose data is shown as ng/per gram adipose wet weight (ww).

Data analysis. All data are shown as mean ± S.E.M. All data were analyzed using a commercially available statistical program (SPSS for Macintosh, version 16.0) and were controlled for normality and homogeneity. Differences in longitudinal BW, food intake, and water intake were assessed using repeated measure analysis, followed by Bonferroni *post hoc* analyses if significant overall interactions were observed. WAT tissue weight and hormone levels in the PF experiment were assessed by one-way ANOVA, followed by Bonferroni *post hoc* analyses if significant overall interactions were observed. All other data were analyzed using a Student's *t*-test. The null hypothesis was rejected at the 0.05 level.

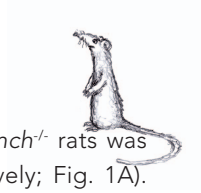

RESULTS

WAT deficiency in *pmch*$^{-/-}$ rats. At PND 40, 60, and 120, the BW of *pmch*$^{-/-}$ rats was decreased as compared to *pmch*$^{+/+}$ rats (82%, 81%, and 77% respectively; Fig. 1A). Subcutaneous adipose mass (SWAT) and visceral perirenal adipose mass (PWAT) was also decreased in *pmch*$^{-/-}$ rats as compared to *pmch*$^{+/+}$ rats at PND 40, 60, and 120 (71%, 65%, and 56% respectively for SWAT; 65%, 52%, and 47% respectively for PWAT; Fig. 1B, and C). Total adipose mass (SWAT and PWAT together) was decreased in *pmch*$^{-/-}$ rats

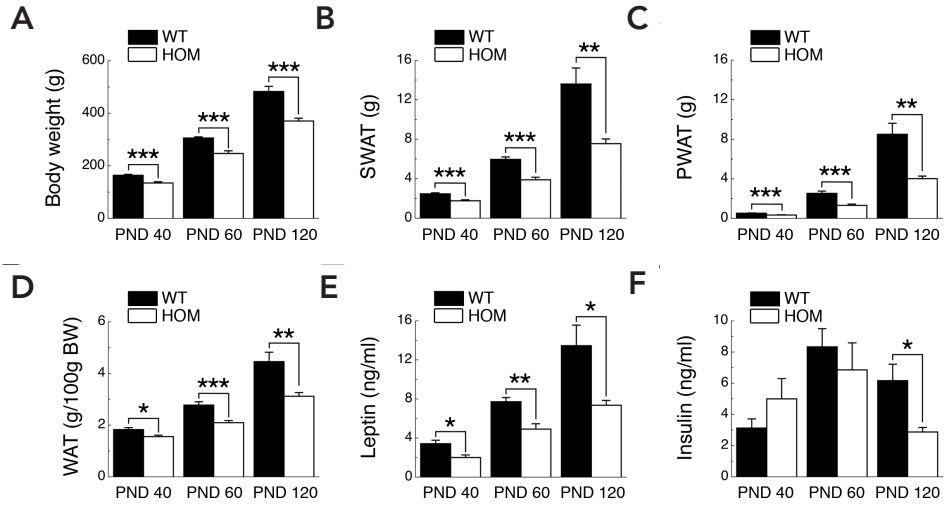

Figure 1. WAT levels in *pmch*$^{-/-}$ rats. Effects of *Pmch*-deficiency on (A) BW, (B) SWAT weight, (C) PWAT weight, (D) WAT weight (SWAT and PWAT combined) normalized for BW (g/100g BW), (E) serum leptin levels, and (F) serum insulin levels in *pmch*$^{+/+}$ and *pmch*$^{-/-}$ rats at PND 40, 60, and 120 (n = 8-15 per group). **P* < 0.05; ***P* < 0.005; ****P* < 0.001. Data are shown as mean ± S.E.M.

as compared to *pmch*$^{+/+}$ rats at PND 40, 60, and 120 (70%, 61%, and 52%, respectively; all *P* < 0.005, Student's *t*-test; data not shown). Moreover, adipose mass normalized for BW (g/100g BW) was also decreased in *pmch*$^{-/-}$ rats as compared to *pmch*$^{+/+}$ rats at PND 40, 60, and 120 (80%, 76%, and 70%, respectively; Fig. 1D), indicative of a decreased ability to accumulate adipose in *pmch*$^{-/-}$ rats compared to *pmch*$^{+/+}$ rats. Nutrient intake levels normalized for BW (kcal/100g body weight) did not differ significantly or were even increased in *pmch*$^{-/-}$ rats as compared to *pmch*$^{+/+}$ rats during adulthood (PND 60 and later), whereas the relative BW of *pmch*$^{-/-}$ rats as compared to *pmch*$^{+/+}$ rats remained stable (~80%) at PND 60 and later (Mul et al., 2010). This observation, in combination with the observation that adipose mass per 100 gram BW kept decreasing between PND 60 and 120, provided additional support that adipose accumulation is decreased in *pmch*$^{-/-}$ rats because of decreased lipogenesis, increased lipolysis, or a combination of both. Serum leptin levels were decreased in *pmch*$^{-/-}$ rats as compared to *pmch*$^{+/+}$ rats at PND 40, 60, and 120 (Fig. 1E), mirroring the decreased adipose levels. Serum insulin levels did not differ significantly between genotypes at PND 40 and 60, but were decreased in *pmch*$^{-/-}$ rats as compared to *pmch*$^{+/+}$ rats at PND 120 (Fig. 1F). The decreased leptin and insulin levels at PND 120 confirmed earlier observations in adult *pmch*$^{-/-}$ rats on a SHP diet (Mul et al., 2010). Liver weights, normalized for BW, were decreased in *pmch*$^{-/-}$ rats as compared to *pmch*$^{+/+}$ rats at PND 40 and 60 (88% and 94%; *P*<0.05, Student's t-test), whereas no significant difference between genotypes was observed at PND 120 (96%; data not shown). Adrenal gland weights, normalized for BW, did not differ significantly between genotypes at PND 40 and 60 (103%, 109%,

respectively), but showed an increased trend in *pmch*$^{-/-}$ rats as compared to *pmch*$^{+/+}$ rats at PND 120 (110%; *P*=0.06, Student's *t*-test; data not shown).

Decreased adipocyte cell size in *pmch*$^{-/-}$ rats. Average adipocyte cell size (ACS) in SWAT of *pmch*$^{-/-}$ rats showed a decreased trend at PND 40 (*P*=0.07, Student's *t*-test), but was decreased as compared to *pmch*$^{+/+}$ rats at PND 60 and 120 (Fig. 2A). ACS in PWAT of *pmch*$^{-/-}$ rats was decreased at all three PNDs as compared to *pmch*$^{+/+}$ rats (Fig. 2B). Average adipocyte cell number (ACN) of SWAT from *pmch*$^{-/-}$ rats was decreased as compared to *pmch*$^{+/+}$ rats at PND 40, but did not differ significantly between genotypes at PND 60 and 120 (Fig. 2C). ACN of PWAT of *pmch*$^{-/-}$ rats did not differ significantly between genotypes at PND 40, but was decreased as compared to *pmch*$^{+/+}$ rats at PND 60, and showed a decreased trend at PND 120 (*P*=0.07, Student's *t*-test; Fig. 2D). In addition, PWAT adipocytes showed an increased ACS as compared to SWAT adipocytes (Fig. 2A, and B).

Less severe WAT reduction in pair-fed *pmch*$^{+/+}$ rats. To investigate if the decreased WAT levels might be a cumulative effect of the hypophagia observed in *pmch*$^{-/-}$ rats (Mul et al., 2010), we pair-fed *pmch*$^{+/+}$ rats (PF) to *pmch*$^{-/-}$ rats from PND 25 till PND 60. The BW of *ad libitum* fed *pmch*$^{-/-}$ rats was decreased as compared to *ad libitum* fed *pmch*$^{+/+}$ rats (78% at PND 60; *P*<0.001, Bonferroni *post hoc* analysis; Fig. 3A, and B). Although the BW of PF and *ad libitum* fed *pmch*$^{+/+}$ rats did not differ significantly at PND 25, the BW of PF rats decreased rapidly and remained decreased as compared to

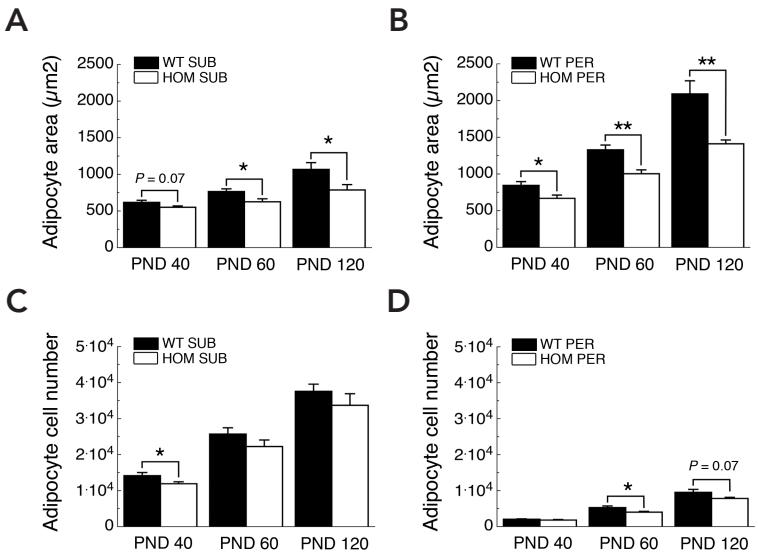

Figure 2. WAT morphology in *pmch*$^{-/-}$ rats. Effects of *Pmch*-deficiency on (A) average SWAT adipocyte area, (B) average PWAT adipocyte area, (C) average SWAT adipocyte cell number, and (D) average PWAT adipocyte cell number in *pmch*$^{+/+}$ and *pmch*$^{-/-}$ rats at PND 40, 60, and 120 (n = 8-15 per group; **P* < 0.05; ***P* < 0.005). Data are shown as mean ± S.E.M.

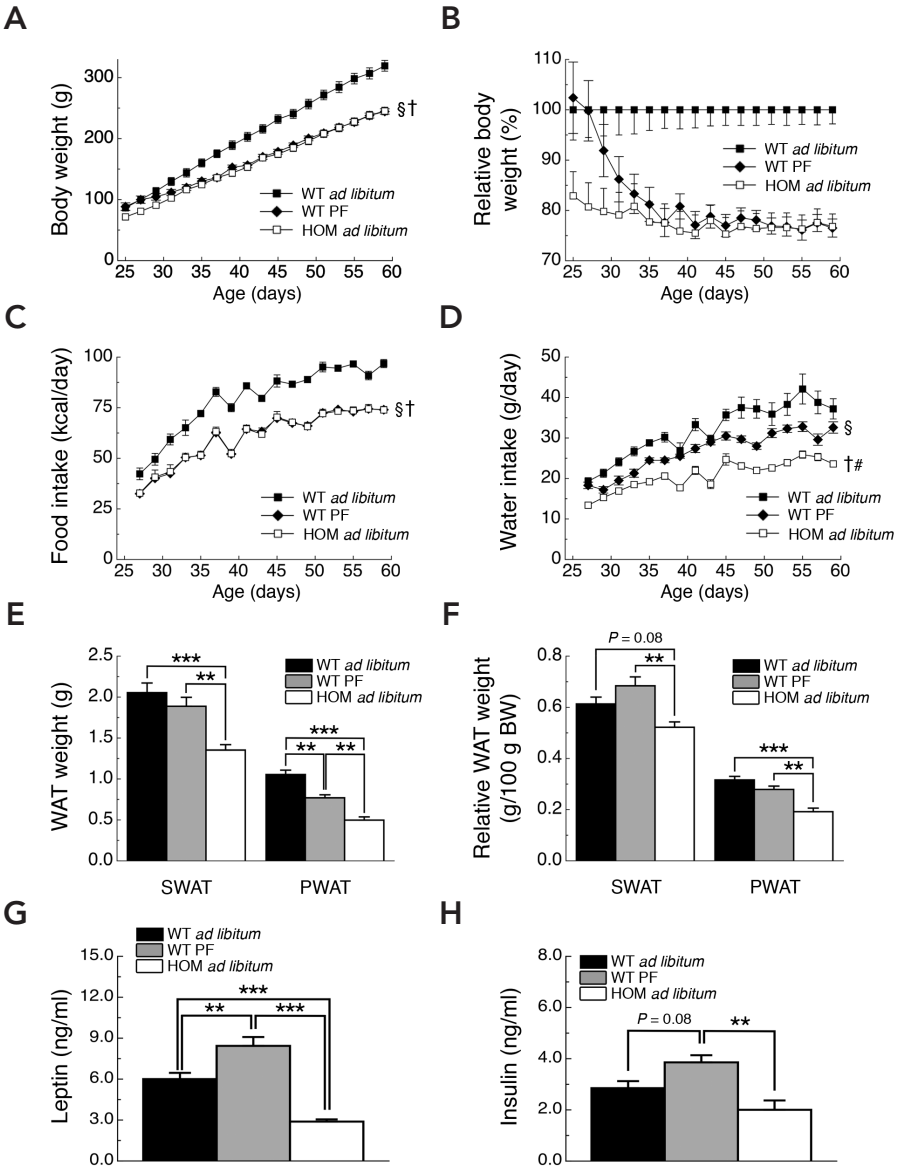

Figure 3. Feeding effects on WAT. Effects of pair-feeding on (A) BW, (B) relative BW, (C) food intake, (D) water intake, (E) SWAT and PWAT weight, and (F) SWAT and PWAT weight normalized for BW, (G) serum leptin levels, and (H) serum insulin levels in *ad libitum* fed *pmch*$^{+/+}$ rats (WT *ad libitum*; n = 6), *ad libitum* fed *pmch*$^{-/-}$ rats (HOM *ad libitum*; n = 14), or *pmch*$^{+/+}$ rats that were pair-fed to *ad libitum* fed *pmch*$^{-/-}$ rats (WT PF; n = 7). $^{\dagger}P< 0.001$, *pmch*$^{+/+}$ rats vs. *pmch*$^{-/-}$ rats; $^{\S}P< 0.001$, *pmch*$^{+/+}$ rats vs. WT-PF rats; $^{\#}P< 0.005$, *pmch*$^{-/-}$ rats vs. WT-PF rats; $^{**}P < 0.005$; $^{***}P < 0.001$. Data are shown as mean ± S.E.M.

ad libitum fed *pmch*$^{+/+}$ rats during the remainder of the experiment (78% at PND 60; $P<0.001$, Bonferroni *post hoc* analysis; Fig. 3A, and B). The BW of PF rats did not differ significantly from the BW of *ad libitum* fed *pmch*$^{-/-}$ rats (Fig. 3A, and B). Food intake of the *ad libitum* fed *pmch*$^{-/-}$ and PF rats was decreased as compared to *ad libitum* fed *pmch*$^{+/+}$ rats during the complete length of the experiment ($P<0.001$, Bonferroni *post hoc* analysis; Fig. 3C). Water intake of the *ad libitum* fed *pmch*$^{-/-}$ rats was decreased as compared to *ad libitum* fed *pmch*$^{+/+}$ rats during the complete length of the experiment ($P<0.001$, Bonferroni *post hoc* analysis; Fig. 3D). Water intake of the PF rats showed an intermediate phenotype and was decreased as compared to *ad libitum* fed *pmch*$^{+/+}$ rats ($P<0.001$, Bonferroni *post hoc* analysis), but was increased as compared to *ad libitum* fed *pmch*$^{-/-}$ rats ($P<0.005$, Bonferroni *post hoc* analysis; Fig. 3D). SWAT mass, harvested at PND 60, was decreased in *ad libitum* fed *pmch*$^{-/-}$ rats as compared to *ad libitum* fed *pmch*$^{+/+}$ rats and PF rats, whereas SWAT mass did not differ significantly between *ad libitum* fed *pmch*$^{+/+}$ rats and PF rats (Fig. 3E). PWAT mass, harvested at PND 60, was decreased in *ad libitum* fed *pmch*$^{-/-}$ rats as compared to *ad libitum* fed *pmch*$^{+/+}$ rats and PF rats, and decreased in PF rats as compared to *ad libitum* fed *pmch*$^{+/+}$ rats (Fig. 3E). SWAT, normalized for BW, showed a decreased tendency in *ad libitum* fed *pmch*$^{-/-}$ rats as compared to *ad libitum* fed *pmch*$^{+/+}$ rats ($P=0.08$, Bonferroni *post hoc* analysis), whereas it was decreased in *ad libitum* fed *pmch*$^{-/-}$ rats as compared to PF rats (Fig. 3F). PWAT, normalized for BW, was decreased in *ad libitum* fed *pmch*$^{-/-}$ rats as compared to *ad libitum* fed *pmch*$^{+/+}$ rats and PF rats (Fig. 3F). Both SWAT and PWAT mass normalized for BW were not significantly different between *ad libitum* fed *pmch*$^{+/+}$ rats and PF rats (Fig. 3F). Serum leptin levels were decreased in *ad libitum* fed *pmch*$^{-/-}$ rats as compared to *ad libitum* fed *pmch*$^{+/+}$ rats, reflecting the decreased adipose levels (Fig. 3E, and 3G). However, serum leptin levels were increased in PF rats as compared to both *ad libitum* fed *pmch*$^{+/+}$ rats and *ad libitum* fed *pmch*$^{-/-}$ rats (Fig. 3G). Serum insulin levels did not differ significantly between *ad libitum* fed *pmch*$^{-/-}$ rats and *pmch*$^{+/+}$ rats (Fig. 3H). Serum insulin levels in PF rats were increased as compared to *ad libitum* fed *pmch*$^{-/-}$ rats, and showed an increased trend as compared to *ad libitum* fed *pmch*$^{+/+}$ rats ($P=0.08$, Bonferroni *post hoc* analysis; Fig. 3H).

BAT weight in *pmch*$^{-/-}$ rats. At PND 140, the BW of *pmch*$^{-/-}$ rats was decreased as compared to *pmch*$^{+/+}$ rats (16% decreased in *pmch*$^{-/-}$ rats; Fig. 4A). Interscapular BAT (IBAT) mass, and IBAT mass normalized for BW did not differ significantly between genotypes (11% decreased, and 4% increased in *pmch*$^{-/-}$ rats, respectively; Fig. 4B, and C).

Increased plasma catecholamine levels in *pmch*$^{-/-}$ rats. Epi and NE levels were determined in SWAT, mesenteric WAT (MWAT), and blood plasma samples of *pmch*$^{+/+}$ and *pmch*$^{-/-}$ rats at PND 120. Epi and NE levels did not differ significantly between genotypes in SWAT and MWAT (Fig. 5A, and B). However, Epi and NE levels in plasma of *pmch*$^{-/-}$ rats showed increased trends compared to *pmch*$^{+/+}$ rats ($P=0.06$ and $P=0.08$, respectively, Student's *t*-test; Fig. 5C).

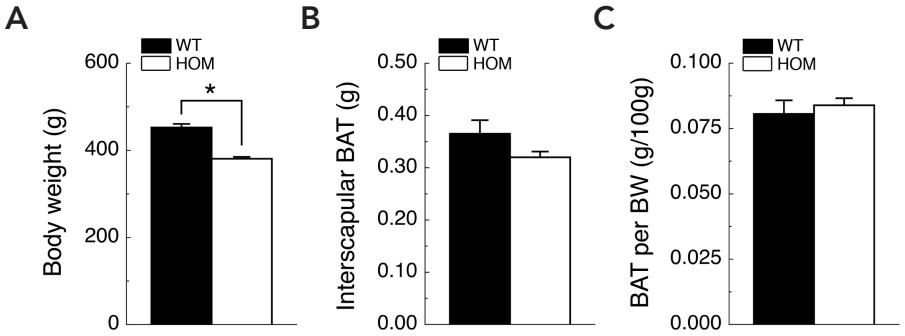

Figure 4. IBAT in *pmch*$^{-/-}$ rats. Effects of *Pmch*-deficiency on (A) BW, (B) interscapular IBAT weight, and (C) IBAT weight normalized for BW (g/100g BW) in *pmch*$^{+/+}$ rats and *pmch*$^{-/-}$ rats at PND 120 (n=6-8 per group; **P* < 0.05) of *pmch*$^{+/+}$ rats and *pmch*$^{-/-}$ rats (n = 6-8 per group; **P* < 0.05) at PND 60. Percentage of *pmch*$^{-/-}$ value relative to control value is shown in bar. Data are shown as mean ± S.E.M.

Thermogenic gene expression in WAT and BAT of *pmch*$^{-/-}$ rats. Relative expression levels of *Ucp1* and *Cox8b*, both highly selective BAT genes (Seale et al., 2007), and β_3*AR* was analyzed in IBAT, SWAT, and PWAT of *pmch*$^{+/+}$ and *pmch*$^{-/-}$ rats by qualitative RT-PCR. Relative expression of *Ucp1*, *Cox8b*, and β_3*AR* in IBAT did not differ significantly between genotypes (Fig. 6). Relative expression of *Ucp1* and *Cox8b* showed an increased trend in SWAT of *pmch*$^{-/-}$ rats as compared to *pmch*$^{+/+}$ rats (*P*=0.11 and *P*=0.12; respectively, Student's *t*-test), whereas no difference in relative β_3*AR* expression was observed (Fig. 6). Relative expression of *Ucp1*, *Cox8b*, and β_3*AR* in PWAT did not differ between genotypes (Fig. 6).

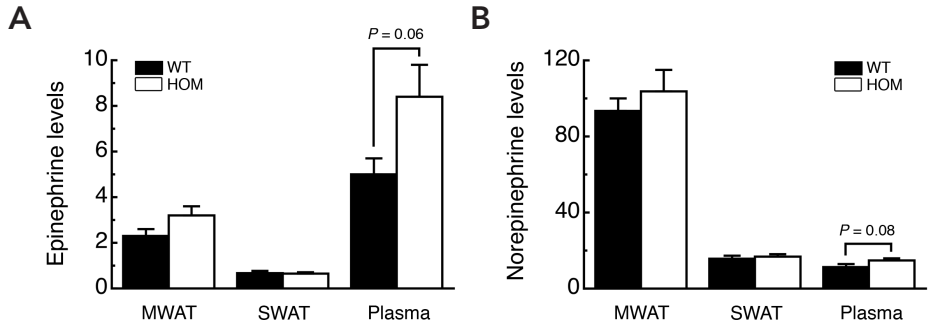

Figure 5. Catecholamine levels in *pmch*$^{-/-}$ rats. Effects of *Pmch*-deficiency on (A) Epi levels in MWAT (ng/gram wet weight), SWAT (ng/gram wet weight), and blood plasma (ng/ml) and (B) NE levels in MWAT (ng/gram ww), SWAT (ng/gram ww), and blood plasma (ng/ml) in *pmch*$^{+/+}$ rats and *pmch*$^{-/-}$ rats at PND 120 (n = 7-10 per group). Data are shown as mean ± S.E.M.

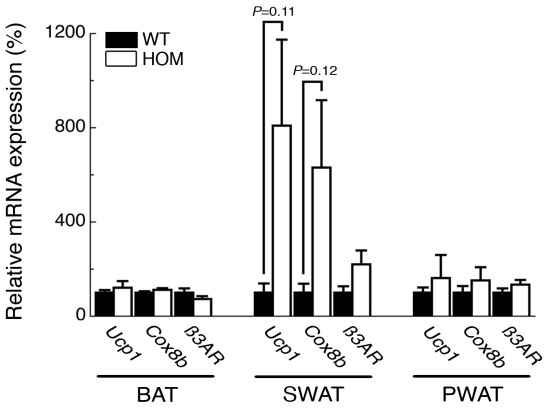

Figure 6. Quantitative RT-PCR analysis in *pmch*$^{-/-}$ rats. Effects of *Pmch*-deficiency on relative *Ucp1*, *Cox8b*, and β_3*AR* expression in BAT, SWAT, and PWAT of *pmch*$^{+/+}$ rats and *pmch*$^{-/-}$ rats at PND 40 (n = 6 per group). Data are shown as mean ± S.E.M.

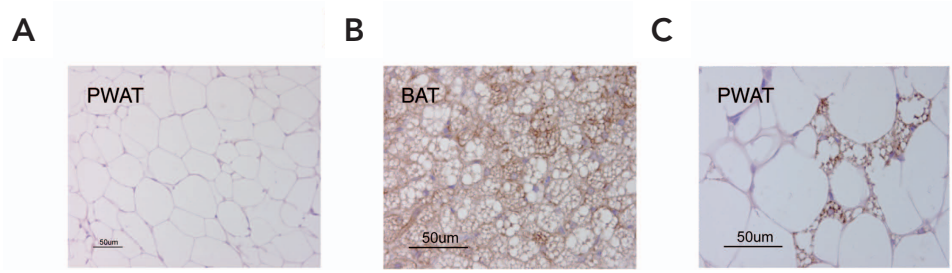

Figure 7. UCP1 Immunohistochemistry. Single-locular white adipocytes in PWAT of a exemplary *pmch*$^{-/-}$ rat stained negative for UCP1 (negative control, x200 magnification; A), whereas multilocular brown adipocytes in BAT stained positive (brown stain; positive control; x400 magnification; B), as well as multilocular brown-like adipocytes surrounded by negatively-stained single-locular white adipocytes in PWAT (x400 magnification; C).

UCP1 immunohistochemistry. Single-locular white adipocytes in PWAT of *pmch*$^{+/+}$ and *pmch*$^{-/-}$ rats at PND 40 stained negative, whereas multilocular brown adipocytes in IBAT or multilocular brown-like adipocytes in PWAT stained positive for UCP1 (Fig. 7A, B, and C).

DISCUSSION

In this study we show that in addition to the pronounced effect of *Pmch*-deficiency on feeding, *Pmch*-deficiency also has an indirect negative effect on lipid accumulation in WAT. We propose that this additional negative effect results from the increased presence of catecholamines in blood plasma of *pmch*$^{-/-}$ rats.

To distinguish between the hypophagic effect of *Pmch*-deficiency on WAT levels and other potential indirect effects, we pair-fed wild type rats to *ad-libitum* fed *pmch*$^{-/-}$ rats from PND 25 till 60. This resulted in equal BW, equal food intake, increased water intake, and increased PWAT and SWAT levels in PF rats as compared to *pmch*$^{-/-}$ rats.

Thus, although BW did not differ significantly between PF and *ad-libitum* fed *pmch*$^{-/-}$ rats, SWAT and PWAT levels were increased. This indicated that other mechanisms in addition to the observed hypophagia affected WAT levels in *pmch*$^{-/-}$ rats as compared to *pmch*$^{+/+}$ rats before PND 60.

However, two things should be noted. First, the pair-feeding paradigm (regularly handling) decreased WAT levels in both *ad-libitum* fed *pmch*$^{+/+}$ and *pmch*$^{-/-}$ rats as compared to *ad-libitum* fed *pmch*$^{+/+}$ and *pmch*$^{-/-}$ rats used for the basal characterization at PND 60 (Fig. 1B, C, and 3E). This was reflected by lower serum leptin and insulin levels in *ad-libitum* fed *pmch*$^{+/+}$ and *pmch*$^{-/-}$ rats of the pair-feeding experiment as compared to *ad-libitum* fed *pmch*$^{+/+}$ and *pmch*$^{-/-}$ rats used for the basal characterization (Fig. 1E, F, 3G, and H). Second, a pair-feeding paradigm likely induces stress-responses, especially when the food intake of the 'paired' rat is not given acutely, but when average food intake is given daily or every two days. Therefore, although not documented well, pair-feeding paradigms potentially dysregulate biological rhythms of for example glucose, insulin, leptin, and corticosterone. However, PF rats demonstrated increased serum leptin and insulin levels as compared to *ad-libitum* fed *pmch*$^{+/+}$ rats. Interestingly, increased leptin levels as compared to *ad-libitum* fed wild type rats were also observed in wild type rats that were fed at six regular time points per day (Kalsbeek et al., 2001). PF rats were slightly food-deprived (~80%) and show decreased BW levels (~80%; this study), whereas regular-fed wild type rats are also slightly food-deprived (~80%), but show no aberrant BW levels (Strubbe et al., 1987; Kalsbeek and Strubbe, 1998; La Fleur et al., 1999; Kalsbeek et al., 2001). Thus, in both scenarios lower leptin levels as compared to *ad-libitum* fed wild type rats would be expected. In addition, increased insulin levels were not observed in regular-fed wild type rats (Strubbe et al., 1987; Kalsbeek and Strubbe, 1998; La Fleur et al., 1999), whereas PF rats showed slightly but not significantly elevated insulin levels as compared to *ad-libitum* fed *pmch*$^{+/+}$ rats. The PF rats were provided with chow every other day, and PF rat chow supplies were always depleted somewhere during the second night (data not shown). As PF rats were sacrificed 24hr after they were provided with chow, enabling active feeding behavior during that time, relative increased leptin and insulin levels might reflect responses to feeding and the subsequent adipocyte nutrient flux (Wang et al., 1998).

Decreased WAT and serum leptin levels at PND 40, 60, and 120 reflected the decreased BW levels at PND 40, 60, and 120, confirming earlier observations in adult rats (Mul et al., 2010). Serum insulin levels were decreased in *pmch*$^{-/-}$ rats at PND 120, again confirming earlier observations in adult animals (Mul et al., 2010). However, insulin levels did not differ significantly between *pmch*$^{+/+}$ and *pmch*$^{-/-}$ rats at PND 40 and 60 during the basal characterization (Fig 1F), or at PND 60 during the pair-feeding paradigm (Fig. 3H). MCH is known to be an enhancer of insulin secretion (Pissios et al., 2007), thus loss of *Pmch* is expected to abolish this enhancement in *pmch*$^{-/-}$ rats. Moreover, *pmch*$^{-/-}$ rats demonstrated decreased WAT levels at PND 40 and 60, and decreased adipose mass is expected to be accompanied by decreased insulin levels. Despite this, insulin levels at PND 40 and 60 did not differ significantly between genotypes, or even appeared

to be slightly but not significantly elevated in *pmch*$^{-/-}$ rats (PND 40). Although insulin levels are not significantly increased in *pmch*$^{-/-}$ rats at PND 40 as compared to wild type rats, this observation is intriguing considering the finding that *pmch*$^{-/-}$ rats showed decreased BW growth as compared to wild type rats until approximately PND 55-60 (Mul et al., 2010). Thus, potential aberrant regulation of insulin release, especially at a younger age (<PND 55-60), might be reflected by relatively high insulin levels in *pmch*$^{-/-}$ rats at PND 40. The relatively high insulin levels might affect central insulin signaling and subsequent body weight growth during this period. However, more studies will be needed to investigate and fully explain our observations.

Liver weights were decreased in *pmch*$^{-/-}$ rats at PND 40, 60, and 120. However, liver weights normalized for BW, remained decreased in *pmch*$^{-/-}$ rats, suggesting decreased cell mass or lipid storage in *pmch*$^{-/-}$ rats at all three time points. In an earlier study, although with a smaller group of animals, no significant difference was observed between genotypes (Mul et al., 2010). Adrenal gland weights were also decreased in *pmch*$^{-/-}$ rats at PND 40, 60, and 120. However, adrenal gland weights, normalized for BW, were slightly albeit not significantly elevated in *pmch*$^{-/-}$ rats at PND 40, 60, and 120. This suggests that the proposed increased sympathetic nervous activity in *pmch*$^{-/-}$ rats might be reflected by increased adrenal gland mass per BW, and subsequent increased plasma catecholamine levels.

A decreased ACS reflected the decreased WAT levels in *pmch*$^{-/-}$ rats, whereas the difference in ACN between genotypes was not as clear. Moreover, *in vitro* treatment of 3T3-L1 cells with MCH did not affect adipocyte differentiation (data not shown). Therefore, we conclude that *Pmch*-deficiency has a primary effect on adipocyte size, whereas a potential effect on adipocyte differentiation, if any, is likely secondary.

As BAT levels have significant effects on thermogenesis (Kopecky et al., 1995; Cannon and Nedergaard, 2004), we measured IBAT levels in adult *pmch*$^{+/+}$ and *pmch*$^{-/-}$ rats. Both absolute IBAT levels, as IBAT levels normalized for BW did not differ significantly between genotypes. Thus, *Pmch*-deficiency in the rat has no clear effects on IBAT mass.

Activation of β_3AR by catecholamines results in lipolysis (WAT and BAT) and thermogenesis (BAT, muscle; Cannon and Nedergaard, 2004). However, both Epi and NE levels measured in MWAT and SWAT did not differ significantly between genotypes, suggesting that *Pmch*-deficiency in the rat did not affect WAT lipolysis by direct effects on the SNS innervation of WAT. However, we did not measure catecholamine-turnover, which can affect lipolysis during prolonged fasting (Migliorini et al., 1997). Therefore, although catecholamine levels in WAT did not differ between genotypes, changes in catecholamine turnover might affect lipolysis in hypophagic *pmch*$^{-/-}$ rats.

Catecholamine levels in blood plasma were increased, although not significantly, and these elevations might have physiological effects. Interestingly, expression of *Ucp1* and *Cox8b*, both highly-selective BAT genes (Seale et al., 2007), were increased, although not significantly in SWAT samples derived from *pmch*$^{-/-}$ rats at PND 40 as compared to *pmch*$^{+/+}$ rats. No changes were observed in PWAT and BAT of *pmch*$^{-/-}$ rats.

Treatment with a β_3AR-agonist increased the expression of *Ucp1* and *Cox8b* in PWAT of obese (*fa*/*fa*) Zucker rats (Oana et al., 2005). Therefore, we hypothesize that the slightly increased plasma catecholamine levels were elevated enough to affect function of BAT-like cells in SWAT, whereas the function of BAT-like cells in PWAT remained unaffected. Moreover, it will be interesting to investigate expression levels in an age-dependent manner.

Mch1r-deficent mice demonstrated an increased heart rate (Astrand et al., 2004). However, administration of metoprolol, an adrenergic antagonist and sympathetic blocker, completely reversed the tachycardia seen in *Mch1r*-deficent mice (Astrand et al., 2004). Although plasma catecholamines levels were not measured in the study, the data strongly suggested that the MCH-system is an important tonic regulator of sympathetic nervous activity (Astrand et al., 2004). Additional studies have shown that chronic MCH-infusions induce brachycardia and reduce mean arterial pressure (hypotension), which is achieved by activating MCH1Rs in the medial nucleus tractus solitarius (mNTS) and the activation of the vagus nerve (Brown et al., 2007; Messina and Overton, 2007). In sum, these data and the data presented in this study indicate that the modification of the MCH-system affects sympathetic nervous activity, thus influencing cardiovascular function and lipid metabolism.

Finally, multiple studies have shown the presence of 'BAT'-like cells in rodent WAT (Cousin et al., 1992; Xue et al., 2007). Using UCP1 Immunohistochemistry, we identified UCP1-positive BAT-like cells in PWAT of *pmch*$^{+/+}$ and *pmch*$^{-/-}$ rats at PND 40. Although we investigated several animals (n=7-11 per group), these UCP1-positive BAT-like cells were rarely present in SWAT of *pmch*$^{+/+}$ and *pmch*$^{-/-}$ rats at PND 40, and in PWAT and SWAT of *pmch*$^{+/+}$ and *pmch*$^{-/-}$ rats at PND120 (data not shown). As SNS innervations of WAT are local, the analysis of the total amount of BAT-like 'islets' in WAT samples can be strongly influenced by the site of immunohistochemistry analysis. Furthermore, several studies have shown that WAT can also contribute to UCP1-independent thermogenesis, especially when treated chronically with a β_3AR agonist (Grujic et al., 1997; Ito et al., 1998; Gong et al., 2000; Granneman et al., 2003). Moreover, chronic treatment with a β_3AR agonist did increase *in vitro* respiration in WAT, but not in BAT (Granneman et al., 2003). In this study, WAT function also appeared affected, whereas no distinct effect on BAT function was observed. UCP1-independent thermogenesis might thus also be affected in *pmch*$^{-/-}$ rats, something that cannot be quantified by just measuring UCP1 positive-stained cells.

The orexigenic hypothalamic neuropeptide MCH has been the subject of many studies, as functional inhibition of MCH or MCH1R might result in an anti-obesity treatment (Handlon and Zhou, 2006). Many studies have focused on the central effects of loss of *Pmch*, resulting in hypophagia and affecting energy expenditure (Shimada et al., 1998; Alon and Friedman, 2006; Pissios et al., 2006; Pissios, 2009; Mul et al., 2010). We now show that *Pmch*-deficiency in the rat has additional effects on WAT levels, independent from its effects via hypophagia. We propose that the deletion of *Pmch* results in an increased sympathetic activity, which selectively affects WAT, thereby

changing the balance more in favor of lipolysis over lipogenesis. Understanding the mechanisms how *Pmch*-deficiency affects the autonomic balance might help the potential development of an obesity treatment based on MCH function.

ACKNOWLEDGMENTS:

We gratefully acknowledge Andries Kalsbeek for critical reading of the manuscript and for suggested improvements.

REFERENCES:

Alon T, Friedman JM (2006) Late-onset leanness in mice with targeted ablation of melanin concentrating hormone neurons. J Neurosci 26:389-397.

Astrand A, Bohlooly YM, Larsdotter S et al. (2004) Mice lacking melanin-concentrating hormone receptor 1 demonstrate increased heart rate associated with altered autonomic activity. Am J Physiol Regul Integr Comp Physiol 287:R749-758.

Bartness TJ, Bamshad M (1998) Innervation of mammalian white adipose tissue: implications for the regulation of total body fat. Am J Physiol 275:R1399-1411.

Bradley RL, Mansfield JP, Maratos-Flier E (2005) Neuropeptides, including neuropeptide Y and melanocortins, mediate lipolysis in murine adipocytes. Obes Res 13:653-661.

Bradley RL, Kokkotou EG, Maratos-Flier E et al. (2000) Melanin-concentrating hormone regulates leptin synthesis and secretion in rat adipocytes. Diabetes 49:1073-1077.

Bradley RL, Mansfield JP, Maratos-Flier E et al. (2002) Melanin-concentrating hormone activates signaling pathways in 3T3-L1 adipocytes. Am J Physiol Endocrinol Metab 283:E584-592.

Brown SN, Chitravanshi VC, Kawabe K et al. (2007) Microinjections of melanin concentrating hormone into the nucleus tractus solitarius of the rat elicit depressor and bradycardic responses. Neuroscience 150:796-806.

Cannon B, Nedergaard J (2004) Brown adipose tissue: function and physiological significance. Physiol Rev 84:277-359.

Cousin B, Cinti S, Morroni M et al. (1992) Occurrence of brown adipocytes in rat white adipose tissue: molecular and morphological characterization. J Cell Sci 103 (Pt 4):931-942.

Cryer PE (1980) Physiology and pathophysiology of the human sympathoadrenal neuroendocrine system. N Engl J Med 303:436-444.

Cypess AM, Lehman S, Williams G et al. (2009) Identification and importance of brown adipose tissue in adult humans. N Engl J Med 360:1509-1517.

Dixon TM, Daniel KW, Farmer SR et al. (2001) CCAAT/enhancer-binding protein alpha is required for transcription of the beta 3-adrenergic receptor gene during adipogenesis. J Biol Chem 276:722-728.

Feve B, Emorine LJ, Lasnier F et al. (1991) Atypical beta-adrenergic receptor in 3T3-F442A adipocytes. Pharmacological and molecular relationship with the human beta 3-adrenergic receptor. J Biol Chem 266:20329-20336.

Garber AJ, Cryer PE, Santiago JV et al. (1976) The role of adrenergic mechanisms in the substrate and hormonal response to insulin-induced hypoglycemia in man. J Clin Invest 58:7-15.

Ghorbani M, Himms-Hagen J (1997) Appearance of brown adipocytes in white adipose tissue during CL 316,243-induced reversal of obesity and diabetes in Zucker fa/fa rats. Int J Obes Relat Metab Disord 21:465-475.

Ghorbani M, Claus TH, Himms-Hagen J (1997) Hypertrophy of brown adipocytes in brown and white adipose tissues and reversal of diet-induced obesity in rats treated with a beta3-adrenoceptor agonist. Biochem Pharmacol 54:121-131.

Gong DW, Monemdjou S, Gavrilova O et al. (2000) Lack of obesity and normal response to fasting and thyroid hormone in mice lacking uncoupling protein-3. J Biol Chem 275:16251-16257.

Granneman JG, Burnazi M, Zhu Z et al. (2003) White adipose tissue contributes to UCP1-independent thermogenesis. Am J Physiol Endocrinol Metab 285:E1230-1236.

Grujic D, Susulic VS, Harper ME et al. (1997) Beta3-adrenergic receptors on white and brown adipocytes mediate beta3-selective agonist-induced effects on energy expenditure, insulin secretion, and food intake. A study using transgenic and gene knockout mice. J Biol Chem 272:17686-17693.

Guerra C, Koza RA, Yamashita H et al. (1998) Emergence of brown adipocytes in white fat in mice is under genetic control. Effects on body weight and adiposity. J Clin Invest 102:412-420.

Handlon AL, Zhou H (2006) Melanin-concentrating hormone-1 receptor antagonists for the treatment of obesity. J Med Chem 49:4017-4022.

Himms-Hagen J, Melnyk A, Zingaretti MC et al. (2000) Multilocular fat cells in WAT of CL-316243-treated rats derive directly from white adipocytes. Am J Physiol Cell Physiol 279:C670-681.

Ito M, Grujic D, Abel ED et al. (1998) Mice expressing human but not murine beta3-adrenergic receptors under the control of human gene regulatory elements. Diabetes 47:1464-1471.

Kalsbeek A, Strubbe JH (1998) Circadian control of insulin secretion is independent of the temporal distribution of feeding. Physiology & behavior 63:553-558.

Kalsbeek A, Fliers E, Romijn JA et al. (2001) The suprachiasmatic nucleus generates the diurnal changes in plasma leptin levels. Endocrinology 142:2677-2685.

Kopecky J, Clarke G, Enerback S et al. (1995) Expression of the mitochondrial uncoupling protein gene from the aP2 gene promoter prevents genetic obesity. J Clin Invest 96:2914-2923.

La Fleur SE, Kalsbeek A, Wortel J et al. (1999) A suprachiasmatic nucleus generated rhythm in basal glucose concentrations. J Neuroendocrinol 11:643-652.

Messina MM, Overton JM (2007) Cardiovascular effects of melanin-concentrating hormone. Regul Pept 139:23-30.

Migliorini RH, Garofalo MA, Kettelhut IC (1997) Increased sympathetic activity in rat white adipose tissue during prolonged fasting. Am J Physiol 272:R656-661.

Mul JD, Yi CX, van den Berg SA et al. (2010) Pmch expression during early development is critical for normal energy homeostasis. Am J Physiol Endocrinol Metab 298:E477-488.

Nagase I, Yoshida T, Kumamoto K et al. (1996) Expression of uncoupling protein in skeletal muscle and white fat of obese mice treated with thermogenic beta 3-adrenergic agonist. J Clin Invest 97:2898-2904.

Oana F, Homma T, Takeda H et al. (2005) DNA microarray analysis of white adipose tissue from obese (fa/fa) Zucker rats treated with a beta3-adrenoceptor agonist, KTO-7924. Pharmacol Res 52:395-400.

Peuler JD, Johnson GA (1977) Simultaneous single isotope radioenzymatic assay of plasma norepinephrine, epinephrine and dopamine. Life sciences 21:625-636.

Pissios P (2009) Animals models of MCH function and what they can tell us about its role in energy balance. Peptides 30:2040-2044.

Pissios P, Bradley RL, Maratos-Flier E (2006) Expanding the scales: The multiple roles of MCH in regulating energy balance and other biological functions. Endocr Rev 27:606-620.

Pissios P, Ozcan U, Kokkotou E et al. (2007) Melanin concentrating hormone is a novel regulator of islet function and growth. Diabetes 56:311-319.

Richard D (2007) Energy expenditure: a critical determinant of energy balance with key hypothalamic controls. Minerva Endocrinol 32:173-183.

Robidoux J, Martin TL, Collins S (2004) Beta-adrenergic receptors and regulation of energy expenditure: a family affair. Annu Rev Pharmacol Toxicol 44:297-323.

Rosenbaum M, Leibel RL, Hirsch J (1997) Obesity. N Engl J Med 337:396-407.

Seale P, Kajimura S, Yang W et al. (2007) Transcriptional control of brown fat determination by PRDM16. Cell Metab 6:38-54.

Shimada M, Tritos NA, Lowell BB et al. (1998) Mice lacking melanin-concentrating hormone are hypophagic and lean. Nature 396:670-674.

Slavin BG, Ballard KW (1978) Morphological studies on the adrenergic innervation of white adipose tissue. Anat Rec 191:377-389.

Spiegelman BM, Flier JS (2001) Obesity and the regulation of energy balance. Cell 104:531-543.

Strubbe JH, Prins AJ, Bruggink J et al. (1987) Daily variation of food-induced changes in blood glucose and insulin in the rat and the control by the suprachiasmatic nucleus and the vagus nerve. J Auton Nerv Syst 20:113-119.

Umekawa T, Yoshida T, Sakane N et al. (1997) Anti-obesity and anti-diabetic effects of CL316,243, a highly specific beta 3-adrenoceptor agonist, in Otsuka Long-Evans Tokushima Fatty rats: induction of uncoupling protein and activation of glucose transporter 4 in white fat. Eur J Endocrinol 136:429-437.

van Marken Lichtenbelt WD, Vanhommerig JW, Smulders NM et al. (2009) Cold-activated brown adipose tissue in healthy men. N Engl J Med 360:1500-1508.

Virtanen KA, Lidell ME, Orava J et al. (2009) Functional brown adipose tissue in healthy adults. N Engl J Med 360:1518-1525.

Wang J, Liu R, Hawkins M et al. (1998) A nutrient-sensing pathway regulates leptin gene expression in muscle and fat. Nature 393:684-688.

Wirsen C, Hamberger B (1967) Catecholamines in brown fat. Nature 214:625-626.

Xue B, Rim JS, Hogan JC et al. (2007) Genetic variability affects the development of brown adipocytes in white fat but not in interscapular brown fat. J Lipid Res 48:41-51.

Yoshida T, Umekawa T, Kumamoto K et al. (1998) beta 3-Adrenergic agonist induces a functionally active uncoupling protein in fat and slow-twitch muscle fibers. Am J Physiol 274:E469-475.

5

LIPIN 1 STIMULATES MYELINATION IN SCHWANN CELLS THROUGH TRANSCRIPTIONAL REGULATION

Joram D. Mul[1*], Karim Nadra[2*], Isaac Nijman[1], Jean-Jacques Médard[2], Pim W. Toonen[1], Alain de Bruin[3], Sandra Grès[5], Gil-Soo Han[4], George M. Carman[4], Jean-Sébastien Saulnier-Blache[5], Dies Meijer[6], Roman Chrast[2,†,*], and Edwin Cuppen[1,8,*]

[1]Hubrecht Institute-KNAW & University Medical Center Utrecht, Utrecht, The Netherlands
[2]Department of Medical Genetics, University of Lausanne, 1005 Lausanne, Switzerland
[3]Department of Pathobiology, Faculty of Veterinary Medicine, Utrecht University, Utrecht, The Netherlands
[4]Department of Food Science and Rutgers Center for Lipid Research, Rutgers University, New Brunswick, New Jersey 08901, U.S.A.
[5]Inserm, U858/I2MR, Department of Metabolism and Obesity, team #3, 1 avenue Jean Poulhès, BP 84225, 31432 Toulouse Cedex 4, France
[6]Department of Cell Biology & Genetics, Erasmus MC University Medical Center, Rotterdam, The Netherlands
[8]Department of Medical Genetics, University Medical Center Utrecht, Utrecht, The Netherlands

*These authors contributed equally

ABSTRACT

In this study we describe a novel rat model of peripheral neuropathy, generated by *N*-ethyl-*N*-nitrosourea mutagenesis, which displays hindlimb paralysis and lipodystrophy. While pronounced early after onset during the second postnatal week, both of these phenotypes attenuated over time. A forward screen identified a region on chromosome 6, suggesting that a mutation in the *Lpin1* gene, which encodes the phosphatidate phosphatase (PAP1) enzyme Lipin 1, could underlie the observed phenotypes. Indeed, the sequencing of *Lpin1* revealed a missense mutation (*Lpin1*^{1Hubr}) in the 5'-end splice site of exon18 affecting splicing, introducing an out-of-frame reading frame and a premature stop codon in exon19. Biochemical and histological analysis of *Lpin1*^{1Hubr} rats revealed that, while loss of PAP1 activity contributes to lipodystrophy and demyelination in sciatic nerve of *Lpin1*^{1Hubr} rats, a potential preserved functional Lipin 1^{1Hubr} transcriptional activity may lead to the phenotype improvements observed in *Lpin1*^{1Hubr} rats. This hypothesis is partially substantiated by our observation that of the two Lipin 1 isoforms, Lipin 1α and Lipin 1β, Lipin 1α modified *in vitro* transcriptional regulation of the myelination regulator *Krox20*. Together these data indicate that the transcriptional function of Lipin 1 is important for myelination and lipid metabolism, and suggest that Lipin 1 might be an important regulator of the Schwann cell myelination program.

INTRODUCTION

Lipid metabolism is crucial for myelinating glial cell maturation and function due to the necessity to synthesize and maintain myelin membrane that contains a high level of cholesterol and phospho- and glycosphingolipids (Garbay et al., 2000). Accordingly, disorders associated with altered cholesterol metabolism (e.g. Tangier disease and Smith-Lemli-Opitz-syndrome) or fatty acid metabolism (Refsum's disease and diabetes mellitus) often produce myelin and axonal defects (Dyck and Thomas, 2005).

Previous studies have suggested that one of the key enzymes regulating nerve lipid metabolism is Lipin 1 (Verheijen et al., 2003; Nadra et al., 2008). Recent biochemical characterization of Lipin 1 indicates that it is an Mg^{2+}-dependent phosphatidate phosphatase (PAP1) enzyme catalyzing the dephosporylation of phosphatidic acid (PA), yielding inorganic phosphate and diacylglycerol needed for the synthesis of triacylglycerol, phosphatidylcholine, and phosphatidylethanolamine in mammals (Han et al., 2006; Donkor et al., 2007; Harris et al., 2007; Carman and Han, 2009). The mammalian Lipin protein family consists of three members, Lipin 1, Lipin 2, and Lipin 3 (Peterfy et al., 2001), which differ in tissue expression (Donkor et al., 2007). Human *Lpin1* is expressed in multiple tissues with highest levels in white adipose tissue (WAT) and muscle (Donkor et al., 2007). Alternate splicing of *Lpin1* generates two Lipin 1 isoforms that play distinct, but complementary, roles in adipogenesis: Lipin 1α, which is predominantly nuclear and affects adipocyte differentiation, and Lipin 1β, which is mostly cytoplasmic and induces lipogenic gene expression (Peterfy et al., 2005). The amino-terminal and carboxy-terminal regions of Lipin 1 (NLIP and CLIP, respectively), and a predicted nuclear localization signal (NLS) are highly conserved among the three mammalian Lipin family members and among species (Peterfy et al., 2001). The CLIP domain contains multiple key protein functional domains: four haloacid dehalogenase motifs and a transcription factor-binding motif (LXXIL) (Finck et al., 2006; Han et al., 2006; Donkor et al., 2009). Moreover, Lipin 1 and Lipin 2 have been predicted to possess the same structural organization as previously characterized HAD protein family members (Donkor et al., 2009).

In addition to its enzymatic function, the transcriptional coactivating role of Lipin 1 has been shown in murine hepatocytes where it regulates expression of genes involved in fatty acid oxidation (Finck et al., 2006). This is achieved by transcriptional activation of the *PPARα* gene, and by direct coactivation of *PPARα* in cooperation with PGC-1α and p300 (Finck et al., 2006). Thus, Lipin 1, but probably also Lipin 2 and Lipin 3, have dual roles in lipid biosynthesis and gene expression (Finck et al., 2006; Reue and Zhang, 2008).

Both increased or disrupted levels of *Lpin1* gene expression lead to altered phenotypes. Overexpression of *Lpin1* in either adipose tissue or skeletal muscle promotes obesity when mice are fed a high-fat (adipose and muscle tissue) or chow diet (muscle tissue; (Phan and Reue, 2005). *Fatty liver dystrophy* (*Lpin1*$^{fld/fld}$) mice, which carry a spontaneous null mutation for *Lpin1* (Peterfy et al., 2001), are characterized by a neonatal fatty liver that resolves at

weaning, a progressive demyelinating neuropathy affecting peripheral nerves visible from postnatal day (PND) 10 onwards, a reduced body size, a floppy gait, tremors, and lipodystrophy (Langner et al., 1991; Peterfy et al., 2001). Recently, mice with a Schwann cell (SC)-specific deletion of *Lpin1* were created resulting in SC abnormalities and neuropathy similar to the full *Lpin1* knockout (*Lpin1*$^{fld/fld}$) mice (Nadra et al., 2008). This indicated that the neuropathy is a direct consequence of the absence op Lipin 1 – and the subsequent dysregulation of storage lipid metabolism – within SCs. Moreover, SC-specific deletion of *Lpin1* also revealed an interaction between PA and the MEK-Erk pathway mediating SC dedifferentiation and proliferation (Nadra et al., 2008). The recently characterized *Lpin1*^{20884} mice show adult-onset transitory hindlimb paralysis (starting around postnatal week 6), characterized by a floppy gait and a tendency to clench the hind limbs in toward the body when suspended by the tail (Douglas et al., 2009). These phenotypes were however less severe compared to *Lpin1*$^{fld/fld}$ mice, probably due to partial retention of PAP activity. The latter observation possibly also explains why *Lpin1*^{20884} mice lack the fatty liver, the delayed hair growth, and the small size seen in preweaning *Lpin1*$^{fld/fld}$ mice (Douglas et al., 2009). In humans, mutations in *Lpin1* resulted in recurrent myoglobinuria or statin-induced myopathy, although these patients were not tested for peripheral neuropathy (Zeharia et al., 2008).

Here we describe an *Lpin1* mutant allele in the rat (hereafter *Lpin1*^{1Hubr}) characterized by early-onset peripheral neuropathy and lipodystrophy. However, these phenotypes attenuated over time. The *Lpin1*^{1Hubr} mutation resulted in out-of-frame transcription, thereby disrupting Lipin 1 HAD domain 4 and completely inactivating PAP1 activity. We also show that Lipin 1α had a positive effect on expression of the important myelination affecter *Krox20* in primary SCs *in vitro*. We thus propose that Lipin 1α might be an important regulator of the Schwann cell myelination program. Moreover, we hypothesize that the transcription factor-binding motif of Lipin 1^{1Hubr} is functional and has kept its capacity to control lipid metabolism gene expression. This may underlay the observed attenuation of the peripheral neuropathy and lipodystrophy phenotype in *Lpin1*^{1Hubr} rats at PND 49 and onward, mirrored by increased adipose mass in adult *Lpin1*^{1Hubr} rats and an adult *Lpin1*^{1Hubr} mutant sciatic nerve morphology at PND 90 that resembles the sciatic nerve morphology of wild type rats at PND 21.

MATERIAL AND METHODS

Identification of Lpin1^{1Hubr} rats. Following an *N*-ethyl-*N*-nitrosourea (ENU)-mutagenesis screen (Smits et al., 2006), an accidental brother-sister mating between two F_3 animals (Wistar/Crl background; outcrossed twice to wild type Wistar background) revealed offspring that could be identified approximately between PND 7 and 14 by hindlimb paralysis and hindquarter muscle wasting.

Forward screen, Sequencing, and Experimental Rats. The Animal Care Committee of the Royal Dutch Academy of Science and the University of Lausanne approved all experiments according to the Dutch and Swiss legal ethical guidelines. For the mapping cross, the two initial F_3 carriers of the *Lpin1*^{1Hubr} mutation were outcrossed with Brown Norway animals (BN/Crl). F_4 Wistar/BN rats were intercrossed to identify them as carriers of the mutation and to generate offspring homozygous

for the mutation. After onset of the phenotype, DNA was isolated from F_5 wild type/heterozygous and homozygous Wistar/BN offspring. DNA was processed as described before (Nijman et al., 2008), and a previous described Wistar/BN SNP panel (Nijman et al., 2008) was used to map the genotype in F_5 Wistar/BN rats. In total, the SNP distribution pattern for 67 mutant Wistar/BN F_5 rats was determined. Primers were designed to cover each exon with partial intron overhang, and sequencing of *Lpin1* in 4 wild type/heterozygous and 4 mutant pups revealed a missense mutation (T>A) in the conserved 5'-end splice site of exon18. In addition to the cross to BN/Crl animals, the initial F_3 carriers of the *Lpin1*^{1Hubr} mutation were also outcrossed to wild type Wistar/Crl animals for 4 additional generations to eliminate confounding effects from background mutations induced by ENU. It has been previously described that outcrossing six times to a wild type background decreases the total number of random background mutations to 1 (Mul et al., 2010). However, we cannot fully exclude the presence of tightly linked confounding mutations in our rat model. F_7 Wistar/Crl rats were used in all described experiments except for the mapping screen.

Animal housing. *Lpin1*^{1Hubr} pups were obtained at the expected Mendelian frequency, and the phenotype was not gender specific. If more than 8 littermates were present and survivability of *Lpin1*^{1Hubr} pups was compromised, wild type/heterozygous pups were removed as soon as the *Lpin1*^{1Hubr} phenotype could be observed, until a total of 8 pups remained. Chow pellets were also added to the maternal cage floor to increase feeding chances of *Lpin1*^{1Hubr} pups. After weaning (PND 21), two rats were housed together, unless noted otherwise, under controlled experimental conditions (12 h light/dark cycle, light period 0600-1800, 21±1°C, ~60% relative humidity). The standard fed diet in our animal facility (semi high-protein chow: RM3, 26.9% crude protein, 11.5% fat, and 61.6% carbohydrates; 3.33 kcal/g AFE; SDS, Witham, United Kingdom) was provided *ad libitum* together with water. For the high-fat (HF) diet experiment, rats were given *ad libitum* access to a HF diet (45%-AFE, 20% crude protein, 45% fat, and 35% carbohydrates; 4.54 kcal/g AFE SDS, Witham, United Kingdom) for 4 weeks starting at PND 90, and food intake and body weight were measured every week.

Genotyping. Genotyping was done using the KASPar SNP Genotyping System (KBiosciences, Hoddesdon, United Kingdom; as described by van Boxtel et al., 2008) using gene-specific primers (forward common, GAGCC CTTTT ATGCT GCTTT TGGGA A; reverse wild type, GAAGG TGACC AAGTT CATGC TCCAC TGACC TCCTC GGGTA; reverse homozygous, GAAGG TCGGA GTCAA CGGAT TCTCC ACTGA CCTCC TCGGG TT). All pups were genotyped at PND 21. Genotypes were reconfirmed when experimental procedures were completed.

Quantitive RT-PCR. For all analyses, total RNA from complete sciatic nerve, endoneurium and WAT was isolated using the Qiagen RNeasy lipid tissue kit (Qiagen) following the manufacturer's instructions. Total RNA from muscle, brain, liver, and rat primary Schwann cells was isolated in TRIzol (Invitrogen) reagent and purified with the RNeasy kit (Qiagen). RNA quality was verified by agarose gel and/or by Qiaxcel capillary electrophoresis device (Qiagen), and the concentration was determined by a ND-1000 Spectrophotometer (NanoDrop). Total RNA (250–500 ng) was subjected to reverse transcription using the SuperScript III First-Strand Synthesis System for RT–PCR (Invitrogen) following the manufacturer's instructions. The resulting cDNA was used as a template for relative quantitative RT-PCR as described previously (de Preux et al., 2007). Results were normalized using the reference gene *Ubiquitin*. See Supplemental Table 1 for a complete list of oligonucleotides used for relative gene expression.

Western blotting. Tissues were lysed in ice-cold lysis buffer (20mM $Na_2H_2PO_4$, 250mM NaCl, Triton X-100 1%, SDS 0.1%) supplemented with Complete protease inhibitors (Roche). Protein levels were quantified using the Bio-Rad protein assay with BSA as a standard. Equal amounts of protein extracts were resolved by 10% SDS-PAGE and electro-transferred onto a polyvinylidene difluoride (PVDF) membrane (Amersham Biosciences). Blots were blocked in tris-buffered saline containing

0.1% Tween (TBS-T) supplemented with 4% milk powder and subsequently incubated overnight at 4°C in the same buffer supplemented with antibodies against Krox-20 (Egr-2, Covance), Krox-24 (Egr-1, Ab-cam), p35 (Santa Cruz Biotechnologies), and Tubulin (Sigma). After washing in TBS-T, blots were exposed to the appropriate horseradish peroxidase-conjugated secondary antibodies (Dako) in TBS-T for 1 h at room temperature. Finally, blots were developed using the ECL reagents (Pierce) and Kodak Scientific Imaging Films (Kodak).

Microdissection of sciatic nerve. Sciatic nerves were harvested at PND 21 or 90 and placed in ice-cold PBS (pH 7.4). The perineurium and epineurium were gently dissected away from the endoneurium along the whole length of the nerve as previously described (Verheijen et al., 2003).

PAP activity measurement. Tissue samples were disrupted using a dounce homogenizer at 4°C in 50mM Tris-HCl (pH 7.5) buffer containing 0.25M sucrose, 1mM EDTA, 10mM β-mercaptoethanol, 1mM benzamidine, 0.5mM PMSF, 5 mg/ml of aprotinin, leupeptin, and pepstatin. The lysed cells were centrifuged at 1,000 × *g* for 10 min at 4°C, and the supernatant was used as cell extract. Total PA phosphatase activity (Mg^{2+}-dependent and Mg^{2+}-independent) was measured at 37°C for 20 min in the reaction mixture (total volume of 100ml) containing 50mM Tris-HCl (pH 7.5), 1mM $MgCl_2$, 10mM β-mercaptoethanol, 0.2mM [^{32}P]-PA (5,000cpm/nmol), 2mM Triton X-100, and enzyme protein. The Mg^{2+}-independent PA phosphatase activity was measured in the same reaction mixture except that 2mM EDTA was substituted for 1mM $MgCl_2$. The Mg^{2+}-dependent PA phosphatase activity was calculated by subtracting the Mg^{2+}-independent enzyme activity from total enzyme activity. A unit of PA phosphatase activity was defined as the amount of enzyme that catalyzed the formation of 1nmol of product/min. Specific activity was defined as U/mg protein.

WAT morphology. Rats were sacrificed at PND 4, 10, 21 or 90 by decapitation after measuring body weight, and the left and right dorsal subcutaneous WAT fat pads were harvested and weighed. Afterwards, WAT samples were collected in 4% formaldehyde, rotated o/n at 4°C, rinsed twice with 100% ethanol for 2 hrs, left in xylene o/n at RT, and embedded in paraffin. Tissue was then cut in 5-*μ*m sections and stained with hematoxylin and eosin. Average adipocyte cell diameter was measured using NIH ImageJ software.

Toluidine blue staining and morphometric analysis. Semi-thin nerve cross-sections were stained with 1% toluidine blue and digitalized using the AxioVision release 4.5 software (Zeiss). For each myelinated axon present, both an axonal area (defined by the inner limit of the myelin sheath) and a total fiber area (defined by the outer limit of the myelin sheath) were automatically measured using image analysis software (G-ratio calculator 1.0, Image J plug-in, Yannick Krempp, Cellular Imaging Facility, Lausanne, Switzerland). The g-ratio was calculated by dividing the axon area by total fiber area. Each experimental group consisted of two rats.

Oil-red-O staining. A fresh working solution of Oil-red-O (Sigma) was prepared by dilution of the Oil-red-O stock solution (5 g/L in 98% isopropanol) in distilled water at a ratio of 3:2. The working solution was allowed to stand for 10 min after mixing and was filtered with a 0.45-μm pore-size filter. Subsequently, sciatic nerve cross-sections were briefly (30 sec) washed in PBS, stained with the filtered working solution of Nile red for 10 min, and washed for 10 min in demineralized water (room temperature). The slides were allowed to dry, mounted with Vectashield mounting medium (Vector Laboratories), and visualized using a Zeiss Axioplan 2 microscope with an AxioCam MRc camera and AxioVision release 4.5 software (Zeiss).

Nile Red staining. Sciatic nerve cross-sections were mounted in Nile red (Sigma) solution (0.5 mg/mL in acetone) diluted 1,000X in 75% glycerol and visualized as described above.

Lentiviral expression in primary rat SC culture. SCs were isolated from sciatic nerves of Sprague–Dawley rat pups shortly after birth (P3–P4). Fibroblasts were eliminated using immunoselection (Brockes et al., 1979). Purified SCs were cultured on poly-L-lysine-coated tissue plastic culture

dishes in DMEM containing 10% fetal calf serum, 10ng/mL neuregulin, and 4μM forskolin (Sigma), and infected with a lentiviral vector expressing either *Lpin1*α or *Lpin1*β. An empty lentiviral vector was used as a negative control. Rat primary SCs were induced to differentiate at 2 days post-infection (designated day 0) with DMEM containing 10% (v/v) FBS, 1μM dexamethasone, 0.5mM isobutylmethylxanthine and 1μg/ml insulin. After 48 h, the cells were re-fed with the same medium and were changed every second day. After 8 days, the cells were harvested and the expression of *Krox20*, *Lpin1* and *Mpz* was analyzed by quantitative PCR. All experimental conditions were done *in triplo*.

BrdU incorporation assay. At PND 21, rats were injected intraperitoneally with 100μg of BrdU per gram of body weight. Six hours later, the sciatic nerves were dissected, fixed in 4% paraformaldehyde for 24 hr, and embedded in OCT medium. Longitudinal cryosections were prepared, post-fixed in 4% paraformaldehyde (10 min), denatured with 2 M HCl for 20 min at 37°C, and neutralized in 0.1M sodium borate (pH 8.5) for 10 min. Sections were incubated with rat anti-BrdU (at a 1:200 dilution; Abcam) in 0.3% Triton X-100 overnight at 4°C. Next day, the sections were incubated with anti-rat secondary antibody conjugated to Alexa Fluor 594 (at a 1:200 dilution; Invitrogen) and visualized with fluorescence microscopy. The nuclei were counterstained with DAPI.

Data analysis. All data are shown as mean ± S.E.M. All data were analyzed using a commercially available statistical program (SPSS for Macintosh, version 16.0) and were controlled for normality and homogeneity. Differences in longitudinal body weight measurements were assessed using repeated measure analysis, followed by Bonferroni *post hoc* analyses if significant overall interactions were observed. All other data were analyzed using a Student's *t*-test. The null hypothesis was rejected at the 0.05 level.

RESULTS

The generation and identification of *Lpin1*^{1Hubr} rats. After an ENU-mutagenesis screen on a Wistar/Crl background (Smits et al., 2006), a brother-sister mating (F_3 generation) revealed offspring that could be identified approximately between PND 7 and 14 by hindlimb paralysis, lipodystrophy, and hindquarter muscle wasting (Supplemental Figure S1A and B; Supplemental Video 1). The phenotype in young *Lpin1*^{1Hubr} rats (PND 28) is characterized by loss of hindlimb joint mobility, hindquarter muscle wasting, lipodystrophy, the absence of characteristic retraction of the hindlimbs when picked up by the neck, and the inability to splay hindlimbs when suspended by the tail (Supplemental Figure S1A, B, C and D). The Wistar/Crl F_3 animals heterozygous for the mutation were outcrossed with Brown-Norway (BN/Crl) animals to generate an F_4 Wistar/BN population for mapping purposes. On PND 21, DNA was collected from wild type/heterozygous and mutant Wistar/BN F_5 animals, and a forward screen was performed using a Wistar/BN-specific SNP marker panel (Nijman et al., 2008). This resulted in the identification of a 3.6Mb region on chromosome 6 between 37.1Mb and 40.7Mb, resulting in the identification of *Lpin1* (Chr.6; 40.3Mb) as a prime candidate gene (Supplemental Figure S2). Sequencing of *Lpin1* revealed a missense mutation (T>A) in the conserved 5'-end splice site of exon18. The mutation impaired the binding of the splicing machinery, and generated a new splice site 16bp downstream of the original site. The new splice site resulted in out-of-frame transcription introducing a premature stopcodon in exon19 (Fig. 1A), and disrupted predicted HAD motif IV (Fig. 1B).

The Lpin1^{1Hubr} phenotype is regressive. In addition to the *Lpin1^{1Hubr}* Wistar/BN line, an *Lpin1^{1Hubr}* Wistar (Wistar/Crl) line was established and used in all described experiments. The *Lpin1^{1Hubr}* phenotype manifested itself approximately between PND 7 and 14. *Lpin1^{1Hubr}* rats that showed an early onset of the phenotype (around PND 7) demonstrated decreased survivability, probably due to decreased mobility and subsequent suckling competition compared to *Lpin1^{1Hubr}* rats with a later onset of the phenotype (data not shown). However, a considerable attenuation of the peripheral neuropathy and lipodystrophy was observed over time. Around PND 49 and onwards, *Lpin1^{1Hubr}* rats had partially regained the ability to use their hindlimbs while walking, although still with a floppy gait, and the characteristic ability to retract their hindlimbs when picked up by the neck (Supplemental Figure S1; Supplemental Videos 1, 2, 3, and 4). In addition, the hindlimb muscle wasting and lipodystrophy became less pronounced (Supplemental Figure S1). The variety in timing of *Lpin1^{1Hubr}* phenotype onset, and thus the severity of the phenotype, was reflected by the variety between strong and moderate phenotype improvement (data not shown).

Loss of PAP1 activity in Lpin1^{1Hubr} rats. Relative expression of the *Lpin1* isoforms, *Lpin1*α and *Lpin1*β (Fig. 2A; (Peterfy et al., 2005), was investigated at PND 21 and 90. In addition, correct splicing of the wild type transcript was investigated using primers spanning

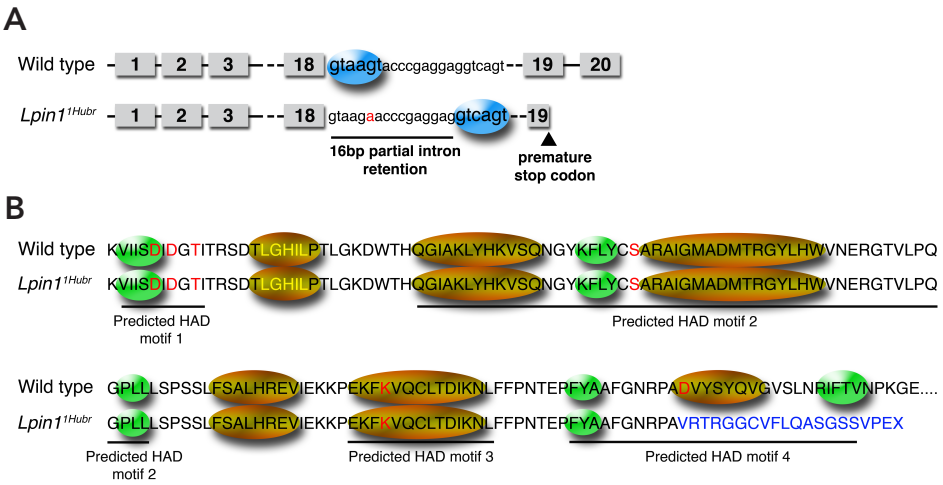

Figure 1. The *Lpin1^{1Hubr}* mutation. ***A***. ENU-mutagenesis introduced an A>T mutation (indicated in red) in intron 18-19 of *Lpin1^{1Hubr}* rats. The mutation disrupted a splice site motif (GTXAGT), creating a new splice site downstream and resulting in 16bp partial intron retention. Blue ellipses indicate a splice motif. The new reading frame resulted in a premature stop codon in exon19. ***B***. Amino acid sequence showing the four predicted HAD motifs, the conserved amino acids from the HAD family of proteins in *red letters*, the transcription coactivator motif LXXIL in *yellow letters*, *green ellipses* indicate predicted ß-strands, and *gold ellipses* indicate predicted α-helices (Donkor et al., 2009). The partial intron retention disrupts the conserved amino acid in predicted HAD motif IV (WT: GNRPAD; HOM: GNRPAV). Moreover, the out-of-frame transcription (indicated in blue) disrupts the predicted α-helice and the second predicted β-strand of predicted HAD motif IV.

the wild type exon18-19 boundary (*Lpin1*$^{Ex18\text{-}19}$; Fig. 2A). Expression of *Lpin1*$^{Ex18\text{-}19}$ was almost undetectable in muscle, WAT, liver, and brain samples of *Lpin1*^{1Hubr} rats at PND 21 or 90 (Fig. 2B and C). Furthermore, expression of *Lpin1*α, *Lpin1*β, and *Lpin1*$^{Ex18\text{-}19}$ was investigated in sciatic nerve endoneurium (Fig. 2D). An ~80% decrease in *Lpin1*$^{Ex18\text{-}19}$ expression was detected in mutants at both PND 21 and 90 as compared to wild type rats (Fig. 2D). Interestingly, *Lpin1*α and *Lpin1*β expression (measured at the level of exons 4-6; Fig. 2A) was increased in *Lpin1*^{1Hubr} rats as compared to wild type rats at PND 21, suggesting absence of nonsense-mediated decay (NMD) mechanism. Later in development (PND 90), only *Lpin1*β expression was increased in *Lpin1*^{1Hubr} rats as

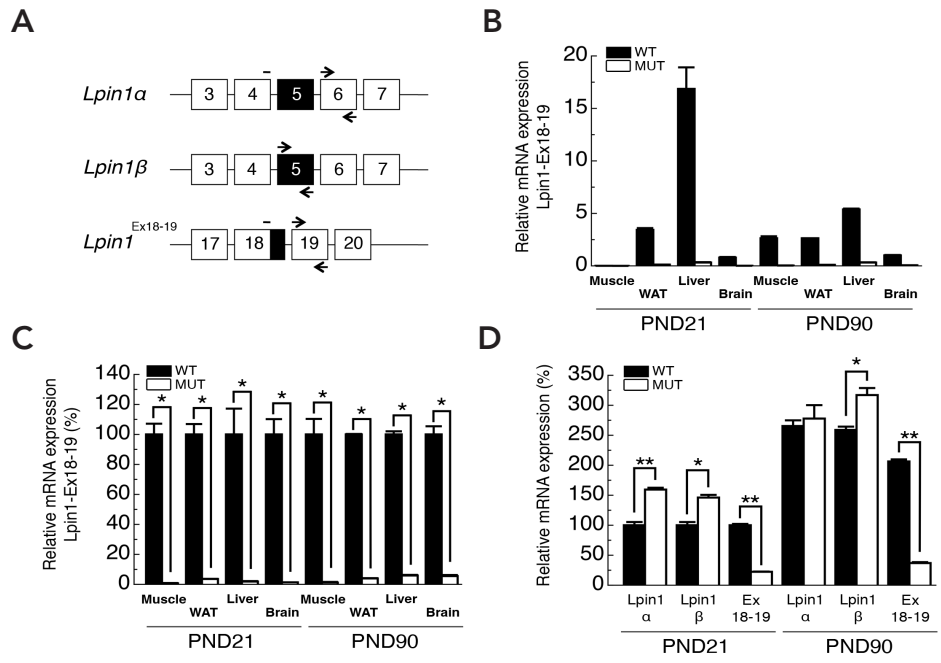

Figure 2. Molecular analysis of *Lpin1*^{1Hubr} expression. ***A***. Schematic overview of primer position to measure expression of *Lpin1*α, *Lpin1*β, and the correctly spliced exon18-19 boundary (*Lpin1*$^{Ex18\text{-}19}$). Exon 5 (shown in black) is included in *Lpin1*β, but is absent in *Lpin1*α. For *Lpin1*$^{Ex18\text{-}19}$, the black part indicates the 16bp intron retention. ***B***. Quantitative PCR measurements revealed high wild-type *Lpin1*$^{Ex18\text{-}19}$ expression in WAT and liver, and low expression in muscle and brain at PND 21. At PND 90, high expression of wild-type *Lpin1*$^{Ex18\text{-}19}$ is observed in muscle, WAT and liver, but expression remained low in brain (n = 2 per group). Wild type *Lpin1*$^{Ex18\text{-}19}$ expression was almost completely absent in all analyzed *Lpin1*^{1Hubr} samples. ***C***. Relative quantification of the expression of wild type transcript in *Lpin1*^{1Hubr} rats at PND 21 and PND 90 (n = 2 per group) revealed its decrease below 10% of wild type levels (**P*<0.001; n = 2 per group). ***D***. Relative expression of *Lpin1*α and *Lpin1*β is increased, whereas *Lpin1*$^{Ex18\text{-}19}$ expression is substantially decreased in sciatic nerve tissue of *Lpin1*^{1Hubr} rats as compared to wild type rats at PND 21. At PND 90, relative expression of *Lpin1*α, *Lpin1*β, and *Lpin1*$^{Ex18\text{-}19}$ is increased, unchanged, and substantially decreased (respectively) in sciatic nerve tissue of *Lpin1*^{1Hubr} rats compared to wild-type rats at PND 21 (**P*<0.05; ***P*<0.001; n = 2 per group). Data are expressed as mean ± S.E.M.

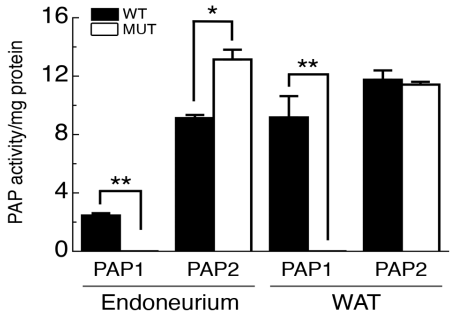

Figure 3. Biochemical analysis of *Lpin1*^{1Hubr} function. PAP1 activity is decreased in sciatic nerve endoneurium and WAT of *Lpin1*^{1Hubr} rats as compared to wild type rats at PND 21. PAP2 activity is increased in sciatic nerve endoneurium of *Lpin1*^{1Hubr} rats as compared to wild type rats, whereas PAP2 activity in WAT was unchanged between genotypes (*P<0.005; **P<0.001; n = 5-6 per group). Data are expressed as mean ± S.E.M

compared to wild type rats (Fig. 2D). However, at PND 21, PAP1 activity was completely inactivated in sciatic nerve endoneurium and WAT of *Lpin1*^{1Hubr} rats as compared to wild type rats (Fig. 3). These data indicate that while the *Lpin1*^{1Hubr} mutation does not lead to NMD, it disrupts HAD motif 4 resulting in a full loss of its enzymatic PAP1 function.

WAT morphology in Lpin1^{1Hubr} rats. The body weight of *Lpin1*^{1Hubr} and wild type rats was equal until PND 10, but from PND 21 and onward, *Lpin1*^{1Hubr} rats showed a reduction in body weight as compared to wild type rats (Supplemental Figure S3A, B, and C). WAT tissue analysis revealed a decreased adipocyte size, both at PND 21 and 90, whereas adipocyte cell size was equal between genotypes at PNDs 4 and 10 (Fig. 4A and B). The decreased ability to store lipids was reflected by a severe reduction in adipose mass (Fig. 4C). Relative expression of peroxisome proliferator-activated receptor receptor-γ (*Pparγ1* and *Pparγ2*), a key affecter of adipocyte differentiation (Rosen and Spiegelman, 2006), and fatty acid-binding protein 4 (*Fabp4*, also designated aP2), that reversibly bind fatty acids and others lipids (Makowski and Hotamisligil, 2005), in WAT derived from *Lpin1*^{1Hubr} and wild type rats was equal between genotypes at PND 4 and 10 (Fig. 4D). However, relative expression of *Pparγ1*, *Pparγ2*, and *Fabp4* was decreased in *Lpin1*^{1Hubr} compared to wild type rats at PND 21 and 90 (Fig. 4D). Relative expression of the wild type transcript *Lpin1*$^{Ex18\text{-}19}$ in WAT was decreased in *Lpin1*^{1Hubr} compared to wild type rats at PND 4, 10, 21 and 90 (Fig. 4D). Adult *Lpin1*^{1Hubr} rats fed a HF diet for 4 weeks demonstrated a decreased body weight increase as compared to wild type rats (Supplemental Figure S4A). However, the percentage increase of body weight normalized for the body weight at the start of the HF feeding did not differ between genotypes, indicating that adult *Lpin1*^{1Hubr} rats are equally capable of storing lipids when fed a HF diet as compared to adult wild type rats (Supplemental Figure S4B). Food intake on a HF diet did not differ between genotypes, although *Lpin1*^{1Hubr} rats were hyperphagic as compared to wild type rats when food intake was normalized for body weight (Supplemental Figure S4C, and D). Finally, although not corrected for lipid loss through feces, *Lpin1*^{1Hubr} rats demonstrated a decreased 'feed efficiency' (Supplemental Figure S4E), as was observed for *Lpin1*$^{fld/fld}$ mice (Phan et al., 2004). In sum, *Lpin1*^{1Hubr} rats demonstrated an aberrant WAT phenotype, consistent with the finding that *Lpin1* is strongly expressed in adipose tissue (Peterfy et al., 2001). However,

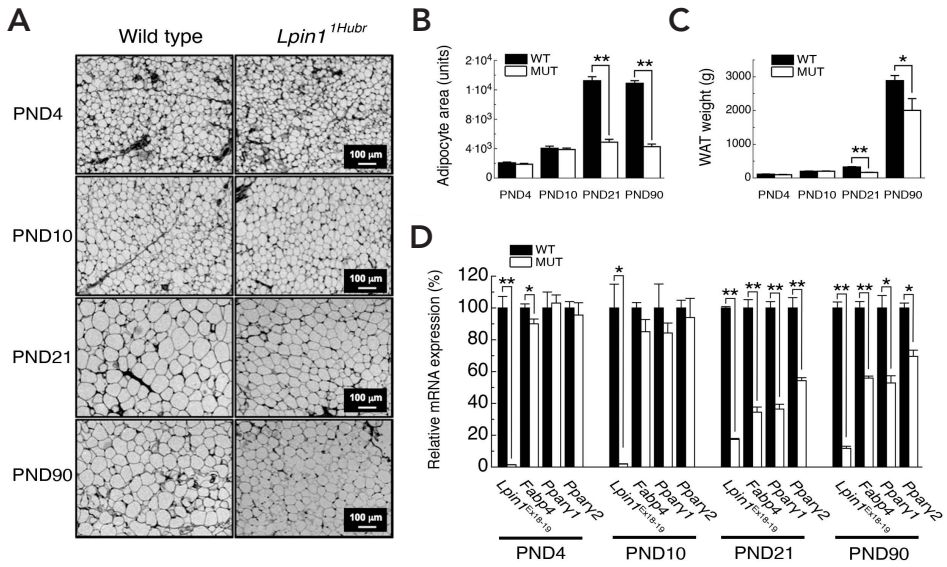

Figure 4. Lipodystrophy phenotype in *Lpin1*^{1Hubr} rats. ***A***. Dorsal subcutaneous adipose tissue sections prepared from *Lpin1*^{1Hubr} and wild type rats at PND 4, 10, 21 and 90 stained with hematoxylin and eosin. Starting from PND 21 the reduced size of adipocytes becomes visible in *Lpin1*^{1Hubr} samples. ***B***. Average adipocyte area is equal between genotypes at PND 4 and 10, but is decreased in *Lpin1*^{1Hubr} rats compared to wild type rats at PND 21 and 90 (n = 2 per group; n = 41-83 adipocytes per group; $^{**}P<0.001$). ***C***. Subcutaneous dorsal WAT weight is equal between genotypes at PND 4 and 10 (n = 2 per group), but is decreased in *Lpin1*^{1Hubr} rats compared to wild type rats at PND 21 (n = 2 per group) and 90 (n = 2-4 per group; $^{*}P<0.05$; $^{**}P<0.001$). ***D***. Relative gene expression analysis in WAT of *Lpin1* (*Lpin1*$^{Ex18\text{-}19}$) and of genes involved in adipocyte differentiation (*Fabp4*, *Pparγ1*, and *Pparγ2*) in WAT. Relative gene expression of *Lpin1*$^{Ex18\text{-}19}$ in *Lpin1*^{1Hubr} rats is decreased compared to wild type rats at PND 4, 10, 21, and 90 (n = 3, n = 3, n = 5, and n = 1 per group, respectively). Relative gene expression of *Fabp4*, *Pparγ1*, and *Pparγ2* was equal between genotypes at PND 4 and 21 (n = 3 and n = 3, respectively). However, at PND 21 and 90, relative gene expression of *Fabp4*, *Pparγ1*, and *Pparγ2* was decreased in *Lpin1*^{1Hubr} rats compared to wild type rats (n = 5 and n = 1 per group, respectively; $^{*}P<0.05$; $^{**}P<0.001$). Data are expressed as mean ± S.E.M.

the WAT phenotype in *Lpin1*^{1Hubr} rats seems to attenuate over time, as reflected by higher expression of adipogenetic factors at PND90 and relatively increased adipose mass at PND 90 (51% at PND 21; 69% at PND 90). Moreover, the ability to accumulate lipids is decreased but not absent in adult *Lpin1*^{1Hubr} rats on a high-fat diet.

Sciatic nerve morphology in Lpin1^{1Hubr} rats. Null deletions of *Lpin1* result in severe sciatic nerve myelin abnormalities (Langner et al., 1991; Nadra et al., 2008), while *Lpin1*^{20884} mutants show a less severe demyelination phenotype (Douglas et al., 2009). We therefore investigated sciatic nerve morphology using toluidine blue-stained semithin nerve sections at PND 4, 10, 21, and 90. At PND 4 and 10, no clear sciatic nerve myelin abnormalities were observed between genotypes (Fig. 5A). This observation was strengthened by an equal axon diameter and g-ratio at PND 4 and 10 (Fig. 5B). At

PND 21, *Lpin1*^{1Hubr} rats showed severe myelin abnormalities compared to wild type rats, characterized by hypo- and demyelination (aberrant g-ratio trend line), a decreased axon diameter, and the presence of dark-colored debris (Fig. 5A and B). Although hypo- and demyelination, a decreased axonal diameter, and dark-colored debris were still present at PND 90, overall sciatic nerve morphology in *Lpin1*^{1Hubr} rats at this late developmental time point showed an improved phenotype resembling sciatic nerve morphology of wild type rats at PND 10 or 21. Thus, *Lpin1*^{1Hubr} rats showed a perturbed

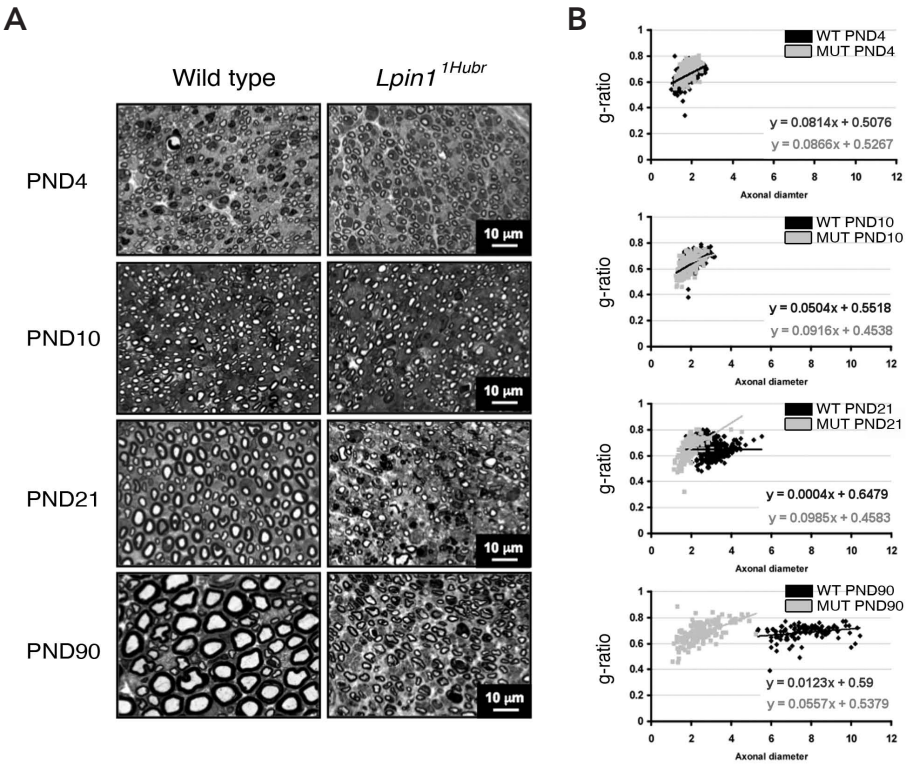

Figure 5. Progression of myelination in *Lpin1*^{1Hubr} rats. ***A***. Toluidine blue-stained semithin sections from the medial region of the sciatic nerve of *Lpin1*^{1Hubr} and wild type rats at PND 4, 10, 21, and 90. At PND 4 and 10, the level of myelination is similar in wild type and mutant nerve. At PND 21 and 90, hypomyelination is visible in sciatic nerves of *Lpin1*^{1Hubr} rats compared to wild type nerves. At PND 90, general morphology of *Lpin1*^{1Hubr} sciatic nerves is improved compared to general morphology of sciatic nerves isolated from *Lpin1*^{1Hubr} at PND 21. ***B***. At PND 4 and 10, average g-ratio, g-ratio trend line, and average axonal diameter of medial sciatic nerve tissue is equal between genotypes. At PND 21, however, axons of *Lpin1*^{1Hubr} rats show a decreased axonal diameter as compared to wild type axons, and an aberrant g-ratio trend line, indicating hypomyelination. At PND 90, axons of *Lpin1*^{1Hubr} rats showed a decreased axonal diameter as compared to wild type axons, and an aberrant g-ratio trend line, indicating hypomyelination. Axons of *Lpin1*^{1Hubr} rats show an increase in trend line at PND 90 compared to PND 21, indicative of myelination improvement. (PND 4, 10, 21, and 90; n = 2, n = 2, n = 2, and n = 1 per group, respectively; n = 107-374 axons per genotype).

sciatic nerve phenotype consistent with the finding that *Lpin1* is critical for normal SC function (Nadra et al., 2008). However, the aberrant SC phenotype seems to attenuate over time. Our observation that *Lpin1*^{1Hubr} rats regain the ability to use their hind limbs when walking, although still with a floppy gait, and regain the ability to splay hindlimbs when picked up by the tail strengthens this observation (Supplemental Figure S1; Supplemental Videos 2, 3, and 4).

Evaluation of myelin defects in Lpin1^{1Hubr} rats. Next, we examined the level of myelination of *Lpin1*^{1Hubr} and wild type sciatic nerve cross-sections at PND 21 and 90, using Nile red staining. AT PND 21, the level of myelination was severely affected. However, the integrity of myelin substantially improved in the older *Lpin1*^{1Hubr} rats (PND 90; Fig. 6A). These findings were confirmed using Oil-red-O staining (Supplemental Figure S5). The level of myelination, as measured by the level of myelin gene expression (*Mpz* [also designated *P0*] and *Pmp22*), was equal between genotypes at PND 4, but was decreased in *Lpin1*^{1Hubr} rats as compared to wild type rats at PND 10, 21 and 90 (Fig. 6B). These observations are in agreement with the observed hypo- and demyelination at PND 21 and 90 (Fig. 5A), and indicate that expression of myelin genes is already affected at PND 10. Relative expression of the POU domain transcription factor *Oct-6/Scip/Tse-1* (hereafter *Scip*), a marker of immature promyelinating SCs (Jaegle et al., 1996; Zorick et al., 1996), and the zinc-finger transcription factor *Krox20/Egr2* (hereafter *Krox20*), a marker of mature SCs (Zorick et al., 1996) and an important controller of myelination, was equal between genotypes at PND 4 (Fig. 6C). At PND 10, relative *Krox20* expression was slightly increased in *Lpin1*^{1Hubr} rats as compared to wild type rats (Fig. 6C). At PND 21, relative *Scip* expression was increased, whereas *Krox20* expression was decreased in *Lpin1*^{1Hubr} rats as compared to wild type rats (Fig. 6C), indicative of a relative increased pool of immature SCs in *Lpin1*^{1Hubr} sciatic nerve. At PND 90, both relative *Scip* and *Krox20* expression was increased in *Lpin1*^{1Hubr} rats as compared to wild type rats (Fig. 6C), suggesting a mixed SC population composed of immature and myelinating SCs. Western blot analysis at PND 21 confirmed decreased protein levels of Krox20 in *Lpin1*^{1Hubr} rats compared to wild type rats (Fig. 6D). Moreover, although Krox24 levels were equal between genotypes, P35 levels were increased in *Lpin1*^{1Hubr} rats as compared to wild type rats (Fig. 6D). Our observations indicate a switch of *Krox20* expression and subsequent protein levels increase between PND 21 and 90 in *Lpin1*^{1Hubr} rat SCs. Together these observations indicate the presence of improvement in myelin phenotype at PND 90. It is however important to mention that using 5-bromo-2'-deoxyuridine (BrdU)/DAPI double-label immunohistochemistry analysis, we observed increased cellularity and increased cell proliferation in sciatic nerve of *Lpin1*^{1Hubr} rats as compared to wild type sciatic nerve at PND 90 (Supplemental Figure S6). This, together with a maintained elevated level of *Cyclin D1* expression in *Lpin1*^{1Hubr} rats as compared to wild type rats at PND 21 and 90, suggests that even at PND 90, mutant endoneurium contains immature and dividing SCs (Supplemental Figure S6).

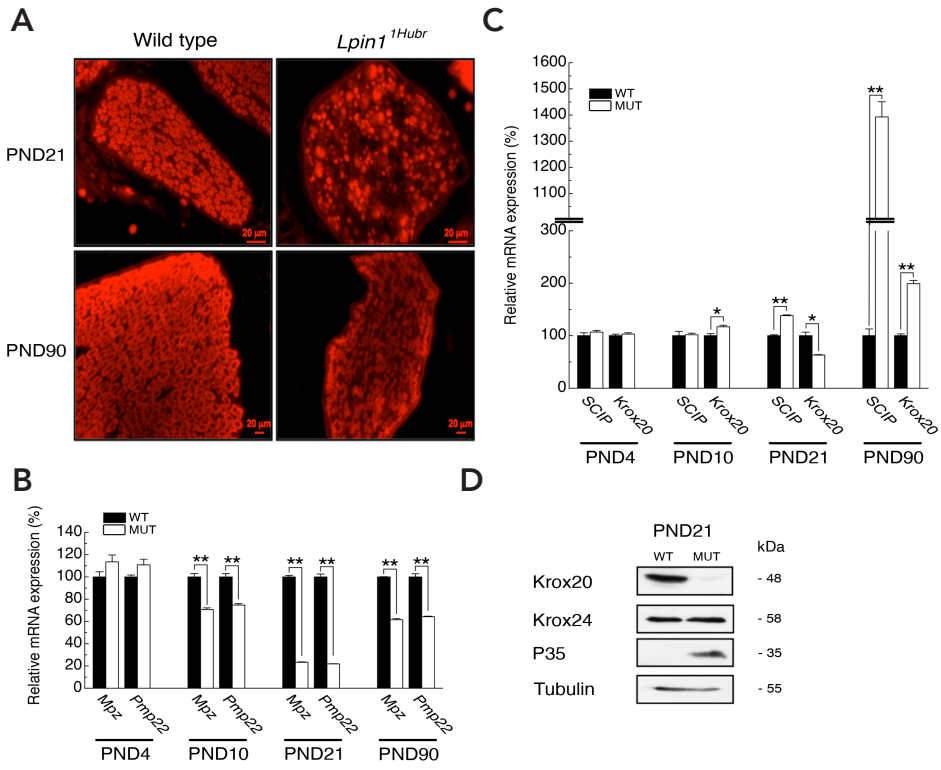

Figure 6. Transitory signaling defects in *Lpin1*^{1Hubr} rats regarding myelination. ***A***. Nile-red staining of sciatic nerve sections from *Lpin1*^{1Hubr} and wild type rats at PND 21 and 90. At PND 21, the typical 'donut'-like myelin structures present in wild type sciatic nerve are replaced in *Lpin1*^{1Hubr} nerves by 'dot'-like structures probably corresponding to the accumulation of debris in demyelinated SCs. *Lpin1*^{1Hubr} nerves partially recover the 'donut'-like myelin staining at PND 90. ***B***. Relative gene expression analysis of *Mpz* and *Pmp22* (mature SC markers) in sciatic nerve tissue of *Lpin1*^{1Hubr} rats as compared to wild type rats at PND 4, 10, 21 and 90 (n = 3, n = 3, n = 3, and n = 1 per group, respectively). Relative *Mpz* and *Pmp22* expression was unchanged between genotypes at PND4, but was decreased in *Lpin1*^{1Hubr} rats compared to wild type rats at PND 10 and 21, and partially recover their levels at PND 90 (**P<0.001). ***C***. Relative gene expression analysis of *Scip* and *Krox20* (immature SC markers) in sciatic nerve tissue of *Lpin1*^{1Hubr} rats as compared to wild type rats at PND 4, 10, 21 and 90 (n = 3, n = 3, n = 3, and n = 1 per group, respectively). At PND 4, relative *Scip* and *Krox20* expression was unchanged between genotypes. At PND 10, relative *Scip* expression was unchanged between genotypes, whereas *Krox20* was increased in *Lpin1*^{1Hubr} rats as compared to wild type rats. At PND 21, relative *Scip* expression was increased, whereas *Krox20* expression was decreased in *Lpin1*^{1Hubr} rats as compared to wild type rats. At PND 90, expression of *Scip*, and *Krox20* was increased (*P<0.05; **P<0.001). ***D***. Western blot analysis showing protein levels of Krox20, Krox24, and P35 in *Lpin1*^{1Hubr} and wild type rats at PND 21. Tubulin was used as input control. At PND 21, protein levels of Krox20 confirmed earlier relative gene expression observations. Data are expressed as mean ± S.E.M.

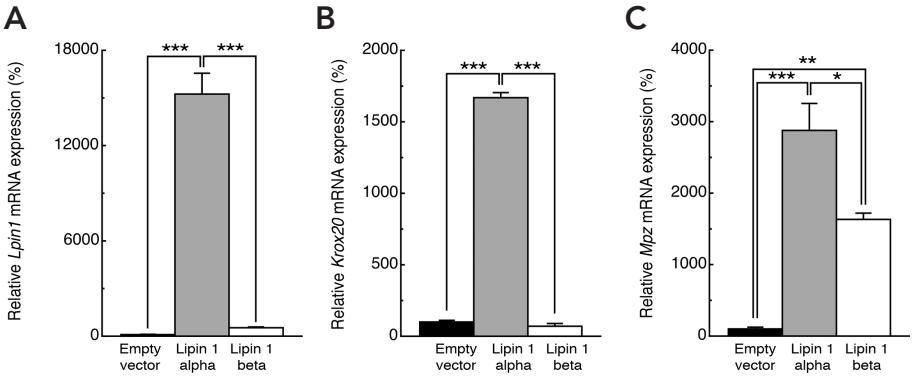

Figure 7. Transcriptional regulatory activity of Lipin 1 in primary SC culture. ***A***. Viral-induced expression of *Lpin1*α or *Lpin1*β increased relative expression of *Lpin1* approximately 150-fold and 6-fold, respectively, in primary rat SC cultures as compared to empty vector control (n = 3 per group; ***P<0.001). ***B***. Viral-induced expression of *Lpin1*α increased relative expression of *Krox20*, whereas viral-induced expression of *Lpin1*β had no effect on relative expression of *Krox20* in primary rat SC cultures as compared to empty vector control (n = 3 per group; ***P<0.001). ***C***. Viral-induced expression of *Lpin1*α and *Lpin1*β increased relative expression of *Mpz* in primary rat SC cultures as compared to empty vector control (n = 3 per group; *P<0.05, **P<0.01, ***P<0.001). Data are expressed as mean ± S.E.M.

Lipin 1 affects myelination through *Krox20* expression *in vitro*. As Lipin 1 affects hepatic metabolic pathways through transcriptional control (Finck et al., 2006), we investigated whether Lipin 1α or Lipin 1ß also affect myelination processes. To investigate lentiviral integration and subsequent expression, we measured *Lpin1* expression in lentiviral-infected primary SCs that were allowed that differentiate for 8 days. *Lpin1*α increased *Lpin1* expression about 150-fold, whereas *Lpin1ß* increased *Lpin1* expression about 6-fold as compared to SCs infected with an empty vector control (Fig. 7A). *Lpin1*α increased expression of *Krox20,* an important regulator of myelination, about 17-fold, whereas *Lpin1ß* had no effect on *Krox20* expression (Fig. 7B). Finally, both *Lpin1*α and *Lpin1ß* increased expression of *Mpz,* a marker myelination, approximately 29-fold and 16-fold, respectively (Fig. 7C).

DISCUSSION

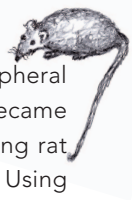

Here we describe an *Lpin1*^{1Hubr} rat model that is characterized by a transitory peripheral neuropathy and lipodystrophy. The deficiencies present in *Lpin1*^{1Hubr} rats became obvious approximately during the second postnatal week, but attenuated during rat maturation, resulting in a considerable improvement of the *Lpin1*^{1Hubr} phenotype. Using an array of histological and molecular techniques we demonstrated that the *Lpin1*^{1Hubr} phenotype improvements are paralleled by improvements in sciatic nerve myelination and lipid accumulation in WAT between PND 21 and 90. In addition, using an *in vitro* analysis we demonstrated that Lipin 1 had the ability to increase *Krox20* expression

in primary rat SCs. We therefore propose that the transcriptional activity of Lipin 1 remains functional in *Lpin1*^{1Hubr} rats, and is responsible for the improvements in sciatic nerve myelin structure and WAT accumulation in mutant rats.

The *Lpin1*^{1Hubr} phenotype was initially discovered in F_3 rats that were already outcrossed twice to wild type Wistar/Crl background. This indicates the importance to outcross ENU-mutagenized rats to clear the background of unwanted mutations. Outcrossing the F_3 Wistar/Crl *Lpin1*^{1Hubr} mutation background for an additional 4 generations (6 outcrosses in total) should theoretically decrease the total number of random background mutations to 1 (Mul et al., 2010). However, we cannot fully exclude the presence of tightly linked confounding mutations in our rat model.

The *Lpin1*^{1Hubr} mutation disrupted 5'-end splice site of the exon 18. Despite this, we observed a small amount (1-6%) of *Lpin1* transcript with the correctly spliced exons 18 and 9 (*Lpin1*$^{Ex18\text{-}19}$) in muscle, WAT, liver, and brain of *Lpin1*^{1Hubr} rats. The amount of correct exon 18 – 19 splicing in sciatic nerve endoneurium harvested from *Lpin1*^{1Hubr} rats was approximately 20%. Both observations indicate that even in the presence of the *Lpin1*^{1Hubr} mutation, the splicing machinery is occasionally able to splice correctly. We did not observe time-related increases in correct *Lpin1*$^{Ex18\text{-}19}$ expression in WAT or sciatic nerve tissue harvested from *Lpin1*^{1Hubr} rats. These data strongly suggest that the attenuation of the different *Lpin1*^{1Hubr} phenotypes is not a consequence of an increased presence of correctly spliced exon 18 – 19 in mutant rats.

We observed increased expression of both *Lpin1*α and *Lpin1*β isoforms (as tested by qPCR using primers locate din the 5' part of the Lpin1 transcript) in sciatic nerve tissue derived from *Lpin1*^{1Hubr} rats at PND 21, suggesting a functional feedback loop affecting their expression. These data, together with our finding that the stop codon is induced in the 19th exon out of 20, close to the last exon-exon junction, suggested that the *Lpin1*^{1Hubr} mutation does not induce nonsense-mediated decay (NMD). The mutation did however completely inactivate the Lipin 1-PAP1 activity, both in nerve tissue as in WAT. As Lipin 1 accounts for all PAP1 activity in murine adipose tissue (WAT and BAT) and muscle (Donkor et al., 2007), our observation that PAP1 activity is completely ablated in WAT derived from *Lpin1*^{1Hubr} rats strengthens these findings, and expands this finding to the rat. In mice, expression of *Lpin2* and *Lpin3* is undetectable in sciatic nerve tissue (Nadra et al., 2008), strengthening our observation that PAP1 activity is completely ablated in nerve tissue. Thus, while *Lpin1* mRNA is present in mutant rats, the *Lpin1*^{1Hubr} mutation disrupts the last HAD motif leading to complete lack of PAP1 activity in corresponding protein.

Until PND 10, *Lpin1*^{1Hubr} pups showed normal WAT levels. At PND 21 however, WAT levels are ~50% reduced, whereas WAT levels are ~30% reduced at PND 90. This transitory lipodystrophy phenotype in *Lpin1*^{1Hubr} rats might be the result of immobility-induced hypophagia and a subsequent decreased lipid accumulation at a young age, while at an older age rats become more able to feed correctly due to increased mobility. This explanation is however unlikely, as most *Lpin1*^{1Hubr} pups retained partial ability to move around after the onset of the *Lpin1*^{1Hubr} phenotype. In addition, chow

pellets were provided to the maternal cage floor to enable feeding under competitional circumstances. An alternative explanation could come from the previously observed regulatory role of Lipin 1 during initial phases of adipogenesis for the induction of adipogenetic factors including PPARγ and CCAAT enhancer-binding protein (C/EBP)α (Peterfy et al., 2001; Phan et al., 2004). Our observation that relative expression levels of *Fabp4*, *PPARγ1*, and *PPARγ2* increased in WAT derived from *Lpin1*^{1Hubr} rats at PND 90 as compared to PND 21, mirrored by relative increased WAT levels, suggests that the regulatory function of Lipin 1^{1Hubr} potentially remained functionally active and able to partially stimulate adipogenesis.

Lpin1$^{fld/fld}$ mice are resistant to high-fat-induced obesity (Phan et al., 2004), whereas mice overexpressing *Lpin1* in adipose tissue (aP2-lipin Tg) demonstrated increased body weight growth on a high-fat diet, but not on regular chow (Phan and Reue, 2005). Interestingly, both *Lpin1*$^{fld/fld}$ and aP2-lipin Tg mice showed normal food intake, but reduced and increased feed conversion efficiency, respectively (Phan et al., 2004; Phan and Reue, 2005). Adult *Lpin1*^{1Hubr} rats on a high-fat diet also showed normal food intake, but did show decreased feed conversion efficiency. The decreased feed conversion efficiency was not as dramatic as in *Lpin1*$^{fld/fld}$ mice, again suggesting that Lipin 1^{1Hubr} was able to partially stimulate adipogenesis in adult mutant rats.

In the PNS, partially recovered *Mpz* and *Pmp22* expression levels accompanied the progression of myelination in *Lpin1*^{1Hubr} sciatic nerves at PND 90. Moreover, expression of *Krox20* was decreased at PND 21, whereas it was increased at PND 90. *Krox20* is an important controller of myelination and a marker of mature SCs (Zorick et al., 1996), thus indicating that myelination processes are down regulated in *Lpin1*^{1Hubr} sciatic nerve tissue at PND 21, but are upregulated at PND 90, resulting in a relative increase in correct myelination at PND 90. The latter finding was mirrored by our behavioral and histological observations. *Scip*, a marker of immature promyelinating SCs (Jaegle et al., 1996; Zorick et al., 1996), is upregulated at PND 21, thus indicative of an increased amount of immature promyelinating SCs. Interestingly, at PND 90, *Scip* levels are even further increased, which, together with the observed increase in cell proliferation, indicate the presence of a mixed population of immature and mature SCs at this time point.

We demonstrated that lentiviral-induced expression of *Lpin1*α increased *Krox20* expression and subsequent *Mpz* expression *in vitro* in primary rat SC cultures. Interestingly, lentiviral-induced expression of *Lpin1*β, even though expressed at a much lower level as compared to *Lpin1*α, did not affect *Krox20* expression but did increase *Mpz* expression. This indicates that *in vivo*, *Lpin1*α is potentially involved in upstream pathways regulating the expression of *Krox20* and subsequent myelination processes. *Lpin1*β also appears to affect myelination processes, potentially via a Krox20-independent pathway. Although more experiments will be necessary to test our hypothesis, our data suggest that in addition to its role in SC fate determination (Nadra et al., 2008), Lipin 1 is also an important regulator of the Schwann cell myelination program.

Krox20 is also an important regulator of adipogenesis via (C/EBP)β-dependent and independent mechanisms (Chen et al., 2005). The nucleocytoplasmic localization of Lipin 1 in adipocytes is regulated by insulin, through interactions with 14-3-3 proteins (Harris et al., 2007; Peterfy et al., 2010). Insulin, also an important factor of serum used to induce adipocyte differentiation, might therefore be an important regulator of Lipin 1 localization and function, thus affecting subsequent *Krox20* expression *in vitro* and *in vivo*. However, more studies will be required to investigate if this hypothesis is valid.

The *Lpin1*^{1Hubr} rat model described in this study is characterized by an early onset peripheral neuropathy and lipodystrophy that are the consequences of a loss of Lipin 1-PAP1 activity. Biochemical and histological analysis of *Lpin1*^{1Hubr} sciatic nerve tissue and WAT revealed pronounced improvements of these phenotypes over time, probably due to the preserved Lipin 1 transcriptional regulatory activity in *Lpin1*^{1Hubr} rats. We demonstrated that viral expression of *Lpin1*β and *Lpin1*α affected myelination processes *in vitro* in primary rat SC culture. Based on these observations, we propose that Lipin 1 is involved in *Krox20*-dependent or -independent regulation of nerve myelination also *in vivo* and it might affect WAT function through similar mechanisms.

REFERENCES

Brockes JP, Fields KL, Raff MC (1979) Studies on cultured rat Schwann cells. I. Establishment of purified populations from cultures of peripheral nerve. Brain Res 165:105-118.

Carman GM, Han GS (2009) Phosphatidic acid phosphatase, a key enzyme in the regulation of lipid synthesis. J Biol Chem 284:2593-2597.

Chen Z, Torrens JI, Anand A et al. (2005) Krox20 stimulates adipogenesis via C/EBPbeta-dependent and -independent mechanisms. Cell Metab 1:93-106.

de Preux AS, Goosen K, Zhang W et al. (2007) SREBP-1c expression in Schwann cells is affected by diabetes and nutritional status. Mol Cell Neurosci 35:525-534.

Donkor J, Sariahmetoglu M, Dewald J et al. (2007) Three mammalian lipins act as phosphatidate phosphatases with distinct tissue expression patterns. J Biol Chem 282:3450-3457.

Donkor J, Zhang P, Wong S et al. (2009) A conserved serine residue is required for the phosphatidate phosphatase activity but not the transcriptional coactivator functions of lipin-1 and lipin-2. J Biol Chem 284:29968-29978.

Douglas DS, Moran JL, Bermingham JR, Jr. et al. (2009) Concurrent Lpin1 and Nrcam mouse mutations result in severe peripheral neuropathy with transitory hindlimb paralysis. J Neurosci 29:12089-12100.

Dyck PJ, Thomas PK (2005) Peripheral neuropathy, 4th ed.: Elsevier Saunders.

Finck BN, Gropler MC, Chen Z et al. (2006) Lipin 1 is an inducible amplifier of the hepatic PGC-1alpha/PPARalpha regulatory pathway. Cell Metab 4:199-210.

Garbay B, Heape AM, Sargueil F et al. (2000) Myelin synthesis in the peripheral nervous system. Prog Neurobiol 61:267-304.

Han GS, Wu WI, Carman GM (2006) The Saccharomyces cerevisiae Lipin homolog is a Mg2+-dependent phosphatidate phosphatase enzyme. J Biol Chem 281:9210-9218.

Harris TE, Huffman TA, Chi A et al. (2007) Insulin controls subcellular localization and multisite phosphorylation of the phosphatidic acid phosphatase, lipin 1. J Biol Chem 282:277-286.

Jaegle M, Mandemakers W, Broos L et al. (1996) The POU factor Oct-6 and Schwann cell differentiation. Science 273:507-510.

Langner CA, Birkenmeier EH, Roth KA et al. (1991) Characterization of the peripheral neuropathy in neonatal and adult mice that are homozygous for the fatty liver dystrophy (fld) mutation. J Biol Chem 266:11955-11964.

Makowski L, Hotamisligil GS (2005) The role of fatty acid binding proteins in metabolic syndrome and atherosclerosis. Curr Opin Lipidol 16:543-548.

Mul JD, Yi CX, van den Berg SA et al. (2010) Pmch expression during early development is critical for normal energy homeostasis. Am J Physiol Endocrinol Metab 298:E477-488.

Nadra K, de Preux Charles AS, Medard JJ et al. (2008) Phosphatidic acid mediates demyelination in Lpin1 mutant mice. Genes Dev 22:1647-1661.

Nijman IJ, Kuipers S, Verheul M et al. (2008) A genome-wide SNP panel for mapping and association studies in the rat. BMC Genomics 9:95.

Peterfy M, Phan J, Reue K (2005) Alternatively spliced lipin isoforms exhibit distinct expression pattern, subcellular localization, and role in adipogenesis. J Biol Chem 280:32883-32889.

Peterfy M, Phan J, Xu P et al. (2001) Lipodystrophy in the fld mouse results from mutation of a new gene encoding a nuclear protein, lipin. Nat Genet 27:121-124.

Peterfy M, Harris TE, Fujita N et al. (2010) Insulin-stimulated interaction with 14-3-3 promotes cytoplasmic localization of lipin-1 in adipocytes. J Biol Chem 285:3857-3864.

Phan J, Reue K (2005) Lipin, a lipodystrophy and obesity gene. Cell Metab 1:73-83.

Phan J, Peterfy M, Reue K (2004) Lipin expression preceding peroxisome proliferator-activated receptor-gamma is critical for adipogenesis *in vivo* and *in vitro*. J Biol Chem 279:29558-29564.

Reue K, Zhang P (2008) The lipin protein family: dual roles in lipid biosynthesis and gene expression. FEBS Lett 582:90-96.

Rosen ED, Spiegelman BM (2006) Adipocytes as regulators of energy balance and glucose homeostasis. Nature 444:847-853.

Smits BM, Mudde JB, van de Belt J et al. (2006) Generation of gene knockouts and mutant models in the laboratory rat by ENU-driven target-selected mutagenesis. Pharmacogenet Genomics 16:159-169.

van Boxtel R, Toonen PW, van Roekel HS et al. (2008) Lack of DNA mismatch repair protein MSH6 in the rat results in hereditary non-polyposis colorectal cancer-like tumorigenesis. Carcinogenesis 29:1290-1297.

Verheijen MH, Chrast R, Burrola P et al. (2003) Local regulation of fat metabolism in peripheral nerves. Genes Dev 17:2450-2464.

Zeharia A, Shaag A, Houtkooper RH et al. (2008) Mutations in LPIN1 cause recurrent acute myoglobinuria in childhood. Am J Hum Genet 83:489-494.

Zorick TS, Syroid DE, Arroyo E et al. (1996) The Transcription Factors SCIP and Krox-20 Mark Distinct Stages and Cell Fates in Schwann Cell Differentiation. Mol Cell Neurosci 8:129-145.

SUPPLEMENTARY MATERIALS

Table S1. Gene name, forward and reverse primer sequences for qPCR analysis.

Gene	Forward primer	Reverse Primer
Ubiquitin	AGTGCGGAAAACTGGAAGCC	GGACTGGATTACTTGGTCAGTCTTG
Lpin$^{Ex18\text{-}19}$	GCCTGCCGATGTGTATTCCTAC	ATTCTATTCAGGGACACTCCCA
Lpin1α	GCCCCAGTCCTTCAGGCTC	GCTCAGAATCACTTTTTGGTGTTG
Lpin1β	GTAGATTGTCAGAGGACTCCCCCT	CAAGAGCTAGAGAGAACTCCCTCG
Fabp4	GGAGACGAGATGGTGACAAGC	TCACGCCTTTCATGACACATTC
Pparγ1	GCAAGAGATCACAGAGTATGCCAA	TCAAGGTTAATGAAACCAGGGATAT
Pparγ2	TTTTGAAAACAAGGACTACCCTTTAC	GGCATCTCTGTGTCAACCATG
Mpz	TTCACAAGTCTTCTAAGGACTCCTCG	GCACTGGCGTCTGCCG
Pmp22	GGAGTCTTCCAAATCCTTGCTG	GATGGCCGCTGCACTCAT
Scip	GAGCTTCAAGAACATGTGCAAGCT	TCCAGCCACTTGTTGAGCAG
Krox20	GGAGGCCCCTTTGATCAGA	TGTTGATCATGCCATCTCCAG
Cyclin D1	GCACTTTCTTTCCAGAGTCATCAA	CAGGCACGGAGGCAGTC

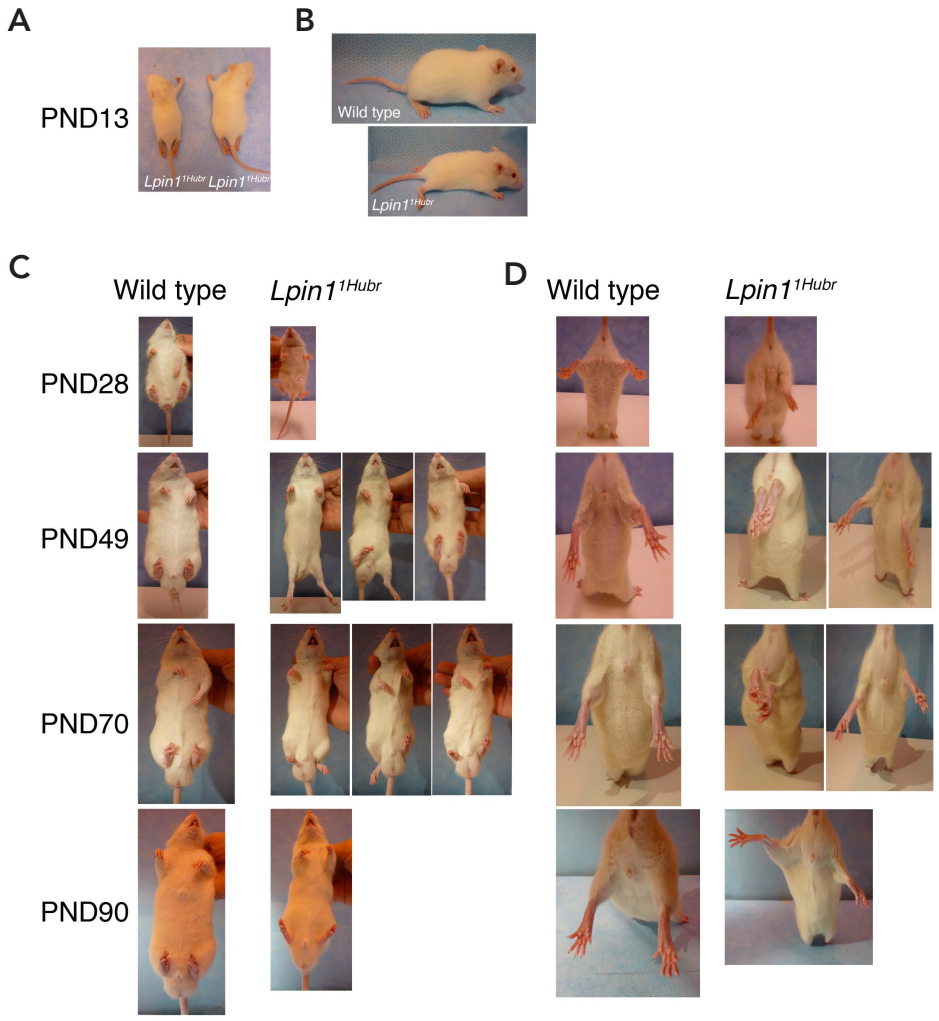

Figure S1. Progression of neuropathy and lipodystrophy phenotypes in *Lpin1*^{1Hubr}. ***A***. The onset of the *Lpin1*^{1Hubr} phenotype occurred between PND 5 and PND 12. Early onset (left male pup) resulted in a more severe phenotype compared to later onset (right male pup) due to decreased mobility, and possibly decreased suckling behavior. ***B***. At PND 13, *Lpin1*^{1Hubr} pups showed severe lipodystrophy, hindquarter muscle wasting, and decreased body length as compared to wild type pups. ***C***. At PND 28, *Lpin1*^{1Hubr} rats showed severe lipodystrophy, hindquarter muscle wasting, a decreased body length, and no characteristic retraction of the hindlimbs as compared to wild type rats. However, at PND 49 and onwards, some *Lpin1*^{1Hubr} rats gain the ability to retract their hindlimbs when picked up, whereas other *Lpin1*^{1Hubr} rats do not gain this ability, or partially. Moreover, the severe lipodystrophy and hindquarter muscle wasting in *Lpin1*^{1Hubr} rats became less pronounced. At PND 90, almost all *Lpin1*^{1Hubr} rats regain the ability to retract their hindlimbs. ***D***. Wild type rats splayed their hindlimbs and toes when picked up by the tail, whereas *Lpin1*^{1Hubr} rats clenched their hindlimbs to their body. However, at PND 49 and onwards, *Lpin1*^{1Hubr} rats splayed their hindlimbs and toes, or clenched their hindlimbs to their body when picked up by the tail. At PND 90, almost all *Lpin1*^{1Hubr} rats regained the ability to splay their hindlimbs.

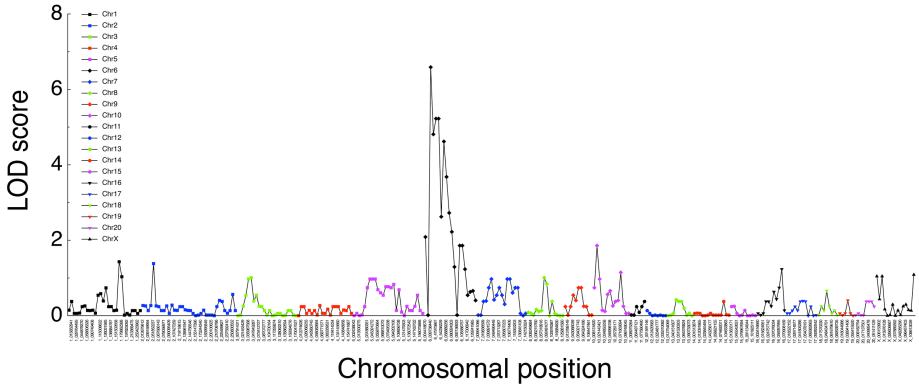

Figure S2. Linkage analysis data. Linkage analysis based on the genotyping results in the Wistar/BN F5 population using 321 informative markers revealed a significant LOD score for the *Lpin1*^{1Hubr} mutation in a region on chromosome 6 between 37.1Mb and 40.7Mb. *Lpin1* is located at 40.3Mb.

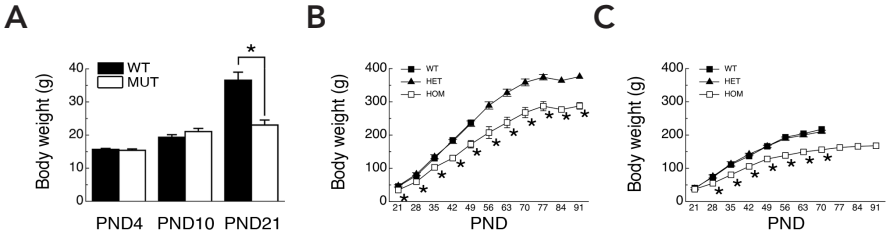

Figure S3. Body weight phenotype in *Lpin1*^{1Hubr} rats. ***A***. No difference in body weight of *Lpin1*^{1Hubr} and wild type rats (mixed gender) is observed at PND 4 (n = 4-9 per group) and PND 10 (n = 7-18 per group). However, as the *Lpin1*^{1Hubr} phenotype develops, body weights start to diverge and body weight is decreased in *Lpin1*^{1Hubr} rats as compared to wild type rats (mixed gender) at PND 21 (n = 8-9 per group; **P*<0.05). ***B***. Body weight of male *Lpin1*^{1Hubr} rats is decreased as compared to male heterozygous and wild type rats between PND 21 and 90 (n = 3-9 per group; **P*<0.001, Bonferroni *post hoc* analysis). ***C***. Body weight of female *Lpin1*^{1Hubr} rats is decreased as compared to female heterozygous and wild type rats between PND 21 and 90 (n = 6-10 per group; **P*<0.001, Bonferroni *post hoc* analysis). Data are expressed as mean ± S.E.M.

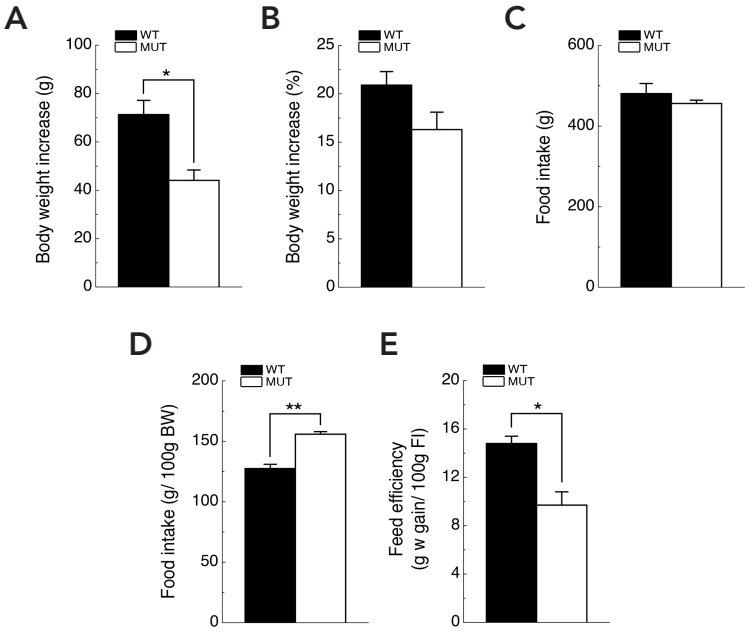

Figure S4. Adult *Lpin1*^{1Hubr} *rats* show decreased weight gain on a HF diet. ***A***. *Lpin1*^{1Hubr} rats showed decreased body weight increase when fed a HF diet for 4 weeks as compared to wild type rats. ***B***. The body weight increase normalized to the body weight at the start of the HF experiment did not differ between genotypes. ***C***. Total food intake during 4 weeks of HF feeding did not differ between genotypes. ***D***. Total food intake during 4 weeks of HF feeding normalized for the average body weight during the 4 weeks was increased in *Lpin1*^{1Hubr} rats as compared to wild type rats. ***E***. Feed efficiency (gram body weight increase per 100 gram food intake) was decreased in *Lpin1*^{1Hubr} rats as compared to wild type rats (n = 2-4 per group; **P*<0.05; ***P*<0.01). Data are expressed as mean ± S.E.M.

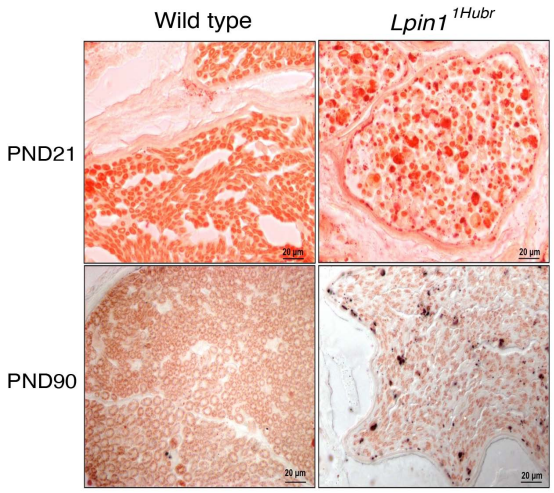

Figure S5. Transitory signaling defects *in Lpin1*^{1Hubr} *rats* regarding myelination. Oil-red-O staining of sciatic nerve sections from *Lpin1*^{1Hubr} and wild type rats at PND 21 and 90. At PND 21, the typical 'donut'-like myelin structures present in wild type sciatic nerve are replaced in *Lpin1*^{1Hubr} nerves by 'dot'-like structures probably corresponding to the accumulation of myelin debris in demyelinated SCs. *Lpin1*^{1Hubr} nerves partially recover the 'donut'-like myelin staining at PND 90.

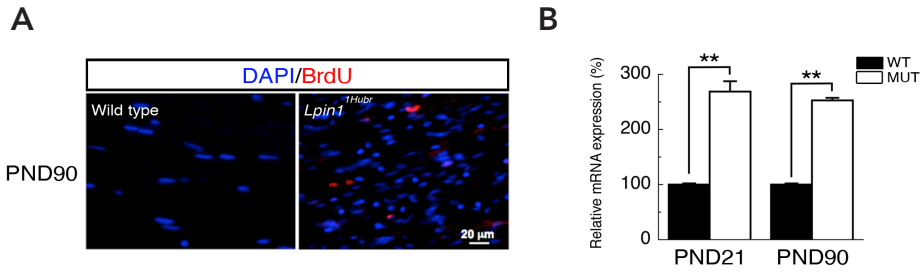

Figure S6. Increased cell proliferation in *Lpin1*^{1Hubr} sciatic nerves. ***A***. Immunohistochemistry of DAPI and BrdU in medial sciatic nerve tissue at PND 90 revealed increased cellularity and cell proliferation in *Lpin1*^{1Hubr} rats as compared to wild type rats. ***B***. Relative expression of *Cyclin D1* (marker of cell proliferation) is increased in *Lpin1*^{1Hubr} rats at PND 21 and 90 as compared to wild type rats (***P*<0.001; n = 2 per group, respectively).

6

SUMMARIZING DISCUSSION

SUMMARIZING DISCUSSION

The future of knockout rat models

As has become clear in this thesis, genetic rat mutants are very valuable models for studying specific aspects of human biology and physiology. However, technology to generate rat models is still in its infancy. Since 2003, investigators have successfully applied target-selected mutagenesis to the rat, generating an impressive amount of mutant and knockout models (Zan et al., 2003; Smits et al., 2004; Smits et al., 2006; van Boxtel et al., 2008). While target-selected mutagenesis is a very labor-intensive approach, it is also highly amendable to scaling. The limitations of the technique are mainly determined by the platform used to screen the F1 cohort for induced mutations, as it will affect the amount of coding sequence screened per rat and thus the number of F1 rats that need to be screened. In sum, the efficiency of the platform will affect the quantity and length of animal housing, and will subsequently influence the cost of the screen. However, the creation of frozen sperm libraries is an efficient way to reduce animal housing (Mashimo et al., 2008). Moreover, recent developments in DNA sequencing methods, such as the application of next generation sequencing, will very likely have profound effects on the efficiency of mutation screening (Cuppen et al., unpublished results).

ENU is a potent mutagen that introduces numerous random point mutations in the genome of the F1 offspring. Although successful in its primary goal, introducing mutations, the success of ENU-mutagenesis is also its downside: when a gene of interest is affected in a rat, the background mutations have to be removed to ensure correct interpretation of the phenotype. Theoretical calculations, taking into account the amount of coding sequence and the mutation frequency of the screen, suggested that the mutated background of the *Pmch* mutation had to be outcrossed six generations to decrease the number of background mutations to 1 (Mul et al., 2010). As the *Lpin1* line was created during the same screen, the same theoretical numbers apply to this rat line. However, as part of the donor chromosome harboring the mutation of interest is still present after six backcrosses (Keays et al., 2006), we cannot fully exclude the presence of tightly linked confounding mutations in our rat models. In sum, continuous outcrossing of the mutant rat lines, after six outcrosses have been performed, is a good initiative to decrease the possible presence of confounding mutations.

Although applying ENU-mutagenesis to the rat has been successful to date, the effectiveness of the technique does rely on the chance of introducing a functional mutation in a specific gene of interest. The technique thus predominantly relies on the number of F1 animals screened (van Boxtel et al., 2008), the rat background used (Smits et al., 2006), and the efficiency of the platform used to detect the mutations (Cuppen et al., unpublished results), and is not suited for the targeted generation of a knockout of a single specific gene. However, the recent successful isolation of embryonic stem cells in the rat (Buehr et al., 2008) and the creation of knockout rats via embryonic microinjection of zinc-finger nucleases (Geurts et al., 2009) have supplied the scientific community with more direct approaches to induce genetic variation in

rats at specific genomic loci. However, both techniques are still relatively laborious, as well as expensive, and experience from the mouse genetics research field (Gondo, 2008) has shown that complementary technologies and resulting models, like the ENU-induced mutants, remain valuable in large-scale studies and for generating alleles that may better reflect human disease-associated variation than full gene knockouts.

MELANIN-CONCENTRATING HORMONE

MCH function

Since the discovery that MCH affects feeding behavior and energy homeostasis (Qu et al., 1996; Shimada et al., 1998), a large quantity of studies has confirmed the important function for MCH regarding these processes (Pissios and Maratos-Flier, 2003; Pissios et al., 2006; Pissios, 2009). In addition, the expression of *Mch1r* in a broad number of brain regions, and the location of MCH neuronal bodies and their projections throughout the mammalian brain has led to the hypothesis that MCH is involved in multiple integrative processes. Indeed, several studies have shown that MCH, and in a lesser degree NGE and NEI, are involved in memory (Monzon et al., 1999), motor activity (Sanchez et al., 1997; Marsh et al., 2002), taste and olfaction (Skofitsch et al., 1985; Bittencourt et al., 1992), depression and anxiety (Borowsky et al., 2002), and learning (McBride et al., 1994). As most of these processes are direct or semi-direct related to feeding behavior and energy metabolism, the regulation of feeding and energy homeostasis can be interpreted as the dominant function of MCH in mammals.

MCH has a clear effect on skin pigmentation in fish, hence its name. However, in mice no clear effects on skin color have been observed in brown or black coat-colored mice that have disrupted MCH function. Therefore, despite its name, a similar function for MCH on mammalian skin pigmentation is possible but unlikely (Pissios et al., 2006).

Murine *Pmch* and MCH1R models

In 1998, the *Pmch* KO mouse was described by the Maratos-Flier group (Shimada et al., 1998). These mice exhibited reduced body weight, fat mass, and leptin levels with reduced food intake, and increased energy expenditure when data were normalized for body weight (Shimada et al., 1998). Locomotor activity of *Pmch* KO mice was not significantly different from wild type mice (Shimada et al., 1998). A subsequent study from the Friedman group reported that use of a toxin (ataxin-3)-mediated ablation strategy in MCH neurons also resulted in leanness (Alon and Friedman, 2006). These transgenic mice exhibited reduced body weight, fat mass, and leptin levels with reduced food intake (although at an older age), and increased energy expenditure when data were normalized for body weight (Alon and Friedman, 2006). Locomotor activity of MCH/ataxin-3 mice was not significantly different from wild type mice (Alon and Friedman, 2006). In sum, these two murine lines with *Pmch* depletion provided strong evidence that the MCH system is involved in the regulation of energy homeostasis. Moreover, the strong similarity between the MCH/ataxin-3 phenotype and the murine *Pmch* KO phenotype, suggested that MCH is the major mediator of MCH neuron function.

Several studies have described independent murine *Mch1r* KO lines resulting in reduced body weight, fat mass, and leptin levels, and increased energy expenditure when data were normalized for body weight (Chen et al., 2002; Marsh et al., 2002; Astrand et al., 2004). Surprisingly, these mice also demonstrated increased food intake and locomotor activity (Chen et al., 2002; Marsh et al., 2002; Astrand et al., 2004).

Depletion of either *Pmch* or *Mch1r* thus results in leanness, although apparently via different mechanisms. Although not yet investigated properly, a possible explanation might be found in the fact that depletion of *Pmch* not only disrupts MCH production, but also the production of NGE and NEI. Neither NGE nor NEI are able to bind MCH1R (Chambers et al., 1999; Lembo et al., 1999; Saito et al., 1999). However, NEI is known to affect locomotor activity (Sanchez et al., 1997; Gonzalez et al., 1998; Sanchez et al., 2001b). Moreover, NEI appears to contain the ability to modify dopamine binding (Sanchez et al., 2001a). NEI might thus be responsible for a significant part of the *Pmch* depletion phenotype. Crossing the *Pmch*-deficient background to the *Mch1r*-deficient background might shed light on the exact function of NEI. Finally a murine or rat line that expresses functional MCH and NGE in combination with non-functional NEI might be of additional value. Additional combinations might also shed light on a possible function for NGE.

Contradictory findings in murine MCH models

The *Pmch* KO mouse line created in the Maratos-Flier group exhibited reduced food intake, one of the key behavioral characteristics of MCH depletion in rodents (Shimada et al., 1998; Mul et al., 2010). It was created by electroporating a modified C129 Sv JP1 clone into the J1 cell line, which was subsequently injected into C57Bl/6 embryos (Shimada et al., 1998). F_3 hybrids were used for the initial characterization (Shimada et al., 1998). However, the same mouse line, this time outcrossed at least 15 times to a C57Bl/6 background, did not display the characteristic reduced food intake in a subsequent study investigating the effects of *Pmch*-deficiency on the limbic dopamine system (Pissios et al., 2008). Another recent report from the same mouse line revealed similar body weight, food intake, and energy expenditure between *Pmch* KO and wild type mice (Glier et al., 2010). More surprisingly, *Pmch* KO mice now demonstrated increased locomotor activity during the night as compared to wild type mice (Glier et al., 2010).

The *Pmch* KO rat line generated in the Cuppen group exhibited reduced body weight, fat mass, and leptin levels with reduced food intake, and increased energy expenditure when data were normalized for body weight (chapter 2; Mul et al., 2010). This phenotype showed great similarity to the initial phenotype observed in *Pmch* KO mice (Shimada et al., 1998) and the MCH/ataxin-3 phenotype (Alon and Friedman, 2006). One possible explanation for the fading of the *Pmch* phenotype in mice on a C57Bl/6 background might be the presence of genetic modifiers, although this has to be investigated in detail. The presence of genetic modifiers might very well be possible, as the C57Bl/6 mouse line is an inbred line and different lines derived from the initial line could result in different phenotypes. The Wistar rat line, the background

on which the *Pmch* mutation was induced, is an outbred line and might therefore display less inter-animal variation. However, the only way to find out if this might be true is outcrossing the *Pmch* generation for many more generations on the Wistar background.

Crossing the *Pmch*-deficiency to the obesity-resistant 129 background or the obesity-prone C57Bl/6 background has provided additional evidence for the influence of the genetic background (Kokkotou et al., 2005). *Pmch* KO mice on both the 129 and the C57Bl/6 background showed increased energy expenditure, when data were normalized per body weight, although this effect was more pronounced on the 129 background (Kokkotou et al., 2005). Moreover, *Pmch*-deficiency on both backgrounds resulted in a phenotype of elevated locomotor activity (Kokkotou et al., 2005). Due to the contradicting findings in *Pmch*-deficient mice, especially on different genetic backgrounds, the *Pmch*-deficient rat could serve as an important complementary model to investigate the function of MCH, NEI and NGE.

The role of MCH in energy expenditure

MCH is an important regulator of energy homeostasis. It has been proposed that in mice, MCH affects energy homeostasis primarily through effects on energy expenditure, and secondary through effects on food intake (Shimada et al., 1998; Alon and Friedman, 2006; Pissios, 2009). However, in these studies, energy expenditure data were always normalized for body weight (Shimada et al., 1998; Alon and Friedman, 2006). As decreased fat mass is the main cause for the leanness in *Pmch*-deficient rodents, normalization for body weight normalizes the data predominantly for the difference in body fat. Moreover, fat is generally thought of as a metabolic inactive organ, although studies have shown that this is not always true (chapter 4; Cousin et al., 1992; Granneman et al., 2003; Xue et al., 2007).

If energy expenditure data is not normalized for body weight, or normalized for lean mass, *Pmch*-deficiency in the rat results in decreased energy expenditure (Mul et al., 2010). As conclusions can differ strongly from the manner data is presented, it is therefore advised, especially for animal models with affected adipose levels, to present energy expenditure data normalized and non-normalized for body weight. In rats, this has generated the hypothesis that the primary cause of leanness in *Pmch*-deficient rats is decreased food intake, followed by decreased energy expenditure (Mul et al., 2010). Moreover, as food intake is known to increase energy expenditure (thermic effect of food; Even et al., 1994), decreased food intake should subsequently result in decreased energy expenditure. Moreover, chronic decreased food intake in combination with chronic energy expenditure as compared to healthy control animals should eventually result in death. In chapter 4 we describe findings that *Pmch*-deficiency affects thermogenesis in WAT through possible secondary effects on the sympathetic nervous system. Although additional studies have to determine the physiological importance of this finding, it indicates that WAT in *Pmch*-deficient rats can have effects on energy expenditure.

In *Mch1r*-deficient mice, increased hyperactivity seems to be causal to an increased metabolic rate observed during the night (Marsh et al., 2002), whereas *Pmch*-deficient rats display similar locomotor activity as compared to control rats (Mul et al., 2010). However, two studies reported *Pmch*-deficient mice with elevated locomotor activity as compared to control mice (Kokkotou et al., 2005; Glier et al., 2010). The increased locomotor activity can additionally complicate the already contradictory findings regarding food intake and energy expenditure in this mouse model.

Finally, the mouse is more prone to temperature changes in the environment as compared to the rat, due to its decreased relative size. Therefore, complementary studies of *Pmch*-deficiency in the rat might aid in understanding the direct and indirect effects of MCH function on energy expenditure.

Is a *Pmch* knockout model the (only) way to go?

Depletion of NPY/AGRP neurons in neonatal mice using a toxin receptor-mediated strategy had no significant effect on food consumption or body weight during early life or adulthood (Luquet et al., 2005). However, depletion of NPY/AGRP neurons in adult mice induced an arrest of food intake and decreased body weight by 20% within 7 days (Luquet et al., 2005). This elegant study demonstrated that if neurons expressing two crucial orexigenic neuropeptides are lost during early development, it had no significant effects. It also indicated that the rodent brain, which is largely developed during the first 3 weeks after birth, is able to produce compensatory adaptations when neuronal bodies are lost during early development.

Therefore, compensatory adaptations could potentially also be induced in *Pmch*-deficient rodents (Shimada et al., 1998; Mul et al., 2010). This possibility could also explain why *Pmch*-deficient rats and rats with acute MCH1R-blockade react differently when self-administrating cocaine (chapter 3; Chung et al., 2009). Humans with a null mutation in *Pmch* have not been described to date. Thus, the potential development of an anti-obesity treatment based on the MCH-MCH1R-system might benefit equally or even favor research in non-chronic knockout animal models. Although knockout models definitely aid in discovering key findings regarding physiological processes such as the regulation of body weight, a complete picture should be obtained by also using inducible knockouts or knockins. This can be achieved by using the above-mentioned toxin receptor-mediated strategy (knockout strategy; (Luquet et al., 2005), by using homologous recombination in embryonic stem cells in combination with the inducible Cre-Lox system (knockout and knockin strategy; hopefully available in the near future), by using lentiviral expression of a short hairpin RNA (shRNA) vector (knockdown strategy; Herold et al., 2008), or by using adeno-associated virus-mediated expression (knockin strategy; Tiesjema et al., 2007). Using a combination of these techniques should result in complementary data, and should provide more insight than data obtained from just a chronic knockout model.

As we showed that, at least in the rat, that *Pmch* expression is important during early development (chapter 2; Mul et al., 2010), it would be very interesting to restore *Pmch*

expression at different time points during development of *Pmch*-deficient rats, and to knockdown *Pmch* expression in young wild type rats at different time points during development. The same strategy, but using *Mch1r* expression, could also be applied to *Mch1r*-deficient mice. Moreover, site-specific effects could then also be investigated.

New observations in the *Pmch* KO rat

Although a significant amount of insight has been gathered using murine *Pmch* models, the availability of the *Pmch* KO rat has provided some additional findings. First, in chapter 2, we describe the novel observation that *Pmch* expression is important during early development and puberty. Although not impossible, food and water intake studies at a young age are limited in the mouse due to its relative small size. However, it will be interesting to see if the same observations can be observed in the *Pmch* mouse model, or if possible even in humans.

Secondly, in chapter 3, we describe that *Pmch*-deficiency affects the meal size pattern of the rat and that *Pmch*-deficient rats demonstrated decreased willingness to exert work for food rewards, while showing increased willingness to exert work for cocaine rewards. Due to its relative big size, and thus its relative big meal size, the rat is very well suited for meal pattern analysis studies, and these studies are hard to perform in young or adult mice. Moreover, due to its relative strong cognitive performance, the rat is very well suited for behavioral experiments like self-administration paradigms. Although, tests have been developed for the mouse to test 'preference' or 'likeness' of substrates (like the conditioned-place preference test), the evaluation of direct 'motivational status' in rodent models in self-administration paradigms is preferred in the rat.

Finally, in chapter 4 we describe that *Pmch*-deficiency in the rat decreases WAT levels as a result of decreased feeding. However, we also observed additional mechanisms that had a negative effect on WAT levels. We propose that increased catecholamine levels in the circuitry might underlie this observation. Although not performed in chapter 4, it might be very interesting to perform denervation studies (Kreier et al., 2002) to measure the effect of direct sympathetic innervation of WAT. Due to the relative large size of the nerves, denervation studies are also preferred in the rat.

In sum, the *Pmch* KO rat has already demonstrated its value in the scientific community. However, to obtain a complete picture of the functions of MCH in humans, multiple animal models, including rat models, mouse models, and maybe even studies in monkeys, might be necessary to accomplish this. It is thus necessary that scientists view the *Pmch* KO rat as a complementary animal model in the MCH-field, and not as competition to the already existing *Pmch* KO mouse models.

MCH2R

Rodents only express MCH1R (Tan et al., 2002), whereas humans, monkeys, dogs and ferrets express both MCH1R and MCH2R (An et al., 2001; Hill et al., 2001; Mori et al., 2001; Rodriguez et al., 2001; Sailer et al., 2001; Wang et al., 2001). Homology between

MCH1R and MCH2R is ~35%, and the function of MCH2R appears to be slightly different (no effect on cAMP; G_q specific; An et al., 2001; Mori et al., 2001; Sailer et al., 2001). However, studies probing the exact function of MCH2R have been limited due to its absence in rodent models. It implies that a potential treatment based on MCH1R function in rodents might result in different effects in humans due to potential effects of MCH2R.

Anti-obesity treatment based on MCH1R signaling

Many pharmaceutical companies have focused on the MCH-MCH1R-system to develop small-molecule MCH1R antagonists for the potential treatment of obesity and/or mood disorders (Handlon and Zhou, 2006; Shimazaki et al., 2006; Tavares et al., 2006; Luthin, 2007). Although many small-molecule MCH1R antagonists have been produced by various laboratories, only three have entered phase I clinical trials before 2007 (Mendez-Andino and Wos, 2007). The main reason for this is that many of the small-molecule MCH1R antagonists display hERG-binding activity *in vitro*. Blockade of hERG-channels can induce QTc (Q wave-T wave interval corrected for heart rate) interval prolongation that is frequently associated with potentially lethal arrhythmias (Schneider et al., 2005). Although some novel and more selective MCH1R antagonists have been developed recently, most of them have limited *in vivo* activity or are unsuitable for clinical development on the basis of their overall Absorption, Distribution, Metabolism, and Excretion (ADME) and safety profile (Mendez-Andino and Wos, 2007). Therefore, several pharmaceutical companies have stopped their research programs regarding MCH1R antagonists. Thus, although the development of an obesity or mood disorder treatment based on MCH1R-antagonsim could be highly valuable, in light of the recent developments, the chance that this will happen is limited.

LIPIN 1

The *Lipin 1*^{1Hubr} protein

In chapter 5 we describe the initial characterization of the *Lpin1*^{1Hubr} rat model. These rats developed a paralysis and lipodystrophy phenotype during the second postnatal week, which attenuated again during development.

The *Lpin1*^{1Hubr} mutation resulted in out-of-frame transcription, thereby disrupting Lipin 1 HAD domain IV and completely inactivating PAP1 activity. Although mRNA levels of *Lpin1*, *Lpin1*α, and *Lpin1*β were present or even increased in *Lpin1*^{1Hubr} rats, at the moment of writing this discussion, we did not yet succeed in demonstrating equal or even increased protein levels in *Lpin1*^{1Hubr} rats as compared to wild type rats due to nonspecific antibodies.

In chapter 5 however we propose that the attenuation of the *Lpin1*^{1Hubr} phenotype results from intact transcriptional activity of the Lipin1^{1Hubr} protein. Therefore, the demonstration that Lipin 1^{1Hubr} protein levels are equal or even increased in *Lpin1*^{1Hubr} rats as compared to Lipin 1 levels in wild type rats is crucial and has be determined as soon a possible.

The transitory phenotype of *Lpin1*^{1Hubr} rats

Lpin1^{1Hubr} rats showed an impressive attenuation of the paralysis and lipodystrophy phenotype. Interestingly, the 20884 double mutant and *Lpin1*^{20884} mice also demonstrated an attenuation of transient paralysis phenotype (Douglas et al., 2009). The *Lpin1* mutation in the 20884 double mutant and *Lpin1*^{20884} mice induced a missense mutation (Y873N) in the last exon of *Lpin1*, and both the 20884 double mutant and the *Lpin1*^{20884} mice showed a significant loss of PAP1 activity (~20% in WAT and nerve tissue as compared to wild type; (Douglas et al., 2009). Moreover, Lipin 1^{20884} protein levels were equal between genotypes, except for WAT, where protein levels were ~200% as compared to wild type protein levels (Douglas et al., 2009).

The *Lpin1*^{1Hubr} mutation in the rat did completely inactivate PAP1 activity in WAT and nerve tissue of *Lpin1*^{1Hubr} rats. Although we did not yet succeed in measuring Lipin 1^{1Hubr} protein levels, mRNA levels of *Lpin1*, *Lpin1*α, and *Lpin1*β in *Lpin1*^{1Hubr} rats might provide an indication that no nonsense-mediated decay mechanism is activated.

In sum, both *Lpin1*^{20884} mice and *Lpin1*^{1Hubr} rats contain a mutation in the one of the last exons of *Lpin1*. In both situations, PAP1 activity is strongly affected, and in both situations mutant rodents demonstrated a pronounced attenuation of the paralysis and lipodystrophy phenotype. Finally, Lipin 1 protein levels are not affected in *Lpin1*^{20884} mice or even increased (Douglas et al., 2009).

On the contrary, a null deletion of *Lpin1* (*Lpin1*$^{fld/fld}$ mice) resulted in complete loss of *Lpin1* mRNA (Peterfy et al., 2001), whereas a near-complete Schwann cell-specific null deletion of *Lpin1* (MPZ$^{Cre/+}$/Lp$^{fE2\text{-}3/fE2\text{-}3}$ mice) resulted in severe loss of *Lpin1* mRNA and Lipin 1 protein levels (Nadra et al., 2008). Moreover, both *Lpin1*$^{fld/fld}$ and MPZ$^{Cre/+}$/Lp$^{fE2\text{-}3/fE2\text{-}3}$ mice developed severe neuropathy that did not improve over time (Langner et al., 1991; Peterfy et al., 2001; Nadra et al., 2008).

Lipin 1 had direct transcriptional effects on genes involved in fatty acid oxidation in the murine liver (Finck et al., 2006). In chapter 5, we proposed and provided preliminary, yet strongly suggestive, evidence that Lipin 1 has a similar function on genes involved in lipogenesis and myelination, in WAT and nerve tissue respectively. Although additional experiments demonstrating a transcriptional function for Lipin 1 in WAT and nerve tissue have to be performed, the *in vivo* data suggest that mutant protein levels, present at normal levels albeit with a decreased or absent PAP1 activity, might be indeed correlated to the transient phenotypes observed in *Lpin1*^{20884} mice and *Lpin1*^{1Hubr} rats.

The role of Lipin 1 in Schwann cell function

In chapter 5 we provided preliminary evidence that Lipin 1α, and probably also Lipin 1β, have the ability to stimulate *Krox20* expression in differentiating primary rat Schwann cell cultures *in vitro*. Although additional experiments are necessary to determine if this observation is real, the observation is of great interest. First of all, it indicates that Lipin 1 could potentially be an important player in the Schwann cell myelination program.

In addition, disorders associated with altered cholesterol metabolism (e.g. Tangier disease and Smith-Lemli-Opitz-syndrome) or fatty acid metabolism (Refsum's

disease and diabetes mellitus) often produce myelin and axonal defects (Dyck and Thomas, 2005). In sum, extended knowledge on how Lipin 1 might affect myelination, potentially through transcriptional effects, could potentially identify new targets for pharmaceutical treatment or stem cell-based gene therapy.

The role of Lipin 1 in WAT

In chapter 5 we provided evidence that attenuation of the *Lpin1*^{1Hubr} phenotype is associated with improvements in the lipodystrophy phenotype. As *Lpin1* is highly expressed in WAT (Peterfy et al., 2001; Donkor et al., 2007) and required for the normal induction of the adipogenetic program (Phan et al., 2004), a transcriptional function for Lipin 1 in WAT should not be excluded. Moreover, *Lpin1*^{1Hubr} rats on a high-fat diet are quite capable of increasing their body weight, whereas this ability is absent in *Lpin1*$^{fld/fld}$ mice (Phan et al., 2004). As both *Lpin1*$^{fld/fld}$ mice and *Lpin1*^{1Hubr} rats demonstrated equal food intake as compared to control animals, these observations indicate that *Lpin1*^{1Hubr} rats have a partially functional adipogenetic program, whereas mice with a null deletion of *Lpin1* do not.

PAP1 activity is fully ablated in WAT of *Lpin1*^{1Hubr} rats, whereas the Lipin 1^{1Hubr} protein, if present at normal levels, might stimulate the adipogenetic program (Phan et al., 2004). Therefore, the lipodystrophy might be induced by absent PAP1 activity, by potential decreased feeding due to decreased mobility in *Lpin1*^{1Hubr} pups, or by a combination of both. Thus, the lipodystrophy phenotypic improvements might result from increased food intake due to relatively increased mobility, correct potential transcriptional activity of Lipin 1^{1Hubr}, or a combination of both. Although it is difficult to measure food intake in weaning pups or very young pups (younger than 15 days), decreased food intake could decrease lipid accumulation in *Lpin1*^{1Hubr} pups, thus partially masking effects of the potential transcriptional activity of Lipin 1^{1Hubr}. However, food intake studies at a young age might add additional information regarding this hypothesis, although such studies will be challenging to set up properly.

CONCLUSION

The number of people that are overweight or obese has shown an alarming increase worldwide in past three decades. Good news however is that, at least in the US, this increase seems to have stalled (Flegal et al., 2010). As mentioned in chapter 1, the obese population can be roughly divided into two groups. The first group is the small fraction (~5-10%) of people with obesity caused by (mono)-genetic mutations, endocrine disorders, or medication. This fraction has remained relatively stable over time. The second group is the large fraction of people with obesity that is caused by a combination of high-caloric food intake, decreased physical activity, and genetic susceptibility.

As the general knowledge regarding energy homeostasis has increased significantly, the development of an anti-obesity treatment based on a key neuropeptide or receptor involved in energy regulation might be not far away. However, the increased general

knowledge has also demonstrated the complexity and integration of different brain systems, all driving one goal: the correct regulation of body weight and subsequent health. Affecting the function of one such brain system through pharmaceutical intervention might thus result in adaptations and subsequent compensation in other brain regions. This will inevitably obstruct or even impair the development and function of a potential anti-obesity treatment.

The chance that such a potential anti-obesity treatment is based on the MCH-MCH1R-system is small, but still present. If Lipin 1 function can be at the basis of a treatment for lipodystrophy, paralysis, or both, has to be investigated in the future. It is conceivable that an effective pharmaceutical anti-obesity treatment with a one-size fits-all characteristic might never be developed. Therefore I advice everybody to first shift their trust from the scientists to themselves: eat healthy and exercise regularly!

REFERENCES

Alon T, Friedman JM (2006) Late-onset leanness in mice with targeted ablation of melanin concentrating hormone neurons. J Neurosci 26:389-397.

An S, Cutler G, Zhao JJ et al. (2001) Identification and characterization of a melanin-concentrating hormone receptor. Proc Natl Acad Sci U S A 98:7576-7581.

Astrand A, Bohlooly YM, Larsdotter S et al. (2004) Mice lacking melanin-concentrating hormone receptor 1 demonstrate increased heart rate associated with altered autonomic activity. Am J Physiol Regul Integr Comp Physiol 287:R749-758.

Bittencourt JC, Presse F, Arias C et al. (1992) The melanin-concentrating hormone system of the rat brain: an immuno- and hybridization histochemical characterization. The Journal of comparative neurology 319:218-245.

Borowsky B, Durkin MM, Ogozalek K et al. (2002) Antidepressant, anxiolytic and anorectic effects of a melanin-concentrating hormone-1 receptor antagonist. Nat Med 8:825-830.

Buehr M, Meek S, Blair K et al. (2008) Capture of authentic embryonic stem cells from rat blastocysts. Cell 135:1287-1298.

Chambers J, Ames RS, Bergsma D et al. (1999) Melanin-concentrating hormone is the cognate ligand for the orphan G-protein-coupled receptor SLC-1. Nature 400:261-265.

Chen Y, Hu C, Hsu CK et al. (2002) Targeted disruption of the melanin-concentrating hormone receptor-1 results in hyperphagia and resistance to diet-induced obesity. Endocrinology 143:2469-2477.

Chung S, Hopf FW, Nagasaki H et al. (2009) The melanin-concentrating hormone system modulates cocaine reward. Proc Natl Acad Sci U S A.

Cousin B, Cinti S, Morroni M et al. (1992) Occurrence of brown adipocytes in rat white adipose tissue: molecular and morphological characterization. J Cell Sci 103 (Pt 4):931-942.

Donkor J, Sariahmetoglu M, Dewald J et al. (2007) Three mammalian lipins act as phosphatidate phosphatases with distinct tissue expression patterns. J Biol Chem 282:3450-3457.

Douglas DS, Moran JL, Bermingham JR, Jr. et al. (2009) Concurrent Lpin1 and Nrcam mouse mutations result in severe peripheral neuropathy with transitory hindlimb paralysis. J Neurosci 29:12089-12100.

Dyck PJ, Thomas PK (2005) Peripheral neuropathy, 4th ed.: Elsevier Saunders.

Even PC, Mokhtarian A, Pele A (1994) Practical aspects of indirect calorimetry in laboratory animals. Neurosci Biobehav Rev 18:435-447.

Finck BN, Gropler MC, Chen Z et al. (2006) Lipin 1 is an inducible amplifier of the hepatic PGC-1alpha/PPARalpha regulatory pathway. Cell Metab 4:199-210.

Flegal KM, Carroll MD, Ogden CL et al. (2010) Prevalence and trends in obesity among US adults, 1999-2008. JAMA 303:235-241.

Geurts AM, Cost GJ, Freyvert Y et al. (2009) Knockout rats via embryo microinjection of zinc-finger nucleases. Science (New York, NY 325:433.

Glier MB, Pissios P, Babich SL et al. (2010) The metabolic phenotype of SCD1-deficient mice is independent of melanin-concentrating hormone. Peptides 31:123-129.

Gondo Y (2008) Trends in large-scale mouse mutagenesis: from genetics to functional genomics. Nat Rev Genet 9:803-810.

Gonzalez MI, Baker BI, Hole DR et al. (1998) Behavioral effects of neuropeptide E-I (NEI) in the female rat: interactions with alpha-MSH, MCH and dopamine. Peptides 19:1007-1016.

Granneman JG, Burnazi M, Zhu Z et al. (2003) White adipose tissue contributes to UCP1-independent thermogenesis. Am J Physiol Endocrinol Metab 285:E1230-1236.

Handlon AL, Zhou H (2006) Melanin-concentrating hormone-1 receptor antagonists for the treatment of obesity. J Med Chem 49:4017-4022.

Herold MJ, van den Brandt J, Seibler J et al. (2008) Inducible and reversible gene silencing by stable integration of an shRNA-encoding lentivirus in transgenic rats. Proc Natl Acad Sci U S A 105:18507-18512.

Hill J, Duckworth M, Murdock P et al. (2001) Molecular cloning and functional characterization of MCH2, a novel human MCH receptor. J Biol Chem 276:20125-20129.

Keays DA, Clark TG, Flint J (2006) Estimating the number of coding mutations in genotypic- and phenotypic-driven N-ethyl-N-nitrosourea (ENU) screens. Mamm Genome 17:230-238.

Kokkotou E, Jeon JY, Wang X et al. (2005) Mice with MCH ablation resist diet-induced obesity through strain-specific mechanisms. Am J Physiol Regul Integr Comp Physiol 289:R117-124.

Kreier F, Fliers E, Voshol PJ et al. (2002) Selective parasympathetic innervation of subcutaneous and intra-abdominal fat--functional implications. J Clin Invest 110:1243-1250.

Langner CA, Birkenmeier EH, Roth KA et al. (1991) Characterization of the peripheral neuropathy in neonatal and adult mice that are homozygous for the fatty liver dystrophy (fld) mutation. J Biol Chem 266:11955-11964.

Lembo PM, Grazzini E, Cao J et al. (1999) The receptor for the orexigenic peptide melanin-concentrating hormone is a G-protein-coupled receptor. Nat Cell Biol 1:267-271.

Luquet S, Perez FA, Hnasko TS et al. (2005) NPY/AgRP neurons are essential for feeding in adult mice but can be ablated in neonates. Science (New York, NY 310:683-685.

Luthin DR (2007) Anti-obesity effects of small molecule melanin-concentrating hormone receptor 1 (MCHR1) antagonists. Life sciences 81:423-440.

Marsh DJ, Weingarth DT, Novi DE et al. (2002) Melanin-concentrating hormone 1 receptor-deficient mice are lean, hyperactive, and hyperphagic and have altered metabolism. Proc Natl Acad Sci U S A 99:3240-3245.

Mashimo T, Yanagihara K, Tokuda S et al. (2008) An ENU-induced mutant archive for gene targeting in rats. Nat Genet 40:514-515.

McBride RB, Beckwith BE, Swenson RR et al. (1994) The actions of melanin-concentrating hormone (MCH) on passive avoidance in rats: a preliminary study. Peptides 15:757-759.

Mendez-Andino JL, Wos JA (2007) MCH-R1 antagonists: what is keeping most research programs away from the clinic? Drug Discov Today 12:972-979.

Monzon ME, de Souza MM, Izquierdo LA et al. (1999) Melanin-concentrating hormone (MCH) modifies memory retention in rats. Peptides 20:1517-1519.

Mori M, Harada M, Terao Y et al. (2001) Cloning of a novel G protein-coupled receptor, SLT, a subtype of the melanin-concentrating hormone receptor. Biochem Biophys Res Commun 283:1013-1018.

Mul JD, Yi CX, van den Berg SA et al. (2010) Pmch expression during early development is critical for normal energy homeostasis. Am J Physiol Endocrinol Metab 298:E477-488.

Nadra K, de Preux Charles AS, Medard JJ et al. (2008) Phosphatidic acid mediates demyelination in Lpin1 mutant mice. Genes Dev 22:1647-1661.

Peterfy M, Phan J, Xu P et al. (2001) Lipodystrophy in the fld mouse results from mutation of a new gene encoding a nuclear protein, lipin. Nat Genet 27:121-124.

Phan J, Peterfy M, Reue K (2004) Lipin expression preceding peroxisome proliferator-activated receptor-gamma is critical for adipogenesis *in vivo* and *in vitro*. J Biol Chem 279:29558-29564.

Pissios P (2009) Animals models of MCH function and what they can tell us about its role in energy balance. Peptides 30:2040-2044.

Pissios P, Maratos-Flier E (2003) Melanin-concentrating hormone: from fish skin to skinny mammals. Trends Endocrinol Metab 14:243-248.

Pissios P, Bradley RL, Maratos-Flier E (2006) Expanding the scales: The multiple roles of MCH in regulating energy balance and other biological functions. Endocr Rev 27:606-620.

Pissios P, Frank L, Kennedy AR et al. (2008) Dysregulation of the mesolimbic dopamine system and reward in MCH-/- mice. Biol Psychiatry 64:184-191.

Qu D, Ludwig DS, Gammeltoft S et al. (1996) A role for melanin-concentrating hormone in the central regulation of feeding behaviour. Nature 380:243-247.

Rodriguez M, Beauverger P, Naime I et al. (2001) Cloning and molecular characterization of the novel human melanin-concentrating hormone receptor MCH2. Mol Pharmacol 60:632-639.

Sailer AW, Sano H, Zeng Z et al. (2001) Identification and characterization of a second melanin-concentrating hormone receptor, MCH-2R. Proc Natl Acad Sci U S A 98:7564-7569.

Saito Y, Nothacker HP, Wang Z et al. (1999) Molecular characterization of the melanin-concentrating-hormone receptor. Nature 400:265-269.

Sanchez M, Baker BI, Celis M (1997) Melanin-concentrating hormone (MCH) antagonizes the effects of alpha-MSH and neuropeptide E-I on grooming and locomotor activities in the rat. Peptides 18:393-396.

Sanchez MS, Salvatierra NA, Vettori G et al. (2001a) Effect of neuropeptide-EI on the binding of [3H]SCH 23390 to the dopamine D1 receptor in rat striatal membranes. Neurochem Res 26:533-537.

Sanchez MS, Barontini M, Armando I et al. (2001b) Correlation of increased grooming behavior and motor activity with alterations in nigrostriatal and mesolimbic catecholamines after alpha-melanotropin and neuropeptide glutamine-isoleucine injection in

the rat ventral tegmental area. Cell Mol Neurobiol 21:523-533.

Schneider J, Hauser R, Andreas JO et al. (2005) Differential effects of human ether-a-go-go-related gene (HERG) blocking agents on QT duration variability in conscious dogs. European journal of pharmacology 512:53-60.

Shimada M, Tritos NA, Lowell BB et al. (1998) Mice lacking melanin-concentrating hormone are hypophagic and lean. Nature 396:670-674.

Shimazaki T, Yoshimizu T, Chaki S (2006) Melanin-concentrating hormone MCH1 receptor antagonists: a potential new approach to the treatment of depression and anxiety disorders. CNS Drugs 20:801-811.

Skofitsch G, Jacobowitz DM, Zamir N (1985) Immunohistochemical localization of a melanin concentrating hormone-like peptide in the rat brain. Brain Res Bull 15:635-649.

Smits BM, Mudde J, Plasterk RH et al. (2004) Target-selected mutagenesis of the rat. Genomics 83:332-334.

Smits BM, Mudde JB, van de Belt J et al. (2006) Generation of gene knockouts and mutant models in the laboratory rat by ENU-driven target-selected mutagenesis. Pharmacogenet Genomics 16:159-169.

Tan CP, Sano H, Iwaasa H et al. (2002) Melanin-concentrating hormone receptor subtypes 1 and 2: species-specific gene expression. Genomics 79:785-792.

Tavares FX, Al-Barazanji KA, Bigham EC et al. (2006) Potent, selective, and orally efficacious antagonists of melanin-concentrating hormone receptor 1. J Med Chem 49:7095-7107.

Tiesjema B, Adan RA, Luijendijk MC et al. (2007) Differential effects of recombinant adeno-associated virus-mediated neuropeptide Y overexpression in the hypothalamic paraventricular nucleus and lateral hypothalamus on feeding behavior. J Neurosci 27:14139-14146.

van Boxtel R, Toonen PW, Verheul M et al. (2008) Improved generation of rat gene knockouts by target-selected mutagenesis in mismatch repair-deficient animals. BMC Genomics 9:460.

Wang S, Behan J, O'Neill K et al. (2001) Identification and pharmacological characterization of a novel human melanin-concentrating hormone receptor, mch-r2. J Biol Chem 276:34664-34670.

Xue B, Rim JS, Hogan JC et al. (2007) Genetic variability affects the development of brown adipocytes in white fat but not in interscapular brown fat. J Lipid Res 48:41-51.

Zan Y, Haag JD, Chen KS et al. (2003) Production of knockout rats using ENU mutagenesis and a yeast-based screening assay. Nat Biotechnol 21:645-651.

&

ADDENDUM

SAMENVATTING IN HET NEDERLANDS (VOOR NIET-INGEWIJDEN)

Help.. ik word dik

Als mensen overmatig energie consumeren beschikt ons lichaam over de mogelijkheid om deze energie op te slaan in de vorm van lichaamsvet. Deze eigenschap is geoptimaliseerd gedurende de evolutie als gevolg van het feit dat voedsel dankzij schaarsheid op onvoorspelde tijden beschikbaar was. Door dan gebruik te maken van reserve energie die zit opgeslagen in het lichaamsvet vergrootte men de kans om te overleven gedurende onfortuinlijke tijden. Echter, onze leefwereld is de laatste eeuwen, en met name de laatste decennia, zo sterk veranderd dat voedsel en met name voedsel met veel energie, aanzienlijk makkelijker beschikbaar is. Dit geldt uiteraard wel slechts voor een (overigens steeds groter wordend) deel van de bevolking, voornamelijk in eerste wereld landen. Het is zelfs zo dat in de meeste (stedelijke) gebieden voedsel bijna vierentwintig uur per dag en zeven dagen per week verkrijgbaar is. Dit heeft er voor gezorgd dat een eigenschap die in het verleden voordelig was, het opslaan van overmatige energie in de vorm van lichaamsvet nu is veranderd in een eigenschap die nadelig is. We worden vaak (te) dik.

Als iemand chronisch teveel energie consumeert, vaak ook in combinatie met verminderde lichaamsactiviteit, dan kan diegene extreem overgewicht, ook wel obesitas genoemd, ontwikkelen. Obesitas wordt gekenmerkt door een extreme ophoping van overmatig lichaamsvet en kan leiden tot secundaire aandoeningen zoals type 2 diabetes, hart- en vaatziekten, ademhalingsproblemen, gewrichtsslijtage, onvruchtbaarheid, en enkele vormen van kanker. Het heeft er dan ook alle schijn van dat obesitas op dit moment de meest voorkombare doodsoorzaak ter wereld is met grote medische en financiële druk op de maatschappij als gevolg. Slechts bij een klein gedeelte van alle mensen met extreem overgewicht (~5-10%) wordt dit veroorzaakt door genetische mutaties, endocriene stoornissen, of medicatie. Het overige en significante percentage is voornamelijk het resultaat van een slechte levensstijl.

Een recent rapport in Nederland heeft aangetoond dat ongeveer de helft van alle volwassenen overgewicht heeft, en dat 11% van hen aan obesitas (extreem overgewicht) lijdt. Voor Nederlandse adolescenten zijn deze aantallen even hoog of zelfs hoger. In landen zoals de Verenigde Staten en China lijdt ongeveer 33% van de volwassenen aan obesitas.

Waarom eet ik?

Voordat we een mogelijke medicatie tegen obesitas kunnen ontwikkelen moeten we eerst begrijpen hoe energiehuishouding gereguleerd wordt in het lichaam. Immers, zonder energie kan ons lichaam niet functioneren en sterven we. Zonder dat we het merken nemen we continue het besluit om te eten, of om juist niet te eten. Dit getuigt van de efficiëntie waarmee onze hersenen een zeer grote hoeveelheid complexe informatie kunnen verwerken. Nutriënten worden immers geïdentificeerd en gescheiden van potentieel gevaarlijk componenten door gebruik te maken van zicht, geur, aanraking, en ervaring, of als voedsel reeds is geconsumeerd via signalen

die onze nutritionele status reflecteren. Deze signalen zijn bijvoorbeeld afkomstig uit de maag of darmen (korte termijn signalen) of via het lichaamsvet (lange termijn signalen). Energiehuishouding is het proces dat probeert energie-inname gelijk te stellen aan energie-uitgave, met als doel een stabiel lichaamsvetgehalte. Als we veel energie verbruiken, dan zal ons lichaam dat proberen te compenseren door meer energie te consumeren. Signalen in het lichaam zullen dan aangeven dat er weinig reserve energie is, en deze signalen zullen centraal in de hersenen verwerkt worden, uiteindelijk resulterend in tijdelijke verhoogde voedselinname.

In de hersenen zijn meerdere gebieden die een belangrijke rol spelen in het proces van energiehuishouding. Belangrijke signalen, zoals het lange termijn signaal leptine dat wordt geproduceerd in vetcellen en dus een indicatie is voor de totale hoeveelheid lichaamsvet, worden voornamelijk verwerkt in de 'Arcuate Nucleus' (ARC), een hersengebied dat in contact staat met de bloedbaan. In de ARC bevinden zich neuronen die een belangrijke rol spelen in de regulatie van energiehuishouding. Deze neuronen 'communiceren', vaak door middel van kleine stofjes zoals neuropeptiden, weer met andere neuronen in andere hersengebieden. Zodoende ontstaat een complex 'communicatie netwerk' waarvan het resultaat een verhoging of een verlaging is in energie uitgave en/of inname.

Het proces van energie regulatie is, zoals eerder aangegeven, zeer complex. Vele neuropeptiden in vele verschillende hersengebieden spelen een rol. Het is daarom een een complexe uitdaging om de functie van elk neuropeptide te achterhalen. De reden waarom wetenschappers veel energie steken in het aangaan van deze uitdaging is dat het wellicht wel mogelijk is om de functie van een enkel neuropeptide (of meerdere neuropeptiden) te beperken of te vergroten om zodoende het lichaamsgewicht te laten verminderen. Het liefst onderzoekt men de functie van elk neuropeptide in een situatie waarin de functie van de andere neuropeptiden gelijk is aan de werkelijkheid. In de realiteit is dit echter vaak lastig. Omdat het ethisch niet te verantwoord is om studies in mensen uit te voeren, gebruiken wetenschappers vaak modelorganismen die de situatie in de mens zo goed mogelijk na bootsen. Dit gebeurd onder strenge begeleiding van ethische commissies. In dit promotieonderzoek gebruiken we ratten (*Rattus norvegicus*) waarbij we een mutatie (foutje) geïntroduceerd hebben in een gen dat belangrijk is voor het proces van energiehuishouding.

Dit proefschrift

Waarom gebruiken we de rat om onderzoek te doen? De rat toont genetisch grote overeenkomst met de mens, en veel genen die betrokken zijn bij energie huishouding zijn vrijwel hetzelfde in rat en mens. Resultaten gevonden in ratten gelden dus waarschijnlijk ook voor mensen. Daarnaast is de rat relatief groot (vergeleken met een vlieg of een muis) en dus beter geschikt voor complexe operaties. Verder is de rat ook relatief slim en dus goed te gebruiken in complexere gedragsstudies. Dit laatste is met name van belang omdat de ontwikkeling van obesitas bij mensen een grote gedragsmatige component heeft.

Hoofdstuk 1 biedt een algemene introductie over de regulatie van energiehuishouding. In **hoofdstuk 2** beschrijven we ratten die een mutatie hebben in het gen dat codeert voor Melanin-Concentrating Hormone (*Pmch*). De mutatie in dit gen heeft er voor gezorgd dat het gen niet meer goed afgelezen kan worden waardoor het neuropeptide, het eindproduct van het gen, niet meer gemaakt kan worden. Ratten die de mutatie dragen (*Pmch*$^{-/-}$) hebben ongeveer 20% minder lichaamsgewicht dan ratten die wel het functionele MCH gen hebben (*Pmch*$^{+/+}$). Dit lijkt voornamelijk te komen doordat *Pmch*$^{-/-}$ ratten minder eten dan *Pmch*$^{+/+}$ ratten. Als een 1-jaar oude *Pmch*$^{+/+}$ rat dus 1 kilogram weegt, dan weegt een *Pmch*$^{-/-}$ rat van gelijke leeftijd ongeveer 800 gram. Dit is een groot verschil, vooral als je het vertaald naar menselijke proporties, en het lijkt er dus op dat MCH dus een belangrijke rol speelt in het proces van energie huishouding. Farmaceutische bedrijven zijn dan ook zeer geïnteresseerd in MCH om te kijken of ze wellicht een medicatie kunnen baseren op basis van de functie van MCH.

Pmch$^{-/-}$ ratten zijn dus lichter, hebben minder vet, eten minder, maar lijken verder normaal. Naast deze algemene beschrijving van het model presenteren we ook een nieuwe vinding, en wel dat het erop lijkt dat MCH erg belangrijk is gedurende de eerste ~55/60 levensdagen van de rat. Het verschil in lichaamsgewicht ontstaat namelijk alleen gedurende deze eerste periode. Als men dit vertaalt naar mensen dan is dat ongeveer tot het einde van de puberteit. Dit zou kunnen betekenen dat MCH belangrijk is gedurende volwassenheid, als men bijvoorbeeld een tekort aan reserve energie hebt, maar misschien nog wel belangrijker gedurende vroeg ontwikkeling en puberteit wanneer mensen hard groeien en veel energie nodig hebben.

In **hoofdstuk 3** bestuderen we wederom *Pmch*$^{-/-}$ ratten, die lichter zijn, maar nu kijken we naar waarom ze minder eten. Het maaltijd patroon van *Pmch*$^{-/-}$ ratten lijkt normaal, maar per maaltijd eten ze beduidend minder. Ook hebben we experimenten gedaan waarbij ratten zichzelf voedselbeloningen kunnen geven door op een pedaaltje te drukken. Als we dit in toenemende mate moeilijker maken (ze moeten vaker drukken voor één beloning) lijkt het erop dat *Pmch*$^{-/-}$ ratten minder 'gemotiveerd' zijn om te werken voor deze voedselbeloningen dan *Pmch*$^{+/+}$ ratten. Dit zou erop kunnen duiden dat MCH een rol speelt in een hersengebied dat belangrijk is voor de belonende waarde van eten. Dit hersengebied speelt ook een rol speelt bij verslavingen. Daarom hebben we dezelfde truc herhaalt, alleen nu mochten de ratten zichzelf kleine hoeveelheden cocaïne toedienen. Verassend genoeg bleek toen dat *Pmch*$^{-/-}$ ratten meer 'gemotiveerd' waren om te werken voor de cocaïne toedieningen dan *Pmch*$^{+/+}$ ratten. Dit is dus precies andersom dan bij voedselbeloningen. Verder tonen we aan dat veranderingen in dopamine huishouding, een stofje dat belangrijk is voor beloningsmechanismen, wellicht onderliggend zijn aan de waargenomen ontkoppeling tussen 'natuurlijke' en 'niet-natuurlijke' beloningen. Dit zou kunnen betekenen dat MCH een rol speelt in de beloningswaarde van voedsel om zodoende van nature voedsel inname te stimuleren.

In **hoofdstuk 4** bestuderen we het lichaamsvet van *Pmch*$^{-/-}$ ratten. *Pmch*$^{-/-}$ ratten hebben namelijk ~20% minder lichaamsgewicht en zelfs ~50% minder lichaamsvet. Dit zou erop kunnen duiden dat niet alleen een verminderde voedselinname leidt

to minder vet opslag, maar dat er wellicht nog additionele mechanismen hierin een rol spelen. Vervolgens hebben we *Pmch*$^{+/+}$ ratten evenveel eten gegeven als *Pmch*$^{-/-}$ ratten. Deze *Pmch*$^{+/+}$ ratten hadden echter aanzienlijk meer vet opslag dan de *Pmch*$^{-/-}$ ratten. Ook dit geeft aan dat er nog meer aan de hand is in het vet van *Pmch*$^{-/-}$ ratten. Voortijdelijk onderzoek geeft aan het niveau van twee stoffen, adrenaline en noradrenaline, verhoogd lijkt in het bloed van *Pmch*$^{-/-}$ ratten. Deze stoffen stimuleren de afbraak van vet en zouden dus een belangrijke rol kunnen spelen in de verminderde vetopslag van *Pmch*$^{-/-}$ ratten. Om dit echter duidelijk aan te tonen is het nodig om verdere vervolgexperimenten uit te voeren.

In **hoofdstuk 5** beschrijven we tenslotte ratten die een mutatie hebben in het gen dat codeert voor Lipin1. De mutatie in dit gen introduceert een foutje, maar het zorgt niet voor afbraak van het eindproduct. Uit literatuur blijkt dat het eindproduct twee verschillende functies heeft: 1) een enzymatische functie die belangrijk is voor vet metabolisme omdat het een stofje omzet in een belangrijk tweede stofje; 2) het is onderdeel van een complex en beïnvloed zodoende de activiteit van weer andere eindproducten.

Ratten met een mutatie in het gen dat codeert voor Lipin1 (*Lpin1*$^{-/-}$) lijken normaal tot ongeveer een week na de geboorte, maar vervolgens groeien ze een stuk minder goed (ze zijn kleiner en hebben minder lichaamsgewicht) en ontwikkelen ze een verlamming, voornamelijk aan het achterlijf. Het blijkt dat de *Lpin1*$^{-/-}$ ratten minder vet opslaan, maar ook dat de beschermlagen om neuronen (eerstgenoemde bestaan ook voor een groot gedeelte uit vet) niet goed ontwikkelen. Tot onze verassing verdwijnen deze aandoeningen grotendeels als de ratten weer ouder worden. Om dit te documenteren hebben we gekeken naar vetopslag en het uiterlijk van de neuronenbeschermlagen in jonge en oudere *Lpin1*$^{-/-}$ ratten. Beide processen verbeteren inderdaad aanzienlijk over tijd. Tot slot geeft eerder onderzoek aan dat het gemuteerde Lipin1 product een mogelijke directe rol speelt in de algemene verbetering van *Lpin1*$^{-/-}$ ratten. Vervolg experimenten zullen echter moeten aantonen of dat werkelijk zo is en welke mechanismen hiervoor verantwoordelijk zijn.

ACKNOWLEDGEMENTS

Hoppa, Gekkenhuis! Het boekje is af.

Een paar jaar geleden begon het met "Nietsch kan je!", maar gelukkig heb ik inmiddels het tegendeel bewezen. Echter, zonder de hulp van vele anderen was het nooit zo ver gekomen.

Edwin, bedankt voor de goede begeleiding, de zakelijke leerschool, maar vooral voor de vrijheid en je vertrouwen. Hierdoor kon ik allerlei samenwerkingen aangaan en zelf op vele verschillende instituten onderzoek doen.

Susanne, ik kan niet vaak genoeg zeggen hoe dankbaar ik ben dat je me welkom heette in de wondere wereld van lichaamsgewicht regulatie. Zonder jou was ik niet verder gekomen dan een ratje in een weegschaal zetten. Je bent een uniek persoon en als er meer mensen zoals jij zouden zijn, dan zou het wetenschapswereldje een stuk leuker zijn. Dries, dit geldt ook voor jou.

De Cuppen groep, alle huidige collega's (en oudgedienden): Wat zijn jullie af een toe een losgeslagen bende projectielen. Daardoor was het wel altijd een genot om met jullie te werken. Bedankt voor de toptijd, de discussies (vaker over andere zaken dan over metabolisme), de biertjes en de mooie uurtjes op borrels, feestjes en in bruine kroegjes. Judith, Harma, Esther, Ruben, Michal, en Jos, bedankt voor de leuke kamer (en dat jullie het uithielden met mijn soms interessante muziekkeuze: boem boem boem boem boem boem boem boem boem!).

Over uithouden gesproken. Alle studenten die dat deden (of niet), Michal, Magdalena, Sabine, Eoghan, en Heleen: Bedankt voor jullie geweldige inzet en bijdrage. Eoghan, I will never forget bringing you (and Daniel) home. I didn't know humans were able to get that drunk!

Het Hubrecht Instituut, het is werkelijk waar een geweldige plaats om te werken. Ira en Janny, jullie zijn geweldig, bedankt voor alle hulp. Alle TD en IT mannen, Jeroen en Harry, de receptionisten, en last but not least, de dierverzorgers. Zonder jullie allemaal zou alles een stuk minder makkelijk gaan. Alle huidige (en verdwenen) gezellige borrelgangers, jullie hebben de afgelopen 4 jaar tot een werkelijk festijn gemaakt: de Rex, VrijMiBo'en, klootschieten, ijsjes, bowlen, rockchicks in de Ekko, knakworsten, de PV, fireballs, stiften, de grote O, MaMiBo'en, DiMiBo'en, WoMiBo'en, DoMiBo'en, happy hardcore feestjes, whisky proeverijen (binnen of buiten een zwembadje), Nieuwjaarsdiners, het bootje, vrijdagmiddag-slechte-muziek-dag, zaalvoetballen, of mexxen op Chrismukkah-borrels: het was altijd super.

All the people that were brave enough to start a collaboration with me: Susanne (RMI/AMC), Roger (RMI), Jean-Louis (IPMC), Dries (NIN/AMC), Peter (LUMC), Bart (Radboud), Ralph (Yale), Taco (VUMC), Roman (Lausanne), Eric (WKZ), Olivier (UCI), Judith (Radboud), Richard (Bratislava), Dies (Erasmus), and Tim (GSU). Thank you! Without your effort and that of your colleagues (Chun-Xia, Karim, Robert, Marieke, Sjoerd, and Arjen to name a few) a significant part of this thesis would be missing.

De Rat Pack: Ruben en Pim. Ik had jullie niet kunnen of willen missen! Van genoom studies naar metabole studies is vaak een grotere stap dan we dachten. Pim, bedankt voor je onmisbare hulp: midden in de nacht rondom een horrorfilm met een Belgisch biertje, bij het vasthouden van een monster van 900 gram die mijn vinger in z'n vizier had, of gewoon als iets weer eens tegen zat. Laat het gaan, laat het vallen, laat het los, of niet?! Ik kan geen lievere papa bedenken voor Noortje. Alhoewel... Rubeninho, hoe doe je het toch? Een tweede kleine donder ~~op komst~~ geboren, op tijd promoveren, altijd vrolijk en enthousiast (nou ja, bijna altijd), en ook nog makkelijk winnen met het 'publicatie wedstrijdje'. Ik bewonder hoe je het allemaal doet. Succes allebei met de nabije toekomst! Vergeet niet dat er altijd een plekje beschikbaar is in Cincinnati...

De Paranimfen: Pim, ik vind het super mooi dat je na 4.5 jaar naast me staat. Ik hoop dat je het net zo leuk vindt als ik. Willem, wat een cola of drie tijdens een groentijd toch niet kan opleveren.. Ik hoop dat we deze zomer nog veel feestjes gaan pakken!

Voor iedereen die zich nu vergeten voelt, dat ben ik niet.

De Familie: Lieve papa, mama, Naomi, Malka, Ernst, kleine Ernst, en Max, bedankt voor jullie onvoorwaardelijke liefde en support als ik weer eens niet kwam opdraven of 2 maanden niet had gebeld. En ondanks dat het af en toe een beetje hogere wiskunde was, vroegen jullie altijd hoe het ging op het werk. Ik ga jullie enorm missen, en ik vind het jammer dat we straks zo ver van elkaar vandaan wonen. Gelukkig is er genoeg logeerruimte in de VS.

Lieve Marieke, zonder jou zou het allemaal leeg zijn. Van 'Cin-ci-net-nie' naar 'Sin city': ik ben blij dat we samen weer eens op avontuur gaan! 'You can always be my wingman'!

LIST OF PUBLICATIONS

Mul JD, Yi CX, van den Berg SA, Ruiter M, Toonen PW, van der Elst MC, Voshol PJ, Ellenbroek BA, Kalsbeek A, la Fleur SE, Cuppen E. *Pmch* expression during early development is critical for normal energy homeostasis. American Journal of Physiology – Endocrinology and Metabolism. 2010 Mar; 298(3): E477-88.

Homberg JR, **Mul JD**, de Wit E, Cuppen E. Complete knockout of the nociceptin/orphanin FQ receptor in the rat does not induce compensatory changes in mu, delta and kappa opioid receptors. Neuroscience. 2009 Sep 29; 163(1): 308-15.

Boxem M, Maliga Z, Klitgord N, Li N, Lemmens I, Mana M, de Lichtervelde L, **Mul JD**, van de Peut D, Devos M, Simonis N, Yildirim MA, Cokol M, Kao HL, de Smet AS, Wang H, Schlaitz AL, Hao T, Milstein S, Fan C, Tipsword M, Drew K, Galli M, Rhrissorrakrai K, Drechsel D, Koller D, Roth FP, Iakoucheva LM, Dunker AK, Bonneau R, Gunsalus KC, Hill DE, Piano F, Tavernier J, van den Heuvel S, Hyman AA, Vidal M. A protein domain-based interactome network for *C. elegans* early embryogenesis. Cell. 2008 Aug 8; 134(3): 534-45.

Homberg JR, Olivier JD, Smits BM, **Mul JD**, Mudde J, Verheul M, Nieuwenhuizen OF, Cools AR, Ronken E, Cremers T, Schoffelmeer AN, Ellenbroek BA, Cuppen E. Characterization of the serotonin transporter knockout rat: a selective change in the functioning of the serotonergic system. Neuroscience. 2007 Jun 8; 146(4): 1662-76.

Smits BM, Peters TA, **Mul JD**, Croes HJ, Fransen JA, Beynon AJ, Guryev V, Plasterk RH, Cuppen E. Identification of a rat model for usher syndrome type 1B by N-ethyl-N-nitrosourea mutagenesis-driven forward genetics. Genetics. 2005 Aug; 170(4): 1887-96.

Mul JD, Sears RM, la Fleur SE, Afrasiab-Middelman A, Verheij MM, Schetters D, Homberg JR, Schoffelmeer AN, Adan RA, DiLeone RJ, De Vries TJ, and Cuppen E. Loss of Melanin-Concentrating Hormone in the rat uncouples operant responding for food and cocaine and affects striatal dopamine function. *Submitted*.

Mul JD, O'Duibhir E, Vargoviç P, Toonen PW, Korving J, Koppen A, Kalkhoven E, Kvetnansky R, and Cuppen E. Adipose function in *Pmch*-deficient rats. *In preparation*.

Mul JD[*], Nadra K[*], Nijman IJ, Médard J-J, Toonen PW, de Bruin A, Grès S, Han G-S, Carman GM, Saulnier-Blach J-S, Meijer D, Chrast R[*], and Cuppen E[*]. Lipin 1 stimulates myelination in Schwann cells through transcriptional regulation. *In preparation*.
[*] authors contributed equally

CURRICULUM VITAE

Joram Mul was born on June 25, 1980 in Arnhem, The Netherlands. In 1998, he received his diploma from the Stedelijk Gymnasium in Arnhem, after which he started his study Biology at Utrecht University in September of that same year. His first internship was performed at the Hubrecht Institute in Utrecht, on "Identification of the rat whirler mutation and exploring a novel MuA-based detection strategy" under supervision of dr. Bart Smits in the group of Prof. dr. Edwin Cuppen. Joram performed his second internship on the subject of "An interaction domain map of *C. elegans* early embryogenesis" in the Center for Cancer Systems Biology and Department of Cancer Biology at the Dana-Farber Cancer Institute in Boston under supervision of dr. Mike Boxem in the group of Prof. dr. Marc Vidal. In 2005 he graduated, receiving a M.Sc. in Biology. In October of the same year he continued his education as a PhD student at the Hubrecht Institute in the group of Prof. dr. Edwin Cuppen (Genome biology). The results of his research performed at the Hubrecht Institute are described in this thesis. In the beginning of 2011, Joram will commence his postdoctoral studies on food intake and body weight regulation in the lab of Prof. dr. Randy Seeley at the Obesity Research Center of the University of Cincinnati, USA.